Developing multiviral nanoparticle vaccines to facilitate proactive vaccinology

Rory Alexander Hills

Department of Biochemistry
Medical Sciences Division
St John's College
University of Oxford
Michaelmas 2024

A thesis submitted to the University of Oxford in partial fulfilment of the requirement for the degree of Doctor of Philosophy

Abstract

Vaccines are a critical public health intervention and have substantially reduced human suffering. The importance of vaccination was demonstrated during the COVID-19 pandemic, where the rapid introduction of safe and efficacious vaccines substantially reduced mortality and morbidity. Innovation is still required to further enhance the speed of vaccine production for protection against newly arising pathogens with pandemic potential. In the 21st century, three lethal zoonotic coronavirus outbreaks (SARS-CoV, MERS-CoV, and SARS-CoV-2) have already been recorded and several zoonotic coronaviruses have been recognized as future threats. In this thesis, I develop a vaccine technology that elicits a broadly protective immune response against a group of coronaviruses to enable proactive vaccine development. I use SpyTag to facilitate the purification and nanoassembly of a panel of receptor-binding domains (RBDs) from different coronaviruses. I examine patient-derived monoclonal antibodies raised against SARS-CoV-2 and identify cross-reactive antibodies that target evolutionarily conserved regions. I then produce a Quartet of tandemly linked coronavirus RBDs as a single polyprotein. I show that immunization with these Quartets as soluble proteins or displayed multivalently on the SpyCatcher003-mi3 Nanocage (Quartet Nanocages) elicits a potent immune response across a group of evolutionarily related coronaviruses. This response includes raising neutralizing antibodies against viruses absent from the vaccine. I demonstrate that Quartet Nanocages raise a broad immune response in mice that have been pre-biased towards a specific virus. I create a Quartet Nanocage vaccine that induces neutralizing antibodies against newly arisen viral variants with potent immune evasion. I produce a Quartet using coronaviruses identified prior to the COVID-19 pandemic and demonstrate that this vaccine raises a potent immune response against SARS-CoV-2. These results highlight the potential of the Quartet Nanocage strategy as a tool for proactive vaccinology, where vaccines are developed against zoonotic pathogens before human transmission has even occurred.

Authorship Declaration

I declare that this thesis is entirely my own work, except for cases described below. This thesis has not been submitted for any other degree at the University of Oxford or any other institution.

Experiments performed by others:

All mouse immunization and sera collection were performed by Jack Tan at the MRC Weatherall Institute of Molecular Medicine, University of Oxford.

Pseudovirus neutralization assays were performed by Jennifer R. Keeffe, Kaya N. Storm, and Priyanthi N. P. Gnanapragasam with supervision provided by Pamela Bjorkman at the California Institute of Technology.

Authentic virus neutralization assays were performed by Sai Liu, Javier Gilbert-Jaramillo, and William S. James at the James & Lillian Martin Centre, University of Oxford.

Deep mutational scanning experiments were performed by Alexander Cohen, Annie Rorick, and Anthony West, Jr. with supervision provided by Pamela Bjorkman at the California Institute of Technology.

Publications arising from this thesis are detailed below:

Proactive vaccination using multiviral Quartet Nanocages to elicit broad anti-coronavirus responses. Hills, R.A.; Tan, T.; Cohen, A.; Keeffe, J.R.; Keeble, A.H.; Gnanapragasam, P.; Storm, K.; Rorick; A., West Jr., A.P.; Hill, M., Liu, S., Gilbert-Jaramillo, J.; Afzal, M., Napier, A.; Admans, G.; James, W.S.; Bjorkman, P.J.; Townsend, A.R.; Howarth, M. Nature Nanotechnology. 2024. https://doi.org/10.1038/s41565-024-01655-9.

Structural Basis for a Conserved Neutralization Epitope on the Receptor-Binding Domain of SARS-CoV-2. Huang, K.-Y. A.; Chen, X.; Mohapatra, A.; Nguyen, H. T. V.; Schimanski, L.; Tan, T. K.; Rijal, P.; Vester, S. K.; Hills, R. A.; Howarth, M.; Keeffe, J. R.; Cohen, A. A.; Kakutani, L. M.; Wu, Y.-M.; Shahed-Al-Mahmud, M.; Chou, Y.-C.; Bjorkman, P. J.; Townsend, A. R.; Ma, C. Nature Communications 2023, 14 (1), 311. https://doi.org/10.1038/s41467-023-35949-8.

SpySwitch Enables pH- or Heat-Responsive Capture and Release for Plug-and-Display Nanoassembly. Vester, S. K.; Rahikainen, R.; Khairil Anuar, I. N. A.; Hills, R. A.; Tan, T. K.; Howarth, M. Nature Communications 2022, 13 (1), 3714. https://doi.org/10.1038/s41467-022-31193-8.

Acknowledgements

As I reflect on my DPhil, it is clear how much my experience has been defined all those who have supported me. I owe so much to so many.

I would like to thank my supervisor Mark Howarth for his mentorship and advocacy. I am consistently inspired by his creativity, work ethic, and focus on translating ideas to real world impact. I will carry many of the lessons that I have learned from Mark for the rest of my career.

I would like to thank my co-supervisor Alain Townsend for his insight and for the joy he brings to research. His enthusiasm for discovery has been motivational, especially through periods of self-doubt.

I am grateful to the Rhodes Trust and the Townsend-Jeantet Charitable Prize Trust for providing the financial support that has allowed me to undertake this degree. I feel so lucky to be part of the Rhodes community and for all of the opportunity and responsibility that this membership has entailed. I am thankful to the Department of Biochemistry and St John's College at the University of Oxford for the vibrant cultures that they have fostered. I am also thankful to the Department of Pharmacology and Darwin College at the University of Cambridge for welcoming me so warmly after our lab's move.

I cannot imagine what my DPhil would have been without the contributions of Jack Tan. I am thankful for Jack's skill, insight, optimism, and friendship.

I have been incredibly fortunate to be part of the Howarth Research Group. My experience would have been unrecognizable without this collection of remarkable people. I would like to thank Rolle for all he taught me and for fostering my independence, Hung-Jen for his friendship and belief at a time I needed it, Lasya for her kindness and for reminding me of home, Susan

for her inspirational research dedication, Claudia for her infectious determination, Gabrielle for approaching science with such humanity, and Anthony for being a fount of knowledge and dad jokes. Thank you to Miha, Dawid, Henry, and Cameron for their scientific insight and some memorable pub nights. Thank you to Ana, Anna, Arne, Christoph, David, Deepak, Dom, Elizabeth, Emily, Jamie, Michal, Niels, Sandra, Sheryl, Vincent, and Yujia for all that they have contributed to this period of my life. I hope that our paths cross again.

My research (and the enjoyment of its pursuit) has been magnified by close scientific collaboration with incredible researchers. I would like to particularly thank Pamela Bjorkman, Alex Cohen, Jennifer Keeffe, and other members of the Bjorkman lab whose work was foundational to this thesis.

I would like to thank Dennis Hore, Alisdair Boraston, Andrew Hettle, Andrew Weaver, and Judy Fainstein for their mentorship earlier in my career. I would not have been at this stage without them.

I am grateful to Connor, Eric, and Brendon for the obscene number of slides that we studied together and for all that they did to bring to joy to my time at UVic.

I am thankful for the support my friends from Oxford, Cambridge, and Victoria who are now beginning to scatter around the world. Noah, Sean, Chloe, Divya, Nina, Sophie, Gorham, Kieran, Owen, Sasha, Longo, Hairy, Josh, Micah, and Andile were all beside me through difficult times and I am indebted to each of them for that.

Finally, on a sombre note, I would like to acknowledge that the experiments presented in this thesis required the deaths of 198 mice. It is my sincere hope that the potential to reduce human suffering justifies the decision to sacrifice these animals. I have hope for a future where experiments of this nature are made obsolete.

Dedication

To my family. So much of what is best in me is a reflection of them.

To all my aunts, uncles, and cousins for their love and support.

To my ‘big sisters’ Katelyn and Alexa, for showing me how to live an authentic life.

To Conor for his integrity and compassion and to Tyler for his persistence and thoughtfulness. To both of them for their kindness. I am so proud to be their brother.

To Dad for teaching me to have fun, to do my best, and to never cheat myself and for always showing up.

To Mom for showing me how to live my values and seek balance in life, for teaching me to communicate with empathy, and for her endless kindness.

To Ana, for choosing to share the big and small moments that make up a lifetime. We’ve come a long way from Thetis and it warms my heart when I think of all that’s left to come.

Table of Contents

Abbreviations

A_{280}	Absorbances at 280 nm
ACE2	Angiotensin-Converting Enzyme 2
Ad26	Adenovirus Type 26
Ad5	Adenovirus Type 5
AIDS	Acquired Immunodeficiency Syndrome
APC	Antigen-Presenting Cell
AUC	Area Under Curve
BCR	B Cell Receptor
cART	Combination Antiretroviral Therapy
CEPI	Coalition for Epidemic Preparedness Innovations
CFPS	Cell-Free Protein Synthesis
ChAd	Chimpanzee Adenovirus
CHO	Chinese Hamster Ovary
CFU	Colony Forming Unit
CnaB2	Second Immunoglobulin-Like Collagen Adhesin Domain
CV	Column Volume
cryo-EM	Cryogenic Electron Microscopy
DLS	Dynamic Light Scattering
DMEM	Dulbecco's Modified Eagle's Medium
DMS	Deep Mutational Scanning
DPP4	Dipeptidyl Peptidase 4
DSPE	1,2-distearoyl-sn-glycero-3-phosphoethanolamine
E	Envelope
EDTA	Ethylenediaminetetraacetic Acid
EGFR	Epidermal Growth Factor Receptor
EU	Endotoxin Unit
eVLP	Enveloped Virus-like Particle
F*	p-azido-L-phenylalanine
FbaB	Fibronectin Binding Protein
FT	Flowthrough
GMP	Good Manufacturing Practice

H1	Hemagglutinin 1
H5	Hemagglutinin 5
H8	Hemagglutinin 8
HCV	Hepatitis C Virus
HIV	Human Immunodeficiency Virus
HRP	Horseradish Peroxidase
HuSA	Human Serum Albumin
ID_{50}	Half-maximal Inhibitory Dilution
IgG	Immunoglobulin G
IgM	Immunoglobulin M
IPTG	Isopropyl β-D-1-thiogalactopyranoside
KDPG	2-keto-3-deoxy-6-phosphogluconate
M	Membrane
MERS	Middle East Respiratory Syndrome–Related Coronavirus
MES	2-(N-morpholino)ethanesulfonic acid
MSP1	Merozoite Surface Protein
N	Nucleocapsid
NHS	N-hydroxysuccinimide
Ni-NTA	Nickel-nitrilotriacetic acid
NSP	Non-structural Protein
NTD	N-terminal domain
OD	Optical Density
PCR	Polymerase Chain Reaction
PEG	Polyethylene Glycol
PEI	Polyethylenimine
PMSF	Phenylmethanesulfonyl Fluoride
PNGase	Peptide N-Glycosidase
PRNT	Plaque Reduction Neutralization Test
QC	Quality Control
qPCR	Quantitative Polymerase Chain Reaction
RBD	Receptor-Binding Domain
RBS	Receptor Binding Site
RLU	Relative Luminescence Unit

S	Spike
SARS1	Severe Acute Respiratory Syndrome Coronavirus 1
SARS2	Severe Acute Respiratory Syndrome Coronavirus 2
SEC	Size Exclusion Chromatography
SN	Supernatant
ST1	SpyTag
TCEP	Tris(2-carboxyethyl)phosphine
TEM	Transmission Electron Microscopy
TMPRSS2	Transmembrane Protease, Serine 2
TMV	Tobacco Mosaic Virus
UTC	Coordinated Universal Time
VOC	Variant of Concern
VLP	Virus-like Particle
W	Wash
WHO	World Health Organization

Figure List

Chapter 1 – Introduction

1.1 Vaccines

The implementation of protective vaccines against an array of communicable diseases has substantially decreased human mortality and morbidity. Vaccine development has been compared with the introduction of sanitation and access to clean water as a cornerstone of public health (Greenwood, 2014; Rodrigues & Plotkin, 2020). Smallpox is an illustrative example of vaccine impact. This contagious and lethal disease, caused by the variola virus, has devastated human populations for centuries. In the 20th century alone, smallpox was responsible for an estimated 300 million deaths (Berche, 2022; Moore et al., 2006).

Beginning in 1966, a concerted global health campaign of surveillance and containment was undertaken. This effort was made possible by the introduction of a heat-stable, freeze dryable and highly effective vaccine. The last naturally occurring case of smallpox was recorded in 1977 and the World Health Assembly officially declared the disease eradicated in 1980 (Henderson, 1987, 2011). Smallpox and rinderpest (also known as cattle plague) remain the only diseases to be completely eradicated through vaccination campaigns (Morens et al., 2011). However, vaccination efforts are responsible for a substantial decline in deaths related to measles, pertussis, polio, typhoid, yellow fever, diphtheria, and various other diseases (Greenwood, 2014).

Vaccines work by stimulating the immune system in a manner that mimics infection by a specific pathogen (Iwasaki & Omer, 2020; Vetter et al., 2018). In some cases, vaccines provoke a strong T cell response in order to induce cell-mediated immunity. Evidence suggests that this response is especially important in vaccines meant to protect against chronic replicating viruses such as human immunodeficiency virus (HIV-1) and hepatitis C virus (HCV). However, the major focus of prophylactic vaccines has commonly been the induction of a strong antibody response (S. C. Gilbert, 2012; Panagioti et al., 2018).

Immunization stimulates B cells to produce antibodies that target the vaccine as well as the pathogen that the vaccine mimics (Elsner & Shlomchik, 2020). Antibody adherence to a pathogen stimulates a broader immune response through recruitment of effector cells and complement factors (Dunkelberger & Song, 2010; Goldberg & Ackerman, 2020; L. L. Lu et al., 2018). Antibodies can also directly neutralize pathogen infection. Neutralization can be achieved by sterically preventing docking with a host cell receptor or any other function that prevents replication of the pathogen (Klasse, 2014). Vaccine induction of neutralizing antibodies is often well correlated with vaccine protection (Cromer et al., 2022; del Moral-Sánchez & Sliepen, 2019; Khoury et al., 2021; Klasse, 2014).

This adaptive immune response allows for immunological memory to be established. Persistent antibodies and memory cells are produced which can more rapidly act upon re-exposure to the antigen (Palm & Henry, 2019). Adaptive immunity forms the basis of the long-term protection which is the goal of vaccination (Corti & Lanzavecchia, 2013).

1.2 Multimeric Plug-and-Display

Vaccination using a whole pathogen administered in an inactivated or attenuated form has been the standard approach for much of the history of vaccinology. More recently developed vaccines often focus on raising a response to specific antigens that are known to convey protection against the pathogen. These antigens may be delivered in a soluble form, presented on a nanoparticle, or encoded as genetic material (Pollard & Bijker, 2021a). When administered as a gene, the antigen may be encoded as RNA or DNA and delivery mechanisms include lipid nanoparticles and viral vectors (Chaudhary et al., 2021; Shafaati et al., 2022; Travieso et al., 2022).

The viral antigens selected for vaccine development are frequently proteins (Pollard & Bijker, 2021a). However, recombinant proteins vaccines administered on their own are often poorly immunogenic. Efforts to directly enhance the immunogenicity of a recombinant protein can

lead to an increase in reactogenicity where a vaccine induces inflammatory response symptoms (Bachmann & Jennings, 2010; Hervé et al., 2019). An effective strategy to increase the immunogenicity of a recombinant protein antigen is multimeric display on a virus-like particle (VLP). This display method allows for an antigen to be presented in a structured, highly repetitive manner that mimics most viral surfaces and facilitates efficient cross-linking by B cell receptors (BCRs). Additionally, VLP presentation increases the size of the antigen, facilitating efficient uptake by antigen-presenting cells (APCs) (Bachmann & Jennings, 2010) and delivery to draining lymph nodes (Moyer et al., 2016), while remaining small enough to retain access to the lymphatic system (Bachmann & Jennings, 2010).

One method to mediate antigen presentation on a VLP is to directly fuse the antigen to the particle sub-unit (Joyce et al., 2021; Ober Shepherd et al., 2024). However, even small changes to a VLP can cause interference to the pathway of assembly meaning that genetic fusion often requires substantial optimization (K. D. Brune & Howarth, 2018; Mateu, 2011). The cooperative assembly of a VLP exacerbates this challenge. If a relatively small percentage of a monomeric protein is misfolded it can often be removed through the purification process. If that same percentage of VLP subunit is misfolded, it has the potential to join an assembling particle and prevent proper formation. Even a small number of sub-units which undergo misfolding induced by antigen-fusion can thwart proper VLP formation by of a large number of properly folded protein sub-units. The optimal expression system and conditions for a viral antigen and VLP are often poorly matched, requiring sacrifices to be made to the production efficiency for one of the components (K. D. Brune & Howarth, 2018).

To address these issues an alternative approach is to express the antigen and the VLP separately and assemble them together post-purification. This strategy can be achieved using high affinity non-covalent interactions such as those between monovalent streptavidin and biotin (Thrane et al., 2015) or histidine and nickel chelates (Chung et al., 2023; Koho et al., 2015). Non-covalent

interactions also form the basis of the two-component computationally-designed I53-50 nanoparticle. In this system the trimeric I53-50A is genetically fused to an antigen and expressed separately from pentameric I53-50B. It is only when the two components are mixed together that they assembly a VLP (Marcandalli et al., 2019; Walls et al., 2021).

Antigens can be linked covalently to a VLP using chemical crosslinking (Cavelti-Weder et al., 2016). For example, a chemical crosslinker can attach one arm to amino groups in lysines or N-termini of VLP sub-units using the *N*-hydroxy succinimide (NHS). The second arm of the linker can then be attached via maleimide coupling to a surface-exposed cysteine. If a surface-exposed cysteine does not occur naturally in the antigen the residue can be introduced via site directed mutagenesis. This chemical crosslinking leads to non-uniform and somewhat unpredictable display of the antigen on the nanoparticle surface (K. D. Brune & Howarth, 2018). Unnatural amino acids can also be introduced into VLPs to facilitate more predictable coupling to an antigen (K. G. Patel & Swartz, 2011).

Antigens can be covalently linked to particles through a variety of protein interactions including split-inteins (Muik et al., 2017), sortase (S. Tang et al., 2016), and isopeptide bond formation (K. D. Brune et al., 2016). Catcher/Tag technology has been developed to facilitate spontaneous intramolecular isopeptide bond formation (Zakeri et al., 2012) and has been shown to couple antigens to a VLP at an efficiency greater than 99% with a moderate 1.5-fold excess of antigen (K. D. Brune et al., 2016).

This strategy was first applied through the fusion of AP205 coat protein to an N-terminally truncated version of SpyCatcher. The AP205 phage coat protein spontaneously forms a nanoparticle (K. D. Brune et al., 2016; Thrane et al., 2016). SpyCatcher is derived from the fibronectin binding protein (FbaB) of *Streptococcus pyogenes*, which naturally forms at least one internal isopeptide bond. When the second immunoglobulin-like collagen adhesin domain

(CnaB2) of FbaB was split into a peptide (Tag) and protein (Catcher) component, reconstitution of the pair would lead to spontaneous covalent bond formation between the lysine on the Catcher and aspartate on the Tag (Figure 1.1). Fusion of the tag to one protein and catcher to another allows for post-translational covalent linkage of the pair. Through rational design, mutations improved the efficiency of the interaction and produced the first-generation SpyTag/SpyCatcher pair (Zakeri et al., 2012).

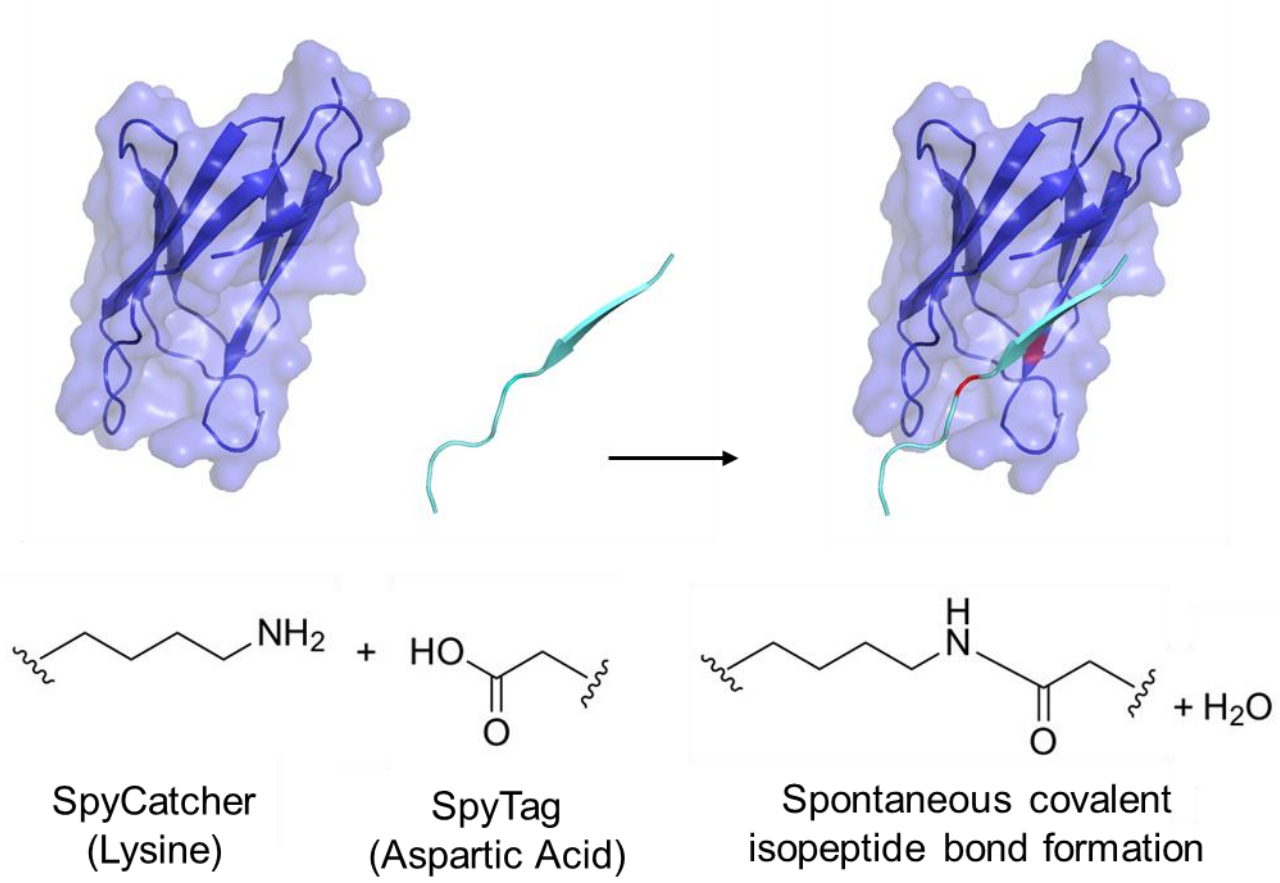

Figure 1.1: Reaction of SpyCatcher and SpyTag. The lysine on SpyCatcher (dark blue) spontaneously forms a covalent isopeptide bond with the aspartic acid on SpyTag (cyan). The reactive lysine and aspartic acid are shown in red in the final SpyTag:SpyCatcher structure. The representation is based on PDB 4MLI.

This approach allows for modular, plug-and-display presentation of different antigens. SpyCatcher functionalized nanoparticles can be produced independently from the SpyTagged antigens that they display. The strategy allows for production of the antigen and nanoparticle scaffold using different expression systems, at different times and locations and could facilitate

stockpiling of nanoparticles separately from the antigens (K. D. Brune & Howarth, 2018). Furthermore, SpyTag is a short (13-residue) peptide that is unlikely to require optimization for genetic fusion to a larger antigen (Zakeri et al., 2012).

An updated nanoparticle based on the Tag/Catcher system has since been introduced, known as SpyCatcher003-mi3, which is a genetic fusion of SpyCatcher003 and mi3 (Rahikainen et al., 2021). SpyCatcher003 is an upgraded version of SpyCatcher, that has undergone further modifications through rational design and phage display evolution to further improve reaction rate. SpyCatcher003 reacts spontaneously and covalently with SpyTag003 at a rate that approaches the diffusion limit. SpyCatcher003 retains back compatibility with SpyTag and, in fact, has an improved reaction rate with SpyTag relative to SpyCatcher (Keeble et al., 2019).

mi3 is a 60-mer porous and hollow protein nanocage that forms the scaffold of the nanoparticle (T. U. J. Bruun et al., 2018). The computationally designed nanoparticle I3-01 served as the template for the development of mi3. Two cysteine to alanine mutations were introduced to improve yield and reduce aggregation (T. U. J. Bruun et al., 2018).. I3-01 itself was based on a trimeric 2-keto-3-deoxy-6-phosphogluconate (KDPG) aldolase with four computationally derived non-polar residues introduced to generate a new interface between the trimers (Hsia et al., 2016). mi3 is a stable scaffold remaining robust to heating (1 hr at 80 °C), freeze-thaw cycling, and lyophilization (T. U. J. Bruun et al., 2018).

SpyCatcher003-mi3 has been used to display a variety of antigens, including monomers like mpox M1 (B. Moss et al., 2023), dimers like *Borrelia burgdorferi* OspC and Newcastle Disease Virus Hemagglutinin-Neuraminidase, trimers like Influenza Hemagglutinin (Rahikainen et al., 2021) and HIV-1 Env (Gristick et al., 2023), and tetramers like Influenza Neuraminidase (Rahikainen et al., 2021) (Figure 1.2). Early in the COVID-19 pandemic, a vaccine candidate was developed that used SpyCatcher003-mi3 to display the receptor-binding domain of SARS-

CoV-2 that elicited strong neutralizing antibodies in pre-clinical animal models (T. K. Tan et al., 2021).

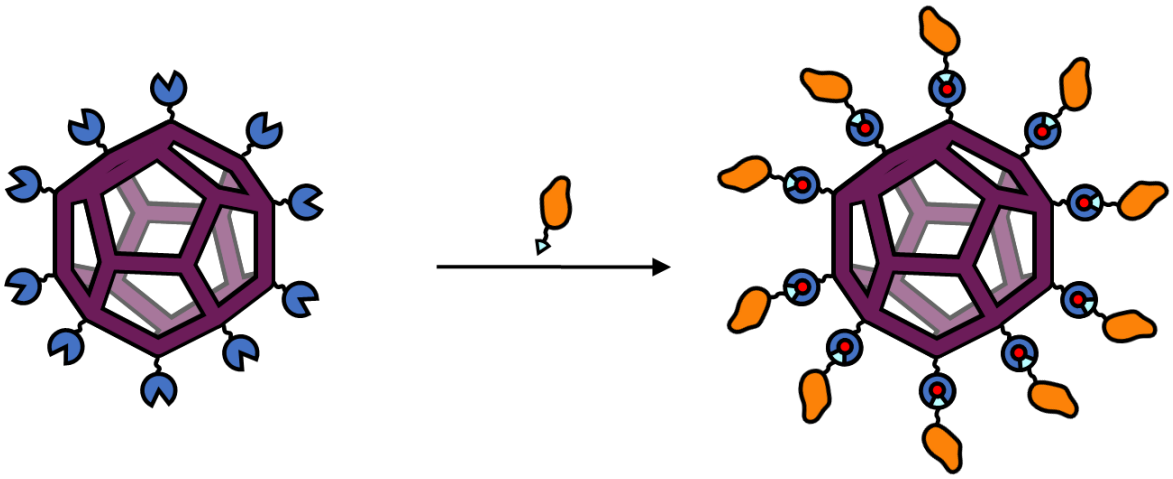

Figure 1.2: Cartoon of SpyCatcher functionalized plug-and-display. A protein (orange) is genetically fused to any generation of SpyTag (cyan) and mixed with the SpyCatcher003-mi3 nanoparticle. This technology facilitates covalent bond (red) formation between SpyTag and SpyCatcher003 (blue) and allows as many as 60 copies of the protein to be displayed per protein nanoparticle formed by mi3 (purple).

1.2.1 Nanoparticle Terminology

Nanoparticles are a broad class of materials which demonstrate diversity in composition, morphology, surface charge, and chemical interaction (I. Khan et al., 2019). The group includes both particles engineered for a specific function and those that occur naturally, including viruses and nanobacteria (Jeevanandam et al., 2018). The defining feature which ties this disparate group together is their size. As defined by the International Union of Pure and Applied Chemistry (IUPAC), a nanoparticle can have any shape as long as its dimensions are in the 1 to 100 nanometre range. This upper limit was chosen as it defines a rough boundary where particles begin to demonstrate novel properties which differentiate them from bulk material (Vert et al., 2012). One of these key properties is their large surface area to volume ratio which can provide more reactive sites than bulk material (Sharma et al., 2018). Nanocages are a

specific form of nanoparticle that have hollow interiors and porous walls (Skrabalak et al., 2008).

Virus-like particle is a somewhat amorphous term and refers to particles that resemble the structure, size, and symmetry of viruses (Mohsen & Bachmann, 2022). These particles can be made from virus structural proteins but also from other naturally occurring proteins or even engineered proteins that have been designed to mimic the structural features of a virus (Heddle et al., 2017). The term can further be applied to enveloped virus-like particles (eVLPs) that mimic enveloped viruses and, typically, display viral glycoproteins on an outer lipid membrane (Tariq et al., 2022). Critically, VLPs lack a genome and replicases, making them non-infectious (Mohsen & Bachmann, 2022).

Considering these definitions, SpyCatcher003-mi3 can be considered a VLP, a nanoparticle, and a nanocage (Rahikainen et al., 2021).

1.3 Induction of Broadly Neutralizing Antibodies

During adaptive immune response development, B cells are selected based on their ability to bind an antigen. There is no evidence that a neutralizing antibody will be selected preferentially relative to an antibody that binds as tightly to the antigen but has no neutralization capacity. Therefore, only a fraction of memory B cells specific to a virus will produce antibodies capable of neutralizing that virus (Bhiman & Lynch, 2017). A subset of non-neutralizing antibodies can still produce an effective response *in vivo* by recruiting other immune system elements. However, other non-neutralizing antibodies will target denatured or internal proteins without therapeutic value. Enhancing the fraction of memory B cells that produce neutralizing antibodies is potential means of increasing the efficiency and effectiveness of vaccines (Bhiman & Lynch, 2017; Corti & Lanzavecchia, 2013).

The protective action of vaccine-induced neutralizing antibodies can be stymied by antigenic drift. Over time, pathogens accumulate mutations which modify their constituent proteins. These modifications can be sufficient to prevent the binding of antibodies that had effectively neutralized an ancestral form of the pathogen (Crespo-Bellido & Duffy, 2023). This effect presents a substantial problem for the production of vaccines that remain effective against rapidly evolving pathogens such as influenza and HIV-1 (Boni, 2008; Carrat & Flahault, 2007; Johnston & Fauci, 2008).

One strategy to address this issue is the elicitation of broadly neutralizing antibodies. These antibodies bind to highly conserved targets on a pathogen and have been identified in convalescent patients (Sok et al., 2013). Some regions of a protein will be more capable of accepting a mutation than others, meaning that there tends to be both conserved and variable regions within a protein. The elicitation of antibodies against conserved regions on a pathogen protein, can allow for a response to a broad range of related pathogens. Broadly neutralizing antibodies are also less susceptible to antigenic variation than traditional antibodies (Bhiman & Lynch, 2017; Corti & Lanzavecchia, 2013).

Broadly neutralizing antibodies have garnered considerable interest for their potential application in vaccines targeting influenza (Corti et al., 2017). Traditional influenza vaccines are widely used and are generally based on whole viruses that have either been inactivated or attenuated (Fiore et al., 2009; Harding & Heaton, 2018). These conventional vaccines primarily elicit an antibody response against the immunodominant head of hemagglutinin. Hemagglutinin is a surface protein essential for invasion of a host cell and is composed of a head and stalk (sometimes called stem) region. The hemagglutinin head is highly variable, meaning that antibodies raised against the heads of one strain are often ineffective against another strain (C.-J. Wei et al., 2020). Because of this restriction, current influenza vaccines induce immunity that wanes in efficacy against newly circulating strains. These vaccines also

rely on constant surveillance of influenza antigenic traits to produce a vaccine that is predicted to be effective. Mismatches can occur when these predictions are incorrect and the vaccine is left ineffective against a prevalent strain (G. Dos Santos et al., 2016; Heikkinen et al., 2014). Furthermore, in the event of newly arisen pandemic influenza strain, a matched vaccine would need to be produced in a process that would take four to six months for preliminary doses (Sparrow et al., 2021). The development of a novel flu vaccine that elicits broadly neutralizing antibodies could solve both of these problems (R. Du et al., 2021; Nachbagauer et al., 2021a; Sok et al., 2013).

The majority of broadly neutralizing antibodies targeting hemagglutinin have been identified as binding the stalk. However, a minor population has also been identified which recognizes the sialic acid binding site on the head. The hemagglutinin stalk is immunoquiescent meaning that after influenza infection antibodies raised against the stalk tend to be substantially less abundant than those raised against the head (Altman et al., 2018). It has been theorized that the lack of anti-stalk antibodies is due to the tight packing of hemagglutinin on a virus reducing stalk accessibility. These anti-stalk antibodies tend to induce less potent neutralization than anti-head antibodies but retain their efficacy across a broad range of influenza strains (Corti & Lanzavecchia, 2013).

Broadly neutralizing antibodies have also drawn interest in the context of HIV-1 (Y. Liu et al., 2020). HIV-1 primarily infects CD4-positive immune cells, causing progressive immune degradation and eventually leading to acquired immunodeficiency syndrome (AIDS) (Deeks et al., 2015). Potent immune evasion strategies and rapid evolution has made HIV-1 a remarkably difficult vaccine target (Letvin, 2005). No viable HIV-1 vaccine has been introduced clinically (Shapiro, 2019). Sustained administration of combination antiretroviral therapy (cART) supresses viral replication, arrests the onset of AIDS, and can prevent transmission of the disease. The introduction of cART has therefore had a monumental impact

on HIV-1 treatment. However, the viral reservoir of HIV-1 is maintained and will reassert itself if the therapy is interrupted or discontinued (Y. Liu et al., 2020).

Broadly neutralizing antibodies against HIV-1 have been identified using a variety of techniques, including high throughput neutralization assays and single-cell antibody cloning. These antibodies target a variety of different conserved regions of the HIV-1 envelope (Y. Liu et al., 2020). Direct administration of broadly neutralizing antibodies against HIV-1 have shown promising preclinical results. Several questions remain unanswered, including whether the antibodies are capable of preventing HIV-1 transmission and progression (Bar-On et al., 2018; Y. Liu et al., 2020; Mahomed et al., 2021).

The existence of broadly neutralizing antibodies raises the possibility that a vaccine can be developed to induce these antibodies (Haynes et al., 2023). Such a vaccine could be a potent therapeutic or prophylactic intervention. The HIV-1 broadly neutralizing antibodies that have been identified to date have undergone extensive affinity maturation in geminal centres. These antibodies have a number of unusual traits including high levels of somatic hypermutation and precursors with especially short or long antigen-binding loops. An HIV-1 vaccine based on this strategy would therefore need to reliably induce these unconventional antibodies (Landais & Moore, 2018; Y. Liu et al., 2020; Sok et al., 2013).

The examples of influenza and HIV-1 highlight the potential of vaccine-induced broadly neutralizing antibodies. This innovative approach could allow for production of vaccines that are less susceptible to evolutionary changes and target a larger range of pathogens. The strategy could additionally allow vaccines to be developed against pathogens that have eluded these efforts to date. Effective elicitation of broadly neutralizing through immunization requires strategies to tailor the immune response towards specific antigenic regions (Corti & Lanzavecchia, 2013).

1.4 Strategies to Achieve Immunofocusing

There are a variety of strategies that have been developed to produce vaccines that elicit antibodies binding specific regions of an antigen. This specificity can produce antibodies that target areas associated with viral neutralization or evolutionary conservation. When these vaccines raise a response to regions of antigen that are both conserved and neutralizing, they can effectively tailor the immune response to be dominated by broadly neutralizing antibodies (Bedi et al., 2023; Cankat et al., 2024; D. Gupta & Mohan, 2023a). This section will explore some of the strategies that have been implemented by a variety of research groups to achieve this immunofocusing.

1.4.1 Antigen Truncation

Pathogenic proteins expressed recombinantly can be administered as subunit vaccines. In contrast to deriving the proteins directly from a pathogen source, recombinant expression removes pathogenicity risk, allows for vaccines that have a defined composition, and facilitates engineering of the antigen (Hansson et al., 2000). One common modification to a recombinant protein antigen is truncation, where a section of the protein is removed. Truncation can be used to allow for prokaryotic expression (J.-F. Han et al., 2017), facilitate purification without detergents (Flach et al., 2011), attenuate features in the antigen that can cause host damage (Sandini et al., 2011), remove sections that may induce host-reactive antibodies (Humbert & Christodoulides, 2018), and stabilize the antigen (B. S. Graham et al., 2019; Pallesen et al., 2017).

Antigen truncation has also been applied as a general strategy to focus the immune response raised by a subunit vaccine. A common approach is to remove an immunodominant, but evolutionarily variable, portion of the protein. This modification can allow for a more robust immune response to be raised against a conserved region that would otherwise be

immunoquiescent (Behrouzi et al., 2017; L. Du et al., 2013; Hallengärd et al., 2013; Peak et al., 2013; To et al., 2010).

An illustrative example of this approach can be found in the truncation of hemagglutinin. Multiple studies have explored removal of the immunodominant hemagglutinin head while retaining the proper folding and overall structure of the stalk. The head is generally replaced with a flexible linker that has been optimized to facilitate protein expression (Mallajosyula et al., 2014; van der Lubbe et al., 2018; Yassine et al., 2015). Different 'headless' hemagglutinin antigens have been expressed as soluble trimers (van der Lubbe et al., 2018) and on ferritin nanoparticles (Yassine et al., 2015). In animal immunizations these strategies have been able to elicit neutralizing antibodies with enhanced breadth across influenza evolutionary diversity (Impagliazzo et al., 2015; Mallajosyula et al., 2014; van der Lubbe et al., 2018; Yassine et al., 2015). Phase I human clinical trials with a stabilized headless hemagglutinin presented on ferritin nanoparticles showed that the vaccine was safe and well tolerated while eliciting durable, cross-reactive neutralizing antibodies (Widge et al., 2023).

1.4.2 Epitope Mimicry

In the epitope mimicry strategy, immunofocusing narrows from a conserved region to a specific epitope (Palma, 2023). Peptides that bind tightly to antibodies can be identified and produced independently of the complete antigenic protein. These peptides can be identified through a variety of display methods and are most frequently selected through phage display. This process has been called reverse vaccinology and the peptides are often called mimotopes, a name derived from the fact that they mimic epitopes. The mimotope term has also been applied more broadly to peptides mimicking any binding site (Geysen et al., 1986; J. Huang et al., 2012; Palma, 2023). A collection of known mimotopes has been collected in the Biopanning Data Bank (B. He et al., 2016) previously known as MimoDB 2.0 database (J. Huang et al., 2012).

On their own mimotopes tend to be too small and unstructured to induce an immune response and can even induce tolerance. This limitation means that a carrier strategy often needs to be employed (Knittelfelder et al., 2009; Leung et al., 2019). Examples of such carrier systems includes fusion to a larger protein that also induces an immune response (Latzka et al., 2011), producing the peptide as several fused repeats (Brämswig et al., 2007), or presentation of the peptide on a VLP (Cuevas-Juárez et al., 2023; O'Rourke et al., 2014).

Some general advantages of using mimotopes are their ability to induce highly specific, often long-lasting, humoral responses as well as their ease of identification, production, and storage. Some disadvantages include the aforementioned lack of immunogenicity, their lack of induction of a T cell mediated response, and the lower affinity of mimotope-induced antibodies compared with those raised against the wild-type antigen (Knittelfelder et al., 2009). It is also important to note that mimotopes are linear epitopes, while many broadly neutralizing antibodies have more complex interactions with their targets that often rely on three-dimensional conformation (K. Y. A. Huang et al., 2023; Y. Liu et al., 2020).

Epitope mimicry has been applied to develop vaccine candidates against a variety of pathogens including respiratory syncytial virus (Chargelegue et al., 1997; Correia et al., 2014; Sesterhenn et al., 2019), *Mycobacterium tuberculosis* (Shah et al., 2018; Shin et al., 2017), HIV-1 (Bianchi et al., 2010; Moseri et al., 2017), and *Measles morbillivirus* (Olszewska et al., 2000). The strategy has also drawn interest in the treatment of cancer where the ability to raise highly specific antibodies is an attractive feature for targeting specific mutant proteins (Riemer & Jensen-Jarolim, 2007; Wen et al., 2016). In an illustrative example of this approach, phage display was used to identify peptides that structurally mimicked the epitope of cetuximab. Cetuximab is a chimeric monoclonal antibody which is known to inhibit epidermal growth factor receptor (EGFR) and is used to treat colon cancer. When mice were immunized with the

identified peptide, the induced antibodies were found to recognize EGFR and elicit cytotoxic effects (Riemer et al., 2005).

1.4.3 Glycosylation

Glycosylation is a common post-translational protein modification, where the addition of a sugar or sugars produces a glycoprotein. In O-linked glycosylation the sugar is attached to a side chain hydroxyl of a serine or threonine and in N-linked glycosylation a sugar is attached to the nitrogen atom in the side chain of asparagine. The initial sugar attachment occurs early in protein synthesis. This attachment is followed by a complex maturation process that includes the trimming and remodelling of the oligosaccharide as the glycoprotein travels through the Golgi and endoplasmic reticulum. This process can produce different carbohydrate patterns on two proteins with identical amino acid sequences meaning that glycosylation produces variance within the population of a protein (B. Lin et al., 2020; Nardy et al., 2016; Vigerust & Shepherd, 2007).

A key feature of viruses is their ability to commandeer host biosynthetic pathways. For viruses that replicate in mammalian cells this process commonly includes the use of glycosylation machinery to produce viral glycoproteins. Through the incorporation of the same sugars that are present on host proteins, a virus is better able to shield itself from host immune recognition. This camouflage is made possible by the potent negative selection undergone by B and T cells that recognize sugars used in host glycosylation. Consequently, proteins covered in these host sugars are rarely immunogenic. Several viruses, such as HIV-1, HCV, and Lassa virus, produce a robust glycan shield that greatly hinders immune recognition (Hariharan & Kane, 2020; Lavie et al., 2018).

This natural immune evasion mechanism has been mimicked as an immunofocusing strategy. In this approach glycosylation is increased on immunodominant regions that do not provoke an effective immune response and the response is, consequently, focused to the desired

antigenic regions (Hariharan & Kane, 2020). This strategy has been applied to develop vaccine candidates for several viruses including HIV-1 (Andrabi et al., 2017), influenza (Eggink et al., 2014; S.-C. Lin et al., 2014), Zika virus (Tai et al., 2019), SARS-CoV2 (Carnell et al., 2023; Guo et al., 2021), and RSV (Frey et al., 2021).

An illustrative example of glycosylation for immunofocusing is demonstrated in the development of a vaccine candidate targeting the receptor-binding domain of the SARS-CoV2 spike protein. This domain contains a number of neutralizing epitopes. Recombinant expression of RBD exposes epitopes that would normally be occluded by the rest of the Spike protein. Mutations in the RBD sequence were used to introduce four new glycans in order to block recognition of these cryptic epitopes. Mice immunization experiments were performed with the newly glycosylated and wild-type RBDs. RBDs with these engineered glycosylation sites induced an enhanced neutralizing antisera response when administer as either a DNA or protein subunit vaccine (Guo et al., 2021).

Glycosylation has also been used to develop a broad influenza vaccine candidate. Using site-directed mutagenesis seven new N-linked glycosylation sites were introduced into the hemagglutinin head of an influenza strain known to have minimal native glycosylation. The large number of engineered sites led this approach to be termed hyperglycosylation. The glycosylation sites were chosen strategically to block known antigenic sites. Immunization with this hyperglycosylated hemagglutinin provided weaker protection against matched influenza viruses but substantially enhanced immune protection against mismatched influenza viruses. The hyperglycosylated hemagglutinin provided protection against challenge with a lethal dose of an influenza virus that contained an exotic head but the same stalk as the vaccine (Eggink et al., 2014).

The inverse of this strategy has also been applied, with immunofocusing being achieved through the removal of existing glycans. Since many viruses are already protected by a glycan shield, the removal of a few native glycans can produce a targeted immunogenic response against the newly revealed region. This approach has been used to elicit an antibody response to the envelope trimer of HIV-1. The CD4-receptor binding site present in this trimer is a highly conserved epitope which is known to produce a broad antibody response. However, the site is blocked by several glycans which inhibit the binding of some antibodies. It has been shown that glycan removal around the CD4-receptor binding site exponentially increases the site-specific immunogenic response. Animal immunization experiments with glycan-hole containing envelope trimers induced high titres of neutralizing antibodies that were not present after vaccination with the wild-type protein. However, antibodies raised against the glycan hole containing envelope timers were not sufficient to neutralize the wild-type virus (T. Zhou et al., 2017).

1.4.4 PEGylation and Related Strategies

The attachment of polyethylene glycol (PEG) to a protein or peptide is a common strategy to reduce immunogenicity. PEG is a general term for polymers of ethylene glycol and PEG molecules demonstrate diversity in chain length and branching. Differences in these properties can lead to varying physical characteristics among different PEGs, although all tend to be extremely soluble in water. The attachment of PEG to another molecule is known as PEGylation and PEGylated proteins have demonstrated reduced antibody binding (Gulati et al., 2018; Yadav & Dewangan, 2021).

PEGylation of protein-based therapeutics has been widely applied in order to reduce clearance and increase circulation time (J. M. Harris & Chess, 2003; Y. Xu et al., 2017). There are several techniques that allow for the attachment of PEG to a protein substrate, most of which involved a functionalized PEG variant. For example, a PEG can be modified to incorporate maleimide.

This maleimide will form a covalent bond to a thiol, allowing for the PEGylation of a protein at any free cysteine residues. The choice of functional group is highly dependent on the nature of the protein and the desired coverage (M. J. Roberts et al., 2002).

An important consideration in the use of PEG is the rise of anti-PEG Immunoglobulin M (IgM) and Immunoglobulin G (IgG) antibodies. In 1984, a sampling of healthy blood donors found that 0.2% of the population had anti-PEG antibodies (Richter & Åkerblom, 1984). In 2009, a similar sampling of a healthy population found that over 25% of individuals had anti-PEG antibodies (Armstrong, 2009). This increase may be due to improved limits of analytical detection or greater population exposure to PEG through its presence in cosmetics, pharmaceuticals, and processed foods. Regardless of whether this is a new trend, the prevalence of anti-PEG antibodies can lead to accelerated clearance of PEGylated substrates as well as the instigation of severe reactogenic symptoms (Garay et al., 2012; Kozma et al., 2020).

An alternative to PEGylation is the incorporation of a polypeptide designed to mimic the features of PEG. For example, XTEN is composed of proline, alanine, serine, threonine, glycine, and glutamine in a non-repetitive manner. The chemical or genetic incorporation of XTEN, known as XTENylation, can allow for the benefits of PEGylation without the need for chemical coupling or lack of biodegradability (Haeckel et al., 2016). PAS is polypeptide composed of proline, alanine and serine which is another PEG alternative that can be chemically or genetically incorporated into a protein with a similar effect to XTEN (Schlapschy et al., 2013). Unlike PEG, both XTEN and PAS have a defined molecular mass which can make their interactions easier to predict. They are also less likely than PEG to have a pre-existing antibody response raised against them (Haeckel et al., 2016; Schlapschy et al., 2013; Zinsli et al., 2021).

An illustrative application of PEGylation for immunofocusing was implemented to elicit broadly neutralizing antibodies against the gp41 subunit of the HIV-1 envelope glycoprotein. Immunizations were performed with the epitope of a known neutralizing antibody. In order to maintain the epitope structure, the antigen was produced as a fusion to a protein scaffold. However, immunization experiments with this chimeric protein elicited a high titre of antibodies against the scaffold. A coat of small molecular weight PEG molecules was added at strategic locations on the scaffold in order to reduce the humoral response raised against it. This reduced the anti-scaffold response while retaining a robust antibody binding to the neutralizing epitope (Bianchi et al., 2009).

A more complex PEG-based immunofocusing approach is nanopatterning. In nanopatterning, the non-canonical amino acid p-azido-L-phenylalanine (F*) is incorporated near the region of the antigen that requires shielding. A PEG derivative incorporating dibenzocyclooctyne (DBCO) is then used to PEGylate the antigen. The shielded region of the antigen can be tuned through the manipulation of the F* location and the modification of the size of PEG added, (Arsiwala et al., 2019).

Nanopatterning has been applied to the malaria vaccine candidate $MSP1_{19}$ which is a terminal fragment of the Merozoite surface protein (MSP1) (Arsiwala et al., 2019). MSP1 is an abundant surface protein on the blood-stage malaria parasite that interact with human blood cell surface proteins and are essential for parasite development. Neutralizing antibodies against MSP1 can prevent invasion of red blood cells by the parasite. However, non-neutralizing antibodies can outcompete neutralizing antibodies prevent the activity of neutralizing antibodies (P. N. Patel et al., 2022). Nanopatterning was applied to occlude the binding epitope of non-neutralizing antibodies that were known to block neutralizing antibodies (Arsiwala et al., 2019).

1.4.5 Antibody Blocking

Monoclonal antibodies have been used to block specific parts of an antigen as an immunofocusing strategy. Since antibodies reliably target a specific epitope, this strategy can allow for a precise portion of the antigen to be blocked from immune recognition (Hioe et al., 2009; Tsouchnikas et al., 2015; Williams et al., 2006). As an added benefit, this antigen-antibody complex can help to induce an immune response against the antigen through Fc-mediated adjuvant activity (Rawool et al., 2008; D.-Z. Xu et al., 2008).

As an example, antibody blocking has been explored as an immunofocusing strategy in the context of HIV-1. These experiments used a monoclonal antibody called 654-D that targets the CD4 binding site of gp120. An immune complex of 654-D and gp120 was used to immunize mice. The presence of 654-D enhanced the immune response raised against regions of gp120 outside the binding site, including the V3 region which contains broadly neutralizing epitopes. Immunization with 654-D:gp120 immune complexes led to a more cross-reactive response than gp120 on its own. However, this immune response was still not effective at neutralizing the majority of the tested HIV-1 isolates (Hioe et al., 2009).

Another immunofocusing strategy incorporates both antibody blocking and PEGylation. This approach has three steps: protect, modify, and deprotect which gives it the name PMD. First, a monoclonal antibody is bound to the antigen at the region that an immune response is desired. Second, the antigen is modified to shield unprotected regions. For example, a PEG derivative that incorporates N-hydroxysuccinimide (NHS) can PEGylate accessible amines on the protein. Amines occluded by antibody binding will not be accessible for PEGylation. Finally, the monoclonal antibody is removed from the antigen which can be achieved using low pH or potassium thiocyanate. At the end of this procedure the antigen is coated in PEG but a hole is present where the monoclonal antibody had previously been bound (Bruun et al., 2024; Weidenbacher & Kim, 2019).

This technique has been validated using hemagglutinin as an antigen. Hemagglutinin was first protected using a known broadly neutralizing antibody raised against the stalk. There was insufficient natural lysine content in the hemagglutinin head for efficient NHS PEGylation and so deep mutational scanning data was used to identify nine locations in the hemagglutinin head where existing residues could be replaced with lysines. To facilitate elution at a neutral pH, the broadly neutralizing antibody was mutated to weaken its interaction with the epitope and allow for removal using potassium thiocyanate. Bio-layer interferometry was used to assess the interaction with known antibodies against hemagglutinin. These results showed that PMD decreased, but did not completely prevent, the binding of anti-head antibodies but did not affect binding of anti-stalk antibodies. The retained binding to the head was attributed to holes in the PEGylation shield. Animal immunization with the PMD hemagglutinin elicited antisera that produced a slightly weaker response against an influenza virus matched to the vaccine but a stronger response to mismatched viruses. This result indicates that PMD produced a broader immune response that has an enhanced potential to protect across strains (Weidenbacher & Kim, 2019).

While this section considers antibody-antigen complexes in the context of immunofocusing, the strategy has been applied vaccine candidates for other purposes including the elicitation of a desired structural conformation (Tsouchnikas et al., 2015) and reduction in residual virulence for inactivated viral vaccine (Iván et al., 2005).

1.4.6 Albumin Shielding

Albumin shielding has been used to reduce immune recognition of nanoparticles, in a strategy that could be implemented for more traditional immunofocusing. Human serum albumin (HuSA) has a variety of roles including maintaining oncotic pressure, acting as an antioxidant, and transporting biomolecules such as fatty acids, steroids, and L-tryptophan as well as ions such as copper, zinc, and calcium. HuSA is also the most abundant human blood protein with

concentrations of 35–50 mg/mL in human serum (Merlot et al., 2014). Several bacterial species use membrane proteins to bind HuSA to their surface in order to protect themselves from immune recognition (Egesten et al., 2011b). The application of HuSA shielding in protein engineering is therefore an application of bio-inspired design (A. S. Pitek et al., 2016).

HuSA shielding has been performed to reduce immune recognition of a nanoparticle derived from the tobacco mosaic virus (TMV). Chemical crosslinking was used to link HuSA to the individual nanoparticle monomers in order to decorate the particle with albumin. Particles that were shielded with HuSA demonstrated reduced macrophage recognition relative to naked particles. This technique has successfully reduced immune recognition of a potential vaccine scaffold (A. S. Pitek et al., 2016).

It is apparent that a similar strategy could be applied attach HuSA to an antigen through chemical coupling or high affinity albumin binding (Dennis et al., 2002; Jonsson et al., 2008). In a similar manner to the TMV-derived nanoparticle, certain antigenic regions could be shielded with albumin to allow for immunofocusing.

1.4.7 Nanoparticle occlusion

As previously outlined, multivalent display of antigens on nanoparticles can lead to substantial enhancements in immune recognition (K. D. Brune & Howarth, 2018). Multivalent display can be used to enhance the immune response raised to antigens that have undergone immunofocusing by other methods (Arsiwala et al., 2019). Antigenic presentation on a nanoparticle can be used as an immunofocusing strategy in its own right. Specific epitopes can be occluded from immune recognition by modifying the position and orientation of an antigen as well as the geometry of the nanoparticle (Ding et al., 2017; Ueda et al., 2020).

As an example of this approach, a soluble and stabilized version of the HIV-1 envelope protein was genetically fused to different computationally-designed nanoparticles. One of these

nanoparticles had a tetrahedral orientation (Ueda et al., 2020) and one had an icosahedral orientation (Brouwer et al., 2019). Six different monoclonal antibodies that bound different known epitopes were assessed for binding to the HIV-1 envelope protein in either presentation. For both nanoparticles, antigen accessibility by monoclonals followed a similar pattern with binding decreasing as epitopes moved from the apex to the base of the immobilized antigen. There was more than a ten-fold decline in binding between the apex and base epitope. Critically, the tetrahedral presentation showed a less rapid decline in antibody interaction as the epitope moved closer to the base, in agreement with the predicted structure of the particles. This result underlines the potential for nanoparticle occlusion to modify the relative response to different antigenic region (Ueda et al., 2020).

1.4.8 Sequential Immunization

Sequential immunization with distinct but related antigens can enhance the immune response to elements shared by the antigens. The immune response is initially raised to the first antigen that is administered. Sequential immunizations will favour activation and expansion of B cells capable of binding the new antigens that are administered. This process favours the selection of B cells capable of binding regions shared between the various administered antigens (Escolano et al., 2016, 2019; Nachbagauer et al., 2021; S. Wang, 2017).

In an example of this approach, sequential immunization has been applied in clinical trials for a broad influenza vaccine. In this trial, two immunizations were performed using different chimeric hemagglutinin proteins. The stalk of these chimeric proteins was derived from a hemagglutinin 1 (H1) known to circulate in humans, while the heads came from hemagglutinin produced in avian influenza strains (H8 and H5). Underlying this strategy is the idea that most individuals have an existing repertoire of anti-hemagglutinin antibodies predominantly focused on the head. Successive immunizations that alter the immunodominant head but maintain the same stalk will select for B-cells producing anti-stalk antibodies, enhancing the anti-stalk titre.

The chimeric hemagglutinins used in these immunizations were administered as part of a full influenza virus that and the most robust immune response was elicited using inactivated influenza viruses adjuvanted with AS03 (Nachbagauer et al., 2021).

Individuals vaccinated with this regimen developed high anti-stalk antibody titres that stabilized after six months and were maintained at similar levels up to 18 months after the initial vaccination. Immune sera were tested using a new chimaera with an H1 stalk and H6 head that came from an avian influenza strain that was not included in the trial. Using this chimeric H1/H6 hemagglutinin, patient antisera demonstrated ability to induce antibody-dependent cellular cytotoxicity, antibody-dependent cellular phagocytosis, hemagglutinin inhibition, and viral neutralization. Patient antisera was passively transferred to mice and provided protection against a cH6/1N5 virus (chimeric H1/H6 hemagglutinin and Neuraminidase 5). Patient antisera bound to other Group 1 hemagglutinins including H2, H9 and H18, demonstrating breadth within Group 1 influenza (Nachbagauer et al., 2021).

Sequential immunization has been widely explored as strategy for eliciting broadly neutralizing antibodies against HIV-1 by manipulating the affinity maturation process of antibodies. This can be especially effective for HIV-1 where broadly neutralizing antibodies tend to have several unusual features and to have undergone high levels of somatic hypermutation. The strategy has been labelled “germline targeting” due to the reliance on evolution of a highly mutated antibody from a germline precursor it (Escolano et al., 2019, 2021; Haynes et al., 2019).

1.4.9 Antigen Mixtures and Mosaic Nanoparticles

Under a similar principle to sequential immunization, immunofocusing can also be achieved by simultaneously immunizing with multiple related antigens. Through the inclusion of multiple evolutionarily-related antigens this strategy provides a competitive advantage for the expansion of B cells that can bind conserved regions. Antigens can be administered in a soluble mixture (referred to as a cocktail or admix) or as nanoparticles displaying several different

antigens (referred to as a mosaic) (Kanekiyo et al., 2019). These approaches have been applied to develop broadly neutralizing vaccine candidates against influenza (Boyoglu-Barnum et al., 2021; A. A. Cohen et al., 2021) and coronaviruses (Cohen et al., 2021; Walls et al., 2021).

A key example of this approach was applied to develop broad influenza protection. This study used the receptor binding domain (RBD) of H1N1 hemagglutinin. In this context, RBD is a portion of hemagglutinin which includes the globular head but excludes most the stalk. The goal was to elicit neutralizing antibodies against the receptor binding site (RBS) present on the hemagglutinin head. RBS is the location of biding between hemagglutinin and sialic acid and is highly conserved within subtypes. Multimeric presentation of the hemagglutinin RBD was achieved through genetic fusion with ferritin. A mosaic nanoparticle co-displaying antigens from several different viruses can be produced through co-transfection with several plasmids expressing different ferritin-fused influenza RBDs (Kanekiyo et al., 2019).

The immunogenic effect of a nanoparticle with hemagglutinins from between one and eight strains of H1N1 were tested through a series of mouse immunization experiments. These experiments demonstrated that the mosaic antigen was capable of inducing responses comparable to a homotypic nanoparticle, which displayed antigen from a single virus. Additionally, the mosaic nanoparticles induced an increased breadth of immune response. Immunization with mosaic nanoparticles was compared with an admix of homotypic nanoparticles. Mosaic display elicited a broader response than that induced by an admix containing the same set of RBDs. A monoclonal antibody was isolated from sera induced by mosaic immunization. This monoclonal (441D6) neutralized all but one (A/Iowa/1943) member of a H1N1 pseudovirus panel, including representatives spanning from 1918 to 2009 (Kanekiyo et al., 2019). A similar strategy has also been applied to develop broad anti-coronavirus vaccines and is outlined in Section 1.7 (Cohen, et al., 2021; Walls et al., 2021).

1.5 Coronaviruses

The term coronavirus typically refers to members of the subfamily *Orthocoronavirinae*, which is part of the family *Coronaviridae* and order *Nidovirales* (Fan et al., 2019). These viruses are enveloped and encode their genome in positive-sense single-stranded RNA (V'kovski et al., 2021). Coronavirus genomes are notably large, in the range 26 – 32 kb (Woo et al., 2010). Coronavirus virions tend to have a diameter between 80-120 nm (Masters, 2006). Electron microscope images of these virions show spike structures that created a fringe around the particle. These images reminded some early observers of the solar corona and led to the name coronavirus (Masters, 2006).

Orthocoronavirinae is further divided into four genera: alphacoronavirus, betacoronavirus, gammacoronavirus, and deltacoronavirus. Alpha- and betacoronaviruses predominantly infect mammalian hosts, while gamma- and deltacoronaviruses primarily infect avian species (Islam et al., 2021; Mei et al., 2022; Mihindukulasuriya et al., 2008; V'kovski et al., 2021; Woo et al., 2012).

At the time of writing, there are seven widely recognized human-infecting coronaviruses that have been shown to undergo human-to-human transmission (Kesheh et al., 2022). Four of these viruses are among several of the causative agents of the common cold (Eccles, 2023). These pathogens are the alphacoronaviruses NL63 and 229E and the betacoronaviruses HKU1 and OC43 (Kesheh et al., 2022). The other three human coronaviruses have caused deadly outbreaks. SARS-CoV (SARS1) first emerged in 2002 and rapidly caused an outbreak of severe acute respiratory syndrome which led to more than 8000 people infected and 774 recorded fatalities. No cases of SARS1 have been reported since 2004 (Ruan & Zeng, 2008; Vijayanand et al., 2004). MERS-CoV (MERS) was first identified in 2012 and causes Middle East respiratory syndrome. Since that initial identification, cases have been reported in more than 25 countries and the virus has caused at least 700 deaths. MERS demonstrates high fatality

rates but relatively poor human-to-human transmission (Ramadan & Shaib, 2019). SARS-CoV-2 (SARS2) was identified in 2019 and is the causative agent of the COVID-19 pandemic (Lamers & Haagmans, 2022).

These three deadly human coronaviruses are all betacoronaviruses. The betacoronavirus genus includes the sub-genera hibecovirus, nobecovirus, embecovirus (HKU1 and OC43), sarbecovirus (SARS1 and SARS2), and merbecovirus (MERS) (Kesheh et al., 2022).

1.5.1 Coronavirus Zoonotic Transmission

Coronaviruses are known to infect a diverse range of animal hosts. Gamma- and deltacoronaviruses have been identified in more than 100 different species of wild bird, across all continents (Wille & Holmes, 2020). In addition to birds, deltacoronavirus have been found in pigs (Woo et al., 2012) and gammacoronaviruses have been found in cetaceans (Mihindukulasuriya et al., 2008; L. Wang et al., 2020). Alpha- and betacoronaviruses been shown to infect members of several mammalian orders including carnivores, lagomorphs, primates, ungulates, and rodents (Ghai et al., 2021).

The diversity of coronaviruses in bats (the Order *Chiroptera*), far exceed those identified in other mammalian hosts. Members of 11 of the 18 extant bat families have been found to be infected by coronaviruses, including species on the six continents inhabited by bats (Drexler et al., 2014). There are a variety of factors that contribute to bats as coronavirus reservoirs. Bats typically demonstrate gregarious behaviour and often live in dense aggregations. Bats also have relatively long lifespans considering their body size, which allows for persistent chronic infection. Sympatry, where a number of related species share geographic distribution, is common in bats and can facilitating interspecific disease transmission. This trait is further enhanced by bats ability to fly which can allows for movement and pathogen dispersal for certain bat species (Luis et al., 2013). Flight also requires high metabolic activity leading to increased body temperature. The “flight-as-fever” hypothesis posits that this increased body

temperature mimics a fever immune response, helping to curtail viral symptoms in bats and enhance their effectiveness as viral reservoirs (O'Shea et al., 2014). However, this hypothesis remains disputed (Letko, Seifert, et al., 2020; Levesque et al., 2021).

Coronaviruses have demonstrated zoonotic transmission from animal hosts to humans (Ghai et al., 2021). A well-studied transmission event is the host switching of SARS1. An analysis was performed of a live animal market in Shenzhen, China as part of the SARS1 response. Evidence of SARS1 infection was found in humans associated with the market as well as Himalayan palm civets (*Paguma larvata*), raccoon dog (*Nyctereutes procyonoides*), and a Chinese ferret badger (*Melogale moschata*)(Guan et al., 2003). In strong suggestion of civets as a direct source of human infection, there is a close sequence match for viral isolates from both humans and civets (H.-D. Song et al., 2005). There remains a possibility that another animal was also involved in human transmission (L.-F. Wang et al., 2006). Civet viral isolates display very little genetic diversity and few instances of infection for wild or farmed palm civets have been detected, suggesting the species is unlikely to be the natural viral reservoir (Shi & Hu, 2008).

A diversity of species closely related to SARS1 have been identified in Asian bat species (W. Li et al., 2005). This has led to the common view that a bat species is the natural reservoir of SARS1 and palm civets served as an intermediate host that facilitated human infection (G. Tang et al., 2022). When compared to civet isolates, human SARS1 isolates show major genetic variation in the spike protein, that facilitates binding to the host-cell receptor. The evolution of SARS1 spike protein appears to be essential to improve the efficiency of human-to-human transmission after the crossover event has occurred (H.-D. Song et al., 2005).

Livestock have also served as a precursor host for human coronaviruses. For example, the human alphavirus OC43 shows genomic similarity to a bovine coronavirus and based on molecular clock and genomic sequence analysis there may have bovine-to-human interspecies

transmission in the late 19th century (Ghai et al., 2021; Vijgen et al., 2005). It has been hypothesized that this crossover event may have caused the "Russian Flu" pandemic of 1889-90 (Brüssow & Brüssow, 2021; Valleron et al., 2010; Vijgen et al., 2005). There is evidence that the human betacoronavirus 229E is associated with dromedary camels (Corman et al., 2016). This link is more firmly established for MERS, where camels are the primary MERS host and repeated, sporadic camel-to-human transmission events are believed to have occurred (Killerby et al., 2020). There are a large diversity of MERS-like viruses circulating in bats (El Sayes et al., 2024) and there is evidence that an ancestral form of the virus may have been transmitted from bats to camels (Corman, Ithete, et al., 2014).

The origin of SARS2 has not yet been determined conclusively (Bloom, 2023; Gostin & Gronvall, 2023; Pekar et al., 2022a; Pipes et al., 2021). There are several coronaviruses closely related to SARS2 circulating in bat populations (Temmam et al., 2022; P. Zhou et al., 2020). There is evidence to suggests that an undetermined mammalian species may have been an intermediate host between bats and humans (Pekar et al., 2022a; Worobey et al., 2022). A zoonotic transmission event similar SARS1 is plausible (Pekar et al., 2022a; Worobey et al., 2022) but has been definitively established (Bloom et al., 2021; Gostin & Gronvall, 2023).

There are several coronaviruses circulating in bats which can bind human cell receptors and have been identified as risks for future zoonotic transmission (Menachery et al., 2017; Mohapatra et al., 2023a; Xiong et al., 2022). In Haiti, a deltacoronavirus (Hu-PDCoV) was recently identified as having undergone two distinct zoonotic spillover events from pig to human hosts (Lednicky et al., 2021). In Malaysia, a canine alphacoronavirus (CCoV-HuPn-2018) was recently identified in patient respiratory swabs (Tortorici et al., 2022; Vlasova et al., 2022). To date, neither of these coronaviruses have been identified as having human-to-human transmission capability (Lednicky et al., 2021; Vlasova et al., 2022). The identification of these novel human infections by coronaviruses suggest that zoonotic transmission may occur more

frequently than previously believed (Sánchez et al., 2022; Tortorici et al., 2022). Each zoonotic spillover event opens the potential for the infecting pathogen to better adapt to its new host becoming more infectious or more transmissible (Ellwanger & Chies, 2021; Recht et al., 2020; C. C. S. Tan et al., 2024).

1.5.2 SARS-CoV-2

As with other coronaviruses, SARS2 is enveloped and encodes its genome with single-stranded positive sense RNA (R. Lu et al., 2020) (Figure 1.3). The genomic size is slightly less than 30 kb and there is diversity in genome length within the viral population (Khailany et al., 2020). The majority of the SARS2 genome constitute two open reading frames: ORF1a and ORF1b (V'kovski et al., 2021). ORF1a begins near the 5' end of genome and is followed directly by ORF1b. There is a partial overlap between ORF1a and ORF1b, with ORF1b being in a different reading frame relative to ORF1a. Within the overlapping region of the two open reading frames there is an RNA element that can cause ribosomes to slip by one base, introducing a frameshift that allows continued translation (Finkel et al., 2021; Kelly et al., 2021). ORF1a encodes the polyprotein pp1a. When the programmed frameshift occurs, the polyprotein pp1ab that is composed of both open reading frame is translated instead (Jahirul Islam et al., 2023; V'kovski et al., 2021). These polyproteins are proteolytically processed by viral proteases encoded within ORF1a in order to produce a total of 16 non-structural proteins (nsp1-16) that play critical roles in viral replication and transcription (Low et al., 2022; Yan et al., 2020).

Downstream of ORF1a and ORF1b, are genes encoding the four structural proteins incorporated in the mature SARS2 virion: spike (S), membrane (M), envelope (E), and nucleocapsid (N) (Jahirul Islam et al., 2023). Interspersed within these genes are several accessory proteins that are not essential for viral replication but play an important role in viral pathogenesis. SARS2 accessory proteins have been implicated in regulating cytokines, induction of apoptosis, and activation of inflammasomes (Fang et al., 2021; Redondo et al.,

2021; Zandi et al., 2022). The structural proteins are well conserved across other coronaviruses (Woo et al., 2012) while there is substantial diversity in the number and identity of accessory proteins across coronaviruses (Fang et al., 2021).

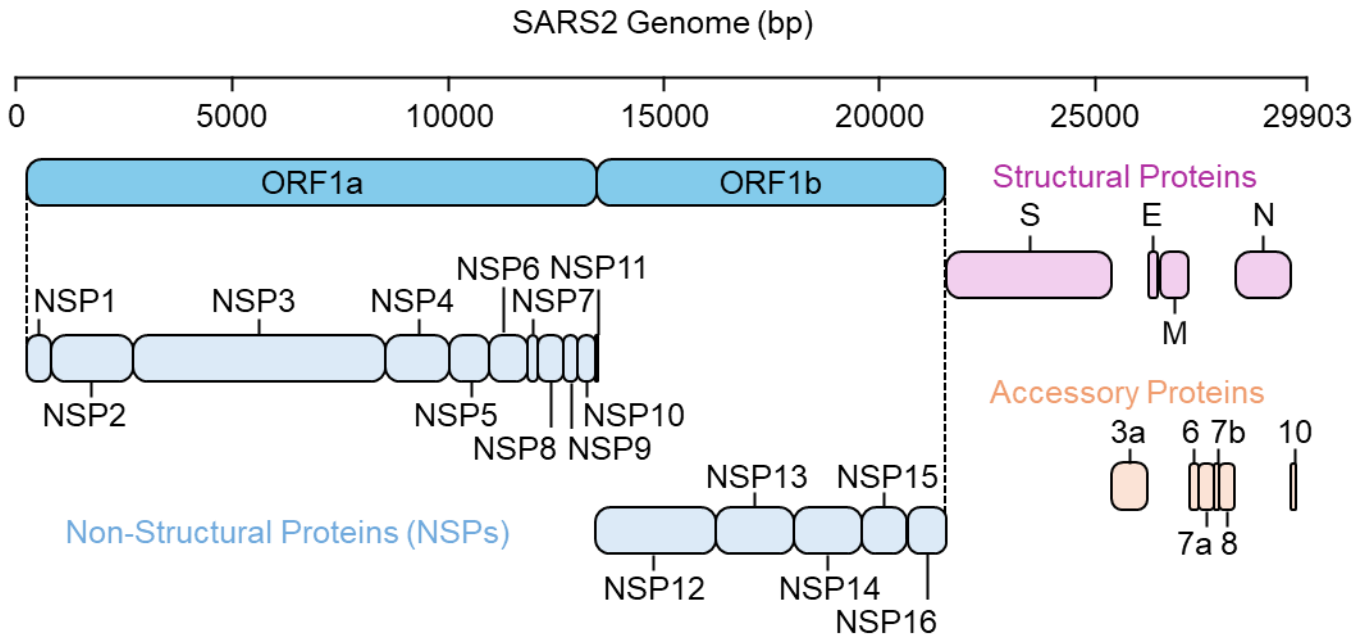

Figure 1.3: Schematic of SARS2 genome. A representation of the SARS2 genome based on the sequence and annotations of GenBank accession number NC_045512.2. Genes encoding non-structural proteins are blue, genes encoding structural proteins are purple, and genes encoding accessory proteins are orange.

SARS-CoV-2 virions have a diameter of approximately 60 to 140 nm and, while typically spherical, display some pleomorphism (N. Zhu et al., 2020). The most abundant structural protein in the SARS2 virion is the membrane protein which plays a critical role in viral assembly and budding (Z. Zhang, Nomura, et al., 2022). The nucleocapsid protein binds to the genomic RNA and facilitates packing within the viral capsid (Wu et al., 2023). The envelope protein is the smallest of the structural proteins present in the virion. Although critical for virulence, the function of the envelope protein role has not been fully elucidated (Cao et al., 2021). Envelope proteins are highly expressed at intracellular transport sites (such as the endoplasmic reticulum and Golgi) in infected cells and form cation-conducting ion channels that enhance pathogenicity (Medeiros-Silva et al., 2023).

The Spike protein plays a key role in host receptor binding and cell membrane fusion. The protein is 180-200 kDa, is heavily glycosylated, and forms a homotrimer (Figure 1.4). The protein is composed of two subunits: S1 and S2. The S2 subunit mediates viral cell membrane fusion and is composed of a fusion peptide, two heptad repeat sequences, and a transmembrane domain. The S1 subunit facilitates host receptor recognition and is composed of an N-terminal domain (NTD) and receptor-binding domain (RBD). SARS2 RBD binds to angiotensin-converting enzyme 2 (ACE2) and is critical for virulence (Y. Huang et al., 2020). ACE2 is a receptor widely expressed in multiple cell types that plays a critical role in blood pressure regulation through the conversion of the peptide angiotensin II to angiotensin-(1-7) (R. A. S. Santos et al., 2018).

The Spike protein folds in a metastable state that, while energetically stable, is capable of undergoing further conformational change to a lower energy state replication (C. B. Jackson et al., 2022). This energetically favourable transition can help overcome the repulsion between the host and viral membranes and is mediated by two proteolytic cleavage steps using host proteases. First, a multibasic site at the junction between S1 and S2 is cleaved by host cell furin. At this stage the S1 site is susceptible to premature shedding away from the rest of the Spike protein. Second, the S2′ site is proteolytically cleaved. The S2′ site on S2 is exposed by confirmational changes induced by RBD biding to ACE2. Cleavage may be performed by transmembrane protease, serine 2 (TMPRSS2) on the cell surface or, if internalization has occurred, by cathepsins in the endosomes. Cleavage causes dissociation of S1 from S2, exposes the fusion peptide, and causes a substantial S2 conformational change that drives the fusion peptide into the host membrane. This forms a fusion pore between the viral and host membrane

that allows dissemination of the viral RNA through the cell cytoplasm, facilitating translation and replication (C. B. Jackson et al., 2022).

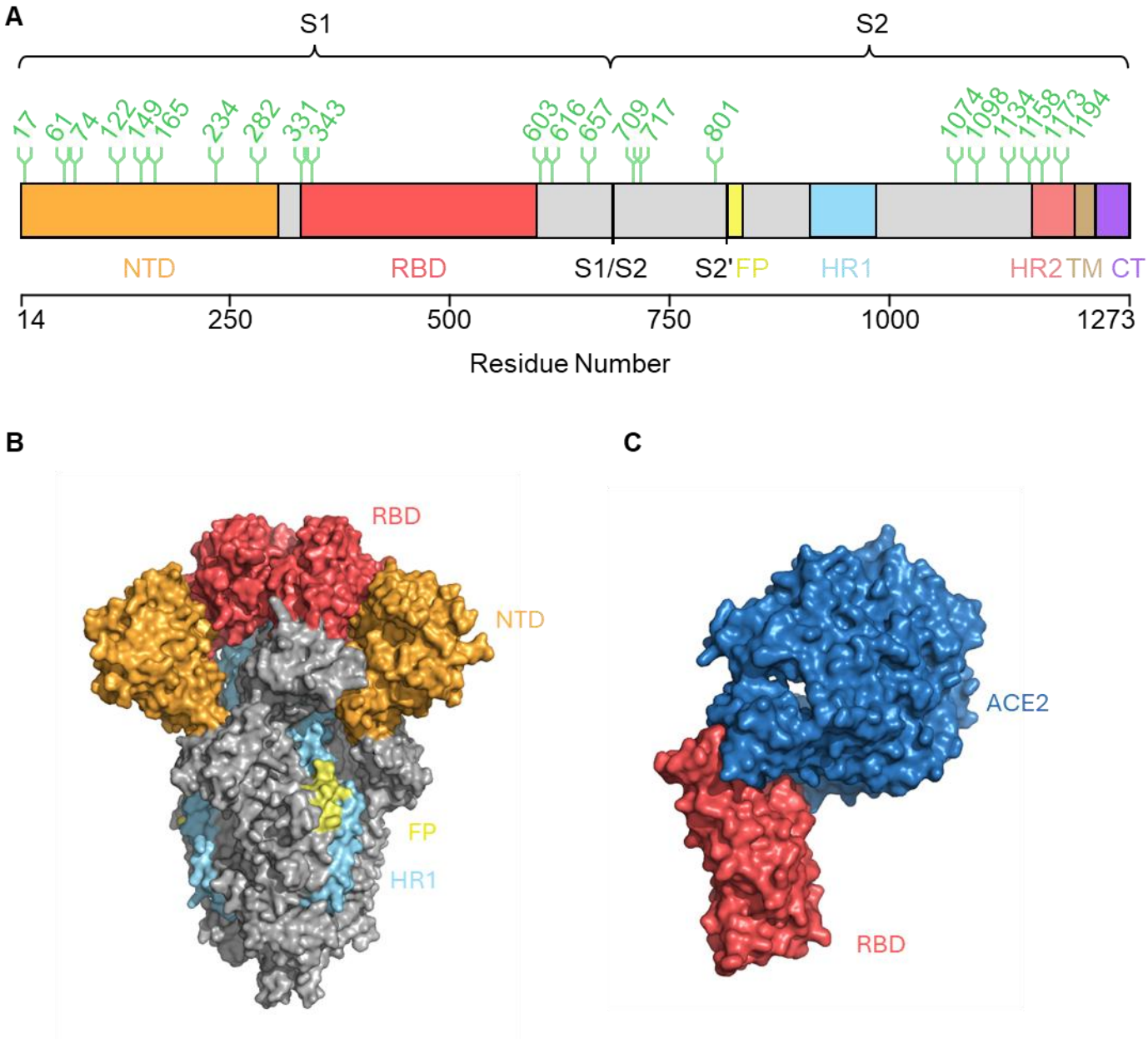

Figure 1.4: SARS2 spike glycoprotein. (A) A map of the SARS2 spike protein showing the location of the N-terminal domain (NTD), receptor-binding domain (RBD), fusion peptide (FP), heptad repeat 1 (HR1), heptad repeat 2 (HR2), transmembrane domain (TM), and cytoplasmic tail (CT). The S1/S2 furin cleavage site and S2′ cleavage site are indicated. The location of glycosylation sites is shown with the residue number indicated (green). Residue numbering starts at 14 as the signal peptide is cleaved during processing and is not present in the mature spike prefusion spike protein. **(B)** The structure of prefusion SARS2 spike protein with all RBDs in the down position with certain domains indicated (PDB 6VXX). **(C)** The structure of an individual SARS2 RBD interacting with human ACE2 receptor (PDB 6M0J).

Human infection with SARS2 causes the disease COVID-19. SARS2 undergoes human-to-human transmission through respiratory droplets and aerosols. After infection, the median incubation period is 4-5 days before the onset of symptoms (Lamers & Haagmans, 2022). Common symptoms are fever, cough, fatigue, and shortness of breath (Alimohamadi et al., 2020), but the disease can be asymptomatic in some cases (Z. Gao et al., 2021). Severe disease is commonly associated with hypoxaemia and can lead to systemic hyperinflammation, progressive respiratory failure, and death (Lamers & Haagmans, 2022).

In a notable fraction of patients that recover from acute COVID-19, there are health effects from the condition 'Long COVID'. This term encompasses dozens of symptoms across several organ systems which can be debilitating to those afflicted. Several non-exclusive causes of Long COVID have been proposed including immune dysregulation, impact on the microbiota, autoimmunity, and persistence viral reservoirs in host tissues. At this time there are no clinically validated treatments for Long COVID (H. E. Davis et al., 2023).

COVID-19 was first identified in December 2019 (C. Huang et al., 2020). Retrospective analysis suggests that the disease may have first emerged as early as October 2019 (D. L. Roberts et al., 2021). By January 2020, the disease had spread to several countries across multiple continents (Caly et al., 2020; Holshue et al., 2020; Imai et al., 2022; Spiteri et al., 2020). On March 11, 2020, the World Health Organization (WHO) declared COVID-19 a global pandemic (Cucinotta & Vanelli, 2020). By July 1st, 2024, the WHO reported more than 7 million deaths confirmed to be due to COVID-19 (WHO, 2023). Statistical measurements have estimated 14.8 million excess deaths associated with the COVID-19 pandemic in the years 2020 and 2021 alone (Msemburi et al., 2023). The COVID-19 pandemic has additionally had far-reaching societal, political and economic impacts (Sachs et al., 2022).

Through the progression of the pandemic, the SARS2 virus has undergone substantial evolution that impacted transmissibility, severity, and immune evasion (Markov et al., 2023). The virus has accumulated mutations through replication errors (Amicone et al., 2022), host-mediated genome editing (Kim et al., 2022), and recombination (T. Tamura et al., 2023). During acute infection, low levels of variance develop within the viral population of an individual host. Each transmission event acts as a genetic bottleneck and typically only the most common variant present in the host will be transferred. Less frequently, a minority variant or a combination of variants will be transferred (Lythgoe et al., 2021). Over time the global variant population will shift and variants with selective advantages may emerge (Markov et al., 2023).

As an early example, the Spike mutation D614G was identified early in the pandemic (Isabel et al., 2020). This mutation has been shown to reduce shedding of S1, increase Spike density in the virion, and increase affinity for the interaction between RBD and ACE2 (despite the mutation occurring outside of RBD) (L. Zhang et al., 2020). D614G quickly became dominant when introduced into a region and became the globally dominant form of the virus (Korber et al., 2020).

Selective pressure has led to the rise of several SARS2 variants of concern (VOCs) (Parums, 2021). One VOC example was the Beta variant (Pango lineage B.1.351) detected in South Africa, which carried three mutations (K417N, E484K, and N501Y) in the RBD and quickly gained regional dominance (Tegally et al., 2021). Another VOC example was the Delta variant (Pango lineage B.1.617.2) detected in India (Dhar et al., 2021) which contained two mutations (L452R and T478K) in the RBD (Dhawan et al., 2022). The Delta variant became globally dominant (Hadfield et al., 2018) leading to a surge of COVID-19 cases (Bolze et al., 2022).

There are multiple hypotheses to explain the emergence of VOCs with several mutations that make them distinct from the dominant circulating variants. These theories include stealth

circulation and genetic drift in populations with poor genomic surveillance, chronic infection and sustained evolution in immunocompromised individuals, and transfer between an undetermined zoonotic reservoir (Markov et al., 2023).

The first three Omicron variants (BA.1, BA.2, and BA.3) were identified in South Africa and Botswana in October 2021 (Viana et al., 2022). These lineages have subsequently undergone substantial further evolution (Roemer et al., 2023), including the emergence of XBB.1 from the recombination of two co-circulating Omicron BA.2 lineages (BJ.1 and BM.1.1.1) (T. Tamura et al., 2023) and further evolution of XBB.1 leading to XBB.1.5 (Uriu et al., 2023). Currently circulating Omicron variants (such as JN.1) demonstrate substantial immune evasion from immune responses raised against earlier variants as well as enhanced cellular infectivity (Kaku et al., 2024). Evasion of pre-existing immune responses targeting previous iterations of SARS2 is a hallmark of several Omicron variants and a challenge for therapeutic and vaccine development (Meng et al., 2022; Qu et al., 2024; Willett et al., 2022).

1.5.3 Sarbecoviruses

Sarbecoviruses are SARS-like betacoronaviruses that have primarily been identified in bats but also include the human pathogens SARS1 and SARS2 (Boni et al., 2020). This group has been broken into four different clades based on their RBD sequences (A. Cohen et al., 2021) (Figure 1.5, 1.6, Appendix 2). It is important to note that these clades are not apparent through phylogenetic analysis of other sarbecovirus sequences, including RNA-dependent RNA polymerase. The clades are named Clade 1a, Clade 1b, Clade 2, and Clade 3 (A. Cohen et al., 2021; Letko, Marzi, et al., 2020; Starr et al., 2022).

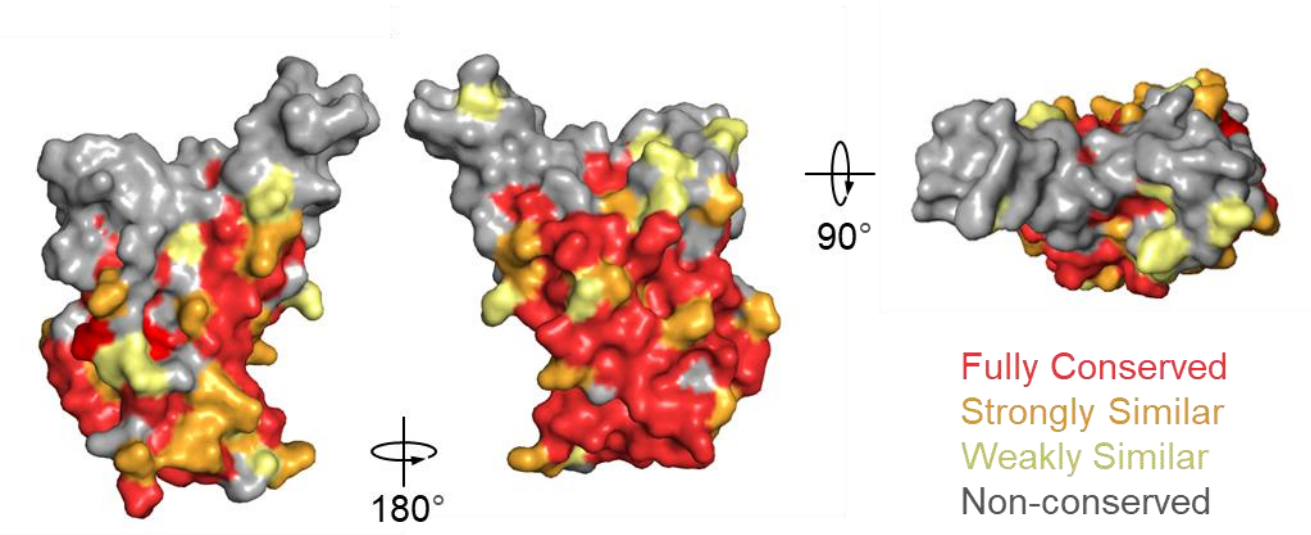

Figure 1.5: Conservation of residues for sarbecoviruses. The conservation of residues for the twelve sarbecovirus RBDs outlined in Figure 1.6 are mapped onto the SARS2 RBD structure (PDB 6ZER). Multiple orientations of the same RBD are shown. Conservation was determined using Clustal Omega (version 1.2.4).

Clade 1a sarbecoviruses are related to SARS1 and demonstrate binding to ACE2. Clade 1b sarbecoviruses are related to SARS2 and also demonstrate binding to ACE2. Several members of Clade 1a and Clade 1b have demonstrated tight binding to the human ACE2 protein. Both of these clades are predominantly found in Asian bat species. Clade 2 sarbecoviruses are also found in Asian bat species but have not been shown to bind human or any other ACE2 protein. The RBD of Clade 2 viruses shows two large deletions in the receptor binding motif. Together these results have led to the hypothesis that Clade 2 viruses use a different, currently unidentified receptor to gain mammalian cell entry. It is unclear if this entry is facilitated by their RBD or a different domain on the Spike protein (Starr et al., 2022).

Clade 3 sarbecoviruses have been found in African and European bats and include the viruses BM48-31, BtKY72, and Khosta-2 (A. Cohen et al., 2021; Letko, Marzi, et al., 2020; Starr et al., 2022). There is variability in ACE2 binding found in this clade (Starr et al., 2022). The BM48-31 virus identified in Bulgarian bats (Drexler et al., 2014) has not demonstrated

binding to any tested human or bats ACE2 receptor (Starr et al., 2022). The BtKY72 virus identified in Kenyan bats demonstrates binding to some bat (*Rhinolophus affinis*) ACE2 receptors but not to human ACE2. However, a double point mutation in BtKY72 can facilitate binding to human ACE2 and entry into human cells with this receptor. The Khosta-2 virus identified in bats in the Russian Greater Caucasus (Alkhovsky et al., 2022) has shown the ability to bind human ACE2 (Starr et al., 2022) and infect human cells (Seifert et al., 2022).

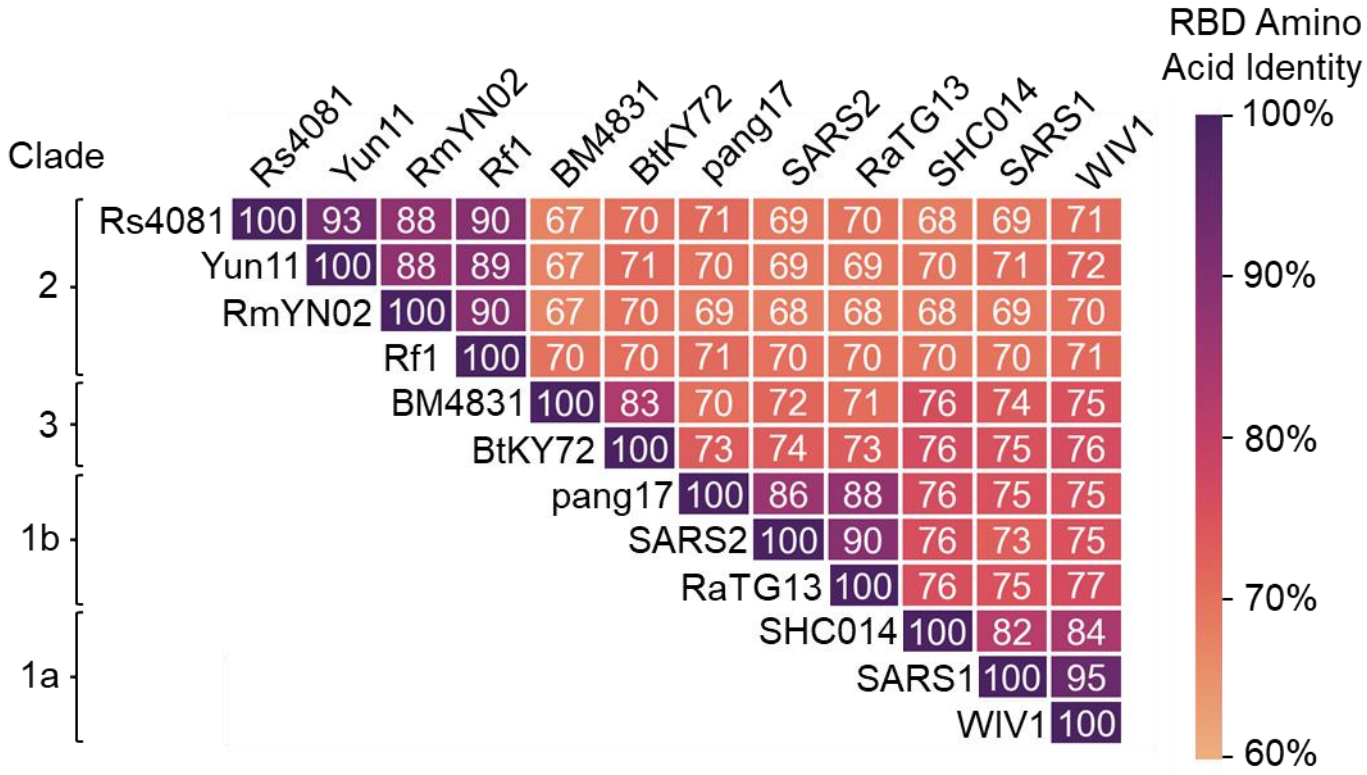

Figure 1.6: Heat map of sarbecovirus RBD conservation. A heat map displaying the percent amino acid identity of selected sarbecovirus RBDs. The colour gradient is based on a range from 60% to 100% amino acid identity. The clades of the viruses that RBDs belong to are indicated.

1.5.4 Merbecoviruses

Merbecoviruses are a subgenus of MERS-like betacoronaviruses. Merbecoviruses have been identified across several continents, circulating in different zoonotic reservoirs, including bats (Woo et al., 2006), camels (Haagmans et al., 2014), hedgehogs (Corman, Kallies, et al., 2014), and pangolins (J. Chen et al., 2023) (Figure 1.3). Some of these merbecoviruses use dipeptidyl peptidase 4 (DPP4) (Letko et al., 2018) to gain entry to mammalian cells while others use ACE2 (C. Ma et al., 2023).

The prototypic merbecovirus is the virus MERS. MERS primarily infects camels but there have been several camel-to-human transmission events. In humans, clinical presentation can range from asymptomatic or mild upper respiratory illness to a rapid pneumonitis progression, respiratory failure, acute respiratory distress syndrome, septic shock, and multiorgan failure leading to death. MERS is still circulating and causes sporadic and intermittent cases in humans (Memish et al., 2020). MERS is relatively poor at human-to-human transmission, with many infections occurring in co-habitation or health care settings (Drosten et al., 2014; Memish et al., 2014).

The MERS virus encodes four structural proteins: spike (S), envelope (E), membrane (M), and nucleocapsid (N) protein. MERS spike is a glycoprotein trimer that plays a critical role in binding to DPP4 and facilitating membrane fusion with host cells. The spike protein includes an RBD which binds the host cellular receptor DPP4 and facilitates viral entry (Memish et al., 2020). DPP4 tends to be well expressed in the upper respiratory tract epithelium for camels but not humans. This differential expression may play a role in the relatively inefficient human-to-human transmission of the disease (Widagdo et al., 2016). In addition to a variety of lung cells, DPP4 is widely expressed on the epithelial cells of other organs and tissues including kidneys, intestine, liver, thymus, and bone marrow which could facilitate wider systemic dissemination (Memish et al., 2020; Meyerholz et al., 2016).

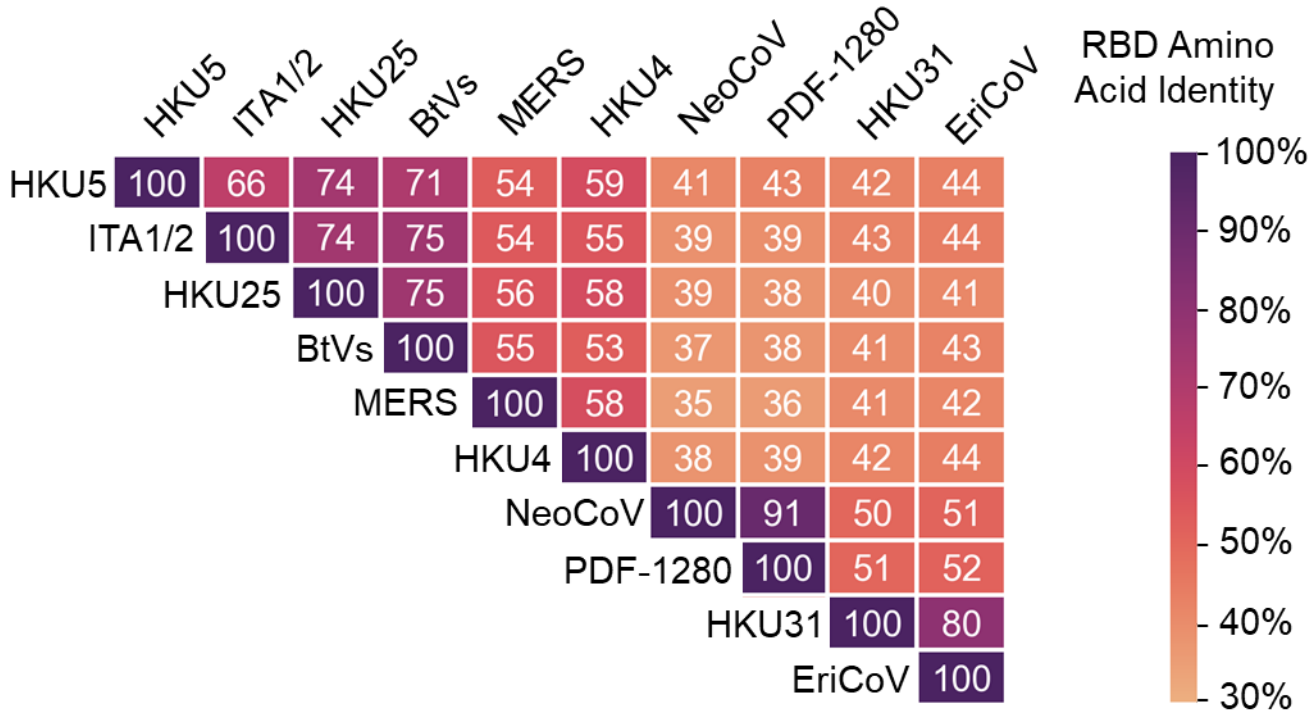

Figure 1.7: Heat map of merbecovirus RBD conservation. A heat maps displaying the percent amino acid identity of selected merbecovirus RBDs. The colour gradient is based on a range from 30% to 100% amino acid identity.

There is currently no clinically approved vaccine to provide human or veterinary protection against MERS (Laydon et al., 2023). MERS vaccines based on the full Spike protein have successfully concluded Phase 1 clinical trials (Bosaeed et al., 2022; Koch et al., 2020; Modjarrad et al., 2019). The candidates are based on Spike delivery using a DNA (Modjarrad et al., 2019) or viral vector platform (Bosaeed et al., 2022; Koch et al., 2020).

Other merbecoviruses have been identified as having risk of zoonotic transmission (Gonzalez-Isunza et al., 2023; Tolentino et al., 2024; Zumla et al., 2024). For example, a relative of the bat merbecovirus HKU4 called MjHKU4r has been identified in pangolins in Malaysia. MjHKU4r is able to use human DPP4 as a receptor for cell entry, as well as host proteases for

enhanced cell infection. MjHKU4r was shown to successfully replicate in human respiratory and intestinal organoids. Transgenic mice with a human DPP4 were infected with MjHKU4r and the virus underwent successful replicating infection causing lung injury (J. Chen et al., 2023).

1.6 COVID-19 Vaccines

The SARS2 genomic sequence was first made publicly available on January 11, 2020 [Coordinated Universal Time (UTC)] (Burki, 2023; Krammer, 2024). By the end of that year, seven different vaccines against COVID-19 had received authorization for clinical use in some jurisdictions (Krammer, 2024). These vaccines included the first clinically approved mRNA vaccines (Vitiello & Ferrara, 2021) mRNA-1273 from Moderna (L. A. Jackson et al., 2020) and BNT162b2 from BioNTech/Pfizer (Polack et al., 2020). Early COVID-19 vaccines also include a vaccine built using viral vector technology (Travieso et al., 2022). ChAdOx1 nCoV-19 from Oxford/AstraZeneca (Falsey et al., 2021) was produced using a Chimpanzee adenoviral (ChAd) vector (Ewer et al., 2017; Watanabe et al., 2021). Ad5-nCoV from CanSino Biologics was produced using Adenovirus type 5 (Ad5) vector (Halperin et al., 2022). Sputnik V from the Gamaleya Research Institute of Epidemiology and Microbiology used heterologous Adenovirus type 26 (Ad26) and Ad5 vectors for prime and boost (Logunov et al., 2021). The group of early vaccines also included more conventional inactivated whole-virus vaccines, namely, CoronaVac from Sinovac Biotech (Tanriover et al., 2021) and BBIBP-CorV from Sinopharm (Al Kaabi et al., 2021; Xia et al., 2021). Both of these vaccines were SARS2 viruses cultured in Vero cells and inactivated with β-propionolactone (Q. Gao et al., 2020; Hotez & Bottazzi, 2022; H. Wang et al., 2020). Later clinically approved vaccines included those based on recombinant spike protein (Heath et al., 2021; Tian et al., 2021), recombinant RBD (Hernández-Bernal et al., 2023), recombinant RBD conjugated to a tetanus toxoid carrier

protein (Toledo-Romaní et al., 2023), spike protein displayed on eVLP (Hager et al., 2022; Ward et al., 2021), and RBD displayed on a protein-based VLP (J. Y. Song et al., 2023).

Vaccines efforts have largely focused on the spike protein, or more narrowly RBD, as an immune target. Antibodies raised against the spike protein have the potential to block interactions between the virus and the host ACE2 receptor or prevent membrane fusion and have been associated with viral neutralization (Krammer, 2024). Passive transfer for mice immunized with SARS2 membrane, nucleocapsid, or envelope has failed to enhance viral clearance, in contrast to sera elicited by spike protein (J. Sun et al., 2020).

The rapid development of safe and efficacious vaccines against COVID-19 was a remarkable achievement that has substantially reduced mortality and morbidity (Oordt-Speets et al., 2023; Watson et al., 2022a; J. Zhang et al., 2022). In the first year of vaccine adoption alone, from December 8th, 2020, when the first administration of clinically approved BNT162b2 vaccine, to December 8th, 2021, vaccines are estimated to have prevented 14.4 million deaths due to COVID-19 (Watson et al., 2022a).

The rise of Omicron variants has led to an increase in breakthrough infections of previously immunized individuals (Jalali et al., 2022; S. T. Tan et al., 2023). Omicron variants have acquired substantial mutations and antibodies raised against ancestral SARS2 variants demonstrate a substantial reduction in Omicron variant neutralization (Planas et al., 2023; Qu et al., 2023; Willett et al., 2022). This development has led to vaccines being updated to include newer Omicron variants (Dixit et al., 2024; Hansen et al., 2024; Winokur et al., 2023). Non-neutralizing antibodies elicited by Wuhan-containing vaccines have still demonstrated binding to Omicron (Carreño et al., 2022). There is evidence that non-neutralizing antibodies against SARS2 can still protect against serious disease and death (Clark et al., 2024; Rahman et al.,

2023). Further innovations in COVID-19 vaccines may focus on developing technologies more resistant to evolution of new variants (Kang et al., 2022; Pang et al., 2022; Pekar et al., 2022b).

1.7 Broad Coronavirus Vaccines

The remarkable impact that vaccines have had on the outcomes of COVID-19 pandemic highlights the importance of vaccines for protection against future pandemic threats (Krammer, 2024; Saville et al., 2022; Watson et al., 2022a). In the 21st century, at least three coronaviruses (SARS, SARS2, and MERS) have undergone zoonotic transmission causing fatalities (G. Tang et al., 2022). There is significant risk of a future coronavirus spillover event, leading to another disease outbreak (Menachery et al., 2017). This risk is exacerbated by the effects of climate change and habitat loss introducing novel points of animal-human contact (Carlson et al., 2022; Keesing & Ostfeld, 2021; The Lancet, 2023).

The risk of zoonotic transmission could be mitigated by the proactive development of broadly protective vaccines. This technology could allow for vaccines to be designed, validated, and stockpiled prior to a transmission event. The potential of these vaccines to target evolutionarily related groups could allow for protection against currently unknown pathogens (Saville et al., 2022). A pan-coronavirus vaccine would effectively accomplish this goal, however, the diversity of coronaviruses makes this approach incredibly challenging (Lewitus et al., 2023). There is sequence conservation within the S2 region of the spike protein and anti-S2 antibodies have shown cross-reactivity, however, the antibodies are often poorly neutralizing (Adams et al., 2023). Broadly neutralizing monoclonal antibodies have been identified that target S2, including S2' and the fusion peptide, and are able to prevent membrane fusion. These results offer tantalizing targets for future vaccine development (Pinto et al., 2021; Poh et al., 2020; X. Sun et al., 2022).

Targeting a narrower group of coronaviruses can still achieve dramatic results. For example, a pan-sarbecovirus vaccine would be able to protect against SARS1, SARS2, and several SARS-

related bat coronaviruses that have been identified as having outbreak potential (Menachery et al., 2015). The benefit to a vaccine targeted towards a narrower group of coronaviruses is that there is a larger area of evolutionary conservation to target. This may produce a response less susceptible to immune evasion through small amounts of antigenic drift (Lewitus et al., 2023).

A T cell-mediated response is critical for viral clearance of SARS2 and plays a key protective role (P. Moss, 2022). Conserved coronavirus T cell epitopes raise exciting possibilities for the induction of a broad and effective cell-mediated immune response (Tarke et al., 2023; van Bergen et al., 2023). There is strong evidence for antibody binding and antibody neutralization as a robust correlate of protection for SARS2 (P. B. Gilbert et al., 2022; Goldblatt et al., 2022; Regev-Yochay et al., 2023) which has focused much of the ongoing broad coronavirus research on a humoral response (Cankat et al., 2024). Several monoclonal antibodies targeting a variety of coronaviruses have been identified (W. ting He et al., 2022; K. Y. A. Huang et al., 2023; Jette et al., 2021; Pinto et al., 2021; Poh et al., 2020; X. Sun et al., 2022). A key question, therefore, is how a vaccine can consistently and dominantly raise broadly neutralizing antibodies against coronaviruses (Cankat et al., 2024).

Several of the strategies outlined in Section 1.4 have been applied to achieve broad coronavirus vaccines. For example, antigen truncation has been performed on the SARS2 spike protein, so that only the S2 domain was included. Immunizations were performed with the vaccine in a DNA format or as bacterially expressed recombinant protein, but only the DNA vaccine successfully raised an S2 response in cell-based assays (Ng et al., 2022). Given that the S2 domain undergoes substantial post-translational glycosylation, it is possible that the recombinant protein result could be improved through mammalian expression (Watanabe et al., 2020). The S2 DNA vaccine raised neutralizing antibodies against several alpha- and betacoronaviruses including HKU1, OC43, 229E, NL63, and SARS2. These results demonstrate antigen truncation can effectively shift the immune response from the

immunodominant S1 domain to the more evolutionarily conserved S2 domain of the spike. Unfortunately, the S2 DNA vaccine failed to protect against a lethal challenge SARS2 Delta virus in K18-hACE2 transgenic mice that utilize a human ACE2 protein. Under these conditions the S2 DNA vaccine provided reduced protection relative to the full spike protein (Ng et al., 2022).

A combination of strategic glycosylation and computational design has also been used to create a pan-sarbecovirus vaccine candidate (Vishwanath et al., 2023). A consensus RBD sequence was produced that maximized phylogenetic similarity within sarbecoviruses. Further modifications were made to introduce a glycosylation site at a poorly conserved region of the RBD and to introduce the epitope of a known broad anti-sarbecovirus monoclonal antibody (S309). This vaccine candidate, designated T2_17, performed favourably when delivered as a viral vector or DNA vaccine (Vishwanath et al., 2023). The antigen is intended to be platform-independent and would accommodate delivery in an mRNA, soluble protein, or VLP display format. The vaccine raised an antibody response against the clade 1a viruses SARS1 and WIV16, as well as the clade 1b viruses SARS2 and RaTG13. No investigation of clade 2 or clade 3 sarbecoviruses was presented. An immunization schedule where K18-hACE2 transgenic mice were primed with ChAdOx1 nCoV-19 and boosted with T2_17 in either DNA or viral vector format, lead to full survival after SARS2 Delta challenge, and weight loss that was comparable to a homotypic ChAdOx1 nCoV-19 prime and boost (Vishwanath et al., 2023).

A computational design strategy has also been undertaken to develop a pan-betacoronavirus vaccine. Researchers analysed the genomes of non-human coronaviruses and identified viruses that had an RBD sequence more similar to a human coronavirus than would be expected based on their overall phylogenetic divergence. These sequences were deemed human-like RBDs. These sequences were optimally clustered into three groups and a consensus sequence was calculated for each of these three clusters. One cluster included RBDs similar to SARS1 and

SARS2, one cluster included RBDs similar to HKU1 and OC43, and one cluster included RBDs similar to MERS. This approach is therefore focused on targeting betacoronaviruses related to existing human pathogens. No results have yet been published to evaluate expression, structural integrity, or immunogenicity of these computationally designed antigens (Lewitus et al., 2023).

Chimeric spike antigens have been produced which can contain an RBD, NTD, and S2 domain from different coronaviruses. For example, a trivalent chimaera was designed to include an NTD from clade 2 HKU3, an RBD from clade 1a SARS1, and an S2 from clade 1b SARS2. Bivalent spike chimaeras were also produced, for example including the RBD of SARS2 and both the NTD and S2 from SARS1. These chimaeras were delivered as mRNA vaccines. A variety of immunization regimens were explored, including homologous doses with a single chimeric antigen, homologous doses with a cocktail of chimaeras, and heterologous doses administering different chimaera cocktails in the prime and boost. The chimeric spike groups were able to raise antibodies to a greater diversity of sarbecoviruses than the wild-type SARS2 spike protein, including to clade 1a WIV1 which was not present in any of the chimaeras. However, the chimeric spike groups raised a lower magnitude antibody response against SARS2 than the wild-type SARS2 spike protein. Administration of chimeric spike cocktails that included SARS1 components enhanced protection from SARS1 challenge compared with the wild-type SARS2 spike, but no enhancement of protection was achieved when no chimeric spikes that included SARS1 were included (Martinez et al., 2021).

In a study focused on protection against human betacoronaviruses, prefusion-stabilized spike proteins were produced for HKU1, OC43, SARS1, SARS2, and MERS. These proteins were fused to one part of a two-component protein nanoparticle (I53_dn5B) and assembled into a full nanoparticle through the addition of the second component (I53_dn5A). A mosaic nanoparticle with these five spike proteins was produced. This mosaic nanoparticle elicited a

potent immune response against the five incorporated human coronaviruses (Hutchinson et al., 2023). Mouse challenge studies were performed using 288/330+/+ mice that were genetically edited to incorporate two point mutations that make them susceptible to MERS infection (Cockrell et al., 2016). The mosaic nanoparticle provided protection against this MERS challenge. This studied was focused on human coronaviruses and there was no analysis on the response raised against zoonotic coronaviruses (Hutchinson et al., 2023).

Both sequential immunization and co-administration of multiple antigens have been explored for mRNA vaccines encoding SARS1, SARS2, and MERS spike proteins. Sequential immunization produced enhanced immune responses relative to co-administration. It is important to note that an additional four doses of the sequential immunization were performed and analysis was performed 14 days after the final sequential boost and 98 days after the final co-administration boost. Both strategies elicited strongly neutralizing immune responses against SARS1, SARS2, and MERS pseudoviruses. The study was solely focused on these pathogens and there was no analysis of immune response raised to any zoonotic coronaviruses (Peng et al., 2022).

As previously referenced, the mosaic nanoparticle strategy has been applied as a broadly effective sarbecovirus vaccine strategy. In one iteration of this strategy, sarbecovirus RBDs were genetically fused to I53-50a, one component of the I53-50 nanoparticle. The RBDs were from clade 1a SARS1 and WIV1 and clade 1b SARS2 and RaTG13. The fusion proteins were expressed as monomers and, when mixed with I53-50b, efficiently formed nanoparticles. This strategy could be used to make homotypic nanoparticles and by pre-mixing different RBD-I53-50a fusion proteins can be used to make mosaic nanoparticles. Both mosaic nanoparticles and cocktails of homotypic nanoparticles were able to raise neutralizing immune responses against the RBDs present on the nanoparticle and provided protection in mice challenged with SARS1 (Walls et al., 2021).

Mosaic nanoparticles have been produced using SpyCatcher003-mi3 (Figure 1.8). A panel of RBDs from the Spike protein of sarbecoviruses infecting humans, bats, and pangolins was produced. All members of this panel were modified to include a C-terminal SpyTag003. Either four (Mosaic-4) or eight (Mosaic-8) different RBDs were incorporated on the same SpyCatcher003-mi3 nanoparticle. Mouse immunization experiments were performed with these mosaic nanoparticles and compared with soluble SARS2 spike trimer and homotypic nanoparticles that only contained SARS2 RBD. These assays showed that spike and Homotypic SARS2 nanoparticles produced a strong immune response against SARS2 but not against any of the other tested sarbecoviruses. In contrast, the antisera induced by the Mosaic-4 and Mosaic-8 nanoparticles demonstrated binding to a large panel of sarbecovirus RBDs and neutralized all of the tested sarbecovirus pseudoviruses. The greatest breadth was achieved with the Mosaic-8 nanoparticle vaccine (A. Cohen et al., 2021).

Critically, the panel of RBDs and pseudoviruses included viruses that were not represented on the mosaic nanoparticles, including zoonotic sarbecoviruses, an early SARS2 variant, and SARS1. The ability of the mosaic nanoparticles to induce an immune response against these RBDs suggests the induction of broadly neutralizing antibodies against common epitopes shared by these viruses (A. Cohen et al., 2021).

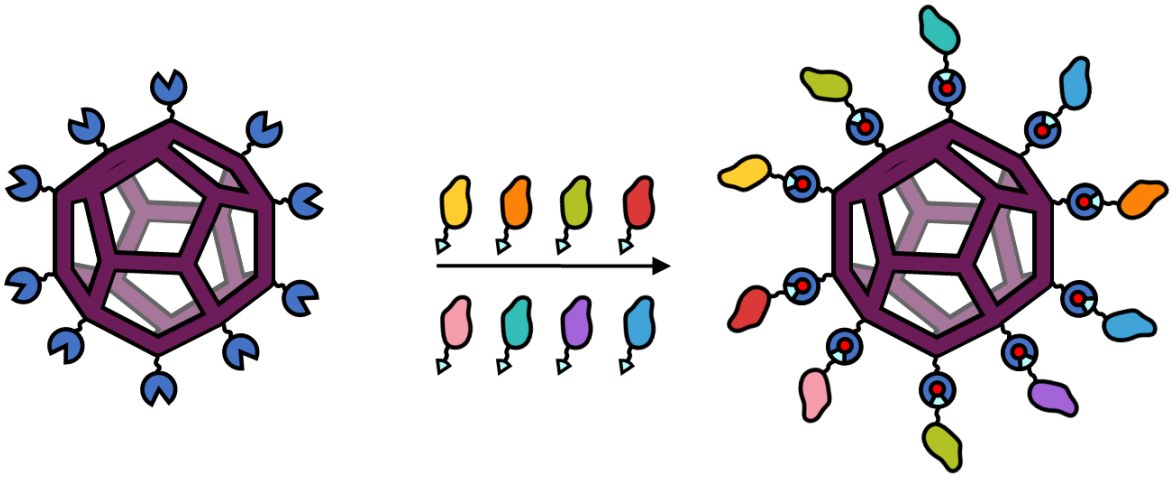

Figure 1.8: Cartoon of Mosaic-8 nanoparticle assembly. SpyCatcher00-mi3 is a nanoparticle formed by monomeric subunits that are a genetic fusion of SpyCatcher003 (dark blue) and mi3 (purple). A mixture of RBDs from different sarbecoviruses (various colours) genetically fused to SpyTag003 (cyan) are incubated with SpyCatcher003-mi3. Covalent bond formation between SpyTag and SpyCatcher facilitates multivalent display of these diverse RBDs and the production of mosaic nanoparticles. Assembly of proteins onto the nanoparticle is stochastic, producing a heterogenous mixture of mosaic nanoparticles.

One may consider the difference in the mechanism for an immune response raised by a homotypic and mosaic nanoparticle. When interacting with B cells in the germinal centre, a homotypic nanoparticle will engage with BCRs that are capable of binding to the single antigen that is being displayed. B cells will be selected for their ability to bind this individual antigen. For a mosaic nanoparticle, B cells that have BCRs capable of binding several different antigens will have a selective advantage over those which can only bind one of the several antigens present. BCRs can bind to multiple related antigens if they target a region conserved across the panel of sarbecovirus RBDs. In this way mosaic nanoparticles may provide selective pressure for the development of antibodies against conserved regions and in doing so raise a response against a greater evolutionary range of viruses (A. Cohen et al., 2021).

In a follow-up study, the SARS2 Wuhan RBD in the Mosaic-8 nanoparticle was replaced with SARS2 Beta RBD, to produce the Mosaic-8b vaccine candidate. This vaccine provided

protection against SARS2 and SARS1 viral challenge of K18-hACE2 mice transgenic mice (A. A. Cohen et al., 2022). Critically, SARS1 was not present in the vaccine itself, indicating breadth of immune protection and the potential to respond to novel pathogenic threats. In non-human primate models, Mosaic-8b vaccines raised neutralizing antibodies against a diverse group of sarbecoviruses, including to viruses absent from the vaccine (A. A. Cohen et al., 2022). In further studies, Mosaic-8b has still been able to raise a broad and neutralizing immune response to a diverse range of matched and mismatched sarbecoviruses in non-human primates or transgenic mice that had previously been immunized with DNA, mRNA, a self-amplifying RNA, or adenovirus-vectored COVID-19 vaccines (A. A. Cohen et al., 2024). The Mosaic-8b vaccine candidate has received support from the Coalition for Epidemic Preparedness Innovations (CEPI) to enter Phase 1 human clinical trials.

1.8 Thesis Objectives

This thesis explores the use of the SpyTag/SpyCatcher system to develop new vaccine candidates capable of protecting against SARS2 and other sarbecoviruses.

The first objective of this thesis is to apply SpyTag/SpyCatcher technologies, such as SpyCatcher-functionalized nanoparticles and a SpyCatcher variant with pH responsive affinity, to facilitate purification and nanoassembly of SARS2 vaccine candidates. I also implement these technologies for streamlined analysis of monoclonal antibodies from convalescent COVID-19 patients.

The second objective of this thesis is to develop a broad anti-sarbecovirus vaccine that raises neutralizing antibodies against evolutionary conserved regions of these viruses. This vaccine candidate is designed to incorporate a minimal number of components to facilitate ease of large-scale vaccine production at Good Manufacturing Practices (GMP). I demonstrate that the vaccine elicits a potently neutralizing responses against the viruses represented on the

vaccine, as well as viruses that are absent from the vaccine. Additionally, I examine the application of this vaccine strategy for proactive vaccinology against future pandemic threats.

Chapter 2 – Materials and Methods

2.1 Cloning

2.1.1 Polymerase chain reactions (PCR)

Polymerase chain reactions (PCR) were performed as part of DNA construct production using Q5 High-Fidelity DNA Polymerase 2× Master Mix (New England Biolabs M0492L). The DNA oligonucleotides used as primers for PCR were purchased from Integrated DNA Technologies (IDT) desalted and desiccated without additional purification. Primers were resuspended in Milli-Q at a stock dilution of 100 µM.

For a typical PCR reaction, a working volume of 25 µL was used with 1 ng of template DNA and a final concentration of 0.5 µM for each primer. The typical thermal cycle began with an initial 98 °C denaturing step for 30 s. 35 cycles of the following was then performed: 98 °C denaturing for 10 s, 65-72 °C annealing for 30 s, and elongation for 30 s per amplified kilobase at 72 °C. Thermal cycling was performed with a C1000 Touch Thermal Cycler (Bio-Rad). Annealing temperatures were calculated with the NEB Q5 Tm calculator (Version 1.16.5) based on the interaction between the primer and the template DNA. After the 35 cycles, a final elongation step was performed at 72 °C for 120 s. In reactions where amplification was initially unsuccessful, PCRs would be repeated testing a range of annealing temperatures between 65 and 72 °C.

2.1.2 Agarose Gel Electrophoresis and gel extraction

PCR products were analysed and purified by running on an agarose gel. Agarose gels were cast with 0.8-1.2% w/v agarose (varied depending on the expected size of the DNA fragment) and 1x SYBR™ Safe DNA Gel Stain (Invitrogen) in TAE (40 mM Tris, 20 mM acetic acid, 1 mM EDTA, pH 8.0). 5 µL of 6× DNA loading dye [0.15 % (w/v) orange G, 60% (v/v) glycerol, 60 mM EDTA in TAE] was mixed with 25 µL of the samples and loaded onto the agarose gel. A Purple Quick-Load 1 kb Plus DNA Ladder (New England Biolabs) was run along with gel

fragments to allow for fragment size determination. Gels were run for approximately 45 min at 130 V in TAE. Gels were imaged using a ChemiDoc XRS+ Imager (Bio-Rad) and analysed with ImageLab version 6.1.0 software (Bio-Rad) or were imaged with an iBright FL1500 imaging system (Thermo Fisher) and analysed with iBright Analysis Software Version 5.2.0 (Thermo Fisher). DNA bands at the appropriate size were excised from the gel and DNA was extracted using Wizard SV Gel and PCR Clean-Up Kit (Promega). DNA concentration was determined using an ND-1000 NanoDrop (ThermoFisher) or NanoDrop One (ThermoFisher) UV-Vis Spectrophotometer.

2.1.3 Gibson Assembly

Plasmid constructs were assembled either entirely from PCR amplicons or from a combination of PCR amplicons and synthesized double-stranded DNA fragments commercially known as gBlocks (Integrated DNA technologies). Gibson assembly (Gibson et al., 2009) was used to assemble the plasmids via overlapping terminal regions in the DNA fragments.

The total DNA concentration for the reaction ranged from 0.02 to 0.5 pmol for 2-3 fragment assembly and 0.2 to 1 pmol for 4-6 fragment assembly. For fragments of similar length an equimolar amount of DNA was added. If one fragment was smaller than the rest, a 3-fold molar excess of the smaller fragment was used. If any of the fragments was below 200 bp, then a 5-fold excess of the smaller fragment was used to account for digestion of this smaller fragment.

A 2× Gibson Assembly mix was made by mixing 320 µL 5× isothermal reaction buffer [25% (w/v) PEG-8000, 500 mM Tris-HCl pH 7.5, 50 mM MgCl2, 50 mM DTT, 1 mM each of the four dNTPs and 5 mM NAD] with 467 µL Mili-Q, 0.64 µL of 10 U/µL T5 exonuclease (New England Biolabs), 160 µL of 2 U/µL Taq ligase (New England Biolabs), and 20 µL of 2 U/µL Phusion polymerase. The Phusion polymerase was produced by Karl Brune (K. Brune, 2019).

The mixture of DNA fragments was mixed 1:1 with 2× Gibson Assembly and incubated isothermally at 50 °C for 1 h.

2.1.4 Assembly from primers

The gene sequences for the merbecovirus RBDs ITA1/2 and HKU5 were assembled from a set of 16 oligonucleotides identified using DNAWorks version 3.2.4 (Hoover, 2002). Aliquots from each of the oligonucleotides were mixed and diluted to 2 μM to create an oligonucleotide stock mixture. 15 μL Q5 High-Fidelity DNA Polymerase 2× Master Mix (New England Biolabs), 13 μL Mili-Q, and 2 μL oligonucleotide stock mixture were mixed. A PCR protocol was run with no initial denaturing step and 35 cycles of: 98 °C denaturing for 10 s, 68-72 °C annealing for 30 s, and 1 min elongation per amplified kilobase at 72 °C. The PCR cycles were followed by a final 2 min incubation at 72 °C. Three annealing temperatures were tested (68, 70, and 72 °C) and the elongation time determined based on the full length of the desired gene. 1.5 μL of this crude extension mixture was then mixed with Q5 High-Fidelity DNA Polymerase 2× Master Mix (New England Biolabs) and two outer primers that amplified the gene of interest from opposite ends of the molecule. These outer primers contained overhang sequences that aligned with the plasmid that the gene would be inserted into. The crude extension mixture and outer primers underwent a conventional PCR reaction, performed according to the thermocycler protocol outlined in Section 2.1.1. The resulting amplicon was run on and extracted from an agarose gel (Section 2.1.2) and inserted into a plasmid by Gibson assembly (Section 2.1.3). This protocol was adapted from Li et al., 2013.

2.1.5 *E. coli* Transformation

20 μL of plasmid from Gibson assembly or approximately 2 ng of previously constructed and validated plasmids were used for bacterial transformations. The plasmid was added to 100 μL of chemically competent *E. coli* DH5 α cells (Invitrogen) for assembly of all Quartet constructs or *E. coli* NEB Turbo (New England Biolabs) for all other constructs. Incubated on ice for 10

min. Cells underwent a heat shock of 42 °C for 45 s in a water bath, followed by a 2 min incubation on ice. 350 µL SOC Media [2% (w/v) tryptone, 0.5% (w/v) yeast extract, 10 mM NaCl, 2.5 mM KCl, 10 mM MgCl2, 10 mM MgSO4, and 20 mM glucose] was added to the transformed cells before incubation for 1 h at 37 °C with 200 rpm shaking. Cells were plated on an LB agar plate with the appropriate antibiotic (100 µg/mL carbenicillin or 50 µg/mL kanamycin) and grown overnight at 37 °C. Carbenicillin plates were used for plasmids with ampicillin resistance genes.

2.1.6 Plasmid Preparation

Bacterial colonies from overnight incubation of transformed cell plates were used to inoculate LB media supplemented with the appropriate antibiotic (100 µg/mL ampicillin or 50 µg/mL kanamycin). For minipreps, 10 mL LB cultures were inoculated and grown for 4-16 h. For midipreps and maxipreps, 200 mL LB cultures were inoculated and grown for 16 h. Cells were pelleted by centrifugation at 4,000 g for 10 min at 4 °C. When a relatively small amounts (less than 30 µg) of a plasmid was needed (for bacterial transformation and sequence validation), the plasmids were obtained from the cell pellet using a GeneJET Plasmid Miniprep Kit (Thermo Fisher). When larger amounts of plasmid were needed (for mammalian transfection), the plasmids were obtained from the cell pellet using a PureLink HiPure Plasmid Midiprep (Thermo Fisher) or PureLink HiPure Plasmid Filter Maxiprep Kit (Thermo Fisher).

2.1.7 Sequencing

For all constructs, the open reading frame of the gene of interest was sequenced via Sanger sequencing by Source BioScience. The DNA sequencing results were compared with the expected construct by sequence alignment using Nucleotide BLAST (NCBI). The sequence of all proteins that I expressed as part of this thesis are included in Appendix 1.

2.1.8 Plasmid Backbones

The SpySwitch construct had the vector backbone pDEST14. The SpyTag-MBP, SpyCatcher003-mi3, and SpyCatcher2-MBP constructs had the vector backbone pET28a. The HexaPro SARS2 Wuhan spike protein had the vector backbone pαH. The twelve sarbecovirus RBD- His8-SpyTag003 constructs had the vector backbone p3BNC. All other proteins expressed in mammalian cells (including all Quartets, merbecovirus RBDS, and SpyTag-RBD derived constructs) had the vector backbone pcDNA 3.1.

2.2 Protein Expression

2.2.1 Bacterial protein expression

Sequence validated plasmids were transformed into *E. coli* BL21(DE3) cells (Agilent). The only exception was the SpySwitch plasmid which was transformed into *E. coli* C41 (DE3), a gift from Anthony Watts (University of Oxford). Transformants were grown overnight on LB-Agar plates with 50 μg/mL kanamycin or 100 μg/mL carbenicillin at 37 °C. A single colony was used to inoculate 10 mL of LB medium containing either 50 μg/mL kanamycin or 100 μg/mL ampicillin depending on the resistance marker of the plasmid used. This starter culture was grown for 16 h at 37 °C with shaking at 200 rpm before being added to 1 L LB containing 50 μg/mL kanamycin or 100 μg/mL ampicillin. This growth flask was cultured at 37 °C and 200 rpm shaking until Optical Density at 600 nm (OD600) reached 0.6-0.8. Protein expression was induced for the culture using 0.5 mM isopropyl β-D-1-thiogalactopyranoside (IPTG). SpyCatcher003-mi3 cultures were grown at 22 °C with shaking at 200 rpm for 16 h. All other cultures were grown at 30 °C with shaking at 200 rpm for 4 h. Cultures were pelleted by centrifugation at 4,000 g.

2.2.2 Expi293F cell maintenance

Expi293F cells (Thermo Fisher, A14635) were cultured under humidified conditions at 37 °C and 8% (v/v) CO2 in Expi293 Expression Medium (Thermo Fisher) with 50 U/mL penicillin and 50 μg/mL streptomycin. Maintenance cells were kept between 0.2 $\times 10^6$ cells/mL and 2.5

$\times 10^6$ cells/mL, by regularly cell passages every 3-4 days. Cells were tested for mycoplasma at least every six months.

2.2.3 Expi293F transfection

All cell culturing for transfection was performed under humidified conditions at 37 °C and 8% (v/v) CO2. For mammalian expression of proteins in Expi293F cells, cells were cultured with 50 U/mL penicillin and 50 µg/mL streptomycin until reaching a concentration of ~3.0 $\times 10^6$ cells/mL. The cells were passaged to a concentration of 2.5 $\times 10^6$ cells/mL. The following day, cells were passaged at concentration of 3.0 $\times 10^6$ cells/mL into fresh Expi293 Expression Medium (Thermo Fisher) without any antibiotic. Transfections were performed using the ExpiFectamine 293 Transfection Kit (Thermo Fisher). 1 µg of plasmid DNA per mL culture was incubated with ExpiFectamine 293 reagent for 20 min, before being added dropwise to the Expi293F culture. After 18-22 h, ExpiFectamine 293 Transfection Enhancers 1 and 2 were added. After 5 days, mammalian cell cultures were centrifuged for 4,000 g at 4 °C for 5 min and supernatants were harvested. The cell supernatants were filtered through a 0.45 µm filter and then a 0.22 µm filter (Starlab). Supernatants were either immediately processed for protein purification using Ni-NTA (Section 2.3.1), SpyDock (Section 2.3.2), or SpySwitch (Section 2.3.4) or were stored at -80 °C.

2.2.4 HEK293 transfection

Due to a brief growth issue with Expi293F cells, SpyTag1-RBD K378Q, and SpyTag1-RBD K378N were expressed in HEK293T cells. A SpyTag1-RBD construct was also expressed in these cells and used for all comparisons to these point mutants.

A T75 adhesive culture flaks (Corning) was seeded with 1-2 million HEK293T. Cells were grown overnight in Dulbecco's Modified Eagle's Medium (DMEM) with 10% (v/v) Fetal Bovine Serum (FBS) and 1% (v/v) Penicillin-Streptomycin at 37 °C with 5% CO_2 . The following day, with the flask at approximately half confluency, the media was removed and

cells were washed twice with 10 mL sterile PBS (137 mM NaCl, 2.7 mM KCl, 10 mM Na_2HPO_4, 1.7 mM KH_2PO_4) pH 7.4. DMEM with 25 mM HEPES was mixed with the plasmid at 30 μg plasmid per 7.5 mL media before being incubated for 5 min at 37 °C. Polyethylenimine (PEI) was added to the mixture at a final concentration of 10 μg/mL. The mixture was incubated for 20 h at 37 °C with 5% CO2 before adding 10 mL DMEM with 25 mM HEPES containing 4.4 μM valproic acid (Sigma-Aldrich), 100 U/mL penicillin, and 100 μg/mL streptomycin. Cells were incubated for 4 days before harvesting the supernatant.

2.3 Protein Purification

2.3.1 Ni-NTA Affinity Purification

SARS-CoV-2 Spike proteins, HuSA, and SpySwitch were purified by nickel-nitrilotriacetic acid (Ni-NTA) affinity chromatography. Purifications were performed at 4 °C. 10× Ni-NTA buffer (500 mM Tris-HCl, 3 M NaCl, pH 7.8) was used to supplement mammalian supernatants or bacterial lysate at 10% (v/v). Econo-Pac Chromatography Columns (Bio-Rad) were packed with Ni-NTA agarose (Qiagen), before being washed with 2 × 10 column volumes (CV) of Ni-NTA buffer (50 mM Tris-HCl, 300 mM NaCl, pH 7.8). Mammalian supernatant or bacterial lysate was incubated in the Ni-NTA column for 1 h at 4 °C with rolling or end-over-end mixing. Supernatant was eluted from the column by gravity, before the column was washed with 2 × 10 CV of Ni-NTA wash buffer (10 mM imidazole in Ni-NTA buffer). A total of six 1 CV elutions were performed by incubating the resin with Ni-NTA elution buffer (200 mM imidazole in Ni-NTA buffer) for 5 min and eluting with gravity. Elution fractions were assessed by SDS-PAGE with Coomassie staining, pooled, and dialysed for 16 h at 4 °C against 1,000-fold excess TBS (pH 7.4 at 25 °C) for spike proteins, PBS pH 7.4 for HuSA, or 50 mM Tris-HCl, 5 mM EDTA, 2 mM tris(2-carboxyethyl)phosphine (TCEP) for SpySwitch.

2.3.2 SpyDock Affinity Purification

SpyDock was used to purify SpyTag-RBD and SpyTag-RBD-ABD035. Mammalian culture supernatant was diluted with 10× TP buffer (250 mM orthophosphoric acid adjusted to pH 7.0 at 25 °C with Tris base). An Econo-Pak column (Bio-Rad) with approximately 1.0 mL of packed SpyDock resin was washed with 2 × 10 CV of 1x TP buffer (25 mM orthophosphoric acid adjusted to pH 7.0 at 25 °C with Tris base). The mammalian culture supernatant was added to the column and incubated at 4 °C for 1 h with rolling or end-over-end mixing. The supernatant was allowed to flowthrough by gravity. The resin was then washed with 2 × 10 CV of TP buffer. The protein of interest was eluted with 2.5 M imidazole in TP buffer adjusted to pH 7.0 at 22 °C (SpyDock Elution Buffer). For each elution step, 1 CV of SpyDock Elution Buffer was added to the resin and incubated for 5 min before being allowed to flow through by gravity. Fractions were analysed using SDS-PAGE with Coomassie staining and fractions containing the protein of interest were dialysed into PBS pH 7.4 at 4 °C.

2.3.3 Production of SpySwitch Resin

SpySwitch was expressed in *E. coli* C41 as outlined in Section 2.2.1. Bacterial cell pellets were resuspended in 20 mL 50 mM Tris-HCl, 300 mM NaCl, pH 7.8 (measured at 25 °C) supplemented with 0.1 mg/mL lysozyme, 1 mg/mL cOmplete mini EDTA-free protease inhibitor (Roche) and 1 mM phenylmethanesulfonyl fluoride (PMSF). This mixture was incubated at 4 °C for 45 min with end-over-end mixing. An Ultrasonic Processor equipped with a microtip (Cole-Parmer) was used to perform sonication on ice. Sonication was performed on the cell pellet for a total of 4 times for 60 s at a 50% duty-cycle (1 s on and 1 s off). Cell debris was cleared from the lysate via centrifugation at 35,000 g for 45 min at 4 °C and the supernatant was retained SpySwitch protein was purified by Ni-NTA as outlined in Section 2.3.1. All elution fractions were pooled and dialysed into 50 mM Tris-HCl, 5 mM EDTA, TCEP pH 8.5 at 4 °C. The SpySwitch protein was run on a HiLoad 16/600 Superdex 75 pg (GE Healthcare)

column. Just prior to loading, 2 mM TCEP was spiked into the sample to account for any oxidization of the TCEP that may have occurred during dialysis. After SEC, elution fractions containing protein were pooled and concentrated to approximately 20 mg/mL using a Vivaspin 20 5 kDa MWCO centrifugal filter (Sartorius). The concentrated protein was reduced in coupling buffer (50 mM Tris-HCl + 5 mM EDTA, pH 8.5) with 1 mM TCEP for 30 min at 25 °C. All subsequent coupling steps were undertaken at 25 °C, protected from light. 20 mg SpySwitch was added per 1 mL of packed SulfoLink Coupling Resin (Thermo Fisher, 20402) in coupling buffer with 1 mM TCEP. Incubation was performed for 30 min with end-over-end rotation, followed by an additional 30 min incubation without rotation. After washing twice with coupling buffer, the resin was blocked with 50 mM L-cysteine in coupling buffer with a 15 min end-over-end incubation followed by a 30 min incubation without rotation. The column was washed with 1 M NaCl, followed by TP buffer, and finally 20% (v/v) ethanol in TP buffer. The coupled resin was stored in 20% (v/v) ethanol in TP buffer.

2.3.4 SpySwitch Affinity Purification

Various RBDs, Quartets and SpyTag-MBP were purified by SpySwitch. Purifications were performed at 4 °C. Cell lysate or mammalian supernatant was supplemented with 10 × SpySwitch buffer (500 mM Tris-HCl pH 7.5 + 3 M NaCl) at 10% (v/v). The pH of this supernatant was tested using Universal pH 1-11 indicator paper (Whatman) to ensure a pH greater than 7.5. SpySwitch resin that was packed in an Econo-Pac Chromatography Column (Bio-Rad) was washed and equilibrated with 2 × 10 CV of SpySwitch buffer (300 mM NaCl, 50 mM Tris-HCl pH 7.5). This supernatant was added to the SpySwitch resin and incubated for 1 h at 4 °C with rolling or end-over-end rotation. The column was washed with 2 × 15 CV SpySwitch buffer. Proteins were eluted using weakly acidic pH elution. The resin was incubated for 5 min with 1.5 CV of SpySwitch Elution Buffer (150 mM NaCl, 50 mM acetic acid/sodium acetate pH 5.0) at 4 °C with the column capped. The cap was removed and the

elution flowthrough was collected into a microcentrifuge tube containing 0.3 CV of neutralization buffer (1 M Tris-HCl pH 8.0). The microcentrifuge tube was immediately mixed by end-over-end inversion. The elution step was repeated for a total of six times. Purification was assessed by SDS-PAGE with Coomassie staining.

2.3.5 SpySwitch Regeneration

Regeneration of SpySwitch columns was performed at 25 °C directly after the final elution. The resin was equilibrated with 1 × 10 CV SpySwitch buffer. First, the resin was treated with 3 × 10 CV of 0.1 M glycine-HCl pH 2.0, incubated for 5 min each time before eluting. The columns were re-equilibrated with 2 × 10 CV SpySwitch buffer. Second, the resin was treated with 3 × 10 CV of 50 mM Tris, 8 M urea, pH 7.5, incubating each time for 5 min. The columns were re-equilibrated with 2 × 10 CV SpySwitch buffer. Third, the resin was treated with 3 × 10 CV of 0.1 M NaOH without incubation. The resin was re-equilibrated in SpySwitch buffer, washed and then stored with SpySwitch Storage buffer (50 mM Tris-HCl pH 7.5, 300 mM NaCl, 20% v/v ethanol).

2.3.6 SpyCatcher003-mi3 Purification

SpyCatcher003-mi3 was expressed in *E. coli* BL21 as outlined in Section 2.2. Bacterial cell pellets were resuspended in 20 mL of 20 mM Tris-HCl, 300 mM NaCl, pH 7.9 (measured at 25 °C) supplemented with 0.1 mg/mL lysozyme, 1 mg/mL cOmplete mini EDTA-free protease inhibitor (Roche) and 1 mM phenylmethanesulfonyl fluoride (PMSF). The solution was incubated with end-over-end mixing at 4 °C for 45 min. An Ultrasonic Processor equipped with a microtip (Cole-Parmer) was used to perform sonication on ice for a total of 4 times for 60 s at a 50% duty-cycle. Cell debris was cleared from the lysate via centrifugation at 35,000 g for 45 min at 4 °C and the supernatant was retained. 170 mg of ammonium sulfate was added to the bacterial lysate for every mL of lysate. The solution was incubated at 4 °C for 1 h, while mixing at 120 rpm. Centrifugation was performed on the solution for 30 min at 30,000 g at 4

°C. The pellet was resuspended in 10 mL mi3 buffer (25 mM Tris–HCl, 150 mM NaCl, pH 8.0) at 4 °C and filtered sequentially through 0.45 µm and 0.22 µm syringe filters (Starlab). This filtrate was dialysed for 16 h against 1,000-fold excess mi3 buffer. The post-dialysis solution was centrifuged at 17,000 g for 30 min at 4 °C, before being filtered through a 0.22 µm syringe filter. The protein sample was loaded onto a HiPrep Sephacryl S-400 HR 16-60 column (GE Healthcare) that had been pre-equilibrated with filtered and degassed mi3 buffer. The column was run using an ÄKTA Pure 25 system (GE Healthcare). The proteins were separated at a rate between 0.1 and 0.5 mL/min while collecting 1 mL elution factions. Absorbance at 280 nm (A280) was recorded and used to determine the presence of protein. The fractions that were determined to contain the purified particles were pooled and concentrated using a Vivaspin 20 100 kDa molecular weight cut-off centrifugal concentrator (Sartorius) and stored at −80 °C.

2.3.7 Size Exclusion Chromatography (SEC)

The protocol for Size Exclusion Chromatography purification of SpySwitch (2.3.3) and SpyCatcher003-mi3 (Section 2.3.6) has already been outlined. Size exclusion chromatography (SEC) was performed on various Quartet constructs. Quartets were loaded onto a HiPrep Sephacryl S-200 HR 16-600 column (GE Healthcare), which was equilibrated with PBS pH 7.4 that had been filtered and degassed. The protein was run over this column using an ÄKTA Pure 25 system (GE Healthcare). The proteins were separated between 0.5 and 1.0 mL/min while collecting 1 mL elution factions. A Gel Filtration Standard (Bio-Rad) containing bovine thyroglobulin (~670 kDa), bovine γ-globulin (~158 kDa), chicken ovalbumin (~44 kDa), horse myoglobin (~17 kDa), and vitamin B12 (~1.35 kDa) was run over the column under the same conditions to allow for comparison. All size exclusion chromatography was performed at 4 °C.

2.4 SDS-PAGE

10 µL of protein solution was mixed with 2 µL 6× SDS loading buffer (234 mM Tris-HCl pH 6.8, 24% (v/v) glycerol, 120 µM bromophenol blue, 234 mM SDS). Samples were heated at

95 °C for 5 min in a C1000 Touch Thermal Cycler (Bio-Rad). A PageRuler Prestained Protein Ladder (Thermo Fisher) or PageRuler Plus Prestained Protein Ladder (Thermo Fisher) was run along with the samples. Samples were loaded onto 12% SDS-PAGE, before staining with Coomassie.

2.5 Site-Specific Biotinylation

HuSA with a C-terminal Avi-tag at ~20 μM was mixed with 5 μL 1 M magnesium chloride, 20 μL 100 mM ATP, 12.8 μL 78 μM GST-BirA and 3 μL 100 mM D-biotin and made up to a final volume of 1 mL with PBS pH 7.4. This mixture was incubated for 1 h at 30 °C. 12.8 μL of 78 μM GST-BirA and 3 μL of 100 mM D-biotin was added for a second time and incubated for an additional 1 h at 30 °C. The protein was dialysed overnight into PBS pH 7.4 at 1,000-fold excess to remove excess biotin. The protein was subsequently run over an S200 column using the protocol outlined in Section 2.3.7. Successful biotinylation was assessed via a biotin gel shift assay. 2 μl of 1 mg/mL streptavidin (New England Biolabs) was mixed with different volumes of post-biotinylation HuSA (0.5, 1.0, and 2.0 μl) and incubated for 10 min at 25 °C. SDS-PAGE was run on the protein without boiling. Successful biotinylation was indicated by an upward shift for the protein in the presence of streptavidin. This protocol was based closely on Fairhead & Howarth, 2015.

2.6 Sarbecovirus SpyCatcher003-mi3 Coupling

For the Figure 3.8 VLP coupling assay, 2 μM sarbecovirus RBD-SpyTag003 protein was incubated for 16 h at 4 °C in neutralized SpySwitch pH elution buffer with 2 μM of SpyCatcher003-mi3. In this and all other cases, the molar concentration of SpyCatcher003-mi3 refers to the concentration of monomeric subunits. Samples were mixed with 6× SDS loading buffer, supplemented with 1 mM DTT, incubated at 95 °C for 10 min. Samples were resolved by 12% SDS-PAGE with Coomassie staining.

2.7 ELISAs

2.7.1 HuSA Binding Assay

Nunc-Immuno 96 MicroWell plates (Thermo Fisher) were coated with 100 µL SpyCatcher002-MBP (5 µg/mL) in TBS (50 mM NaCl, 50 mM Tris-HCl, pH 7.4 at 25 °C) and incubated overnight at 4 °C. Plates were washed three times with TBST (TBS with 0.1% Tween) before being blocked with 300 µL 0.25% (w/v) N,N-dimethylcasein in TBS pH 7.4 and incubated for 2 h at 37 °C. Plates were washed three times with TBST. 100 µL of SpyTag construct of interest was added and incubated for 1 h. SpyTag-RBD-ABD035 and appropriate controls were tested at 3.125 µg/mL while SpyTag-Quartet-ABD05 and appropriate controls were tested at 1.0 µg/mL. Plates were washed three times with TBST before 50 µL of biotinylated HuSA was added at the 0.2 µg/mL and incubated for 1 h at room temperature. Plates were washed three times with TBST. 100 µL Streptavidin conjugated to Horseradish Peroxidase (HRP) (Thermo Scientific) was added at a 1/5,000 dilution in TBS. Plates were incubated for 1 h at room temperature, before being washed six times with TBST. 100 µL of 1-Step Ultra TMB-ELISA Substrate Solution (Thermo Fisher) was added and a time course measurement of absorbance at 652 nm was recorded using a FLUOstar® Omega plate reader (BMG Labtech).

2.7.2 Mouse Antisera ELISAs for Albumin-Hitchhiking Immunizations

Mouse antisera ELISAs were performed on post-prime and post-boost samples for the Albumin-Hitchhiking ELISAs presented in Figure 3.4. SpyCatcher2-MBP in PBS pH 7.4 was adsorbed to the wells of a Nunc-Immuno 96 MicroWell plate (Thermo Fisher) at 80 nM and incubated overnight at 4 °C. Plates were washed three times with PBST (PBS with 1% (v/v) Tween 20). Plates were incubated for 2 h at 37 °C with PBS pH 7.4 with 0.1% BSA. Plates were washed three times with PBST. Plates were incubated for 1 h at 25 °C with 80 nM SpyTag-RBD. Plates were washed three times with PBST. Mouse antisera that had been heat inactivated (30 min incubation at 56 °C) were diluted into PBS pH 7.4 with 0.1% BSA using an 8-point dilution series, starting at 1:40 with three-fold dilutions. Plates were incubated with antisera

for 1 h at 25 °C. Plates were washed three times with PBST. Plates were incubated for 1 h at 25 °C with a 1:1,600 dilution of horseradish peroxidase-conjugated goat anti-mouse IgG antibody (Sigma-Aldrich A9044). Plates were washed three times with PBST. Plates were then incubated at 25 °C for 5 min with 1-Step Ultra TMB-ELISA Substrate Solution (Thermo Scientific) before the reaction was stopped with 1 M H2SO4. A450 measurements were taken with a FLUOstar Omega plate reader (BMG Labtech) using Omega MARS software (BMG Labtech). Data analysis is outlined in Section 2.7.8.

2.7.3 Monoclonal antibodies on VLP presentation of sarbecovirus RBDs

This is the method for the monoclonal antibody ELISA presented in Figure 3.9, where patient-derived antibodies were tested for binding to a panel of sarbecovirus RBDs presented on SpyCatcher003-mi3. 25 nM sarbecovirus RBD-SpyTag003 constructs were incubated with 25 nM SpyCatcher003-mi3 at 4 °C for 48 h in neutralized SpySwitch pH elution buffer. The proteins were adsorbed to the wells of a clear flat-bottom Immuno Nonsterile 96-Well Plate (Thermo Fisher) via incubation for 16 h at 4 °C. Uncoupled SpyCatcher003-mi3 was used for the 'No RBD' control. The wells were washed three times with PBST, before blocking with blocking buffer (5% [w/v] skim milk in PBS pH 7.4) for 2 h at 25 °C. The wells were washed three times with PBST. 50 nM of the specified antibody in blocking buffer was incubated for 1 h at 25 °C. The wells were washed three times with PBST, before incubation with a 1/1,600 dilution of goat anti-human IgG conjugated with HRP (Sigma-Aldrich, A8667) in blocking buffer for 1 h at 25 °C. A final three washes with PBST were performed. 1-Step™ Ultra TMB-ELISA Substrate Solution (Thermo Fisher) was added to the wells. A time-course of A652 measurements was recorded using a FLUOstar Omega plate reader (BMG Labtech) at 25 °C. The mean absorbance from triplicate wells at 6 min is presented as a heat map in Figure 3.9.

2.7.4 Monoclonal antibody ELISAs on RBD point mutants

This is the method for the monoclonal antibody ELISA presented in Figure 3.10, where CR3022 and EY6A antibodies were tested for their ability to bind RBD K378 point mutants. The SpyTag-RBD constructs or the negative control SpyTag-Hemagglutinin were adsorbed directly to the wells of a Nunc-Immuno 96 MicroWell plate (Thermo Fisher) at 80 nM in PBS pH 7.4 overnight at 4 °C. The plate was washed three times with PBST. The wells were incubated with blocking buffer 2 h at 25 °C before being washed three times with PBST. The wells were incubated for 1 h at 25 °C with 80 nM of the specified monoclonal antibody. The plate was washed three times with PBST before incubating for 1 h at 25 °C with 1/1,600 dilution of goat anti-human IgG conjugated with HRP (Sigma-Aldrich, A8667). The plate was washed three times with PBST. 1-Step™ Ultra TMB-ELISA Substrate Solution (Thermo Fisher) was added to the wells, incubated for five min, and stopped with 1 M HCl. Absorbance at 450 nm (A450) were read using a FLUOstar Omega plate reader (BMG Labtech) at 25 °C. The mean absorbance from triplicate wells presented as a heat map in Figure 3.10.

2.7.5 Monoclonal antibody ELISAs on sarbecovirus RBDs

This is the method for the monoclonal antibody ELISA presented in Figure 3.11, where patient-derived primarily Class 4 antibodies are tested for binding to a panel of sarbecovirus RBDs. 50 nM of specified RBD in PBS pH 7.4 were adsorbed to Nunc MaxiSorp flat-bottom plates (Thermo Fisher) by incubating for 16 h at 4 °C. The plates were incubated for 2 h at 25 °C with blocking buffer. The plates were washed three times with PBST and then incubated for 1 h with the specified antibody at 50 nM in Blocking buffer. The plates were washed three times with PBST and then incubated for 1 h at 25 °C with a ½,500 dilution of goat anti-human IgG HRP antibody (Sigma-Aldrich A8667) in Blocking Buffer. The plates were washed three times with PBST. 1-Step™ Ultra TMB-ELISA Substrate Solution (Thermo Fisher) was added to the wells, incubated for 2 min, and stopped with the addition of 1 M sulfuric acid. The absorbance at

450 nm was measured with a FLUOstar Omega microplate plate reader (BMG Labtech). The mean absorbance from triplicate wells is presented at a heat map in Figure 3.11.

2.7.6 Mouse Antisera ELISAs for Quartet Immunizations

This is the mouse antisera ELISA protocol followed for all mouse antisera results in Chapter 4 and Chapter 5. Nunc MaxiSorp plates (Thermo Fisher) were coated with 80 nM purified antigen (RBD, MBP or SpyCatcher003-mi3) in PBS pH 7.4 at 4 °C for 16 h. The only exception was for Figure 4.6 where the plate was coated with 1 µg/mL of the indicated HexaPro Spike protein in PBS. Plates were washed three times with PBST. Plates were blocked by 2 h incubation at 25 °C with blocking buffer. Plates were washed three times with PBS. Mouse antisera that had been heat inactivated (30 min incubation at 56 °C) were serially diluted into the blocking buffer using 8-point, starting at 1:100 and diluting 4-fold at each point. Plates were incubated with sera for 1 h at 25 °C. Plates were washed three times with PBST and incubated at 25 °C for 1 h with a 1/1,600 dilution of horseradish peroxidase-conjugated goat anti-mouse IgG antibody (Sigma-Aldrich A9044). Plates were washed three times with PBST and were then incubated at 25 °C for 5 min with 1-Step™ Ultra TMB-ELISA Substrate Solution (Thermo Scientific). The reaction was stopped with 1 M H2SO4. Absorbance at 405 nm (A405) measurements were taken with a FLUOstar Omega plate reader (BMG Labtech) using Omega MARS software (BMG Labtech).

2.7.7 Analysis for mouse antisera ELISAs

The data obtained using the mouse antisera ELISA methods outlined in Section 2.7.2 and 2.7.6, were treated according to the same procedure. The optimize.curve_fit() function from the Python SciPy library (Virtanen et al., 2020) was used to fit a sigmoidal dose response curve to the absorbance versus sera dilution data. The sigmoidal dose response function was:

$$y = \text{Bottom} + \frac{\text{Top} - \text{Bottom}}{1 + 10^{\log_{10}(\text{IC}_{50}) - x}}$$

The trapz function from the Python Numpy library (C. R. Harris et al., 2020) was used to determine the area under the fitted curve (AUC). Area under the curve was selected as opposed to endpoint titre to better account for data across the entire range of dilution values (Hartman et al., 2018). Results were plotted using GraphPad Prism (GraphPad Software version 9.4.1).

2.7.8 Monoclonal Quartet ELISAs for Quartet Accessibility

This is the methods for the monoclonal antibody ELISA presented in Figure 4.16, where monoclonal antibodies were used to test binding to Quartets. For Quartets displayed on SpyCatcher003-mi3, 2 μM SpyTag-Quartet or 2 μM Quartet-SpyTag was incubated with SpyCatcher003-mi3 in 25 mM Tris–HCl, 150 mM NaCl, pH 8.0 for 16 h at 4 °C to allow for coupling. The protein samples, SpyTag-Quartet or Quartet-SpyTag, with or without SpyCatcher003-mi3 were adsorbed to Nunc MaxiSorp plates (Thermo Fisher) at 50 nM and incubated for 16 h at 4 °C in PBS pH 7.4. The plates were washed three times with PBST and incubated with blocking buffer for 2 h at 25 °C. The plates were washed three times with PBST and incubated for 1 h at 25 °C, with 50 nM of the specified antibody. The plates were washed three times with PBST, and incubated with a 1/2,500 dilution of anti-human IgG horseradish peroxidase (Sigma-Aldrich A8667) for 1 h at 25 °C. The plates were washed three times and incubated with TMB for 2 min (for comparison of SpyTag-Quartet and Quartet-SpyTag) or 30 s (for comparison of coupled and uncoupled Quartet) before the reaction was stopped with 1M HCl. A405 measurements of triplicate wells per condition were taken at 25 °C with a FLUOstar Omega plate reader (BMG Labtech) using Omega MARS software (BMG Labtech).

2.8 Immunogen Preparation

2.8.1 Endotoxin Depletion and Quantification

Removal of endotoxin from all vaccine components was accomplished using Triton X-114 phase separation (Aida & Pabst, 1990b; K. D. Brune et al., 2016). 1% (v/v) Triton X-114 was incubated with the protein of interest on ice for 5 min. The solution was then incubated for 5

min at 37 °C. The solution was centrifuged for 1 min at 16,000 g at 37 °C and the top phase was transferred to a fresh tube. This procedure was repeated according to these specifications for a total of three times. The procedure was repeated a fourth time without the addition of Triton X-114, to reduce residual Triton-X114. A LAL assay was performed using a Pierce Chromogenic Endotoxin Quant Kit (Thermo Fisher) in order to quantify the final endotoxin concentration. All vaccine components were below the accepted endotoxin levels of 20 Endotoxin Units (EU) per mL for pre-clinical protein subunit vaccine products (Brito & Singh, 2011). All endotoxin depletion and quantification steps were performed using filtered tips and pyrogen-free microcentrifuge tubes.

2.8.2 Immunogen Preparation

Concentration of all vaccine components was determined using a Bicinchoninic acid (BCA) assay (Pierce). When multiple antigens were coupled to the same SpyCatcher003-mi3, the antigens were first mixed in equimolar amounts. Doses were normalized by the number of SpyTags, to allow for each condition to have an equimolar amount of SpyCatcher003-mi3 nanocages with similar occupancy. SpyTag-RBD and SpyTag-RBD-ABD035 immunogens were aliquoted at equimolar levels so that each 25 µL dose contained 10 µg of SpyTag-RBD or 12.25 µg SpyTag-RBD-ABD035 (Figure 3.4). For "High Dose" Quartet immunizations (Figure 5.2-5.4), SpyTagged antigen at a total of 8 µM was incubated with SpyCatcher003-mi3 at 8 µM for 48 h at 4 °C in TBS pH 8.0. For other Quartet immunizations, 0.8 µM total SpyTagged antigen was incubated with SpyCatcher003-mi3 at 0.8 µM for 48 h at 4 °C in TBS, pH 8.0. Uncoupled RBD and Uncoupled Quartet were incubated at 0.8 µM for 48 h at 4 °C in TBS pH 8.0, without the addition of SpyCatcher003-mi3. Prior to immunization, samples were analysed by SDS-PAGE/Coomassie and Dynamic Light Scattering. For Figure 4.19-4.21, SARS2 Spike prime and boost doses were performed with 10 µg SARS2 Wuhan Spike (HexaPro) protein in TBS pH 8.0 at 4 °C.

2.8.3 Immunization

Animal experiments were performed according to the UK Animals (Scientific Procedures) Act 1986, under Project License (PBA43A2E4 and PP9362617), and approved by the University of Oxford Animal Welfare and Ethical Review Body. Mice were obtained from Envigo and were 6 weeks old at the time of the first immunization. For high dose immunizations (Figure 5.2-5.4), BALB/c female mice were used. For all other immunizations we used C57BL/6 female mice. Mice were housed in accordance with the UK Home Office ethical and welfare guidelines and fed on standard chow and water ad libitum.

Prior to immunization, immunogens were mixed 1:1 (25 µL + 25 µL) with either AddaVax (Invivogen) for Albumin Hitchhiking immunizations (Figure 3.4) and High Dose Quartet (Figure 5.2-5.4) immunizations or with VAC 20 adjuvant (SPI Pharma) for all other immunogens. For albumin hitchhiking constructs this gave a final dose of 0.4 nmol SpyTagged antigen. For High Dose Quartet immunizations this gave a final dose of 0.2 nmol total SpyTagged antigen. For all other Quartet immunizations this gave a final dose of 0.02 nmol total SpyTagged antigen, which relates to 0.6 µg Uncoupled RBD. Isoflurane (Abbott)-anesthetized mice were immunized on day 0 and day 14 intramuscularly in the gastrocnemius muscle with the specified antigen-adjuvant mix. On day 14, post-prime blood samples were obtained via tail vein using Microvette (CB300, Sarstedt) capillary tubes. On day 32 to 41 (the exact day for each set of immunizations is indicated in the figure) post-boost samples were obtained via cardiac puncture of humanely sacrificed mice. The collected whole blood in microtainer SST tubes (Becton Dickinson) was allowed to clot at 25 °C for 1-2 h, before spinning down at 10,000 g for 5 min at 25 °C. All immunizations and sera sampling were performed by Jack Tan (University of Oxford). The sera were heat-inactivated at 56 °C for 30 min, before storing at −20 °C.

2.9 Peptide:N-glycosidase (PNGase) Digest Assay

2 µg of Quartet protein was incubated with 1 µL 10 × Glycoprotein Denaturing Buffer (New England Biolabs) at 100 °C for 10 min using a C1000 Touch Thermal Cycler (Bio-Rad). The denatured protein was then chilled on ice for 1 min and centrifuged for 10 s at 2,000 g with a MiniStar silverline (VWR). 2 µL 10×GlycoBuffer 2 (New England Biolabs), 2 µL 10% (v/v) NP-40, 6 µL MilliQ water and 1 µL PNGase F (New England Biolabs) at 500,000 units/mL were added. This mixture was incubated at 37 °C for 1 h. Proteins were resolved on 12% SDS-PAGE, stained with Coomassie.

2.10 Dynamic Light Scattering (DLS)

2 µM SpyCatcher003-mi3 was incubated with 2 µM SpyTag-antigens for 48 h at 4 °C. 45 µL of protein solution was centrifuged for 30 min at 16,900 g at 4 °C and 30 µL of the supernatant was loaded into a quartz cuvette. Samples were measured using a Viscotek 802 (Viscotek) at 20 °C with 20 scans of 10 s each, using 50% laser intensity, 15% maximum baseline drift, and 20% spike tolerance. Before data collection, the cuvette was incubated in the instrument for 5 min to allow the sample temperature to stabilize. The intensity of the size distribution was normalized to the peak value using OmniSIZE version 3.0 software, calculating the mean and standard deviation from the multiple scans (Viscotek).

2.11 Negative Stain Transmission Electron Microscopy (TEM)

2 µM SpyCatcher003-mi3 was incubated with 2 µM of the appropriate antigen for 48 h at 4 °C to make Mosaic-8 and Quartet Nanocage. Incubation was performed in 25 mM Tris–HCl, 150 mM NaCl, pH 8.0. For uncoupled SpyCatcher003-mi3 Nanocage sample, the incubation was performed without the addition of any SpyTagged antigen. Samples were applied to a freshly glow-discharged TEM grid and blotted twice with water. Samples were stained with 2% (w/v) uranyl acetate for 30 s. Samples were imaged using a Tecnai G2 80-200 keV

transmission electron microscope at the Cambridge Advanced Imaging Centre. The particle diameter was measured manually (n = 75) and plotted with 2 nm bin size in Excel (Microsoft).

2.12 Viral Neutralization

2.12.1 Authentic Virus Neutralization

These assays were performed by Sai Liu, Javier Gilbert-Jaramillo, and William S. James at the James & Lillian Martin Centre, University of Oxford, operating under licence from the Health and Safety Authority, UK, on the basis of an agreed Code of Practice, Risk Assessments (under the Advisory Committee on Dangerous Pathogens) and standard operating procedures.

The authentic virus neutralization assay determines the serum concentration required to induce a 50% reduction in focus-forming units of SARS2 in Vero cells (American Type Culture Collection, CCL-81). A serial dilution of immunization sera (seven steps from 1/40 to 1/40,000 diluted into DMEM) was pre-incubated for 30 min at 25 °C with a fixed dose of 100-200 focus-forming units (20 μL) of the specified SARS-CoV-2 variant. This procedure was performed in quadruplicate. DMEM alone was used for serum-free control wells and was used to define 100% infectivity. The Victoria 01/2020 isolate (Pango B) was used for Wuhan neutralization (Caly et al., 2020). The isolate for Delta (Pango B.1.617.2) was kindly supplied by Gavin Screaton (University of Oxford). This mixture of virus and sera was incubated with 100 μL of Vero cells (4.5 × 104) at 37 °C with 5% (v/v) CO2. After 2 h incubation, a 1.5% (w/v) carboxymethyl cellulose-containing overlay was applied in order to prevent satellite focus formation. After 18 h incubation, the monolayers were fixed with 4% (w/v) paraformaldehyde in PBS and then permeabilized with 2% (v/v) Triton X-100. The cells were stained using 1 μg/mL of the FB9B monoclonal antibody (K.-Y. A. Huang et al., 2021). These samples were treated with a 1:5,000 dilution of anti-human IgG (Fc-specific) peroxidase-conjugated antibody (Sigma-Aldrich, A0170-1ML) and True Blue peroxidase substrate. The infectious foci were counted using a Classic ELISpot Reader (AID GmbH). Data were analysed using four-

parameter logistic regression (Hill equation) using GraphPad Prism (GraphPad Software version 8.3). A one-way analysis of variance (ANOVA) test, followed by Tukey's multiple comparison post hoc test of ID50 values converted to log10 scale using GraphPad Prism (GraphPad Software version 9.4.1) was used to determine statistical significance of differences between groups.

2.12.2 Pseudovirus Neutralization

These assays were performed by Jennifer R. Keeffe, Kaya N. Storm, Priyanthi N. P. Gnanapragasam with supervision provided by Pamela Bjorkman (California Institute of Technology).

Pseudotyped viruses for SARS2 BQ.1.1, SARS1, WIV1, SHC014, and BtKY72 K493Y/T498W were prepared as previously described (Crawford et al., 2020; Robbiani et al., 2020). The BtKY72 Spike protein was modified with the double mutation K493Y/T498W in order to enable entry to human cells via ACE2 (Starr et al., 2022). This pseudovirus technique employs HIV-based lentiviral particles with genes encoding the appropriate Spike protein lacking the cytoplasmic tail. Pseudotyped virus was incubated for 1 h at 37 ˚C with sera that underwent a serial dilution with threefold steps. The sera and pseudovirus mixture was incubated with 293TACE2 target cells for 48 h at 37 ˚C. Cells were washed twice with PBS, and then lysed with Luciferase Cell Culture Lysis 5× reagent (Promega). The Nano-Glo Luciferase Assay System (Promega) was used to measure NanoLuc Luciferase activity in the lysates. The relative luminescence units (RLUs) were normalized to values derived from cells infected with pseudotyped virus in the absence of serum. 4-parameter nonlinear regression in AntibodyDatabase (West et al., 2013), was used to determine half-maximal inhibitory dilution (ID50). These values were plotted using GraphPad Prism (GraphPad Software version 9.4.1). Statistical significance of differences between groups was determined using an ANOVA test,

followed by Tukey's multiple comparison post hoc test of ID50 values converted to log10 scale using GraphPad Prism (GraphPad Software version 9.4.1).

2.13 Deep Mutational Scanning (DMS)

Deep Mutational Scanning assays were performed by Alexander Cohen, Annie Rorick, and Anthony West, Jr. with supervision provided by Pamela Bjorkman (California Institute of Technology) following a previously established approach (A. A. Cohen et al., 2022; Greaney et al., 2022). All sera used in this assay had previously been heat-inactivated using a 30 min incubation at 56 °C. The sera were depleted of non-specific yeast-binding antibodies by twice incubating with 50 optical density (OD) units of AWY101 yeast containing an empty vector. Yeast were generously provided by Tyler Starr (University of Utah) and were induced to express the SARS-CoV-2 RBD library in galactose-containing synthetic defined medium with 6.7 g/L Yeast Nitrogen Base, 5.0 g/L Casamino acids, 1.065 g/L 2-(N-morpholino)ethanesulfonic acid (MES), 2% (w/v) galactose and 0.1% (w/v) dextrose (Greaney et al., 2022). After a 16–18 h induction, cells were washed and incubated for 1 h at 25 °C along with serum at a range of dilutions under gentle agitation. A sub-saturating dilution was determined for each serum sample that enabled the fluorescent signal from antibody binding to be equivalent across samples. The libraries were washed and labelled for 1 h with 1:200 Alexa Fluor-647-goat anti-mouse-IgG Fc-gamma (Jackson ImmunoResearch 115-605-008) to detect mouse antibodies from serum and 1:100 fluorescein-conjugated anti-myc tag antibody (Immunology Consultants Lab, CYMC-45F) to quantify RBD expression. Approximately, 5×10^6 RBD-positive yeast cells were processed on a SH800 cell sorter (Sony). A flow cytometric gate was drawn to for yeast with RBD mutants that demonstrated reduced antibody binding compared to their level of RBD expression (Greaney et al., 2022). These cells were grown overnight in a synthetic defined medium with 6.7 g/L Yeast Nitrogen Base, 5.0 g/L Casamino acids, 1.065 g/L MES, 2% (w/v) dextrose, 100 U/mL penicillin and 100 µg/mL streptomycin.

Plasmid samples were prepared from 30 OD units (1.6 × 108 colony forming units; cfu) of pre-selection yeast populations and 5 OD units (~3.2 × 107 cfu) of overnight cultures of serum-escaped cells (Zymoprep Yeast Plasmid Miniprep II). The 16-nucleotide barcodes identifying each RBD variant were amplified by PCR and sequenced on an Illumina HiSeq 2500 using 50 bp single-end reads. Variants with >1 amino acid mutation, low sequencing counts, or highly deleterious mutations that might escape antibody binding because of poor RBD expression or folding were computationally filtered out. The escape fraction is the proportion of cells expressing that specific variant that falls in the escape bin. An escape fraction value of 0 means that the variant is always bound by serum antibody and an escape fraction value of 1 means that the variant always escapes serum antibody binding. The height of each letter in the logo plots indicates the escape fraction for that amino acid mutation, calculated as described above. The static logo plots feature any site where, for at least one serum sample, the site-total antibody escape was >10× the median across all sites and at least 10% the maximum of any site. RBD sites are categorized based on antibody epitope region (Barnes et al., 2020). Class 1 epitopes are defined as residues 403, 405, 406, 417, 420, 421, 453, 455–460, 473–478, 486, 487, 489, 503 and 504. Class 2 epitopes are defined as residues 472, 479, 483–485 and 490–495. Class 3 epitopes are defined residues 341, 345, 346, 354–357, 396, 437-452, 466–468, 496, 498–501 and 462. Class 4 epitopes are defined as residues 365–390 and 408.

2.14 Bioinformatics

MEGA X version 11.0.13 software (K. Tamura et al., 2021) was used to determine the phylogenetic tree of sarbecovirus and merbecovirus RBD sequences using an unweighted pair group method with arithmetic mean (UPGMA) method. Multiple sequence alignment and calculation of amino acid identity was performed using Clustal Omega version 1.2.4 (Madeira et al., 2019).

2.15 Statistics

There was no statistical method used to predetermine sample size. When only two conditions are tested (Quartet vs. Quartet-ABD035, Quartet vs. No Linker Quartet, Quartet vs. 2017 Quartet), the significance for ELISAs was calculated using a one-way ANOVA with Bonferroni's test in GraphPad Prism (GraphPad Software version 9.4.1). Significance for all other ELISAs was calculated with an ANOVA test using Tukey's post hoc test in GraphPad Prism (GraphPad Software version 9.4.1). Comparisons for neutralizations were calculated with an ANOVA test, followed by Tukey's multiple comparison post hoc test of ID50 values converted to log10 scale with GraphPad Prism (GraphPad Software version 9.4.1). Stars for figures were assigned according to: * $p < 0.05$, ** $p < 0.01$, *** $p < 0.001$. On graphs where statistical tests were performed, where no test is marked the difference was non-significant. The experiments were not randomized and the investigators were not blinded to allocation during experiments and outcome assessment.

2.16 Software

Annealing temperatures for PCRs were calculated using the NEB Q5 Tm calculator (Version 1.16.5). For gene assembly from primers, constituent primers were identified using DNAWorks version 3.2.4 (Hoover, 2002). Gel analysis was performed using ImageLab version 6.1.0 software (Bio-Rad) or iBright Analysis Software Version 5.2.0 (Thermo Fisher). DLS analysis was performed using the OmniSIZE version 3.0 software.

For mammalian expression constructs, signal peptide cleavage was predicted by SignalP (version 5.0 or 6.0) (Almagro Armenteros et al., 2019; Teufel et al., 2022). Final protein sequences, with the N-terminal fMet (bacterial expression) or signal peptide (mammalian expression) removed, were analysed using ExPASy ProtParam (Gasteiger et al., 2005). ExPASy ProtParam was used to determine a variety of properties including molecular weight, extinction coefficient, and theoretical isoelectric point. PyMOL version 2.5.2 was used for

visualization of protein structures. ChemDraw JS (version 19.0, PerkinElmer) was used for visualizing chemical reactions.

Curve fitting for ELISA results was performed using the Python (version 3.9.7) SciPy library (version 1.7.1) (Virtanen et al., 2020). For authentic virus neutralizations, infectious foci versus sera dilution data were curve fit using GraphPad Prism (version 8.3). For pseudovirus neutralizations, RLUs versus sera dilution data were curve fit using GraphPad Prism (version 9.4.1). All ELISA, pseudovirus neutralization, and authentic virus neutralization graphs presented in this thesis were plotted using GraphPad Prism (version 9.4.1).

Chapter 3 – SpyTag Facilitates Purification and Nanoassembly for Vaccine Development

The COVID-19 pandemic spurred an unprecedented global drive towards the development of a protective vaccine. The unified focus of scientists, regulators, and funding bodies contracted the typical 5–10-year timeline for clinical development and approval of vaccines. Several COVID-19 vaccines had received approval for clinical use within less than a year of the first detection of the SARS-CoV-2 virus (Daems & Maes, 2022; Excler et al., 2023; Krammer, 2024).

The experience of vaccine development during the COVID-19 pandemic highlights the importance of technologies that can speed vaccine research and development. Given the impact of vaccines on public health outcomes, any innovations that can streamline vaccine development for newly emerging diseases or difficult to target existing pathogens can have enormous downstream effects (Gouglas et al., 2023; Pollard & Bijker, 2021; P. Singh et al., 2023).

In this chapter I will explore the use of the SpyTag, SpyCatcher, and related proteins to advance efficient vaccine research.

I will apply SpyDock for the Spy&Go affinity purification of a new COVID-19 vaccine candidate that uses albumin hitchhiking to substantially increase the immune response that is elicited. I will pilot the use of SpySwitch, a next generation of Spy&Go purification technology, to purify a panel of sarbecovirus RBDs. Many of these RBDs either have zoonotic crossover potential or have already infected humans. I will demonstrate that each of these RBDs can be efficiently multimerized on the SpyCatcher003-mi3 nanoparticle in a modular manner that does not require optimization.

Finally, I will apply this panel of sarbecovirus RBDs to assess the breadth of binding for antibodies isolated from COVID-19 patients or vaccine recipients. These experiments identified two broad-spectrum monoclonal antibodies that bound to all tested sarbecoviruses. The identification of broadly binding monoclonal antibodies provides therapeutic potential and a goal for future vaccine development.

3.1 – Harnessing albumin-binding domains for COVID-19 vaccine development

I cloned a SARS-CoV-2 RBD construct with an N-terminal SpyTag and C-terminal ABD035 albumin-binding domain. ABD035 is an engineered protein that had previously been evolved from an albumin-binding domains in streptococcal protein G (G148-GA3) using phage display to select for high affinity binding to human serum albumin (HuSA). This selection was successful, with the three-helix bundle protein displaying femtomolar (50-500 fM) affinity for human serum albumin (HuSA), as well as strong cross-species albumin-binding (Jonsson et al., 2008).

I expressed this SpyTag-RBD-ABD035 protein along with SpyTag-RBD in Expi293F cells. I purified both constructs using the SpyDock system, eluting with 2.5 M imidazole. The bands on both purification gels were disperse and migrated slightly larger than predicted, which aligns with the expected glycosylation of RBD (Figure 3.1). After dialysing into PBS pH 7.4 to remove excess imidazole, I performed size exclusion chromatography (SEC) using an S200 column to remove any aggregate and demonstrated that a single dominant population was present for each antigen (Figure 3.2). As expected, the SEC trace suggested that SpyTag-RBD-ABD035 was larger than SpyTag-RBD.

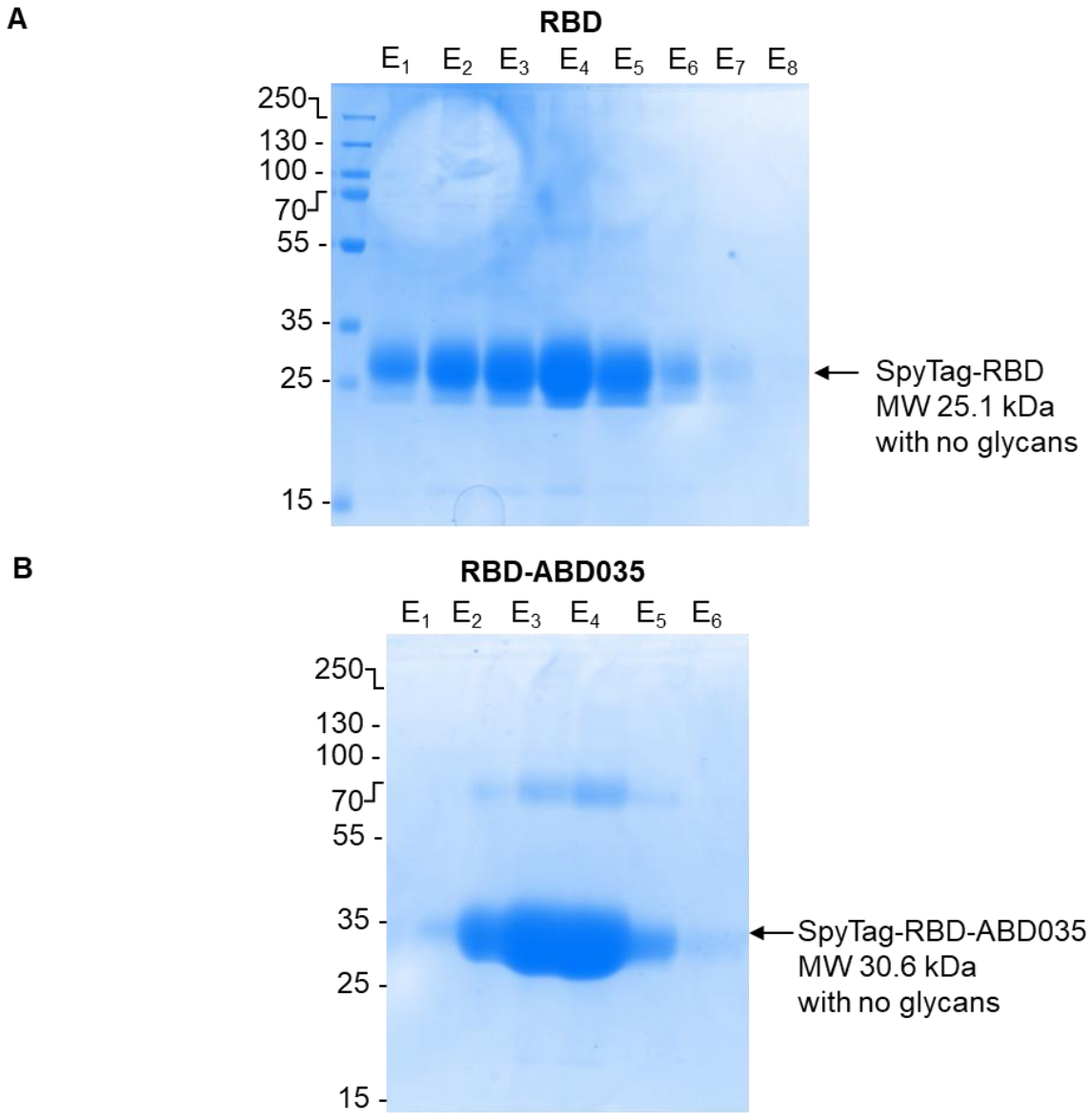

Figure 3.1: SpyDock Purification of RBD with an albumin-binding domain. (A) SARS-COV-2 WA1 RBD with an N-terminal SpyTag was purified by SpyDock. **(B)** The SpyTag-RBD construct with an additional engineered albumin-binding domain genetically fused at the C-terminus was purified by SpyDock. For all purifications, elution fractions were run on SDS-PAGE with Coomassie staining under non-reducing conditions.

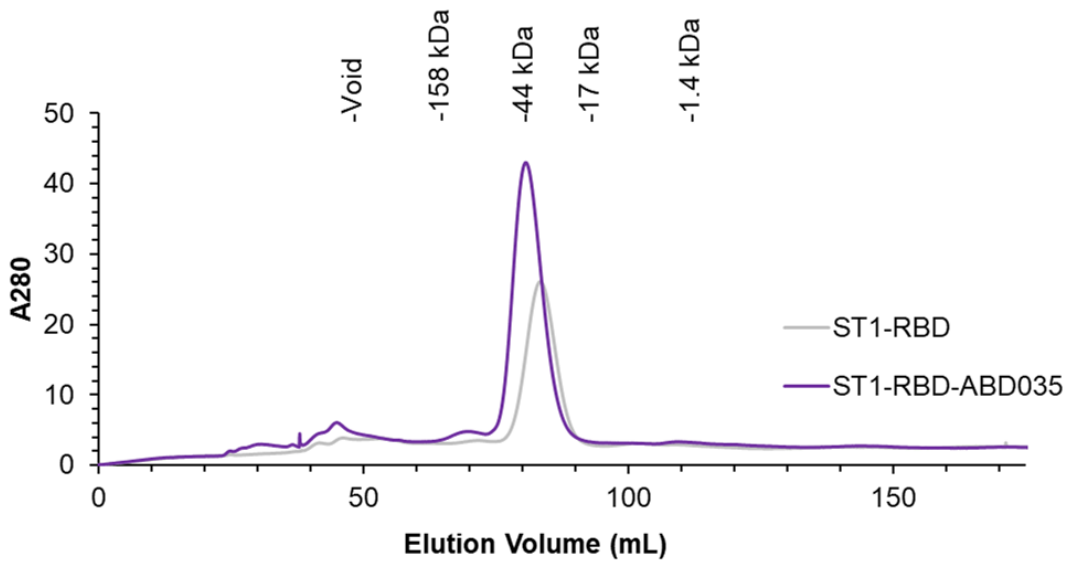

Figure 3.2: Size Exclusion Chromatography of RBD with an albumin-binding domain. SARS-CoV-2 RBD constructs with N-terminal SpyTag (ST1) were run over a HiPrep Sephacryl S-200 HR 16-600 column in PBS pH 7.4 after purification by SpyDock. One of these constructs had a C-terminal albumin-binding domain (ST1-RBD-ABD035) and one had no additional C-terminal domain (ST1-RBD). Bio-Rad gel filtration standards were run over the same column under the same conditions and the elution volume based on these standards are presented.

The ABD035 engineered albumin-binding domain had previously been well characterized for high affinity binding to both human and mouse serum albumin (Jonsson et al., 2008). I wanted to ensure that genetic fusion to RBD had not induced misfolding, caused steric hindrance, or prevented albumin-binding by any other means. To this end, I developed a plate assay to assess albumin-binding to SpyTag-RBD constructs. In this assay, the protein of interest was immobilized on the plate using SpyCatcher002-MBP. This step was included to remove potential variability caused by certain regions of the analysed protein having enhanced interactions with the plate. Albumin binding was assessed using a biotinylated HuSA that was subsequently detected using streptavidin-HRP. To implement the plate assay, I cloned and expressed a human serum albumin construct with a C-terminal Avi-tag to facilitate site-specific biotinylation using BirA (Fairhead & Howarth, 2015).

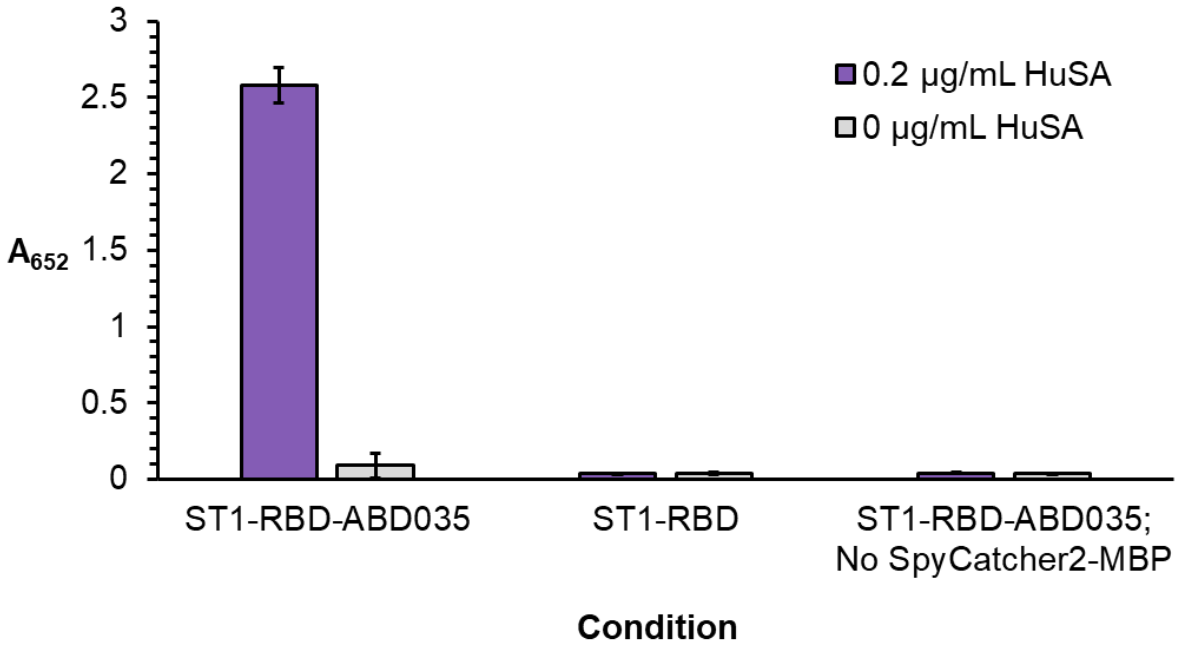

Figure 3.3: Confirmation of albumin-binding by RBD with an albumin-binding domain. Results of the albumin-binding ELISA. Unless otherwise indicated, SpyCatcher2-MBP was coupled to all wells. After adsorption and blocking the indicated antigen was coupled to the well. Bars represent the mean absorbance at 652 nm (A652) measurement 5 minutes after the addition of TMB (n=3) while the error bars are ±1 standard deviation.

When SpyTag-RBD-ABD035 was assessed using the outlined plate assay there was a substantial colour change in the presence of biotinylated HuSA, indicating that SpyTag-RBD-ABD035 has retained its ability to bind albumin (Figure 3.3B). There was no evidence of HuSA biding to SpyTag-RBD (Figure 3.3B).

I prepared samples of SpyTag-RBD and SpyTag-RBD-ABD035 for immunization by endotoxin-depletion with Triton-X114 phase separation (Aida & Pabst, 1990). I performed endotoxin quantification using a Limulus amebocyte lysate assay. All samples were under 20 EU/mL, the maximum recommended endotoxin levels for recombinant subunit vaccines (Brito & Singh, 2011).

Immunizations were performed with either SpyTag-RBD or SpyTag-RBD-ABD035 in female C57BL/6 mice. I aliquoted immunization doses so that each immunization contained a molar equivalent of 0.4 nmol antigen (10 µg of SpyTag-RBD and 12.25 µg SpyTag-RBD-ABD035)

and AddaVax was used as an adjuvant. Immunizations were performed according to the timeline outlined in Figure 3.4A. All immunizations and sera sampling were performed by Jack Tan (University of Oxford).

I performed antisera ELISAs to determine the results of the mouse immunizations. Prime sera samples showed little detectable response to RBD and there was no significant difference between the two antigens (Figure 3.4C). For both antigens, boost sera demonstrated a significantly enhanced immune response to RBD relative to prime sera (Figure 3.4C). SpyTag-RBD-ABD035 elicited a significantly greater anti-RBD humoral response than SpyTag-RBD (Figure 3.4B,C).The mean area under curve (AUC) for mice immunized with SpyTag-RBD was 2.0 and with SpyTag-RBD-ABD035 was 5.3 meaning that the inclusion of a C-terminal ABD035 more than doubled the AUC for antisera dilution curves.

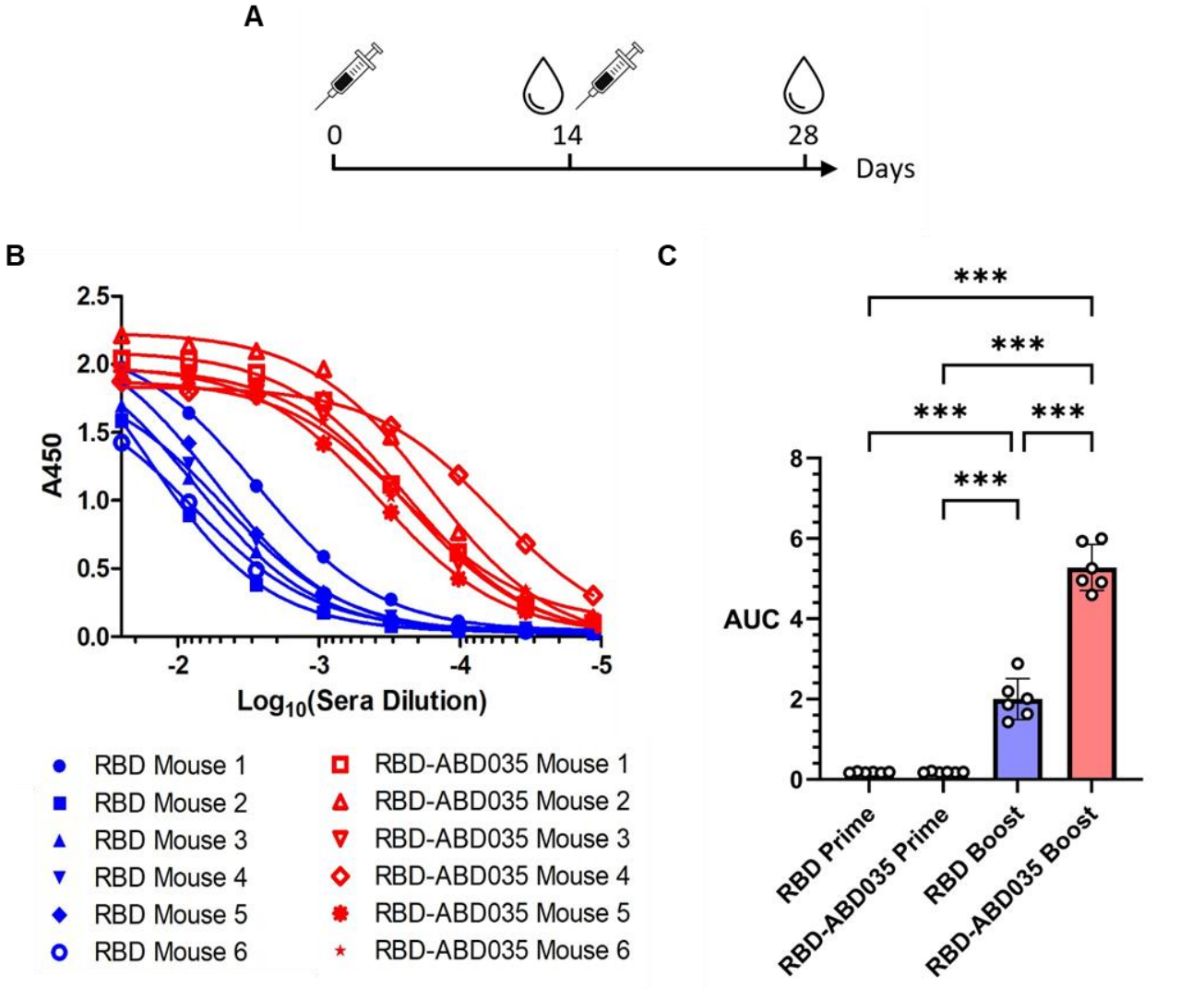

Figure 3.4: Mouse Immunization with RBD fused to Albumin-binding Domain. (A) Dose administration and sampling timeline for female C57BL/6 mice immunization with soluble RBD and RBD-ABD035. **(B)** Post-boost mouse antisera dilution series using A450 to measure antisera binding to RBD. Each point represents a mean of two absorbances for a single mouse at a single dilution. Points and curves are coloured blue for mice administered RBD and red for mice administered RBD-ABD035. **(C)** The area under the curve (AUC) for post-prime and post-boost antisera elicited by administration of RBD (blue) and RBD-ABD035 (red). Bars represent mean AUC (n=6) with error bars being ±1 standard deviation. Individual points represent the AUC for a single mouse. Significance was calculated with an ANOVA test using Tukey's post hoc test. *P < 0.05, **P < 0.01, ***P < 0.001; other comparisons were non-significant.

3.2 – SpySwitch purification of sarbecovirus RBDs with moderate pH elution

Adoption of the SpyTag/SpyCatcher system for a wide variety of applications (Keeble & Howarth, 2020), has enhanced the desire for a switchable system to isolate SpyTagged proteins. This approach would allow for purification of proteins functionalized by SpyTag (or a more

recent iteration such as SpyTag003) without any additional purification tags. Affinity purification via SpyTag has been named Spy&Go (Khairil Anuar et al., 2019).

SpyDock was previously developed by members of our lab and was the Spy&Go purification system I used to purify SpyTag-RBD and SpyTag-RBD-ABD035. SpyDock is a modified version of SpyCatcher002 (Keeble et al., 2017) that included an E77A mutation Khairil Anuar et al., 2019). By removing this catalytic residue SpyDock is unable to form a covalent bond with a SpyTag. An additional S49C mutation was introduced to allow anchoring of SpyDock to SulfoLink resin. SpyDock forms a tight, non-covalent interaction with SpyTag, facilitating capture even at low levels from a mixed supernatant. However, the release requires harsh conditions such as 2.5 M imidazole or pH 2 that induce global disruption of SpyDock and have the potential to perturb the protein being purified (Khairil Anuar et al., 2019).

To address this issue members of our lab (Rolle Rahikainen, Irsyad N. A. Khairil Anuar, and Susan K. Vester,) developed a new protein, named SpySwitch, to facilitate Spy&Go purification using gentler elution conditions. SpySwitch was based on SpyCatcher003 with a total of ten mutations added. These included the E77A and S49C mutation previously included in SpyDock (Vester et al., 2022).

Four mutations (K28H, S30H, Y84H and E85H) were introduced based on histidine mutations scanning. In these experiments, rationally determined residues were mutated to histidine and mutants were assessed for their ability to bind SpyTag003-sfGFP at pH 8.0 and release the protein with sequential elutions at pH 6.0, pH 5.0 and pH 4.0 (Vester et al., 2022).

An additional four mutations (R32H, S59T, V94I, A111P) were identified by phage display. In this directed evolution campaign, an intermediate form of SpySwitch was randomized by error-prone PCR and displayed on phage. Phage were selected for their ability to bind SpyTag003-MBP at pH 8.0 and release the bait at a lower pH. The stringency of this release step was

increased over the course of the selections beginning at pH 5.0 and being raised to pH 7.0 by the final selections (Vester et al., 2022).

The final SpySwitch protein facilitates purification of proteins with SpyTag or SpyTag003 from bacterial and mammalian supernatant with high yield, efficiency, and purity. SpySwitch purification can be accomplished using pH elution where binding occurs at pH 8.0 and elution occurs at pH 5.0. Proteins purified by SpySwitch are eluted directly into a basic neutralization buffer so that the protein spends minimal time at this moderately acidic pH. SpySwitch purification can also be accomplished using temperature change for elution. In this protocol, binding occurs at 4 °C, elution occurs at 37 °C, and the protein is kept at pH 8.0 through the entire purification process (Vester et al., 2022).

I expressed the SpySwitch protein in *E. coli* C41 (DE3) cells and purified the protein by Ni-NTA (Figure 3.5A). SpySwitch (like most SpyCatcher derived proteins) has a tendency to run slightly larger than expected on SDS-PAGE, which may be linked to the low pI of SpyCatcher (Bio-Rad Laboratories, 2023) repelling SDS from binding (Tiwari et al., 2019).

I pooled all elution fractions and dialysed into 50 mM Tris-HCl, 5 mM EDTA, 2 mM Tris(2-carboxyethyl) phosphine hydrochloride (TCEP) (pH 8.5 at 25 °C). The reducing agent TCEP was included to decrease the potential dimerization through the S49C mutation present in the SpySwitch. I ran the SpySwitch protein over an HiLoad 16/600 Superdex 75 pg column size exclusion chromatography column, producing a single peak consistent with the SpySwitch monomer (Figure 3.5B). Just prior to loading on the SEC column, I added 2 mM TCEP to the sample to account for any oxidization of the TCEP that may have occurred during dialysis. I ran elution fractions on a non-reducing SDS-PAGE gel and found a single population providing

further evidence for the identity of the protein (Figure 3.5B). I pooled elution fractions from the major SEC peak and coupled the SpySwitch protein to SulfoLink Coupling Resin beads.

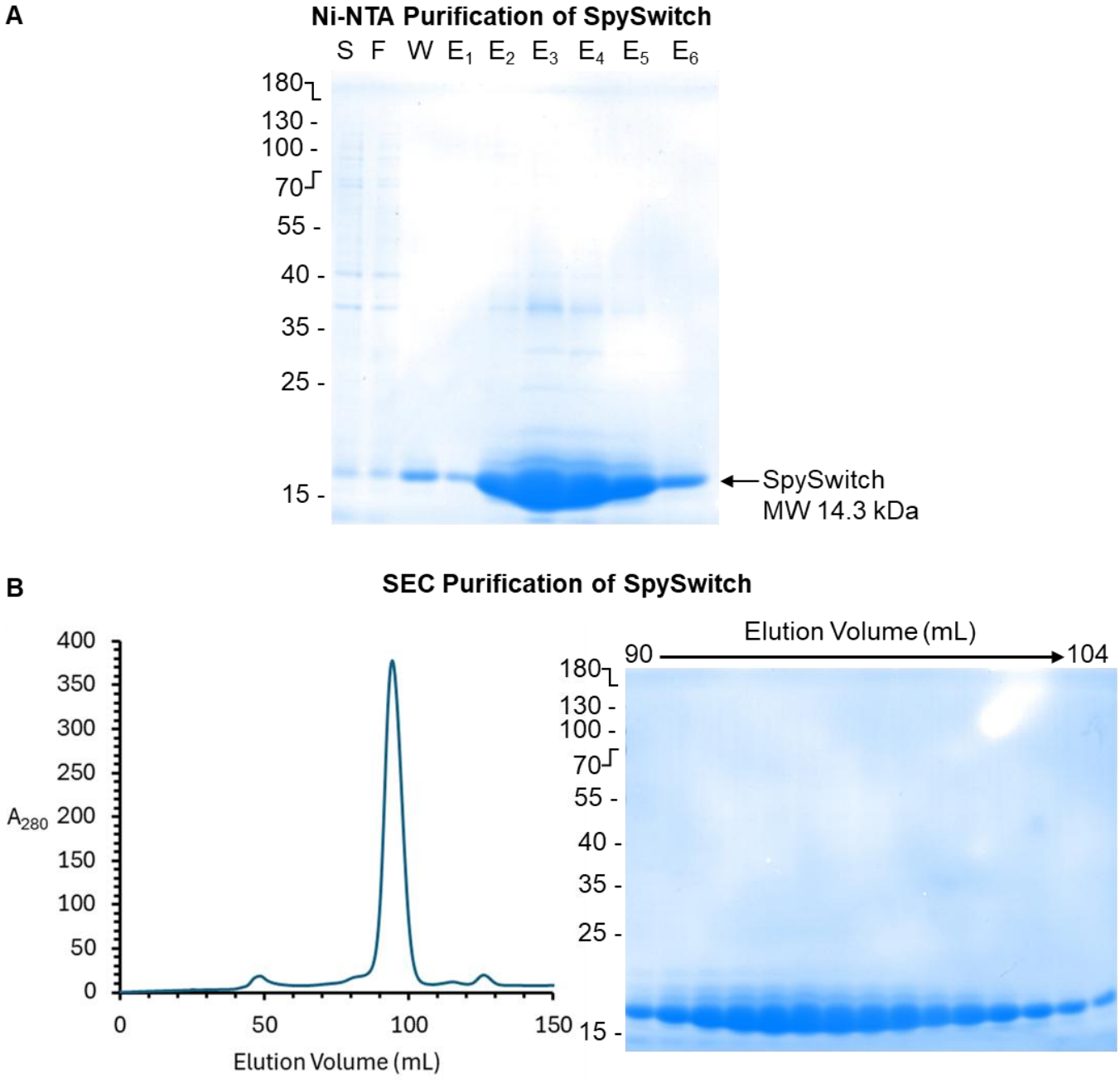

Figure 3.5: Production of SpySwitch. (A) SpySwitch was purified from *E. coli* C41 (DE3) expression strain by Ni-NTA. An SDS PAGE gel with Coomassie staining was run using the supernatant (S), flowthrough (F), wash (W), and elution fractions (E1 – E6). **(B)** SpySwitch elution fractions were pooled and run on over an S75 column. The protein was run using the following buffer: 50 mM Tris-HCl, 5 mM ethylenediamine tetraacetic acid (EDTA), 2-4 mM TCEP (pH 8.5 at 25 °C). The 1 mL elution fractions from 90-104 mL run on an SDS PAGE gel with Coomassie staining and pooled for coupling to SulfoLink beads.

I applied SpySwitch to purify a panel of twelve sarbecovirus RBDs by pH elution (Figure 3.6A). The plasmids in this panel were produced by and obtained from Pamela Bjorkman's lab (California Institute of Technology) (Figure 3.6B). All of these RBDs belong to bat viruses except for SARS1 and SARS2 that infect humans and pang17 that infects pangolins (Manis javanica) (A. A. Cohen et al., 2022). Several of these viruses have been identified as having the potential to cross over into humans (T. S. Evans et al., 2023; Muylaert et al., 2022).

The panel contained RBDs from viruses belonging to all sarbecovirus clades (Figure 3.6B). Clade 1a contains ACE2 binding SARS1-like viruses and includes SARS1, WIV1, and SHC014. Clade 1b contains ACE2 binding SARS2-like viruses and includes SARS2, pang17, and RaTG13. Clade 2 contains non-ACE2 binding viruses and includes Rs4081, Yun11, RmYN02, and Rf1. Clade 3 is the most distantly related sarbecovirus clade with members identified in European (BM48-31) and African (BtKY72) bats (Starr et al., 2022). Some but not all members of Clade 3 bind ACE2 (Mohapatra et al., 2023b; Seifert et al., 2022; Starr et al., 2022) (Figure 3.6B).

At the N-terminus all of these sarbecovirus constructs contain a signal peptide to facilitate mammalian cell secretion. At the C-terminus the constructs contain a His8-tag followed by a SpyTag003 (Figure 3.6C). I expressed all twelve sarbecovirus proteins in Expi293F cells. I purified the proteins using SpySwitch with pH elution. A representative purification gel is included for SARS-CoV-2 RBD-SpyTag003 purified by SpySwitch (Figure 3.6D).

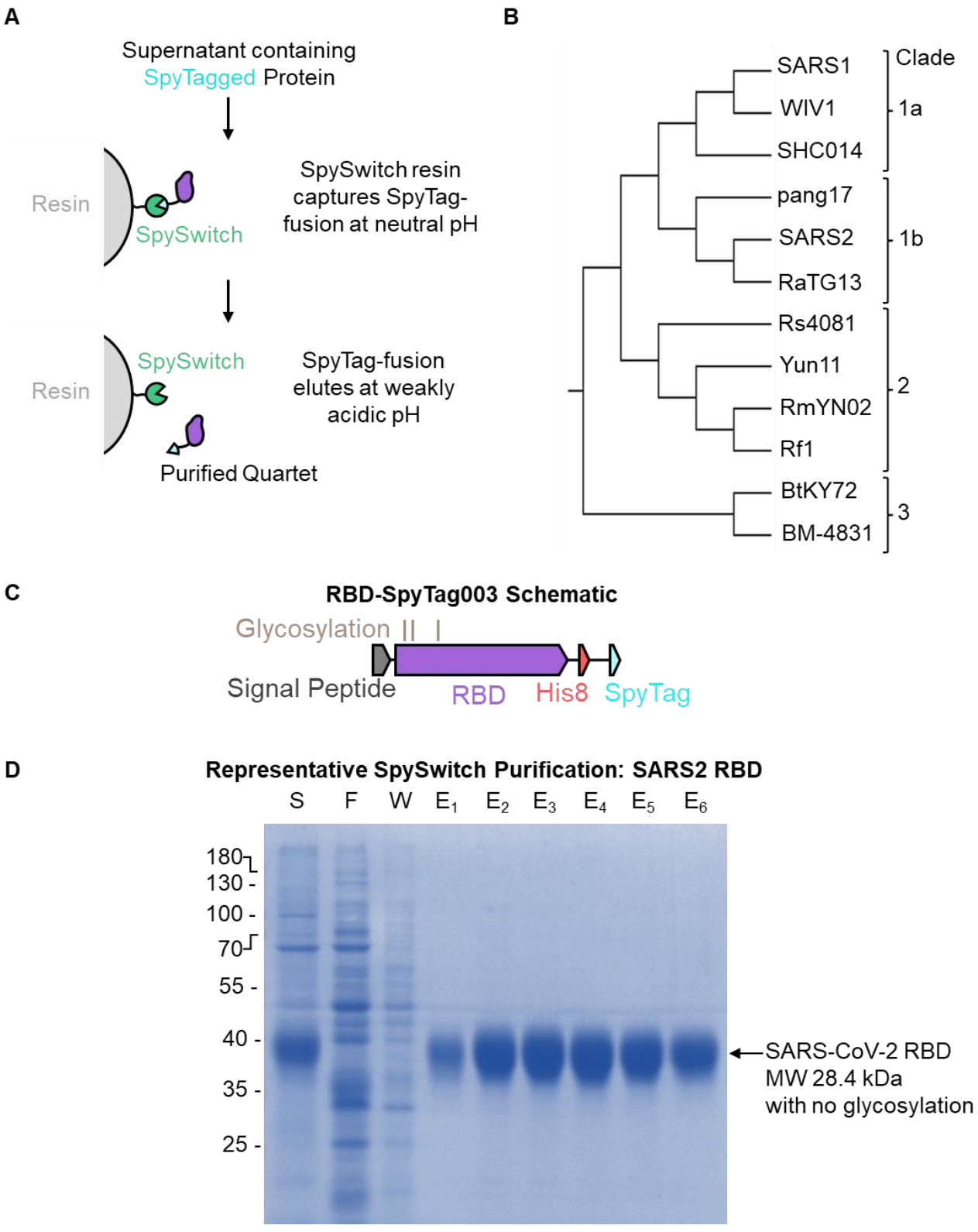

Figure 3.6: Purification of a panel of Sarbecovirus RBDs by SpySwitch. (A) A cartoon schematic showing SpySwitch purification by pH elution. **(B)** A phylogenetic tree showing the sarbecovirus RBDs that were included in this panel. **(C)** The schematic for the RBD constructs in the panel. **(D)** A representative purification SDS PAGE gel with Coomassie staining for the RBDs purified by SpySwitch. The lanes include the mammalian supernatant (S), flowthrough (F), wash (W), and elution fractions (E_1 _ E_6).

3.3 Implementing SpyTag for Nanoassembly

As previously outlined (Section 1.2), the SpyCatcher003-mi3 nanoparticle was developed by our group to provide a simple route for modular multivalent display of SpyTagged proteins.

I expressed SpyCatcher003-mi3 in *E. coli* BL21 (DE3) cells and purified the nanoparticle by ammonium sulfate precipitation. I dialysed the protein using 100 kDa molecular weight cutoff tubing to remove protein impurities and excess ammonium sulphate. I ran the post-dialysis protein over an S400 size exclusion chromatography column to separate the properly formed nanoparticle from aggregate (Figure 3.7A). I performed dynamic light scattering on the nanoparticle to verify that the particle was formed at the appropriate size (Figure 3.7B). This result showed a nanoparticle with a hydrodynamic diameter of 37.0 ± 9.6 nm which aligns well with previous reports for SpyCatcher003-mi3 (Rahikainen et al., 2021).

I then tested the coupling of the sarbecovirus RBD-SpyTag003 panel to SpyCatcher003-mi3. I performed this coupling interaction with an excess of SpyCatcher003-mi3 directly in neutralized SpySwitch elution buffer without the any additional dialysis or buffer exchange step. The results were analysed by SDS-PAGE after 16 hours coupling at 4 °C. All twelve sarbecovirus RBDs reacted to completion with SpyCatcher003-mi3 (Figure 3.8). No optimization was required to achieve efficient coupling with these twelve viral antigens highlighting the effective flexibility of the SpyCatcher003-mi3 nanoparticle for vaccine development.

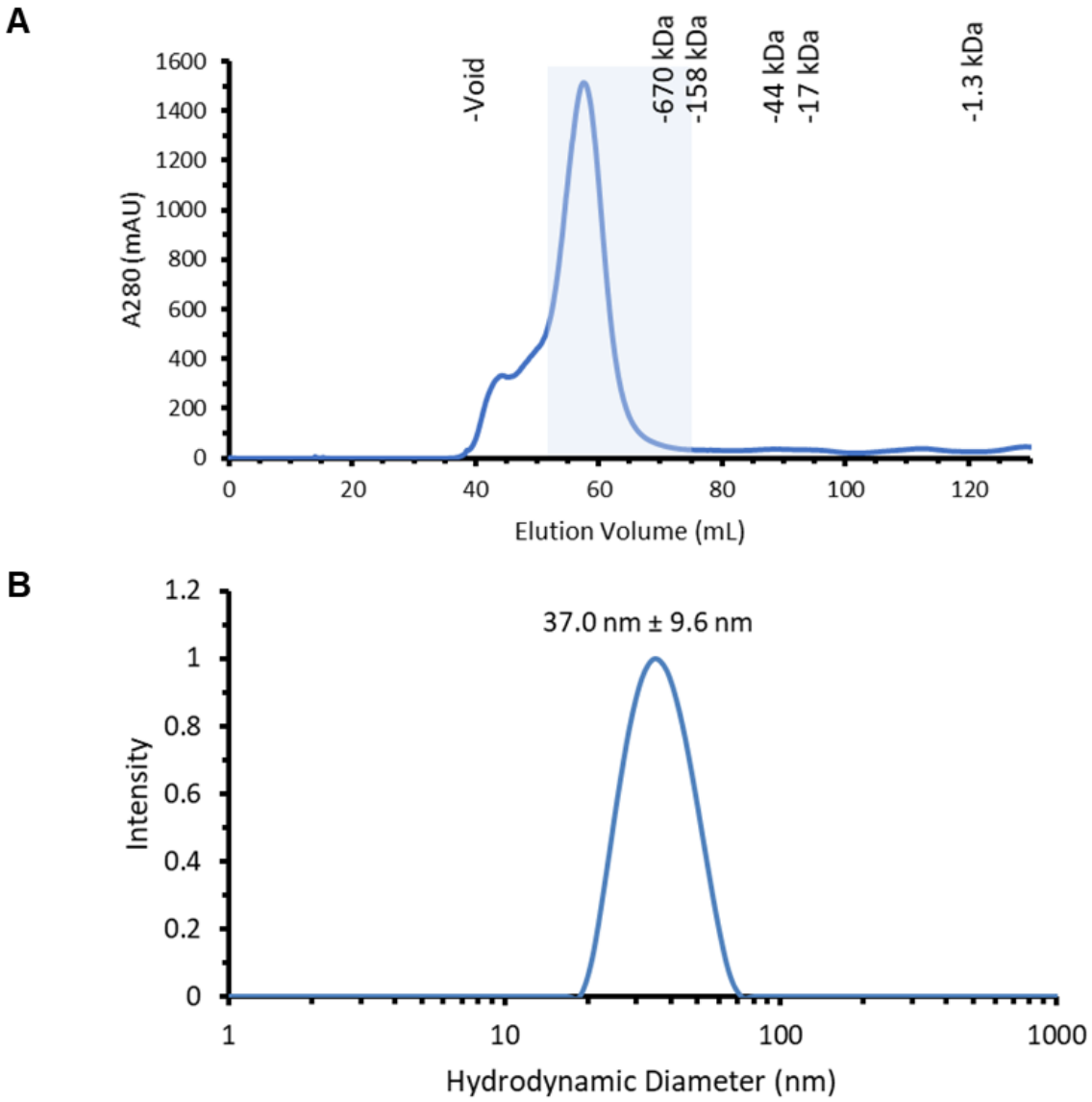

Figure 3.7: Purification and validation of SpyCatcher003-mi3. (A) Size Exclusion Chromatography results using a HiPrep Sephacryl S-400 HR 16-60 column for the production of SpyCatcher003-mi3, showing A280 measurements at different elution volumes. The fractions that we retained and pooled are shaded in blue. Bio-Rad gel filtration standards were run over the same column under the same conditions and the elution volume of these known standards are placed on the figure. **(B)** Dynamic light scattering result for SpyCatcher03-mi3. Hydrodynamic diameter is shown ± 1 standard deviation.

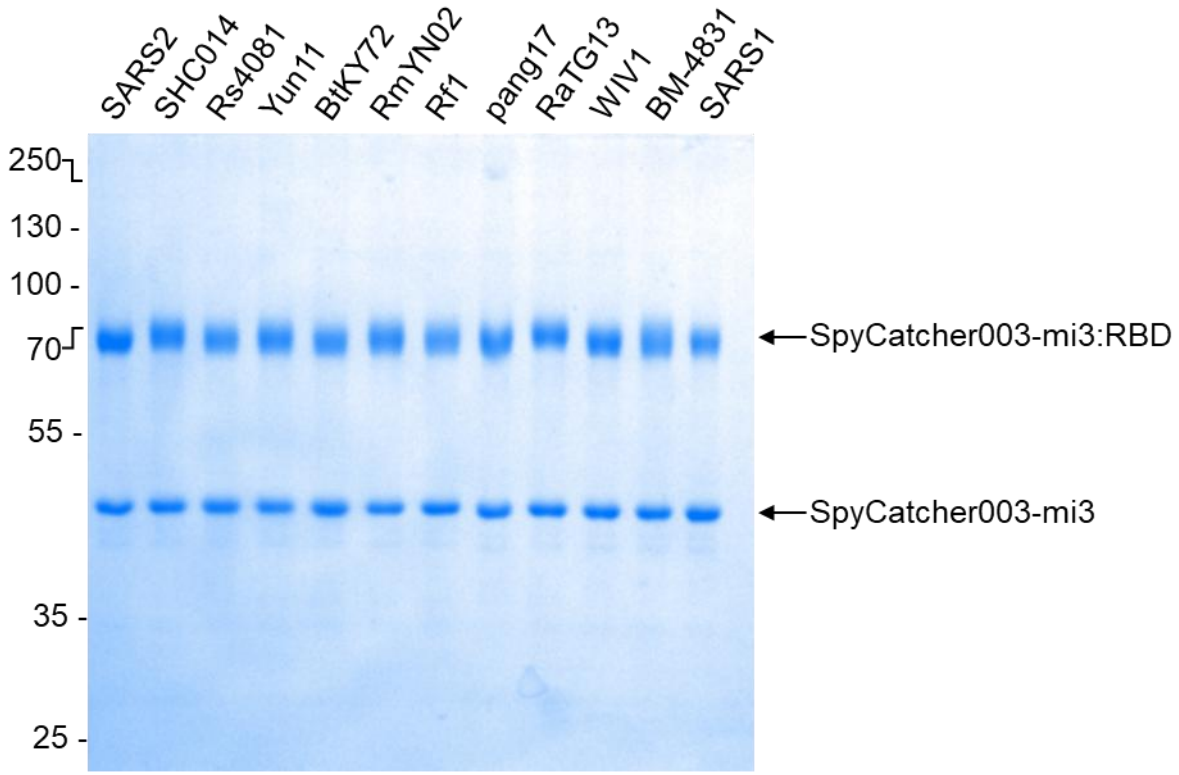

Figure 3.8: Coupling of sarbecovirus RBD to SpyCatcher003-mi3. The twelve sarbecovirus RBD-SpyTag003 constructs included in the panel were incubated with excess SpyCatcher003-mi3 for 16 h at 4 °C in neutralized SpySwitch elution buffer. SDS-PAGE gel with Coomassie staining is presented after coupling reaction. A colon between the name of two proteins indicates a covalent bond has been formed between them.

3.4 Identification of monoclonal antibodies with broad anti-sarbecovirus function

Understanding the breadth of SARS2-binding antibodies across related coronaviruses can give important insight for development of future vaccines, especially when considering the creation of vaccines against evolving SARS2 variants or newly arising zoonotic threats (Cankat et al., 2024). The identification of new broad spectrum monoclonal antibodies may also be applied for therapeutic development (Y. Chen et al., 2023).

I tested the ability of several antibodies to bind our panel of sarbecovirus RBDs when coupled the SpyCatcher003-mi3 nanoparticle. I was interested in understanding whether these individual monoclonal antibodies could (i) bind several different sarbecovirus RBDs and (ii)

bind to RBDs that were coupled to SpyCatcher003-mi3. This result would underscore the potential of a SpyCatcher003-mi3 based vaccine to elicit monoclonal antibodies with substantial anti-coronavirus breadth. The identification of a pan-sarbecovirus monoclonal antibody would be a useful resource for coronavirus research in addition to therapeutic value.

I selected the antibodies EY6A (D. Zhou et al., 2020), FI-3A, FP-8A, FI-3A, and FP-12A (K. Y. A. Huang et al., 2022) which had been identified in convalescent COVID-19 patients and were generously provided by Prof. Kuan-Ying Arthur Huang (Chang Gung University). I additionally selected CR3022, an anti-SARS1 monoclonal antibody (Ter Meulen et al., 2006) that had been identified as binding SARS2 (Yuan et al., 2020) and received interest as a COVID-19 therapeutic (Atyeo et al., 2021).

The antibodies selected belonged to multiple SARS2 RBD antibody classes (Figure 3.9A) (Barnes et al., 2020). Class 4 was overrepresented in selection as the Class 4 epitope had the greatest conservation across the sarbecoviruses included in the panel.

At the time this assay was performed, the selected anti-SARS2 antibodies were of research interest to several groups. Members of the antibody panel had recently undergone or were in the process of undergoing a variety of analyses including viral neutralization, cryogenic electron microscopy (cryo-EM), and protection studies in animal models (K. Y. A. Huang et al., 2022; Jette et al., 2021; D. Zhou et al., 2020).

I also included the anti-MERS-CoV RBD monoclonal antibody LCA60 in the panel (Corti et al., 2015). Given the substantial difference in sequence and structure of the SARS2 and MERS RBDs (Lewitus et al., 2023) we did not expect this monoclonal to bind sarbecovirus RBDs. Any binding would have been an interesting result, while a lack of binding would validate LCA60 as a negative control for future experiments using this sarbecovirus RBD panel.

I tested antibody binding to RBDs displayed on SpyCatcher003-mi3 by ELISA. As predicted, all of the antibodies bound to SARS2 RBD except for the anti-MERS LCA60. None of the Class 1-3 antibodies tested demonstrated binding to any sarbecovirus other than SARS2. The Class 4 antibody FP-12A showed strong binding to SARS2 and weak binding to RaTG13 and pang17, both close relatives of SARS2, as well as to the more distantly related BtKY72.The Class 4 antibody EY-6A bound to all twelve of the tested sarbecovirus RBDs (Figure 3.9B).

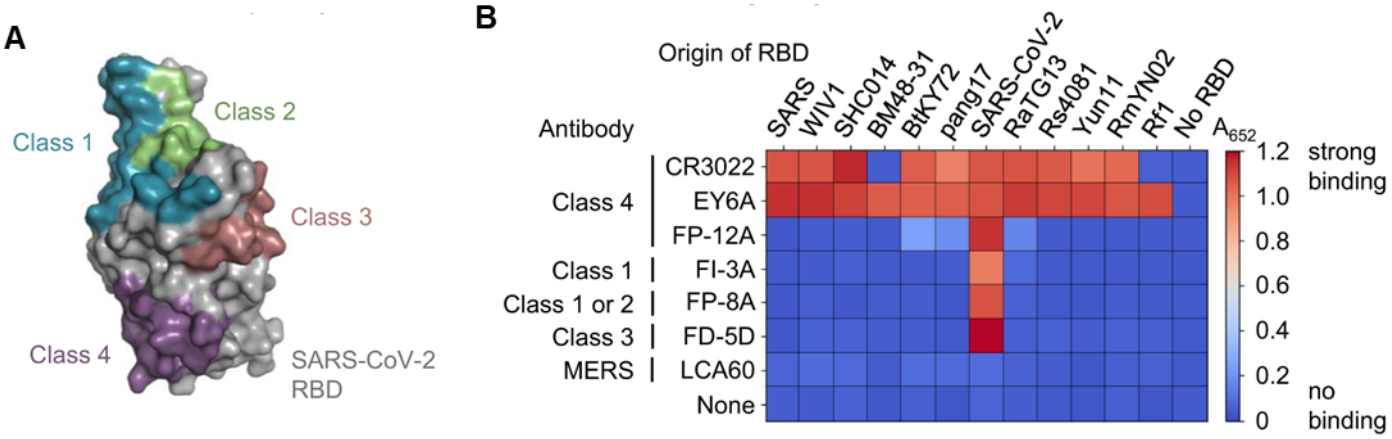

Figure 3.9: Recognition of sarbecovirus RBDs by a panel of antibodies. (A) SARS-CoV-2 RBD is shown with the binding sites defined by the Barnes classification system showing class 1 (blue), 2 (green), 3 (bronze) and 4 (purple). **(B)** Recognition of sarbecovirus RBDs by a panel of SARS-CoV-2 antibodies. The mean absorbances at 652 nm (A652) from ELISAs are plotted as a heat map (n = 3). Strong binding is represented by red and no binding is represented by blue.

The Class 4 antibody CR3022 bound to only ten of the twelve tested RBDs. The two RBDs not bound by CR3022 were from the viruses BM48-31 and Rf1 (Figure 3.9B). Notably, these viruses do not belong to the same clade and share only 70% identity in RBD (Figure 1.5). In contrast, BM48-31 shares 83% identity with the RBD of fellow Clade 3 virus and CR3022-binder BtKY72. Likewise, Rf1 shares 90% identity with the RBD of fellow Clade 2 virus and CR3022-binder RmYN02.

This raises the question of why CR3022 is unable to bind these two RBD when the antibody binds to the RBDs of related sarbecoviruses. A related question is why does EY6A bind BM48-31 and Rf1 while CR3022, an antibody with a similar binding footprint, does not.

I considered the structure of SARS2 RBD bound to CR3022 (Figure 3.10A) and EY6A (Figure 3.11B) and noted the residues that might interact with CR3022 but not EY6A. One of these residues, K378, was conserved in the ten sarbecovirus RBDs that bound CR3022 but not the two non-binders. BM48-31 RBD has a glutamine at the position aligned with K378 and Rf1 RBD has an asparagine at the position aligned with K378. I hypothesized that these mutations played a key role in the CR3022 escape.

To test this hypothesis, I cloned SpyTag-SARS2 RBD constructs with a single point mutation at position K378. This position was modified with either a K378Q mutation to match BM48-31 or a K378N mutation to match Rf1. I expressed these proteins in HEK293T cells and purified by SpySwitch.

I performed ELISAs to test binding to EY6A, CR3022, and LCA60 (Figure 3.10B). No non-specific binding was recorded to SpyTag-Hemagglutinin or by the LCA60 antibody. EY6A bound to the wild type RBD and both point mutants. This demonstrates that the K378 substitutions present in BM48-31 and Rf1 do not negatively impact EY6A binding. This also provides evidence that the point mutants were properly folded. CR3022 showed strong binding to the wild-type SARS2 RBD but no binding to either of the point mutants. This provides evidence that the K378Q (BM48-31) and K378N (Rf1) mutations play an important role in CR3022 escape for these sarbecoviruses (Figure 3.10B). These results highlight the impact that a single mutation can have in escaping an otherwise broad monoclonal antibody.

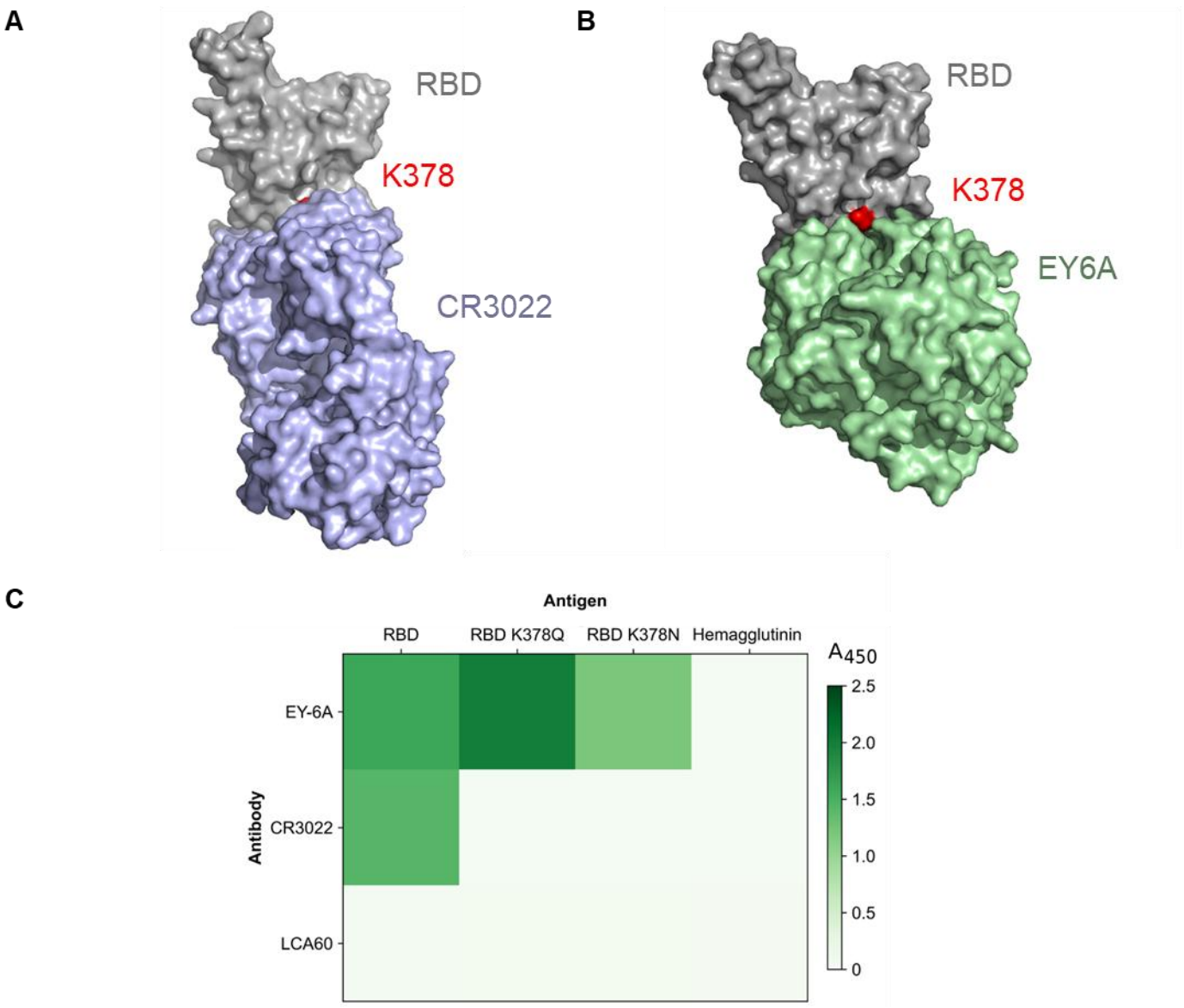

Figure 3.10: Investigating differences in CR3022 and EY6A binding. The crystal structure of SARS-CoV-2 RBD binding by **(A)** CR3022 (PDB 6W41) and **(B)** EY6A (PDB 6ZDH). For both structures, the K378 residue identified as potentially responsible for ablated CR3022 binding in BM48-31 and Rf1 is indicated in red. **(C)** EY6A and CR3022 binding to SARS-CoV-2 RBD wild-type and RBD point mutants that matched BM48-31 (K378Q) or Rf1 (K378N) at a single position. The mean absorbance at 450 nm (A_{450}) from ELISAs are plotted as a heat map (n = 3). Strong binding is represented by green and no binding is represented by white. An anti-MERS RBD antibody, LCA60, was included as a negative antibody control and SpyTag-Hemagglutinin was included as a negative antigen control.

The identification of EY6A as a broad anti-sarbecovirus antibody highlighted the potential for other Class 4 antibodies to be identified with similarly broad binding. Prof. Kuan-Ying Arthur

Huang (Chang Gung University) had identified a group of Class 4 individuals from individuals that were either convalescent from COVID-19 (EY-6A and FP-12A) or had received two doses of a COVID-19 vaccine (IY-2A, IV-6D, IV-4B, IS-9A, IS-11B and IV-10C) and supplied our lab with aliquots of these antibodies. These antibodies had been identified as Class 4 based on their competition with EY6A for SARS2 RBD binding.

I tested the binding of these purified monoclonal antibodies to our panel of sarbecovirus RBDs by ELISA (Figure 3.11). As the previous ELISA had demonstrated that Class 4 antibodies were capable of binding RBDs coupled to SpyCatcher003-mi3, I chose to perform this ELISA with a more conventional setup and adsorbed the proteins directly onto the plate.

As expected, every Class 4 antibody tested bound tightly to SARS2 RBD. Interestingly, all of the antibodies demonstrated at least some binding to Clade 1a RBDs, particularly WIV1. IV-6D came close to binding every member of the panel but did bind Yun11 RBD. IY-2A was identified as binding every member of the sarbecovirus RBD panel (Figure 3.11).

Further analysis of IY-2A, demonstrated that the antibody uses a novel RBD-binding strategy to facilitate this broad-spectrum binding and was able to potently neutralize several different sarbecoviruses including SARS1, SHC014, WIV1, BtKY72, and all tested SARS2 VOCs (including Omicron BA.4/5) (K. Y. A. Huang et al., 2023).

Figure 3.11:

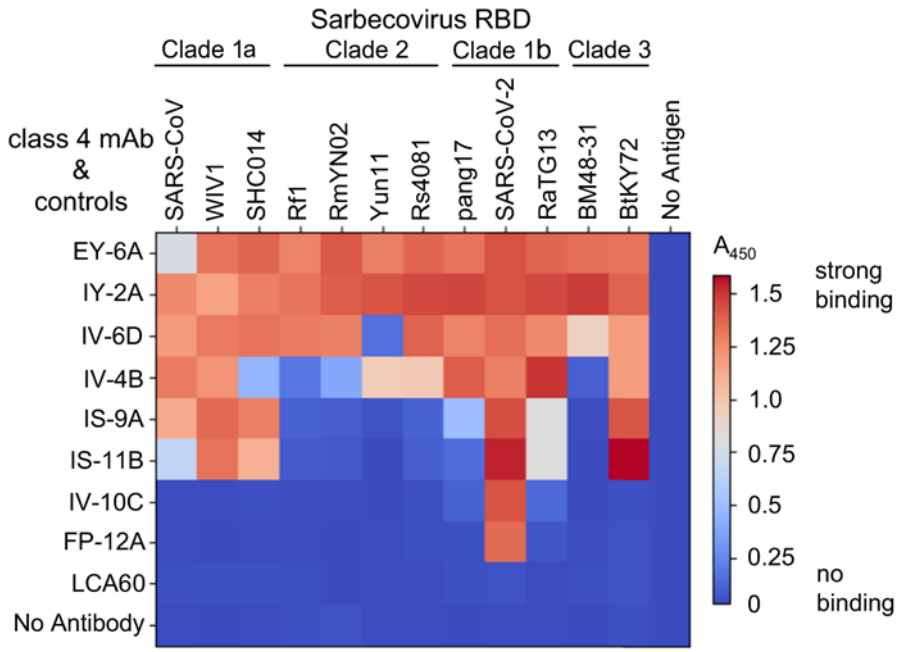

Recognition of sarbecovirus RBDs by a panel of Class 4 antibodies. The mean absorbance at 450 nm (A450) from ELISAs are plotted as a heat map (n = 3). Strong binding is represented by red and no binding is represented by blue. An anti-MERS LCA60 was included as a negative antibody control.

3.5 Discussion

In this chapter, I have implemented SpyTag-enabled technologies to both facilitate and streamline the vaccine research.

I used SpyTag as an affinity purification tag to produce a novel COVID-19 vaccine candidate. Purified using SpyDock, this vaccine was a genetic fusion of the SARS2 RBD and the engineered albumin-binding domain ABD035 (Jonsson et al., 2008). From several well characterized albumin-binding domains and peptides, ABD035 was selected due to its remarkably high affinity (50–500 fM) for HuSA and its breadth of binding including mouse and macaque serum albumin. This cross-species breadth would simplify the translation of any albumin-binding vaccine candidate from pre-clinical models to clinical application in humans (Jonsson et al., 2008).

The fusion of ABD035 to RBD significantly increased the response relative to RBD alone, when two doses of either immunogen were administered to mice. The mean AUC for RBD-

ABD035-treated mice (5.3) more than doubled the mean AUC for RBD treated mice (2.0). Every individual mouse dosed with RBD-ABD035 had an increased immune response relative to every individual mouse that received RBD alone.

As a highly abundant serum protein (35–50 mg/mL) with multiple binding sites and a long circulatory half-life (19 days), human serum albumin has been a frequent target for attachment of a drug to improve pharmacokinetics (Tao et al., 2021). This albumin-hitchhiking strategy has recently begun to be applied for vaccine development. For example, the attachment of lipid tails to CpG or peptide vaccines has been shown to significantly increase lymph node accumulation and subsequent immune response (H. Liu et al., 2014; Rakhra et al., 2021). Similar work has used Evans Blue (G. Zhu et al., 2017), a highly water-soluble dye that binds albumin-binding site I (H. M. Evans & Schulemann, 1914; Yao et al., 2018), to facilitate albumin hitchhiking for CpG and cancer neoantigen peptides (G. Zhu et al., 2017).

Part of this enhanced immune response comes simply from albumin attachment increasing the molecular weight of the antigen (Moyer et al., 2016). Physical size plays an important role in dictating fluid clearance with larger macromolecules being more likely to be delivered to draining lymph nodes. Above a molecular weight of approximately 45 kDa, proteins tend to be entirely trafficked via the lymphatic system (Miller et al., 2011; Moyer et al., 2016). Albumin hitchhiking of RBD is also likely to have directed this relatively small viral antigen (25.4 kDa) to draining lymph nodes. This would increase the effective dose of the vaccine and contribute to the enhanced humoral response. Linking RBD to HuSA via a high-affinity protein binder may also take advantage of the long-lasting nature of HuSA to increase antigenic half-life of the antigen (Moyer et al., 2016).

In a study that was published after I had concluded my albumin hitchhiking research, SARS2 RBD was modified with the lipophilic diacyl tail 1,2-distearoyl-sn-glycero-3-

phosphoethanolamine (DSPE). DSPE binds HuSA with a KD of approximately 125 nM. This was accomplished through the addition of a free cysteine at the N-terminus of the antigen, with the authors demonstrating that this modification did not affect production, stability, or antigenicity profile. The authors attached DSPE to SARS2 RBD using maleimide coupling with a hydrophilic polyethylene glycol (PEG) spacer separating the lipid and antigen to produce a DSPE-PEG2K-RBD vaccine candidate (Hartwell et al., 2022).

It is important to consider the impact of including PEG in clinical vaccines, given the prevalence of pre-existing anti-PEG antibodies in humans (B. M. Chen et al., 2016). While successful COVID-19 mRNA vaccines have included PEG, these both induced and boosted anti-PEG antibodies in the global population (Guerrini et al., 2022; Kozma et al., 2023). It has been shown that pre-existing anti-PEG antibodies can increase the reactogenicity of vaccines that contain PEG (Ju et al., 2022). PEGylated drugs have demonstrated enhanced systemic clearance in the presence of pre-existing anti-PEG antibodies (B. M. Chen et al., 2021). There is no evidence that the efficacy of PEG-containing mRNA vaccines was negatively impacted by pre-existing anti-PEG antibodies (Ju et al., 2023) but the clinical impact of pre-existing anti-PEG antibodies binding to a PEG containing protein sub-unit vaccine remains unknown. Given this uncertainty and the substantial investment of a human clinical trial, I believe it would be optimal to develop an albumin hitchhiking strategy that avoids the use of PEG.

In agreement with the results for SpyTag-RBD-ABD035, immunization with a DSPE-PEG2K-RBD construct showed remarkable improvement relative to RBD alone. The researchers performed intranasal immunizations and found significant improvements in IgG and IgA titres for sera and various mucosal samples. The attachment of an albumin-binding lipid additionally improved SARS2 pseudovirus neutralization by both sera and bronchoalveolar lavage fluid (Hartwell et al., 2022).

The success of both an albumin-binding protein and lipid at enhancing immune response to SARS2 RBD highlights the potential of albumin hitchhiking to enhance recombinant protein vaccines, especially for antigens that are typically poorly immunogenic. In future work it would be useful to compare these two approaches to determine whether there is any difference in the response that is achieved. It would also be useful to test other albumin-binding proteins and peptides (Dennis et al., 2002; Johansson et al., 2002; Y. Ma et al., 2015) to assess whether the high affinity of ABD035 (50-500 fM) elicits a different response compared with relatively low affinity binders. The importance of mucosal immune response in reducing morbidity and mortality for SARS2 (Puhach et al., 2023) suggest that intranasal delivery of SpyTag-RBD-ABD035 could provide further enhanced immune response and could be worthy of future study.

My research demonstrates that genetically encodable protein-mediated albumin hitchhiking can enhance overall antibody titres for recombinant protein sub-unit vaccines. Future work may explore whether this strategy can be further optimized to alter the nature of the antibodies that are elicited.

Several bacterial species use membrane proteins to bind HuSA to their surface in order to protect themselves from immune recognition(Egesten et al., 2011a). A similar approach has used covalent albumin decoration of a tobacco mosaic virus (TMV) derived nanoparticle to reduce macrophage recognition and immune clearance (A. S. Pitek et al., 2016).

The location that elicited antibodies bind to is unlikely to be altered by the inclusion of a terminal albumin-binding domain separated from the antigen by a flexible linker (SpyTag-RBD-AD035). However, the strategic incorporation of a high affinity albumin-binding peptide within the protein could facilitate albumin-binding to and consequent shielding of certain regions of an antigen.

While the SpyTag-RBD-ABD035 vaccine candidate was effectively purified by SpyDock, not all proteins are able to withstand the harsh elution conditions required for purification by this route (wither 2.5 M imidazole or pH 2.0) (Khairil Anuar et al., 2019). To facilitate ease-of-use and more widespread technology adoption our lab developed the SpySwitch protein. This system allows for purification with gentler elution conditions, using a short incubation at pH 5.0 or 37 °C to release a SpyTag from the SpySwitch protein. The option for temperature elution is especially important for purification of proteins that have evolved pH-responsive changes (Vester et al., 2022).

I used this newly developed technology to purify a panel of twelve different sarbecovirus RBDs, all at high yields and purity. I coupled each member of sarbecovirus RBD panel to SpyCatcher003-mi3 in neutralized SpySwitch elution buffer. Neutralization of the elution buffer was performed by eluting directly into neutralization buffer (Tris pH 8.0), meaning that no additional dialysis or buffer exchange steps were required between purification and multimerization. Despite the sequence diversity and evolutionary distance present in the panel, all of these RBDs were efficiently displayed on the nanoparticle without the need for any modification or optimization. This result highlights the modularity of using the SpyTag/SpyCatcher system for nanoparticle display.

While a His-tag was present in these constructs, only the SpyTag was required and was used for both purification and multimerization. The development allows for vaccine constructs to be produced without the inclusion of a potentially immunogenic His-tag (F. Khan et al., 2012; M. Singh et al., 2020) or an extra step to remove excess tags (Raran-Kurussi et al., 2017). These results highlight the ability of SpySwitch to facilitate simpler vaccines constructs and a streamlining of antigen display on nanoparticles.

In addition to piloting SpySwitch purification, I used the RBD panel to test monoclonal antibodies that were identified in human patients and were known to bind SARS2 RBD. By assessing the ability of these antibodies to bind several related RBDs we sought monoclonal antibodies capable of binding to the broad spectrum of sarbecoviruses. A pan-sarbecovirus antibody would be a useful reagent for the study of sarbecoviruses. Understanding RBD and monoclonal antibody features that influenced breadth of binding would also give important insight into how a broad spectrum humoral immune response might be elicited. An antibody that demonstrates broad binding and the ability to effectively neutralize viruses it binds could be an important therapeutic against newly arising zoonotic coronaviruses or novel SARS2 VOCs.

In my first effort at testing monoclonal antibody binding, I identified two antibodies as being broad anti-sarbecovirus binders: EY6A and CR3022.

CR3022 bound to ten of the twelve tested sarbecovirus RBDs. Notably, the two tested sarbecoviruses that CR3022 was unable to bind were not closely related. Rf1 is a Clade 2, BM48-31 is Clade 3, and their RBDs shared only 70.0% identity with one another. I considered the mutations in these RBDs relative to SARS2, focusing on residues that are part of the RBD:CR3022 binding site. Almost every mutation present in Rf1 or BM48-31 relative to SARS2 was shared by viruses that are susceptible to CR3022 binding. It is therefore unlikely that any of these mutations were responsible for the ablated binding. At the position aligned with SARS2 K378 a different residue was present for Rf1 (asparagine) and BM48-31 (glutamine). This position also appeared to interact more significantly with the binding of CR3022 than EY6A. I hypothesized that a mutation at K378 played a key role in CR3022 escape. When I added a single point mutation to SARS2 RBD to match either Rf1 (K378N) or BM48-31 (K378Q), I demonstrated that binding to CR3022 was lost entirely. The RBDs

retained binding to EY6A, indicating that loss of binding was not an issue with mutations inducing protein misfolding.

The ability of a single point mutation to ablate broad spectrum binding highlights the danger of overreliance on a single broad spectrum monoclonal therapeutically. Even a remarkably broad binder like CR3022 can be overcome by small antigenic changes.

Unlike CR3022, EY6A bound to all of the tested sarbecovirus RBDs. EY6A is a monoclonal antibody that was identified in an individual convalescent from SARS2. Based on structural characterization and competition assays, EY6A is a Class 4 antibody, meaning it bound to a region of the SARS2 RBD that was highly conserved amongst sarbecoviruses.

At the time I identified EY6A as broadly binding it had been shown to neutralize SARS2 in quantitative polymerase chain reaction (qPCR) and plaque reduction neutralization test (PRNT) assays. EY6A had been characterized as 'highly neutralizing' (D. Zhou et al., 2020). Later work demonstrated that EY6A was a relatively poor SARS2 neutralizer, compared with several other monoclonal antibodies (K. Y. A. Huang et al., 2023), especially when considering neutralization of SARS2 VOCs (K. Y. A. Huang et al., 2023) While this result removes the therapeutic application of EY6A, the antibody still demonstrates broad spectrum binding which could be useful for sarbecovirus RBD detection by ELISA, flow cytometry, mass photometry, and other assays.

In a second effort using our panel of sarbecovirus RBDs for monoclonal antibody assessment, I tested a new group focused on Class 4 antibodies. These antibodies were of our interest to an international collaboration that our group belonged to and were undergoing active structural and functional characterization. As expected, all of the tested antibodies bound to SARS2 and many displayed some level of sarbecovirus breadth. IY-2A was the only tested antibody that bound to all of the sarbecovirus RBDs in our panel.

This antibody was subsequently tested in pseudovirus neutralization assays performed by Jennifer R. Keeffe, Alexander A. Cohen, and Leesa M. Kakutan in Pamela J. Bjorkman's lab (California Institute of Technology). IY-2A demonstrated a remarkable neutralizing titre (IC50) of 0.03 μg/mL against SARS2 Wuhan and demonstrated strong neutralization of all tested SARS2 VOCs. The most recent VOC tested was Omicron BA.4/5 against which IY-2A demonstrated an IC50 of 0.17 μg/mL. For context, EY6A neutralized SARS2 Wuhan at 0.56 μg/mL. IY2A also demonstrated potent neutralization of several bat coronaviruses that I had demonstrated binding to, including SHC014 (Clade 1a), WIV1 (Clade 1a), and BtKY72 (Clade 3). The weakest neutralization observed for IY-2A was an IC50 of 0.57 μg/mL for SARS1 (Clade 1a) (K. Y. A. Huang et al., 2023).

Crystal structures were determined for IY-2A bound to SARS2 RBD (PDB 8HHH) by Arpita Mohapatra and Hong Thuy Vy Nguyen (Academia Sinica). IY-2A demonstrated a unique binding footprint compared with previously described antibodies. Unlike most Class 4 antibodies the binding footprint of IY2A extends to the bottom part of the RBD (residues 364–368) (K. Y. A. Huang et al., 2023). This region is buried in the apo RBD but interaction with IY-2A causes the region to become exposed. More specifically the blade-like HCDR3 of IY-2A intrudes into the hydrophobic core of RBD, causing the 364-375 residue region of SARS2 RBD to be partially refolded. This conformational change provides the final binding surface for the tight interaction between IY-2A and RBD. The 364-375 region is known to be structurally conserved across various sarbecoviruses and SARS2 VOC, helping to explain the breadth demonstrated by IY-2A (K. Y. A. Huang et al., 2023).

The identification of IY-2A, and other broadly neutralizing anti-sarbecovirus antibodies such as C118 (Jette et al., 2021), CC25.36, CC25.53, and CC25.54 (W. ting He et al., 2022), highlights the potential to raise a pan-sarbecovirus immune response. Finding a method to reliably and predominantly elicit broadly neutralizing antibodies like IY-2A could offer

proactive protection against evolutionarily related zoonotic viruses and newly evolved variants of existing human pathogens. Additionally, this strategy would elicit a polyclonal antibody repertoire that would be less susceptible to point mutation escape exhibited with CR3022. IY-2A originated in an individual who had been administered two doses of mrna-1273 from Moderna, a SARS2 specific vaccine. Despite the presence of some antibodies like IY-2A, the predominant immune response raised by a conventional clinically approved vaccine does not protect against a broad range of sarbecoviruses (C.-W. Tan et al., 2021). This discrepancy raises the question of whether a vaccine can be created that will reliably raise a cross-neutralizing immune response? The next chapter will explore one strategy that seeks to achieve this.

Chapter 4 – Multiviral Quartet Nanocages Elicit Broad Anti-Coronavirus Antibody Responses

Clinically approved SARS2 vaccines have shown remarkable success in reducing both death and serious illness from COVID-19 infection (Sachs et al., 2022). Given the substantial impact of these vaccines, it is critical to consider the development of vaccines with the potential to protect against future coronavirus pandemic threats. In this century, two other coronavirus crossover events, SARS1 and MERS-CoV, have led to outbreaks in humans (De Wit et al., 2016). Several zoonotic sarbecoviruses have been identified as future pandemic threats (Menachery et al., 2017). Immunizations using a single antigen tend to elicit immune responses that are narrow and strain-specific (Cohen et al., 2021). This raises the important question: how can a vaccine response be broadened to target an existing pathogen as well as newly arising variants and newly infectious relatives?

In a previously outlined approach, antigenic protein variants are arranged stochastically on the surface of a VLP. This varied arrangement led the particles to be named ‘mosaic nanoparticles’. The presentation of several related antigens in this manner favours the expansion of B cells that recognize the common features. This strategy was first applied with a mosaic of different hemagglutinin head domains on ferritin nanoparticles and elicited cross-reactive antibodies against diverse influenza strains within the H1 subtype (Kanekiyo et al., 2019). The technique has subsequently been applied to coronaviruses, with mosaic nanoparticles displaying multiple RBDs from the spike protein of different sarbecoviruses (A. Cohen et al., 2021; A. A. Cohen et al., 2022; Walls et al., 2021).

In one promising mosaic nanoparticle strategy, eight different sarbecovirus RBDs were displayed on the SpyCatcher003-mi3 nanoparticle (A. Cohen et al., 2021; A. A. Cohen et al., 2022). These particles, termed Mosaic-8 nanoparticles, raised immune responses against a

range of different sarbecoviruses in multiple animal models (A. A. Cohen et al., 2022). These responses were not limited to the RBDs present on the nanoparticles. Mosaic-8 immunization raised neutralizing antibodies to viruses with RBDs present on the particle (matched) and evolutionarily related viruses that were absent from the particle (mismatched) (A. Cohen et al., 2021; A. A. Cohen et al., 2022). This vaccine candidate has received support from the Coalition for Epidemic Preparedness Innovations (CEPI) to enter Phase I clinical trials.

There are two important hurdles which the Mosaic-8 nanoparticles will need to overcome in order to reach the clinic. The first is their inherent heterogeneity. Mosaic-8 nanoparticles are assembled by combining a mixture of SpyTagged sarbecovirus RBDs with SpyCatcher003-mi3. The RBDs spontaneously couple to the nanoparticle leading to a stochastic arrangement. The inherent heterogeneity and the difficulty in determining batch-to-batch consistency has been raised as a potential regulatory issue for the vaccine. This hurdle may be overcome through the development of effective batch release assays in consultation with regulatory bodies.

The second hurdle is more fundamental. The Mosaic-8 vaccine is complex and requires the production of nine different components (eight RBDs and SpyCatcher003-mi3) at Good Manufacturing Practice (GMP) level. This requirement creates an inherent challenge that needs to be overcome to achieve broad scaling of the vaccine.

In this chapter, I will seek to sidestep these two hurdles with the introduction of the multiviral Quartet Nanocage strategy. This technology combines RBDs from four different sarbecoviruses into a single polyprotein with a terminal SpyTag. This facilitates multivalent display of the Quartet on SpyCatcher003-mi3, with fewer components and a greater number of RBDs per particle compared with Mosaic-8. I will assess the ability of Quartet Nanocages to raise both matched and mismatched responses against various sarbecoviruses. I will then

compare the responses raised by Quartet Nanocages directly with those elicited by Mosaic-8. Finally, I will examine the ability of Mosaic and Quartet antigens to raise an immune response in animals that have been pre-biased to a single virus. Together these results will examine whether Quartet Nanocages may provide a scalable route to raise broadly neutralizing antibodies against a range of related viruses.

4.1 Production of a Multiviral Quartet

The RBDs of four different, evolutionarily related sarbecoviruses were genetically fused and expressed as a single polypeptide chain that I named a Quartet. The RBDs concatenated to form this construct came from the sarbecoviruses SHC014, Rs4081, RaTG13 and SARS2 Wuhan (Figure 4.1A).

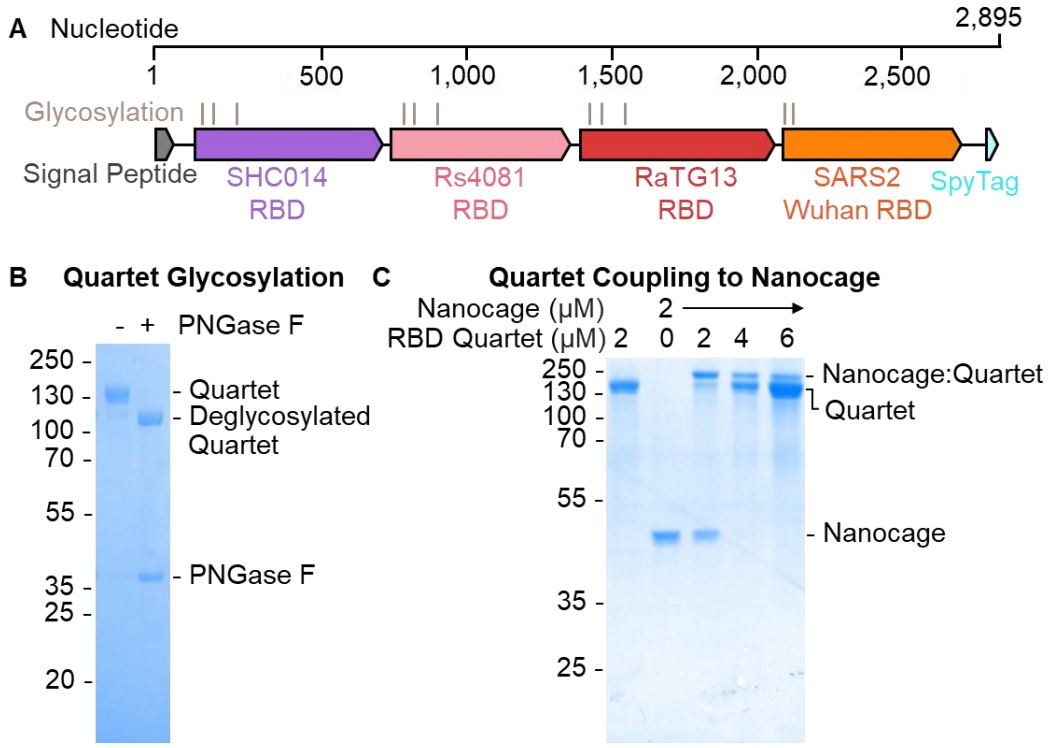

Figure 4.1: Production of Multiviral RBD. (A) Schematic showing the genetic organization of the Quartet-SpyTag construct. The identity of constituent RBDs and location of SpyTag, Signal Peptide and predicted glycosylation sites are indicated. Flexible linkers are shown as a black line. **(B)** A Coomassie stained SDS-PAGE gel displaying Quartet with and without the treatment of PNGase F. **(C)** Coupling of Quartet to the SpyCatcher003-mi3 Nanocage at the specified molar ratios analysed by SDS-PAGE with Coomassie staining. All molecular weight markers are in kDa.

SHC014 is a clade 1a sarbecovirus, closely related to SARS1, and first identified from a Chinese horseshoe bat *(Rhinolophus sinicus*) (Ge et al., 2013a). SHC014 was identified as a zoonotic spill-over risk and has a spike protein that is capable of mediating human cell infection (Menachery et al., 2015). Rs4081 is a clade 2 sarbecovirus that was also identified in *R. sinicus* (Hu et al., 2017a). Rs4081 is capable of infecting human cells, in contrast to several clade 2 viruses (Khaledian et al., 2022). Rs4081 does not enter cells via ACE2 (Starr et al., 2022). RaTG13 is a clade 1b virus with very high sequence identity with SARS2 (90% RBD sequence identity) and was identified in the Intermediate horseshoe bat (*Rhinolophus affinis*) (P. Zhou et al., 2020a). This collection of RBDs were chosen to allow comparison to the previously described Mosaic-4 vaccine (A. Cohen et al., 2021).

The Quartet construct included a signal sequence for secretion from mammalian cells and a C-terminal SpyTag, for purification and multivalent display on the SpyCatcher003-mi3 nanocage. RBDs were separated from one another by with an eight or nine residue Gly-Ser linker (Figure 4.1A). I expressed the Quartet protein in Expi293F cells. The Quartet secreted efficiently and was purified using SpyTag via the SpySwitch affinity purification system (Vester et al., 2022). The Quartet band was relatively broad on SDS-PAGE which I attributed to natural variation in protein glycosylation. When the Quartet was treated with Peptide N-Glycosidase (PNGase) F to remove N-linked glycans, the Quartet band became more uniform and shifted downward (Figure 4.1B). The Quartet was capable of coupling to completion with the SpyCatcher003-mi3 nanocage (Figure 4.1C).

I wanted to produce a larger concatenated protein that would include all eight sarbecovirus RBDs present in the Mosaic-8 vaccine. Towards this goal I produced a sextet that included the four RBDs present in the Quartet in addition to RBDs from RmYN02 and pang17. I expressed this construct in Expi293F cells and purified by SpySwitch (Figure 4.2). The yield for this

construct (~7.5 mg/L culture) was substantially lower than the typical Quartet yields (70-100 mg/L culture). Facilitating ease of production was the primary motivation in pursuing RBD concatenation. Given that the addition of two further RBDs to the sextet was likely to further reduce yields, I chose not to pursue larger RBD chains for these experiments.

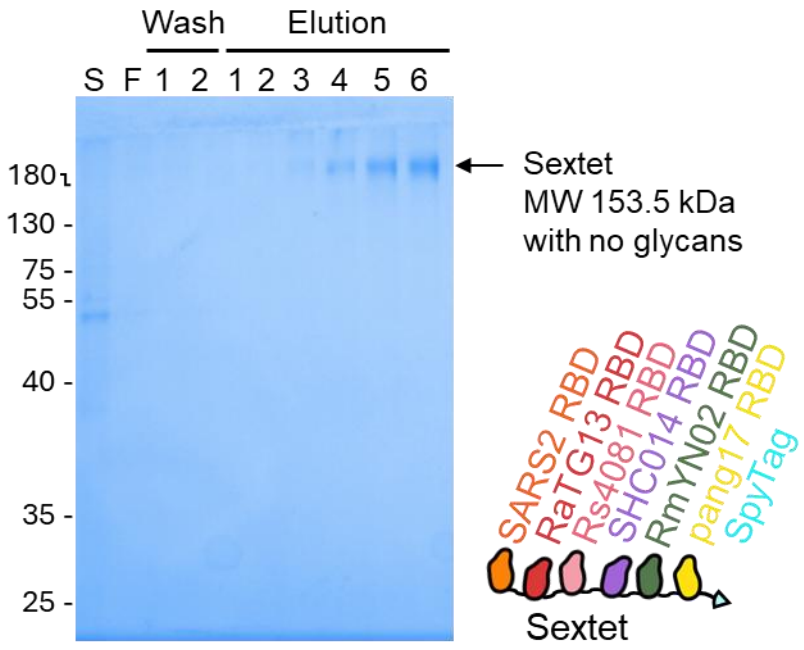

Figure 4.2: Purification of Multiviral RBD. An SDS-PAGE gel with Coomassie staining analysing the SpySwitch purification of a multiviral RBD Sextet. The lanes include the mammalian supernatant (S), flowthrough (F), wash (W), and elution fractions (E1 – E6). A cartoon of the Sextet indicates the viral origin of the RBDs and the location of the SpyTag.

4.2 Multiviral Quartet Nanocage Induces Broad Anti-Sarbecovirus Response

I then examined the immunogenicity of these Quartet when administered as a soluble protein (Uncoupled Quartet) or presented multivalently on SpyCatcher003-mi3 (Quartet Nanocage). I compared Quartets with SARS2 Wuhan RBD as a soluble (Uncoupled RBD) or nanocage displayed (Homotypic Nanocage) antigen (Figure 4.3A). I endotoxin-depleted all vaccine components and using a LAL assay I determined that the final endotoxin levels were below 20 EU/mL. I prepared these four immunogens, normalizing by the number of antigen molecules.

This molar normalization can be thought of as normalizing by the number of SpyTags or the number of SARS2 RBDs. Two mouse immunizations used the alum-based VAC 20 adjuvant (Figure 4.3B). All immunization and sera sampling were performed by Jack Tan (University of Oxford).

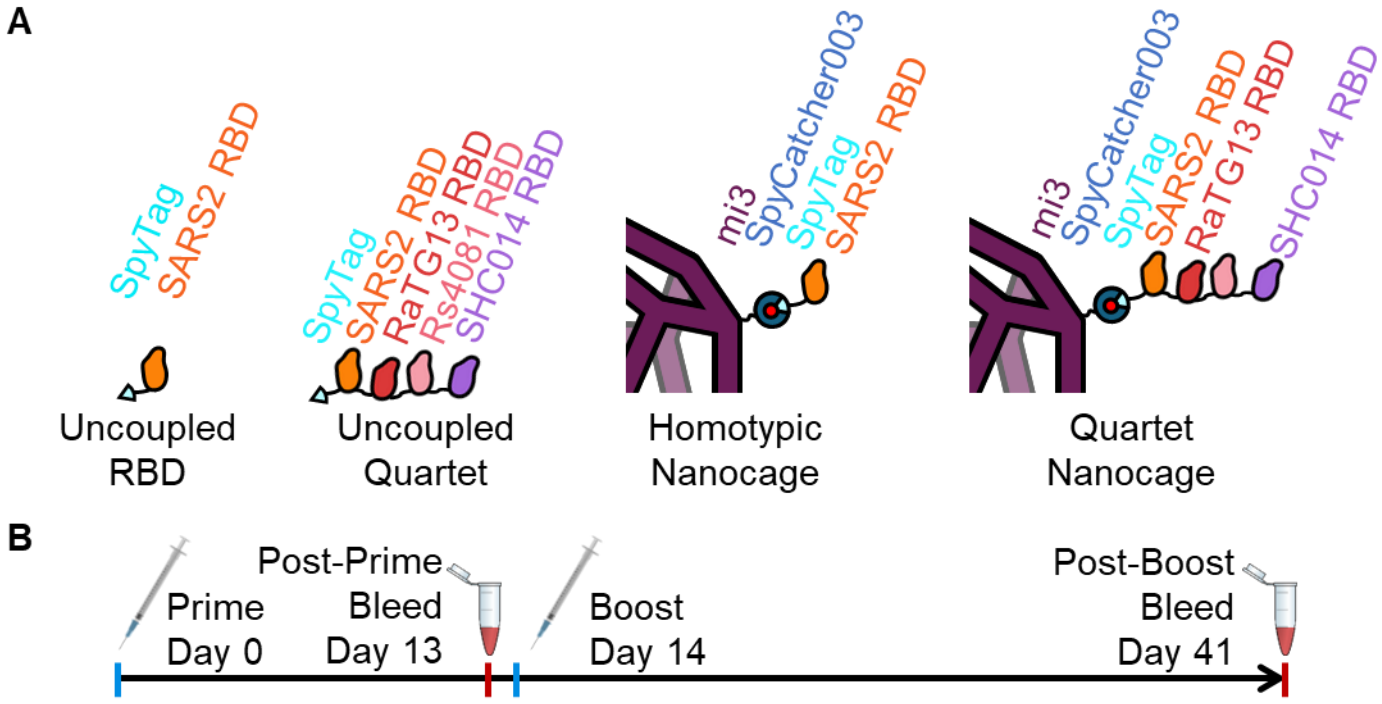

Figure 4.3: Parameters for the Initial Quartet. (A) Cartoon of the four different immunogens used in these immunizations comparing single RBD and Quartet antigens with and without presentation on SpyCatcher003-mi3. **(B)** Immunization timeline showing the timepoint for dosing (needle) and sampling (microcentrifuge tubes).

I performed mouse antisera ELISA on the post-prime samples (Figure 4.4). It is important to note that these ELISAs and all future ELISAs were performed with a different sera dilution series than the previously presented albumin-hitchhiking ELISAs (Figure 3.4).

Of all tested immunogens, the Quartet Nanocage elicited the strongest post-prime response to SARS2 RBD. The strongest SARS1 response was raised by Quartet Nanocage, followed by Uncoupled Quartet, with the Uncoupled RBD and Homotypic Nanocage giving a weak

response. The SARS1 AUC raised by the Quartet Nanocage was greater than the SARS2 AUC raised by the Homotypic Nanocage. SARS1 RBD was a mismatched antigen, not represented in any of the immunogens, and so an anti-SARS1 response indicates induction of broadly binding antibodies (Figure 4.4).

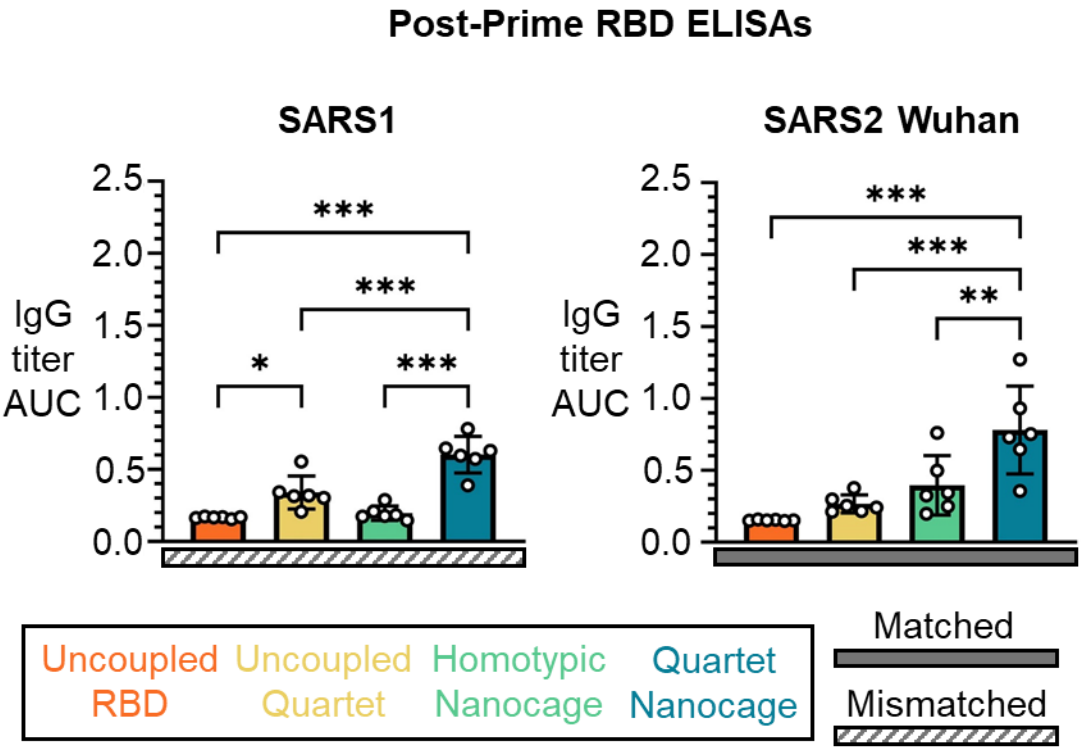

Figure 4.4: Post-Prime ELISA results for Initial Quartet Immunization. ELISA binding for mouse antisera IgG antibodies after a single dose (post-prime) of either uncoupled SARS2 RBD (orange), Uncoupled Quartet (yellow), Homotypic Nanocage displaying SARS2 RBD on SpyCatcher003-mi3 (green), and Quartet Nanocage (blue). A solid gray rectangle under a sample indicates that the ELISA is against a component present in the vaccine (matched) while a striped rectangle indicates that the ELISA is against a component absent from the vaccine (mismatched). Each individual dot represents serum from one animal. The mean (n = 6) is denoted by a bar, shown ± 1 standard deviation. Significance was calculated with an ANOVA test using Tukey's post hoc test. * $p < 0.05$, ** $p < 0.01$, *** $p < 0.001$; other comparisons were non-significant.

In the post-boost samples, I again determined that the strongest response against SARS2 was raised by the Quartet Nanocage. The next strongest anti-SARS2 response was raised by the Uncoupled Quartet, followed by the Homotypic Nanocage, and finally the Uncoupled RBD (Figure 4.5). When I performed post-boost ELISAs against the SARS2 Wuhan, Beta, and Delta spike proteins this same pattern was retained (Figure 4.6).

Immunizations with Uncoupled RBD and Homotypic Nanocage elicited low response levels against all of the non-SARS2 sarbecoviruses RBDs that were tested. The strongest response raised by the Homotypic Nanocage to an RBD other than SARS2 was the closely related RaTG13 (Figure 4.5).

In contrast, the Uncoupled Quartet and Quartet Nanocage elicited substantial immune responses against all tested RBDs. The Quartet Nanocage raised the strongest response of the immunogens to all tested RBDs and in each case raised a significantly greater response than the Uncoupled RBD or Homotypic Nanocage. A strong response was raised by the Quartet Nanocage against the mismatched SARS1 and BM48-31 RBDs that were absent from the Quartet. The Quartet Nanocage antibody response raised to these mismatched RBDs was only slight lower than the anti-SARS2 response raised by the Homotypic Nanocage (Figure 4.5).

I had initially hypothesized that there would likely be variability in the immune response raised against RBDs based on their location on the chain. My hypothesis was that steric hindrance would reduce BCR accessibility for the RBDs nearer the nanocage surface, leading to a stronger response to RBDs on Quartet further from the SpyTag. In practice, I did not observe any clear relationship between the RBD chain location and antibody response (Figure 4.5). These ELISAs results indicate that the Quartet Nanocage approach is able to induce broadly binding antibodies against a group of evolutionarily related viruses.

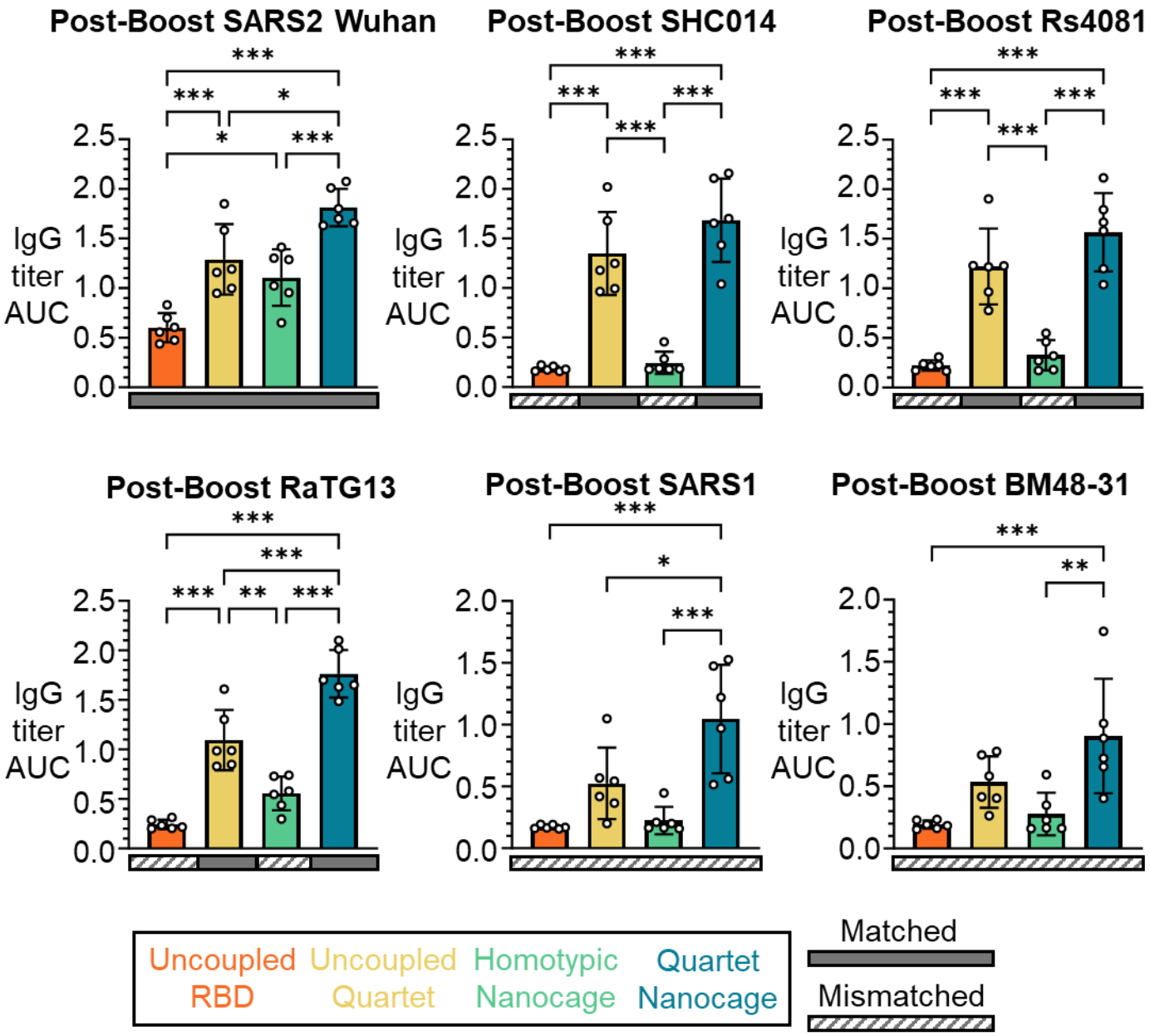

Figure 4.5: Post-Boost anti-RBD ELISA results for Initial Quartet Immunization. ELISA binding for mouse antisera IgG antibodies after two doses (post-boost) of either uncoupled SARS2 RBD (orange), Uncoupled Quartet (yellow), Homotypic Nanocage displaying SARS2 RBD on SpyCatcher003-mi3 (green), or Quartet Nanocage (blue). A solid gray rectangle under a sample indicates that the ELISA is against a component present in the vaccine (matched) while a striped rectangle indicates that the ELISA is against a component absent from the vaccine (mismatched). Each individual dot represents serum from one animal. The mean (n = 6) is denoted by a bar, shown ± 1 standard deviation. Significance was calculated with an ANOVA test using Tukey's post hoc test. * $p < 0.05$, ** $p < 0.01$, *** $p < 0.001$; other comparisons were non-significant.

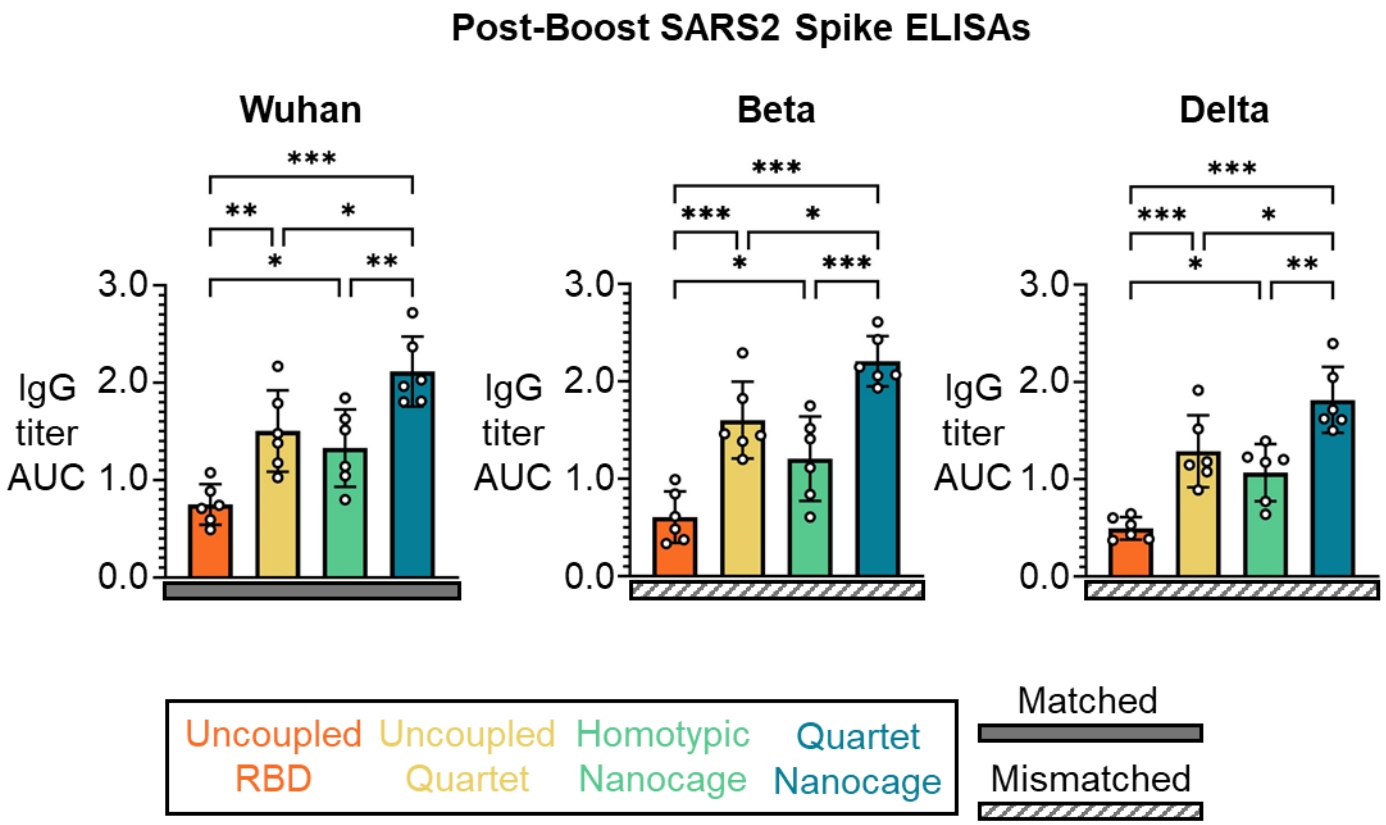

Figure 4.6: Post-Boost anti-spike ELISA results for Initial Quartet Immunization. ELISA binding for mouse antisera IgG antibodies after two doses (post-boost) of either uncoupled SARS2 RBD (orange), Uncoupled Quartet (yellow), Homotypic Nanocage displaying SARS2 RBD on SpyCatcher003-mi3 (green), or Quartet Nanocage (blue). A solid gray rectangle under a sample indicates that the ELISA is against a component present in the vaccine (matched) while a striped rectangle indicates that the ELISA is against a component absent from the vaccine (mismatched). Each individual dot represents serum from one animal. The mean (n = 6) is denoted by a bar, shown ± 1 standard deviation. Significance was calculated with an ANOVA test using Tukey's post hoc test. * $p < 0.05$, ** $p < 0.01$, *** $p < 0.001$; other comparisons were non-significant.

4.3 Comparison of Quartet Nanocages and Mosaic nanoparticles

Given the success of mosaic nanoparticles at inducing broadly neutralizing antibodies (Cohen et al., 2021, 2022) and their support to enter Phase I clinical trials, I wanted to compare the immune responses raised by Mosaic nanoparticles and Quartet immunogens.

For these experiments, I cloned a version of the Quartet with the SpyTag at the N-terminus (Figure 4.7A). This SpyTag-Quartet construct would couple to SpyCatcher003-mi3 in the opposite orientation and allow further interrogation into the relationship between location on the chain and potency of immune response. I expressed SpyTag-Quartet in Expi293F cells and efficiently purified the construct by SpySwitch (Figure 4.7C). This SpyTag-Quartet construct was used for all subsequent immunizations, unless stated otherwise.

In order to produce a Quartet immunogen that incorporated all eight RBDs in the Mosaic-8 nanoparticle, I cloned the Alternate Quartet. This Quartet contained the RBDs from pang17, RmYN02, Rf1, and WIV1 (Figure 4.7B). The Alternate Quartet was expressed in Expi293F cells and was efficiently purified by SpySwitch (Figure 4.7D). Coupling both the Quartet and the Alternate Quartet to SpyCatcher003-mi3 allows for the display of all eight RBDs present in Mosaic-8. Dual Quartet Nanocage is the name I gave to SpyCatcher003-mi3 displaying both the Quartet and Alternate Quartet. This Dual Quartet Nanocage displays the same number of RBDs as Mosaic-8 but uses only three components instead of the nine required for Mosaic-8.

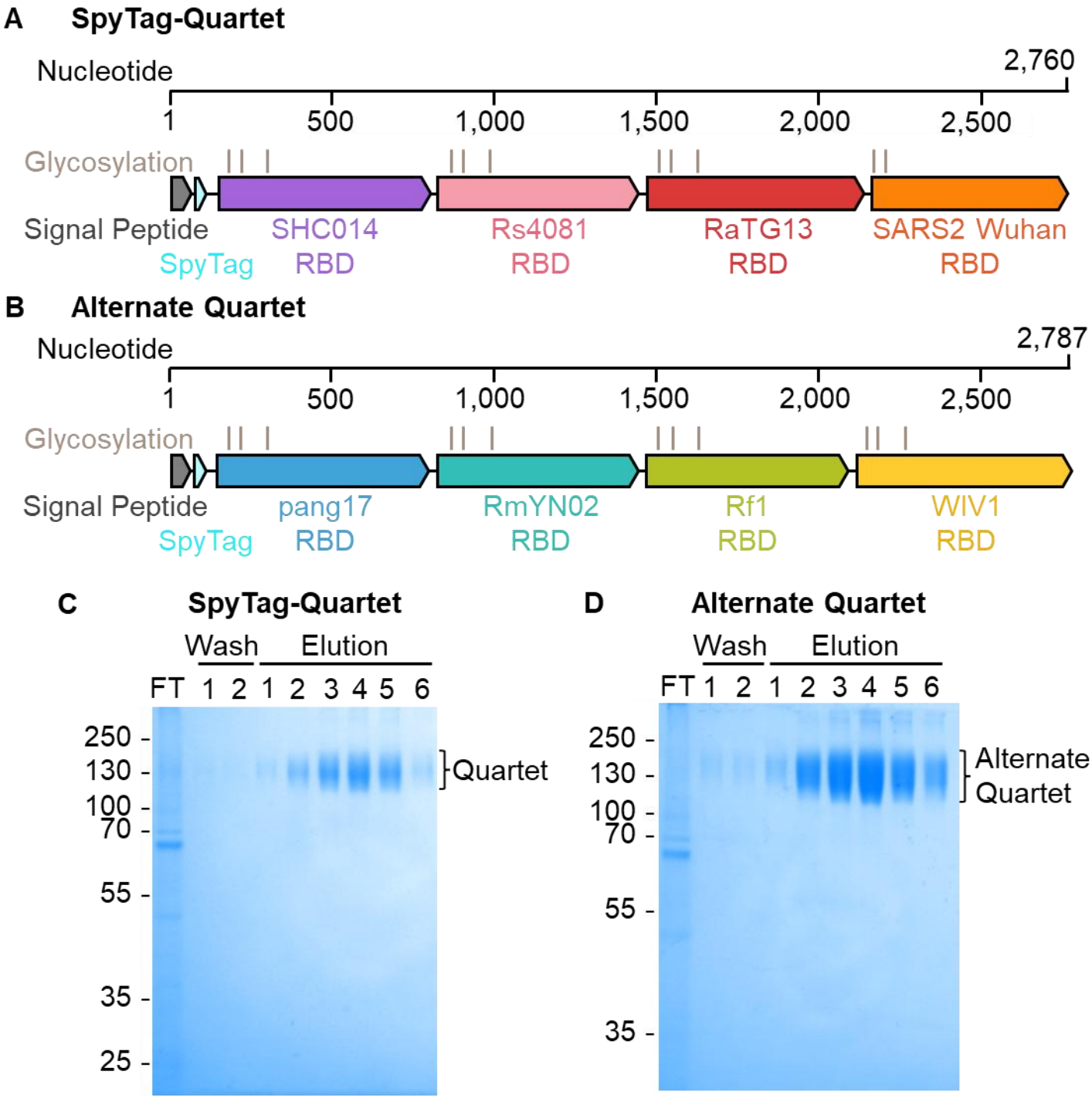

Figure 4.7: Expression of additional Quartets. (A) Schematic showing the genetic organization of the SpyTag-Quartet construct. **(B)** Schematic showing the genetic organization of the Alternate Quartet construct. The identity of constituent RBDs and location of SpyTag, Signal Peptide and predicted glycosylation sites. Flexible linkers are shown as a black line. **(C)** SpySwitch purification of SpyTag-Quartet. **(D)** SpySwitch purification of Alternate Quartet. Both SpySwitch purifications are analysed using an SDS-PAGE gel stained with Coomassie. The lanes include the flowthrough (FT), wash (1-2), and elution fractions (1-6).

I ran both the SpyTag-Quartet and SpyTag-Alternate Quartet over an S200 column in PBS pH 7.4 and demonstrated a single population for both constructs. Both constructs eluted at a similar volume (Figure 4.8) suggesting that there is minimal aggregation or multimerization for either immunogen.

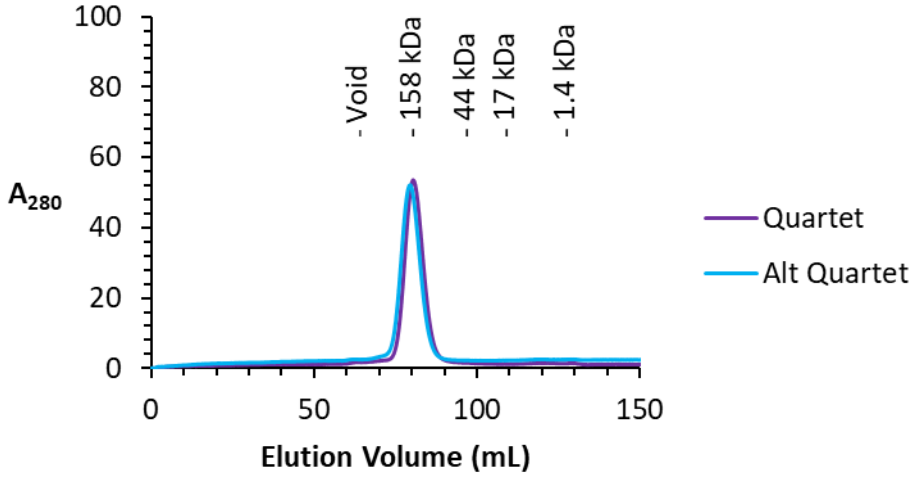

Figure 4.8: Size Exclusion Chromatography on Quartets. SpyTag-Quartet and Alternate (Alt) Quartet were run over an S200 column in PBS pH 7.4 after purification by SpySwitch. Bio-Rad gel filtration standards were run over the same column under the same conditions and the elution volume based on these standards are presented. A280 is measured in mAU.

I produced five nanoparticle-based immunogens by coupling SpyTagged RBDs or Quartets to SpyCatcher003-mi3 (Figure 4.9A). The Homotypic Nanocage displayed only SARS2 RBD. Both the Mosaic-4 and Quartet Nanocage immunogen displayed SHC014, Rs4081, RaTG13 and SARS2 Wuhan RBD. The Dual Quartet Nanocage and Mosaic-8 nanoparticle display these same RBDs along with pang17, RmYN02, Rf1, and WIV1. DLS was performed on these immunogens and demonstrated homogenous assembly after coupling to SpyCatcher003-mi3 (Figure 4.9B).

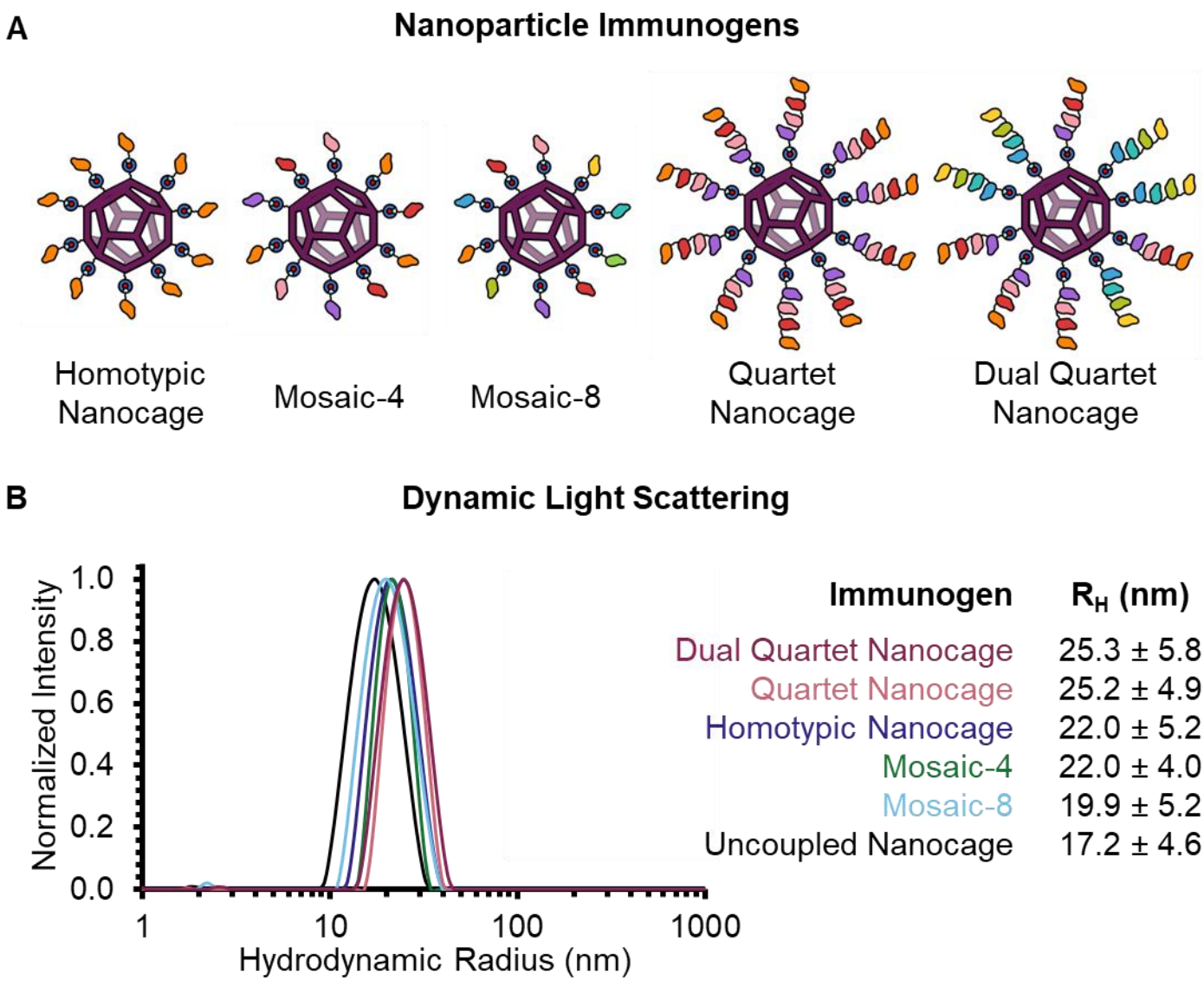

Figure 4.9: Dynamic Light Scattering on Nanoparticle Immunogens. (A) A cartoon schematic of the nanoparticle immunogens analysed by DLS. **(B)** DLS results for SpyCatcher003-mi3 alone (Uncoupled Nanocage) and each of the nanoparticle immunogens. The mean hydrodynamic radius ±1 standard deviation is derived from 20 scans of the sample and are displayed in the table.

I performed negative stain transmission electron microscopy (TEM) on SpyCatcher003-mi3 (Nanocage), Mosaic-8, and Quartet Nanocage. This technique allowed for visualization of individual nanoparticle immunogens and confirmed the integrity of the Quartet Nanocages. An equivalent visible particle diameter was found for uncoupled Nanocage, Mosaic-8 and Quartet Nanocages. This is consistent with dynamic arrangement of the Quartets on the nanocage surface not allowing for TEM visualization (Figure 4.10).

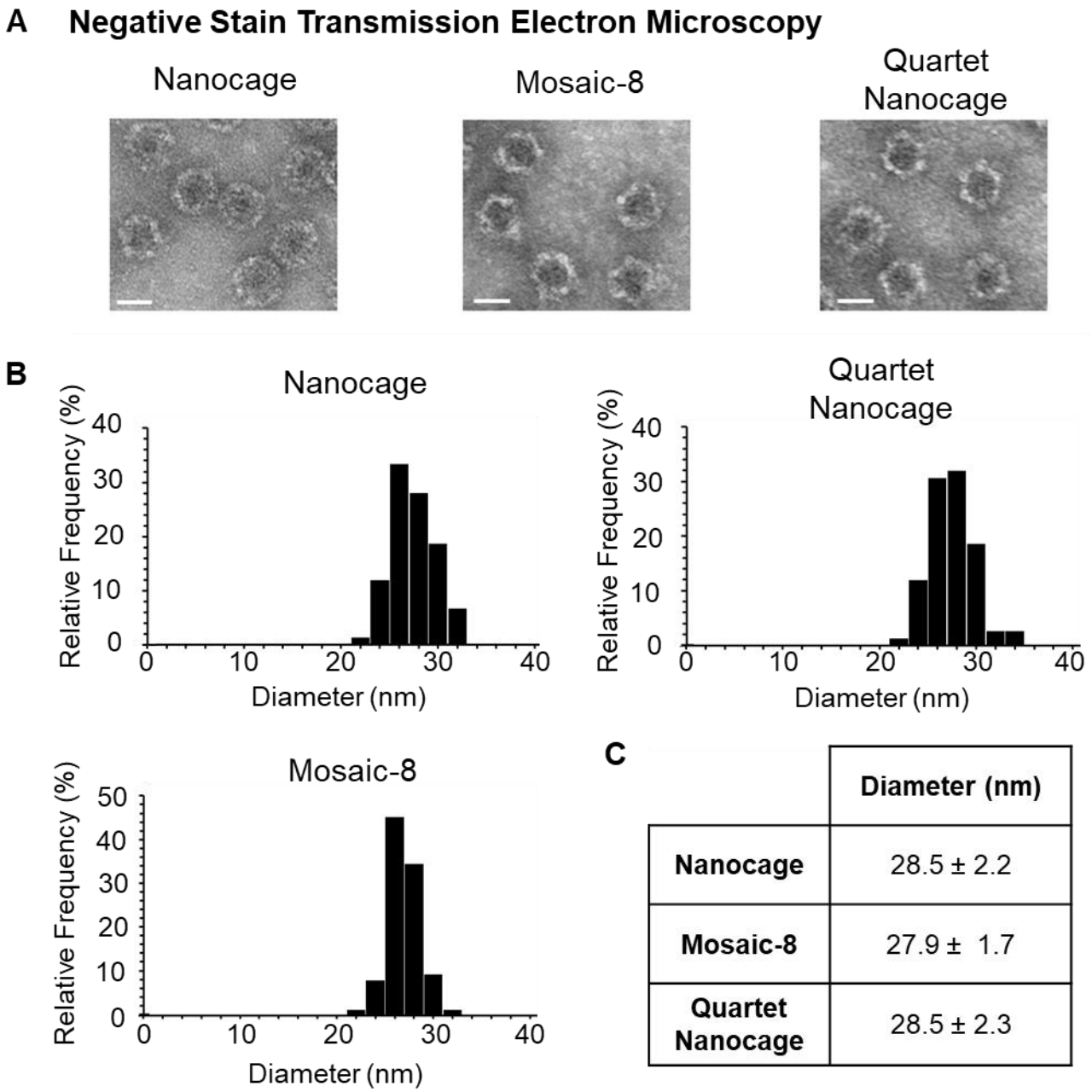

	Diameter (nm)
Nanocage	28.5 ± 2.2
Mosaic-8	27.9 ± 1.7
Quartet Nanocage	28.5 ± 2.3

Figure 4.10: Negative stain TEM of nanocage immunogens. (A) Representative images for negative stain TEM of uncoupled Nanocage, Mosaic-8 nanoparticles, and Quartet Nanocages. Scale bar is 20 nm. **(B)** Nanoparticles size distribution as measured by TEM with 2 nm bin size (n = 75). **(C)** Table of the size distribution of different nanoparticles: mean ± 1 standard deviation (n = 75).

I endotoxin-depleted all immunization components and determined that the final endotoxin levels were below 20 EU/mL. I produced and aliquoted the following immunogens: Homotypic SARS2 Nanocage, Mosaic-4, Mosaic-8, Quartet Nanocage, Dual Quartet Nanocage, and Uncoupled Quartet. As in previous immunizations, I performed molar normalization and included a molar equivalent of immunogens in each dose. Under this protocol the same concentration of SpyCatcher003-mi3 is used for the five nanoparticle-based immunogens. Two immunizations were performed by Jack Tan (University of Oxford) using the alum-based VAC 20 as an adjuvant (Figure 4.11A).

I analysed post-prime sample response to SARS2 (matched) and SARS1 (mismatched) RBD by mouse antisera ELISA. The two strongest responses against SARS2 were raised by the Quartet Nanocage and Dual Quartet Nanocage. The Dual Quartet Nanocage raised the strongest mismatched response to SARS1. Mosaic-8 and Quartet Nanocage raised similar responses to SARS1 that were greater than the Homotypic Nanocage. The Uncoupled Quartet raised relatively poor responses to both SARS1 and SARS2 (Figure 4.11B).

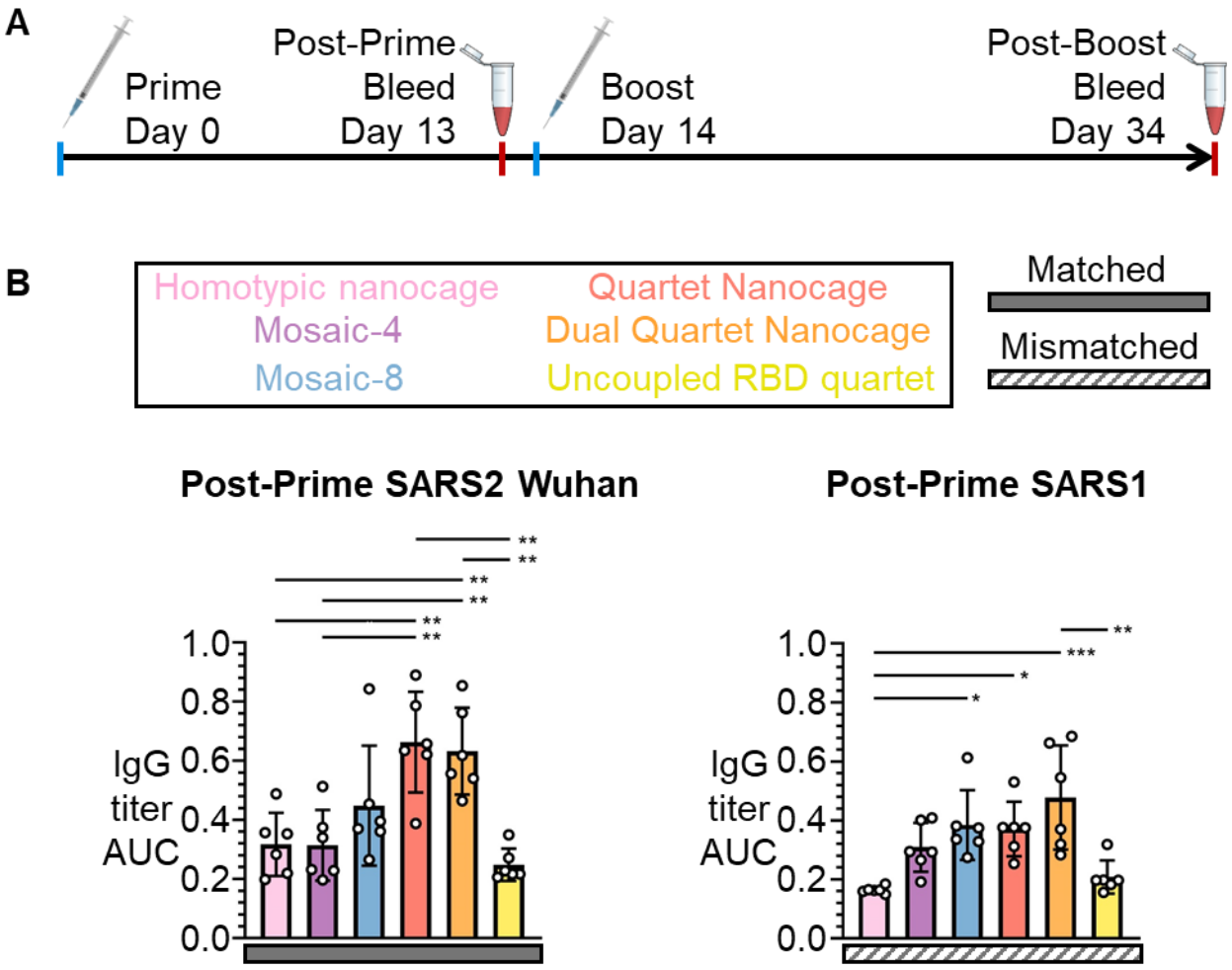

Figure 4.11: Antibody induction by Quartet and Mosaic Immunogens. (A) Summary of timeline (doses and sampling) for this set of immunizations with 0.02 nmol antigen per dose. **(B)** ELISA for serum IgG from mice immunized with a single dose (post-prime) of the indicated immunogen. Each dot represents serum from one animal. The mean is denoted by a bar (n=6), with error bars ± 1 standard deviation. Significance was calculated with an ANOVA test using Tukey's post hoc test. * $p < 0.05$, ** $p < 0.01$, *** $p < 0.001$; other comparisons were non-significant.

I subsequently performed antisera ELISAs on the post-boost sera samples. I found that the two highest antibody titres against all tested sarbecovirus RBDs were raised by the Quartet and Dual Quartet Nanocage (Figure 4.12-4.14). There was no statistically significant difference between this pair for any of these tested antigens (Figure 4.14). This result was surprising for WIV1 and pang17, given that these RBDs are present in the Dual Quartet Nanocage but not the Quartet Nanocage. Supporting previous work (A. Cohen et al., 2021), the Mosaic-4 and Mosaic-8 nanoparticles raised a broad anti-sarbecovirus response that exceeded the Homotypic Nanocage. The Homotypic Nanocage gave relatively poor responses to the non-SARS2 RBDs, with the two strongest responses raised to the closely related RaTG13 and pang17 RBDs (Figure 4.12-4.14).

The Uncoupled Quartet had a stronger performance in the post-boost samples and consistently elicited similar responses to Mosaic-4 and Mosaic-8 (Figure 4.12-4.14). There was no statistically significant difference between the Uncoupled Quartet response and either mosaic nanoparticle for any of the tested sarbecovirus RBDs (Figure 4.14).

As anticipated, all condition except for the Uncoupled Quartet induced similar antibody responses against the SpyCatcher003-mi3 platform (Figure 4.15). As a negative control, SpyTag003-Maltose Binding Protein (MBP) was included and ELISAs demonstrated minimal response against SpyTag003 in all cases (Figure 4.15).

As with the previous Quartet immunizations (Figure 4.5) and in spite of the flipped orientation of the Quartets, there was no apparent relationship between the position of the RBD on the chain and the strength of immune response the RBD elicited (Figure 4.12).

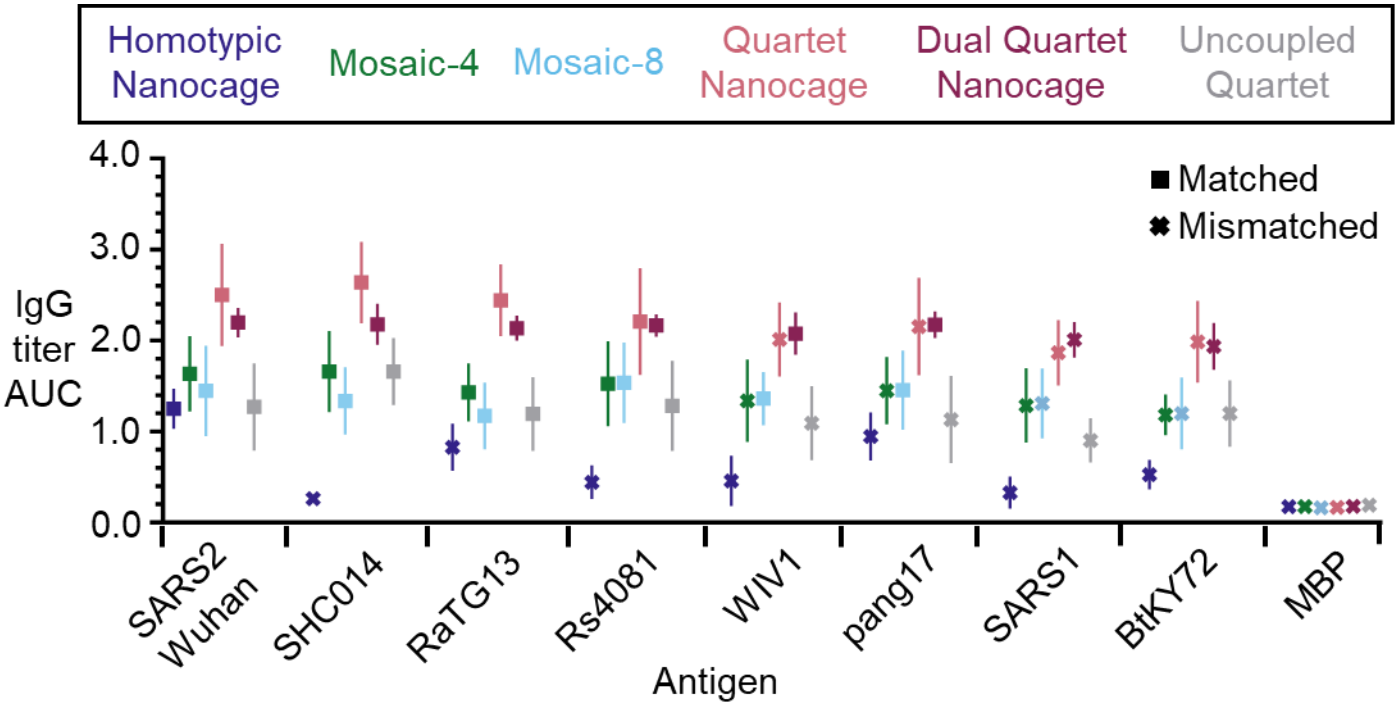

Figure 4.12: Post-boost antibody induction by Quartet and Mosaic immunogens. Post-boost serum IgG was analysed by ELISA. The results are presented as AUC for sera from mice immunized with Homotypic SARS2 Nanocages (dark blue), Mosaic-4 (green), Mosaic-8 (light blue), SpyTag-Quartet Nanocage (pink), Dual Quartet Nanocage (purple) or Uncoupled Quartet (grey). The mean AUC for ELISAs against a component of that vaccine (matched) is indicated with squares. The means AUC for ELISAs against an antigen absent in that vaccine (mismatched) are indicated with crosses. Responses are shown to a panel of sarbecovirus RBDs, with SpyTag-MBP as a negative control. The mean (n=6) is shown ±1 standard. Individual data points and statistics are shown in Figure 4.16.

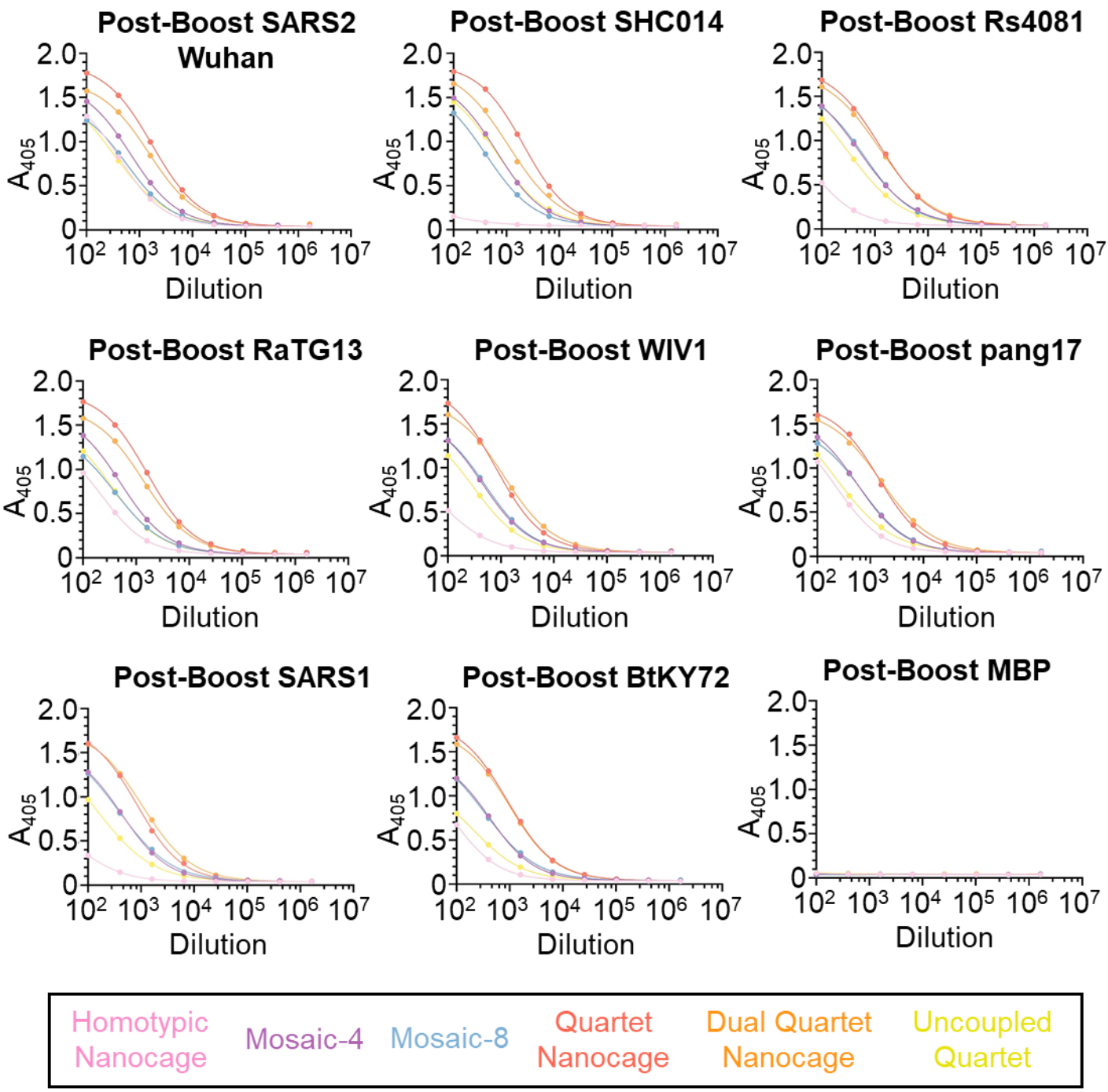

Figure 4.13: Serum binding curves for comparison of Quartet and Mosaic immunogens. ELISA binding data are presented for a serial dilution of mice sera after immunization with either uncoupled SARS2 Wuhan RBD (orange), Uncoupled Quartet (yellow), SARS2 Wuhan RBD coupled to SpyCatcher003-mi3 (Homotypic Nanocage, green), and Quartet Nanocage (blue) as outlined in Figure 4.13. The mean absorbance (duplicate measurements for n=6 serum samples) for each immunization condition at each dilution is plotted with a curve fit for each immunization condition.

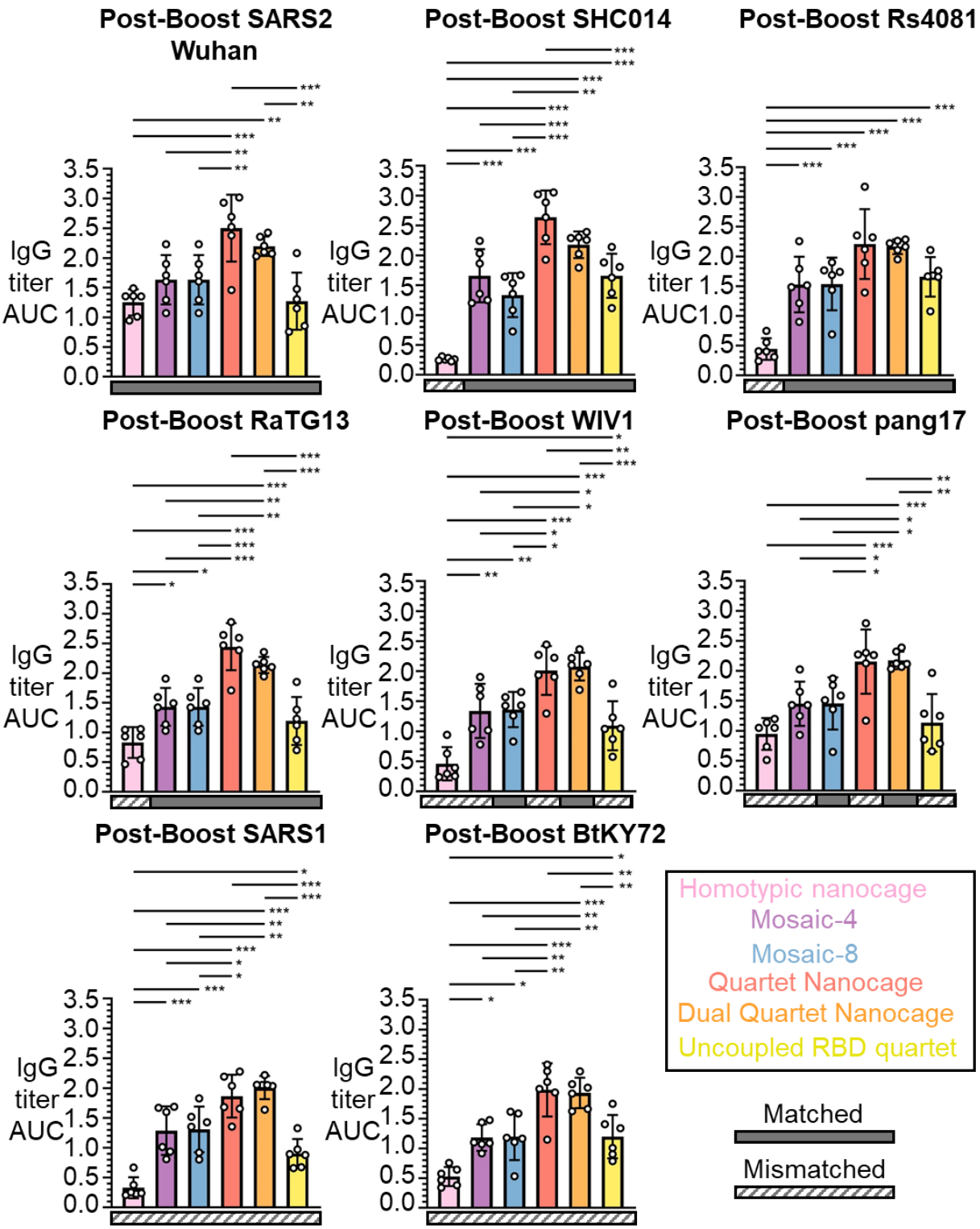

Figure 4.14: Analysis of antibody induction by Quartet and Mosaic immunogens. ELISA for post-boost serum IgG from mice immunized with the indicated immunogen with 0.02 nmol antigen per dose, presented as area under the curve of a serial sera dilution. Each dot represents serum from one animal. The mean is denoted by a bar, with error bars ± 1 standard deviation, n = 6. Significance was calculated with an ANOVA test using Tukey's post hoc test. * $p < 0.05$, ** $p < 0.01$, *** $p < 0.001$; other comparisons were non-significant.

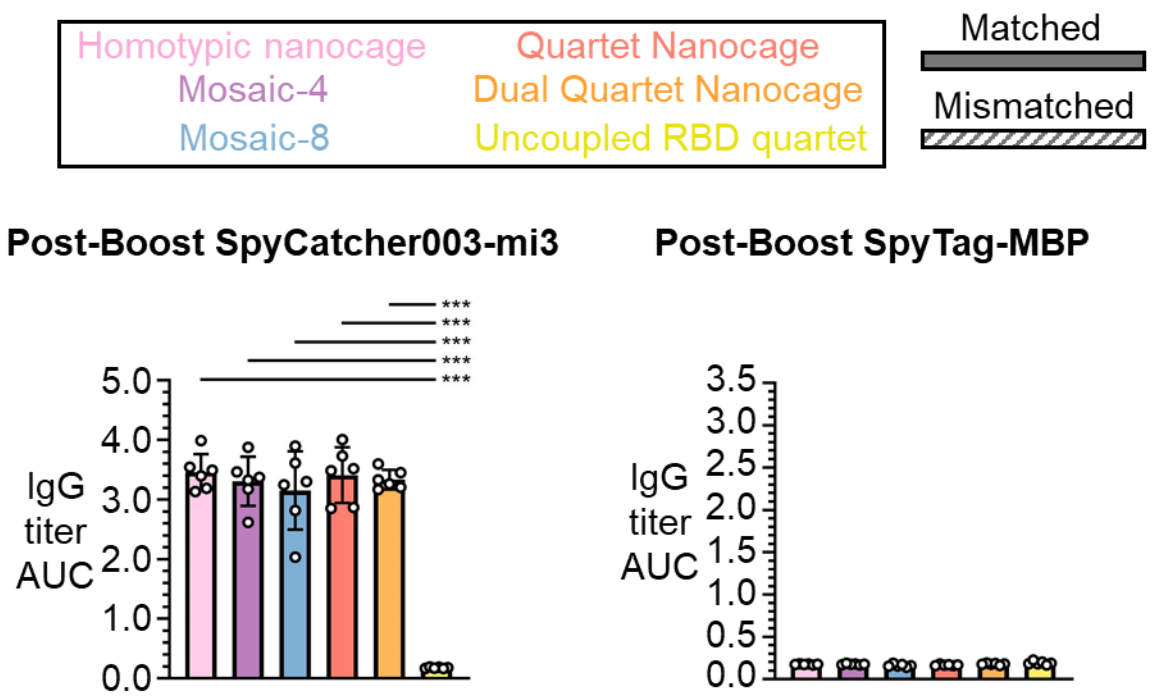

Figure 4.15: Breadth of antibody induction by Quartet and Mosaic Immunogens. ELISA for serum IgG from mice immunized with the indicated immunogen. The response is measured against SpyCatcher003-mi3 or SpyTag-MBP. Each dot represents serum from one animal. The mean is denoted by a bar, with error bars ± 1 standard deviation, n = 6. Significance was calculated with an ANOVA test using Tukey's post hoc test. No significance test was performed for SpyTag-MBP responses. * $p < 0.05$, ** $p < 0.01$, *** $p < 0.001$; other comparisons were non-significant.

In order to further interrogate the response to RBDs at different distances from a Nanocage, I performed ELISAs on Quartet antigens using a set of previously described monoclonal antibodies (Figure 4.16A). I found minimal difference between the monoclonal antibody binding with and without coupling to SpyCatcher003-mi3 (Figure 4.16B). However, there was a consistent reduction in anti-SARS2 monoclonal antibody binding when SARS2 was the innermost RBD (as in Quartet-SpyTag) compared to when SARS2 was the outermost RBD (as in SpyTag-Quartet) (Figure 4.16C). Despite this apparent difference in monoclonal antibody binding, I have not determined any relationship between antibody response and chain location for any of the Quartet immunizations that I have performed.

A

Antibody	Class of RBD Epitope	Specificity
FI-3A	1	SARS2
C121	2	SARS2
FP-8A	1 or 2	SARS2
FD-5D	3	SARS2
FP-12A	4	SARS2
IY-2A	4	Broad
EY-6A	4	Broad
LCA60	n/a	MERS

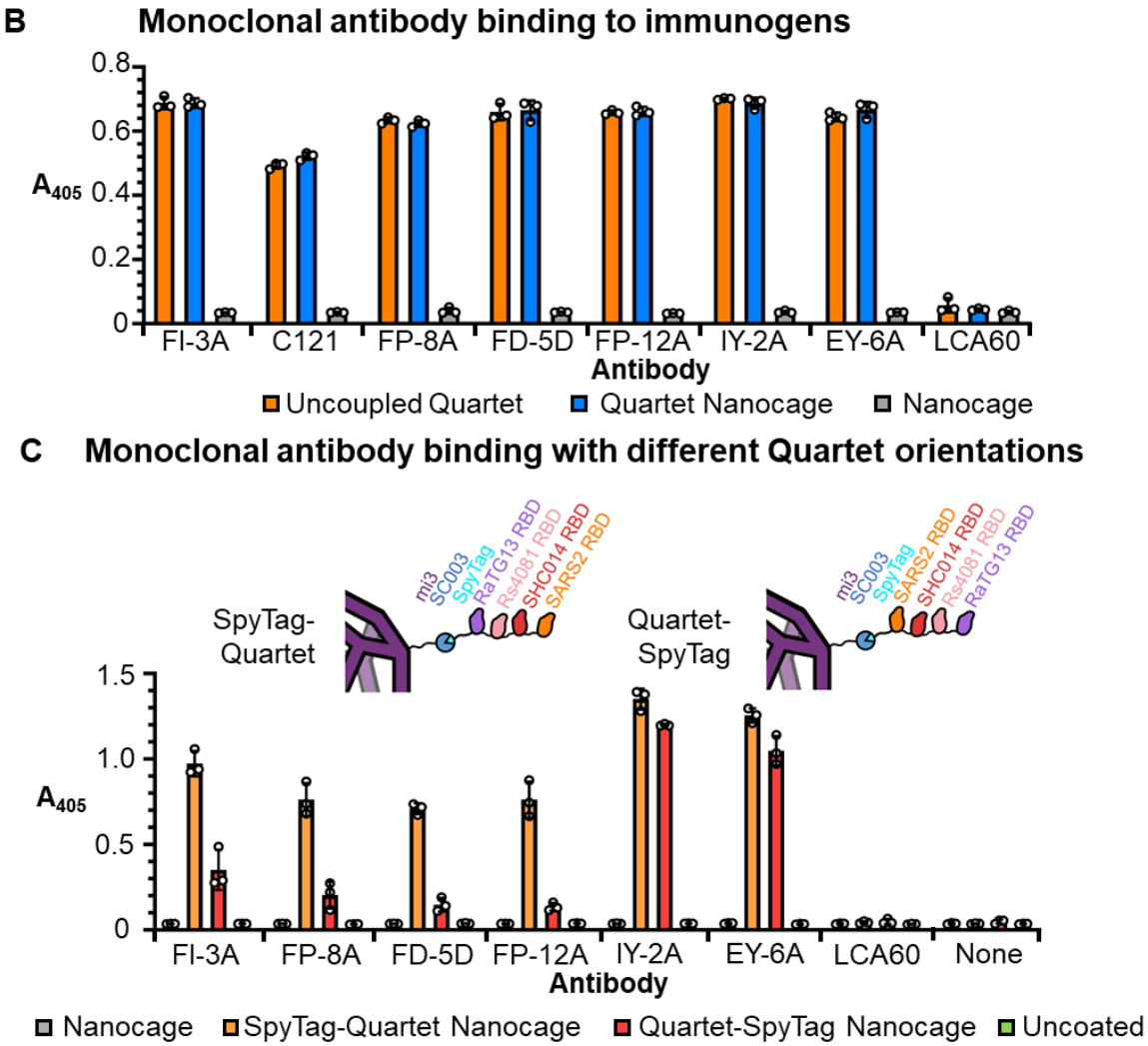

Figure 4.16: Monoclonal antibody binding to Quartet Nanocages. (A) A summary of monoclonal antibodies used in these experiments. **(B)** Monoclonal antibody binding to Quartet with and without coupling to SpyCatcher003-mi3. The mean absorbance for replicate wells (n=3) is denoted by a bar, with error bars ± 1 standard deviation. **(C)** Monoclonal antibody binding to Quartet coupled to SpyCatcher003-mi3 with different orientations. The mean absorbance for replicate wells (n=3) is denoted by a bar, with error bars ± 1 standard deviation.

To relate the levels of antibody binding to antibody efficacy, we worked with collaborators to perform virus and pseudovirus neutralizations with the collected mouse antisera. Sera were tested for neutralization of the SARS2 Wuhan or Delta virus and the strongest neutralization for both pathogens was induced by the Quartet Nanocage (Figure 4.17A,B). The Uncoupled Quartet provided poorer neutralization of both viruses than Homotypic Nanocage (Figure 4.17A). This result is notable as the Uncoupled Quarte demonstrated a higher antibody binding titre than Homotypic Nanocage against SARS2 Wuhan RBD (Figure 4.5), SARS2 Wuhan spike, and SARS2 Delta spike (Figure 4.6). These neutralization assays were performed by Sai Liu, Javier Gilbert-Jaramillo, and William S. James (Oxford).

SARS1 neutralization was compared for sera elicited by Quartet and Mosaic antigens using a pseudotyped virus neutralization assay. SARS1 was mismatched for all tested immunogens, giving insight into breadth of neutralization. Pseudotyped virus neutralization has been shown to correlate well with neutralization of authentic virus (Schmidt et al., 2020). In these assays, the Dual Quartet Nanocage gave the strongest mismatched neutralizing response to SARS1. Quartet Nanocage and Mosaic-8 gave similar levels of neutralization that were the next strongest (Figure 4.17C). These neutralization assays were performed by Jennifer R. Keeffe, Kaya N. Storm, Priyanthi N. P. Gnanapragasam with supervision provided by Pamela Bjorkman (California Institute of Technology).

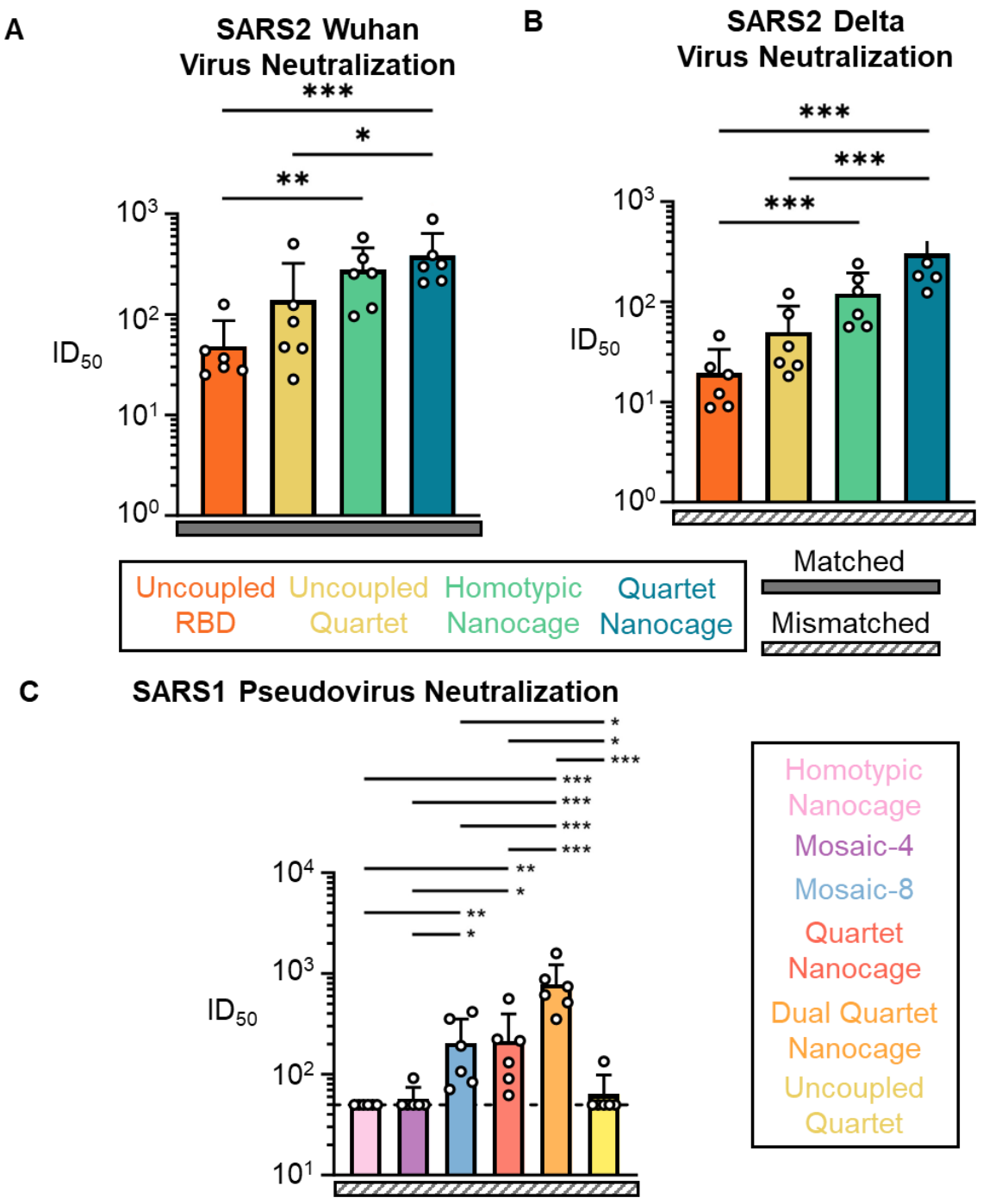

Figure 4.17: Neutralization by sera elicited from Quartet Immunizations. (A) Neutralization of SARS2 Wuhan and Delta virus by mice treated with Uncoupled RBD (orange), Uncoupled Quartet (yellow), Homotypic Nanocage (green) or Quartet Nanocage (blue). Neutralizations were performed by Sai Liu, Javier Gilbert-Jaramillo, and William S. James (Oxford). **(B)** Neutralization of SARS1 pseudovirus (mismatched) treated with different Quartet and Mosaic immunogens. Neutralizations were performed by Jennifer R. Keeffe, Kaya N. Storm, and Priyanthi N. P. Gnanapragasam (California Institute of Technology). Dashed horizontal lines represent the limit of detection. For all neuralizations, each dot represents one animal, showing the serum dilution giving 50% inhibition of infection (ID50). The mean (n=6) is denoted by a bar + 1 standard deviation. Significance was calculated with an ANOVA test, followed by Tukey's multiple comparison post hoc test of ID50 values converted to log10 scale. *P < 0.05, **P < 0.01, ***P < 0.001; other comparisons were non-significant.

4.4 Quartet Nanocage immunization in mice with existing immunity

Given that a large portion of the global population has been vaccinated for or previously infected with SARS2 (Mathieu et al., 2021; H. Wang et al., 2022; Watson et al., 2022b; WHO, 2023), it is critical to understand whether a broad antibody response can be achieved when immunity to a specific virus has already developed. A wide variety of vaccine regimens have been applied globally, including different administration schedules and different combinations of vaccines. It was not a feasible to experimentally match this diversity. I chose to use soluble SARS2 Wuhan spike protein to induce pre-bias and investigate the impact of pre-existing immunity on Quartet Nanocage immunogens.

I wanted to be able to compare immunogens that included SARS2 RBD with those that lacked the RBD in the context of an immune system pre-biased to SARS2. A reasonable hypothesis would be that administration of a SARS2-containing immunogens to animals with a pre-existing response to SARS2 would boost the existing response at the expense of other antigens in the chain. In this scenario, inclusion of SARS2 RBD would narrow the immune response.

To test this hypothesis, I cloned a new version of SpyTag-Quartet which replaced SARS2 RBD with SARS1 RBD (Figure 4.18A). This construct was called Quartet[SARS1] and allows for creation of Quartet Nanocages where SARS2 RBD was absent. I expressed Quartet[SARS1] in Expi293F cells and purified by SpySwitch (Figure 4.18B). I performed SEC on the protein using an S200 column in PBS pH 7.4 and found a single population that eluted similarly to all other Quartet constructs (Figure 4.18C).

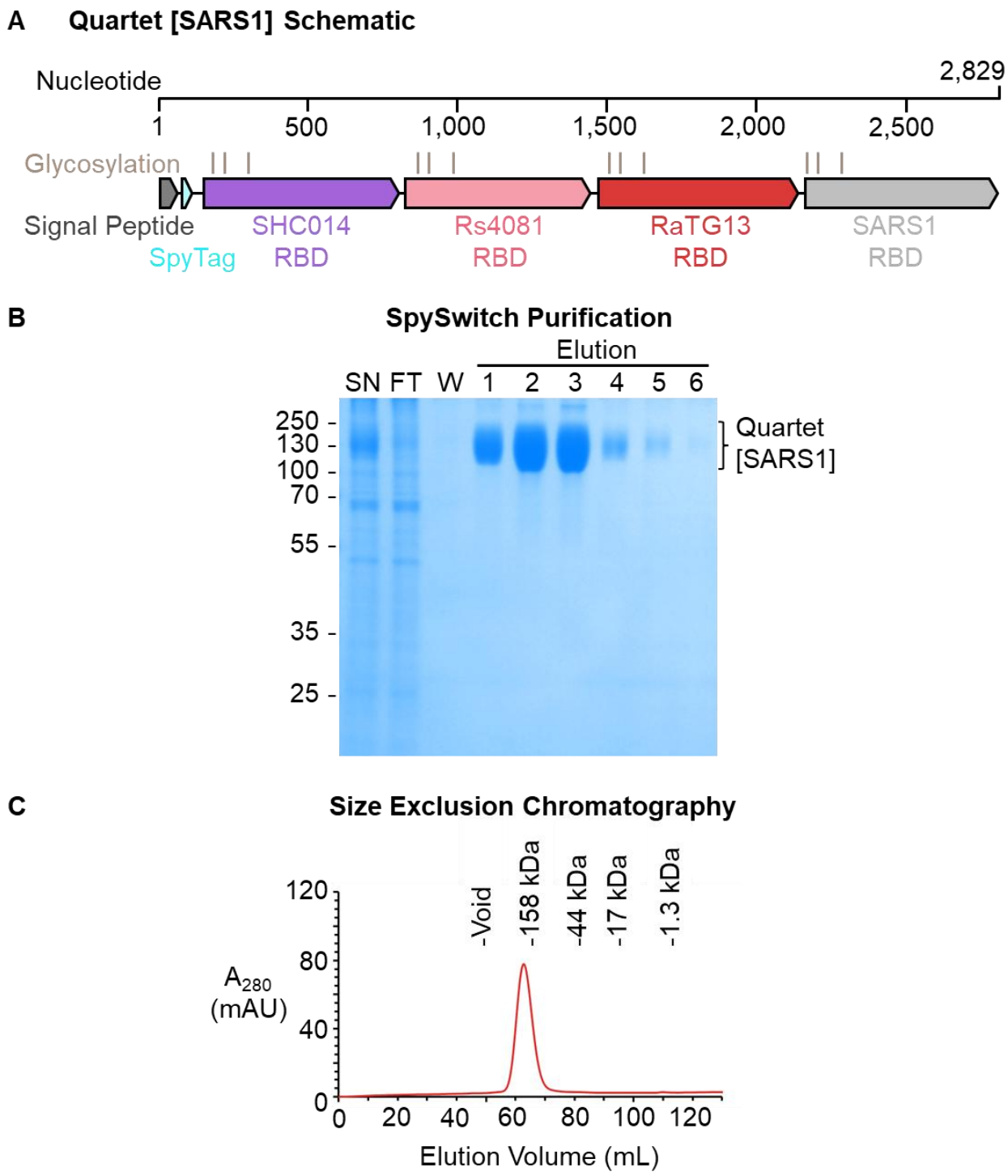

Figure 4.18: Purification of the Quartet[SARS1] Construct. (A) Schematic showing the genetic organization of the Quartet[SARS1] construct. The identity of constituent RBDs and location of SpyTag, Signal Peptide and predicted glycosylation sites are indicated. Flexible linkers are shown as a black line. **(B)** SpySwitch purification of SpyTagQuartet analysed using SDS-PAGE with Coomassie staining. The lanes include the supernatant (SN) flowthrough (FT), wash (W), and elution fractions (1-6). **(C)** Quartet[SARS1] was run over a HiPrep Sephacryl S-200 HR 16-600 columnin PBS pH 7.4. Bio-Rad gel filtration standards were run over the same column under the same conditions and the elution volume based on these standards are presented.

In this experiment, all mice were primed using a soluble SARS2 Wuhan spike (HexaPro) protein. Mice were than boosted with different immunogens. Two of these boost immunogens lacked SARS2 RBD: Quartet Nanocage [SARS1] and Dual Quartet Nanocage [SARS1]. The other boost immunogens were Homotypic SARS2 Nanocage, Mosaic-8, Quartet Nanocage, Dual Quartet Nanocage, and, as a control, a second dose of Wuhan spike (Figure 4.19). I prepared all immunogens, endotoxin-depleted them and established acceptable endotoxin levels by a LAL assay. All immunization and sampling were performed by Jack Tan (University of Oxford).

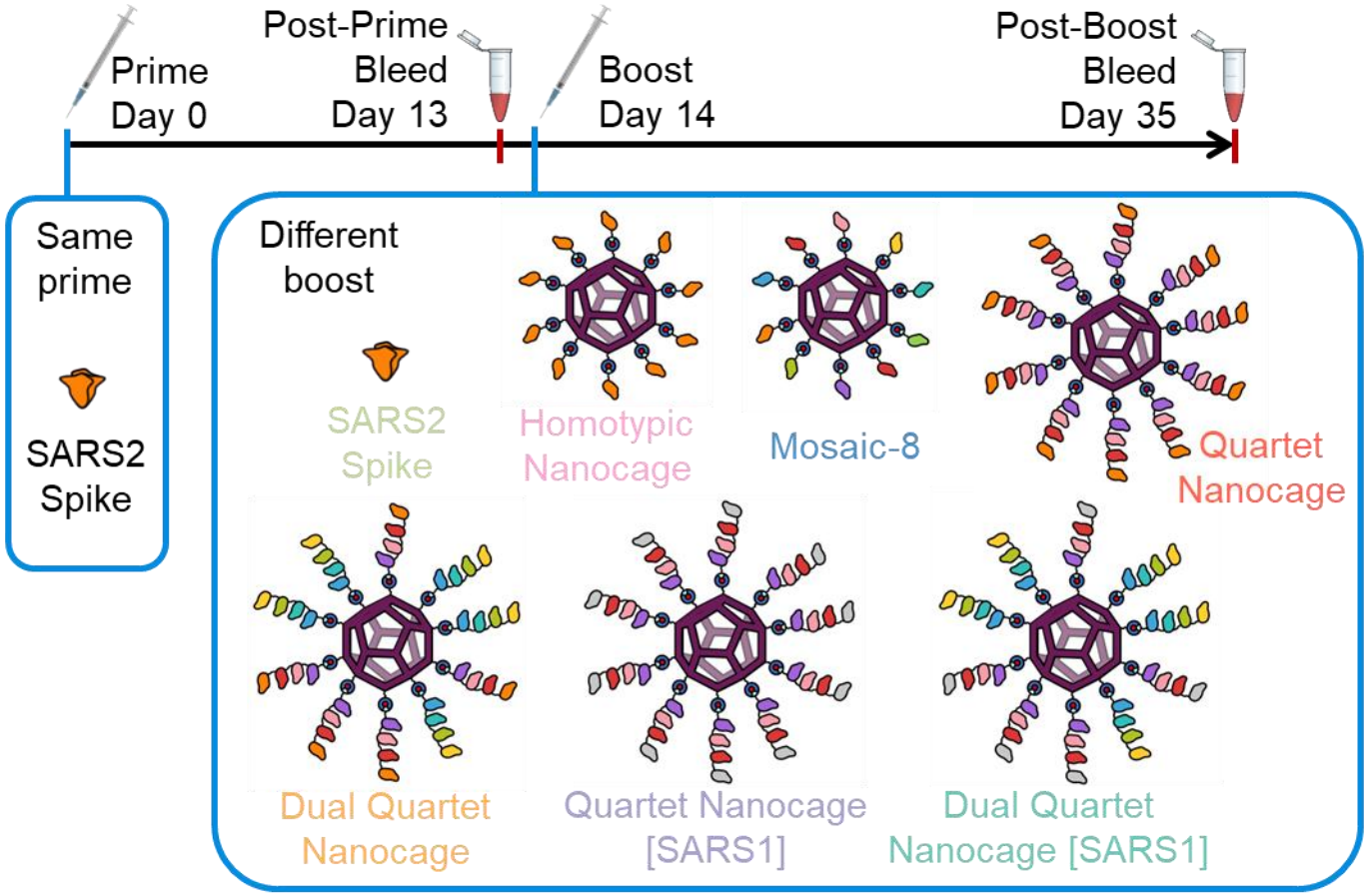

Figure 4.19: Quartet and Mosaic Immunizations with heterologous prime. Summary of timeline (dosing and sampling) for immunizations with a pre-primed response against SARS2. All mice receive the same SARS2 spike boost. Different groups receive a different immunogen boost, as outlined in this schematic.

I performed post-prime antisera ELISAs on the sera treated with Wuhan spike protein. As expected, these immunizations elicited a narrow antibody response that bound to SARS2 RBD but raised negligible response to SARS1 or BtKY72 (Figure 4.20).

When I performed antisera ELISAs on the post-boost sample, all of the boost immunogens had raised similar responses against SARS2 RBD. This result was notable as SARS2 RBD was absent from both the Quartet Nanocage [SARS1] and Dual Quartet Nanocage [SARS1]. This means that these Quartet-based immunogens were able to boost an anti-SARS2 response despite lacking any SARS2 sequences (Figure 4.21).

All of the Quartet Nanocage vaccines, as well as Mosaic-8, raised greater antibody response than the Homotypic Nanocage or spike boost against the mismatched SARS1 and BtKY72 RBDs. Quartet Nanocage and Mosaic-8 raised similar responses to mismatched SARS1 and BtK72 (Figure 4.21), which aligned with the results for a single dose of these candidates in naïve mice (Figure 4.11). Intuitively, the Quartet Nanocage [SARS1] and Dual Quartet Nanocage [SARS1] raised the strongest anti-SARS1 RBD response.

These results demonstrate the Quartet Nanocage vaccines can achieve a broad anti-sarbecovirus response in spite of an initial bias towards a specific virus. Under the conditions tested there was not a clear benefit to removing the pre-biased antigen from the vaccine. Excitingly, the results also suggest that a Quartet Nanocage lacking SARS2 sequence can still boost strong levels of anti-SARS2 response.

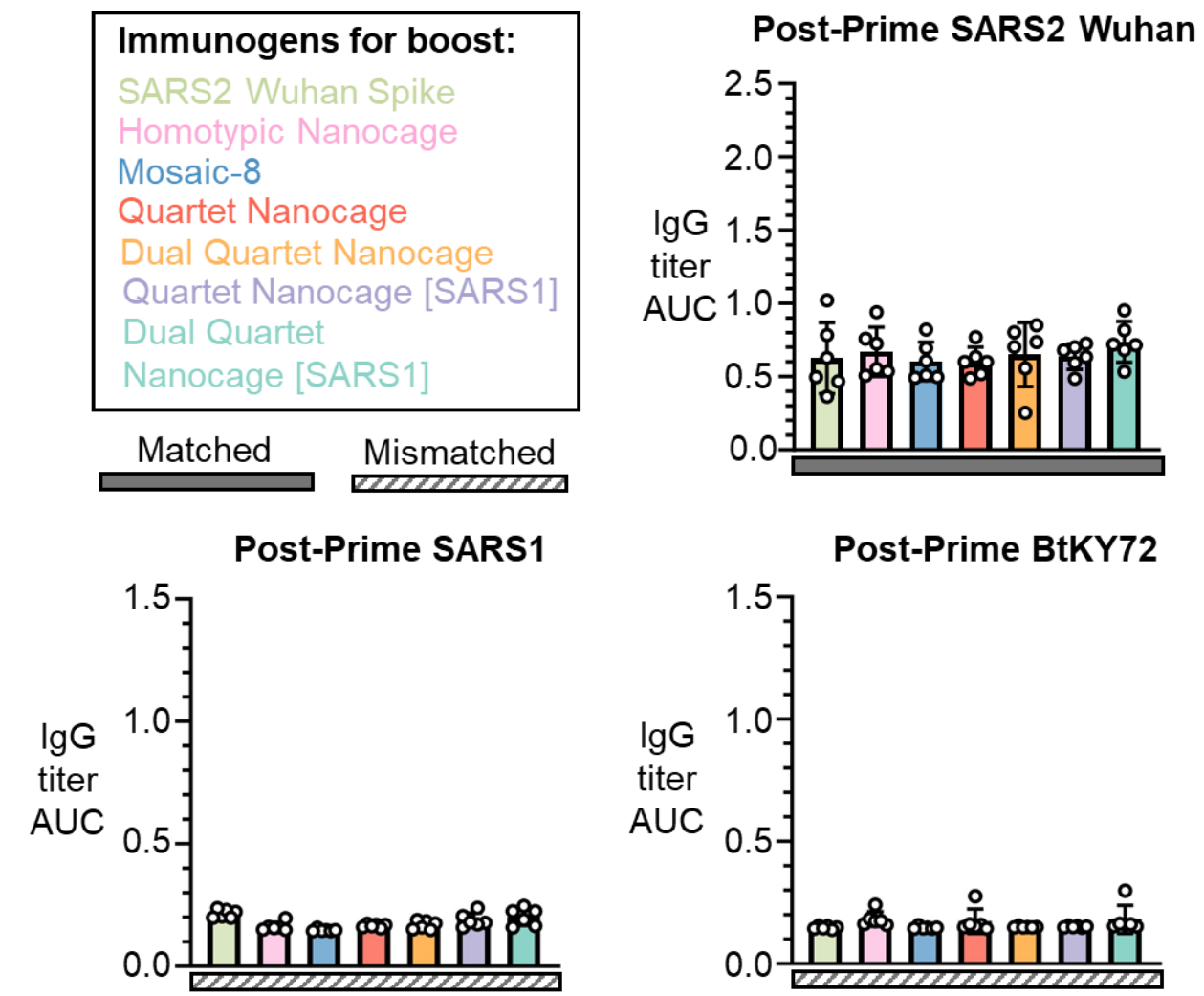

Figure 4.20: Post-Prime results for Quartet and Mosaic Immunizations with Wuhan spike Prime. ELISA for serum IgG from mice immunized with a single dose of SARS2 Wuhan spike protein, grouped by the second dose of 0.02 nmol antigen they will receive. No significance test was performed on post-prime samples. Each dot represents serum from one animal. The mean (n = 6.) is denoted by a bar, with error bars ± 1 standard deviation.

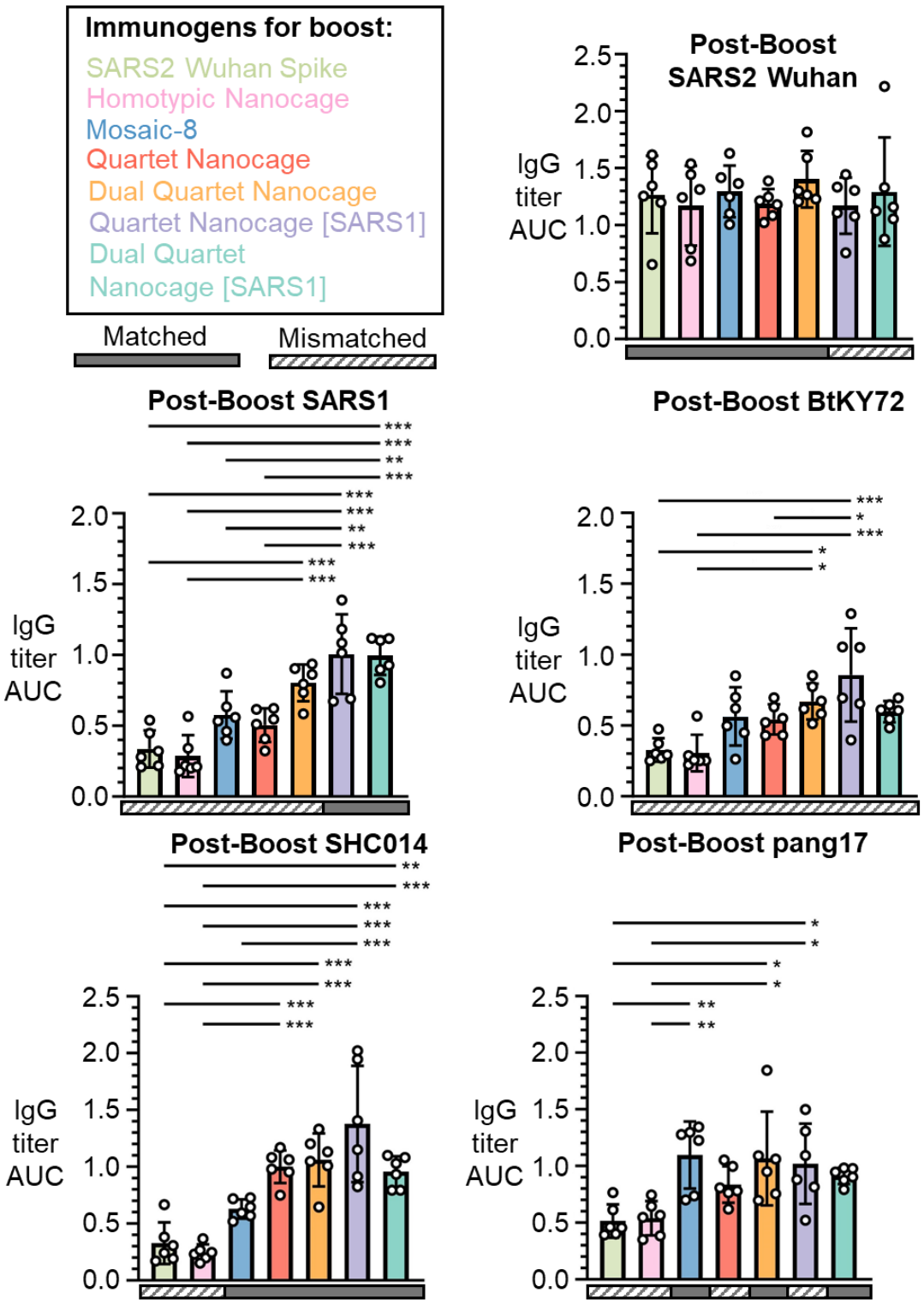

Figure 4.21: Post-Boost results for Quartet and Mosaic Immunizations with Heterologous Boost. Mice were primed using Wuhan SARS2 spike, before boosting with the specified immunogen. Solid rectangles under samples matched ELIESA and striped rectangles indicate mismatched ELISAs. Each dot represents one animal. The mean (n=6) is denoted by a bar ±1 standard deviation.; n = 6. Significance was calculated with an ANOVA test using Tukey's post hoc test. *P < 0.05, **P < 0.01, ***P < 0.001; other comparisons were non-significant.

4.5 Discussion

In this chapter, I have established that the RBDs from multiple sarbecoviruses can be expressed in tandem as a single concatenated polyprotein. These proteins, which I have named Quartets, can be efficiently expressed, purified, and assembled onto protein nanocages. I have shown that mouse immunization with a soluble Quartet protein can elicit antibodies to the antigens represented on the Quartet and, critically, to evolutionarily related viruses not present on the Quartet. This indicates that Quartets can raise a broad humoral response that may provide protection against a range of viruses. The single-component Uncoupled Quartet vaccine was shown to raise similar antibody binding titres as the nine-component Mosaic-8 vaccine. It is, however, important to note that Uncoupled Quartets moderately underperformed in neutralization assays relative to what might be expected based on binding titres.

The highest level of matched and mismatched immune response raised by Quartets required the tandemly linked antigen to be displayed on SpyCatcher003-mi3. The two-component Quartet Nanocage and three-component Dual Quartet Nanocage raised neutralizing antibodies that bound a range of different matched and mismatched sarbecoviruses. The responses raised to the mismatched SARS1 and BtKY72 were similar to the specific immune response raised against SARS2 by a Homotypic SARS2 Nanocage. Both Quartet Nanocages and Dual Quartet Nanocages elicited higher levels of antibodies than Mosaic-8 which is a leading pan-sarbecovirus vaccine candidate (Cankat et al., 2024; C. Q. Huang et al., 2023).

Tandemly linked sequential antigens have previously been explored for linear T cell epitopes (Skwarczynski & Toth, 2016). In this context there is no requirement for the linked antigens to fold into a three-dimensional. Cell secretion machinery can be challenged by repeats of related structured domains and undesired pairings of the domains can occur (Borgia et al., 2015). This has proven not to be a substantial issue for our purposes, with the multiple Quartets being

efficiently expressed. There are a variety of factors which may have aided the expression of these Quartets. First, there is sequence divergence between the RBDs present (~70-90%). Secondly, sarbecovirus RBDs demonstrate favourable solubility and thermostability (Vester et al., 2022). Thirdly, there is a flexible region at the termini of RBDs which was supplemented with additional flexible linkers further delineating the different domains. There was a substantial reduction in expression levels for a construct containing six different sarbecovirus RBDs, indicating a limitation to these benefits.

Previous studies with RBD genetic fusion have largely focused on eliciting protective responses against SARS2 or existing human coronaviruses. A tandem homodimer has been previously implemented as a COVID-19 vaccine with the fusion of two SARS2 Wuhan RBDs (Dai et al., 2022). An updated version of this vaccine has formed a heterotrimer by tandemly linked the Delta and Omicron BA.2 RBD (P. Du et al., 2024). One vaccine candidate that has entered clinical development is a heterotrimer with one RBD from Wuhan, Beta and Kappa SARS2 (Liang et al., 2022). Another strategy has involved the fusion of individual RBDs to proliferating cell nuclear antigen to make a ring with coronavirus antigens from five different human coronaviruses (Lee et al., 2023).

My work builds on these approaches and seeks to elicit a broad and robust response across sarbecoviruses. Critically, this approach aims to target the humoral response towards evolutionarily conserved regions of the antigen. In doing so the strategy may provide protection against related zoonotic viruses that may be unknown at the time the vaccine is developed.

To consider the potential mechanism for the Quartet Nanocage, one may consider the Darwinian evolution process central to the function of the germinal centre (De Silva & Klein, 2015; Laidlaw & Ellebedy, 2022). Upon immunization with a Homotypic Nanocage, B cells are selected for the ability of their BCRs to interact with that virus RBD alone. There is no

selective pressure for broad binding and so any breadth that is achieved is simply a happy accident. With Quartet Nanocage immunization, BCRs that only recognize the RBD of one virus are less likely to be activated than BCRs capable of recognizing several different RBDs present in the vaccine. BCRs will be capable of recognizing multiple different RBDs if they bind to regions that are conserved across the RBDs included in the vaccine. Quartet Nanocages, therefore, provide selective pressure for BCR binding to the evolutionarily-conserved regions on the RBD and facilitates the production of broadly binding antibodies.

I was surprised to discover that there was no apparent relationship between location on the RBD chain and the level of antibody response. I had anticipated differential accessibility being an issue and had begun work exploring cyclization of the Quartets by SnoopLigase (Buldun et al., 2018) or SnoopCatcher (Veggiani et al., 2016) to try to overcome this potential bias. However, even when the orientation of the Quartet was flipped, there remained no difference in the relative response elicited to the different RBDs in the chain. These immune response observations were made in spite of the monoclonal antibody ELISAs demonstrating that there were differences in accessibility to RBDs at different locations on the chain.

A potential explanation for this observation is reliant on flexibility within the Quartet chain. Between each RBD there is a mobile region formed by a combination of Glycine-Serine linkers and flexible regions at the termini of the RBD. The flexibility of these Quartet may produce a dynamic arrangement RBDs at the surface of the nanoparticle. This situation would produce a functionally non-uniform surface for B cell stimulation while employing a uniformly made antigen. The flexibility of the Quartets makes the nanoparticle surface difficult to probe by cryo-EM or crystallography (Palamini et al., 2016). SpyCatcher003-mi3 displaying SARS2 RBD alone, without any additional fusion partners, showed minimal RBD electron density in single-particle cryo-EM (T. K. Tan et al., 2021).

The challenge of eliciting novel protective immunity in individuals with pre-existing immune responses is a critical challenge for many diseases, including malaria and influenza (Vatti et al., 2017). In this chapter, I have demonstrated that even after priming with SARS2 Wuhan spike, different Quartet Nanocage immunogens were able to raise antibodies to diverse sarbecovirus RBDs. In these pre-biased mice, the Quartet Nanocages also elicited equivalent antibody titres against SARS2 RBD as SARS2-specific immunogens. These data provide initial support that Quartet Nanocages could be an effective vaccine boost administered in human populations with an existing SARS2 response from immunization and infection.

It is important to note that I did detect induction of antibodies against the SpyCatcher003-mi3 scaffold. I detected a uniform level of response across the Homotypic, Mosaic, and Quartet Nanocages. Unlike viral vector vaccines that need to function and infect cells to be efficacious, anti-platform antibodies against VLPs do not appear to impair response against target antigen (Kraft et al., 2022; Marini et al., 2019). The results in pre-clinical work are promising but it remains an open question whether anti-SpyCatcher003-mi3 antibodies will have clinically relevance, especially in terms of reactogenicity. The upcoming Phase I Mosaic-8 clinical trial will administer SpyCatcher003-mi3 to humans and may provide important insight.

It is important to note two differences between the Mosaic-8 antigen I used as a comparison in these immunizations and the Mosaic-8 antigen that will be entering clinical trials. Firstly, we used SARS2 Wuhan RBD instead of SARS2 Beta RBD. Secondly, we presented RBDs on the nanocage at sub-saturating levels. Saturating the nanoparticle requires the introduction of excess antigen (A. Cohen et al., 2021; Rahikainen et al., 2021). This excess antigen is then removed by SEC or dialysis, both of which can lead to the introduction of endotoxin. More importantly, these steps can vary the concentration of antigen and nanoparticle. This variance can be accounted for, but it will not be as accurate as taking antigens and nanoparticles from

the same stock. Sub-saturating presentation has been shown to elicit strong humoral responses (Marini et al., 2019). While there are valid arguments towards both approaches, I ultimately chose to use sub-saturating levels for all Homotypic, Mosaic, and Quartet antigens.

My research has focused on applying Quartet Nanocages as a protein-based nanoparticle vaccine administered through intramuscular injections. The recognition of mucosal immunity induction as a potent tool to defend against SARS2 (Mitsi et al., 2023; Pilapitiya et al., 2023; Russell & Mestecky, 2022) makes exploration of intranasal delivery of the Quartet Nanocage an obvious next step. Beyond nanoparticle vaccines, the demonstration that RBD Quartets are potently immunogenic and can be expressed efficiently, which opens the door to other vaccine delivery mechanisms. It would be valuable to explore RBD Quartet delivery via viral vectors (Dicks et al., 2022; Folegatti et al., 2020) or messenger RNA vaccine (Hoffmann et al., 2023; Z. Zhang, Mateus, et al., 2022). Such a vaccine could include broadly conserved T cell epitopes (Russell & Mestecky, 2022) to facilitate a broadly effective B and T cell response. To this end, I am actively working with research groups at California Institute of Technology and University of California San Francisco to apply RBD Quartets using mRNA vaccine technology.

Beyond sarbecoviruses, the Quartet Nanocage approach may be applied to other pathogens. An obvious next step would be raising responses to other coronavirus groups such as embecoviruses and merbecoviruses (Y. Han et al., 2023; Rabaan et al., 2023), the latter of which is explored in the following chapter. Outside of coronaviruses, one can consider the application of this tandemly-linked antigen strategy for any pathogen with an effective antigen that fulfils two criteria. Firstly, the antigen must contain conserved regions capable of eliciting effectively protective antibodies. Secondly, the antigen must be robust enough to facilitate tandem expression. In a pre-print published subsequent to our research, the tandem approach

was applied with tandemly linked influenza hemagglutinin head domains displayed on ferritin-based nanoparticles. This approach effectively raised a cross-reactive, neutralizing antibody responses to influenza subtypes that were not included in the vaccine (Lamson et al., 2023).

The Mosaic-8 vaccine has demonstrated impressive pre-clinical results (A. A. Cohen et al., 2022) however regulatory questions about particle heterogeneity and the inherent complexity of vaccine production have been challenges to overcome as the vaccine enters clinical trials. In this chapter, I elucidate the Quartet Nanocage strategy to address these issues. The vaccine candidates I present use only two (Quartet Nanocage) or three (Dual Quartet Nanocage) components. The Quartet Nanocage can be produced homogenously. Presentation of RBD antigens as a Quartet, allows for a greater number of RBDs to be displayed per nanoparticle, which appears to have benefits for antibody induction. In all cases, the level and breadth of antibodies elicited by Quartet Nanocages were at least comparable to, and in many cases greater than, those raised by Mosaic-8.

Despite the rapid generation of effective vaccines, the devastating impacts of the COVID-19 pandemic have been far reaching (Msemburi et al., 2023; Sachs et al., 2022; WHO, 2023). There remains a substantial risk of future outbreaks caused by a novel coronavirus (Menachery et al., 2017). It is, therefore, critical to develop technologies that can facilitate the rapid generation of effective vaccines against newly arising pathogens. One approach to achieve this goal is to develop and validate a vaccine before an outbreak has even begun. This could be facilitated by the development of broad-spectrum vaccines that can protect against a group of related viruses, including those absent from the vaccine itself (Gouglas et al., 2023; Saville et al., 2022). Quartet Nanocages are capable of eliciting antibodies across a range of often mismatched viruses they may prove to be an important tool for this proactive vaccinology

approach. A further exploration of the Quartet Nanocage strategy and investigation of potential applications will be examined in the following chapter.

Chapter 5 – Expanding the Use of Multiviral Quartets for Proactive Vaccinology

The Quartet immunization strategy has been shown to elicit a humoral response that targets a wide array of sarbecoviruses. Critically, this response includes sarbecoviruses that were not represented in the Quartet, indicating that the antibody response has targeted regions of the antigen shared by different viruses. Quartet Nanocages compare favourably with the Mosaic-8 nanoparticle vaccine that is entering Phase I clinical trials, while requiring the production of fewer components and allowing for greater nanoparticle homogeneity.

In this chapter I will explore how the Quartet strategy for broad immune response can be improved and better understood. Building on past results, I will examine albumin hitchhiking as a means to improve the soluble Quartet immunogen to optimize a broad single-component vaccine. I will consider the impact of changing dose and adjuvant on the immunogenicity of the vaccine. Based on deep mutational scanning (DMS) experiments performed by collaborators, I will examine the impact of Quartets on the binding profile of antibodies. In an attempt to better understand how breadth is achieved using a uniform antigen, I will examine the immunogenic impact of removing linkers in the Quartet.

I will seek to broaden the application of the Quartet Nanocage strategy. This effort will first involve examining the responses raised to SARS2 Omicron variants by Quartet Nanocage immunogens. Next, a Quartet that could have been designed prior to the COVID-19 pandemic will be assessed for induction of anti-SARS2 antibodies. Finally, I design and express new Quartets that target an entirely new group of potentially dangerous coronaviruses.

5.1 Exploring albumin-hitchhiking for multiviral Quartets

The Quartet Nanocage has streamlined production requirements, decreasing the nine proteins needed for Mosaic-8 production to two proteins for Quartet Nanocage or three proteins for

Dual Quartet Nanocage. This simplification has the potential to ease scale-up to high levels of vaccine production. There was a desire to augment these outcomes with an enhanced single-component broadly neutralizing vaccine.

Immunization with the Uncoupled Quartets were shown to raise broadly binding antibodies at titres that were comparable to Mosaic-4 and Mosaic-8 (Figure 4.12). However, when assessed in neutralization assays, the Uncoupled Quartet tended to moderately underperform relative to the nanocage-displayed antigens (Figure 4.17). Given the positive impact that albumin-hitchhiking via high-affinity protein binders had on soluble SARS2 RBD (Figure 3.4), I decided to explore a similar strategy with Quartets.

I cloned an iteration of SpyTag-Quartet with a C-terminal ABD035 albumin-binding domain. I expressed the Quartet-ABD035 construct in Expi293F cells and purified by SpySwitch (Figure 5.1A). I used the previously outlined biotinylated HuSA binding plate assay (Figure 3.3) to determine whether fusion of the Quartet to ABD035 prevented binding. This assay demonstrated strong binding of HuSA to Quartet-ABD035 but not to the original Quartet construct (Figure 5.1B). I prepared immunization samples by Triton X-114 phase separation endotoxin-depletion and performed a LAL assay to determine that endotoxin levels were below 20 EU/mL (Brito & Singh, 2011). I aliquoted immunization samples normalizing by antigen molarity. Immunizations were performed by Jack Tan (University of Oxford) according to the timeline outlined in Figure 4.11A.

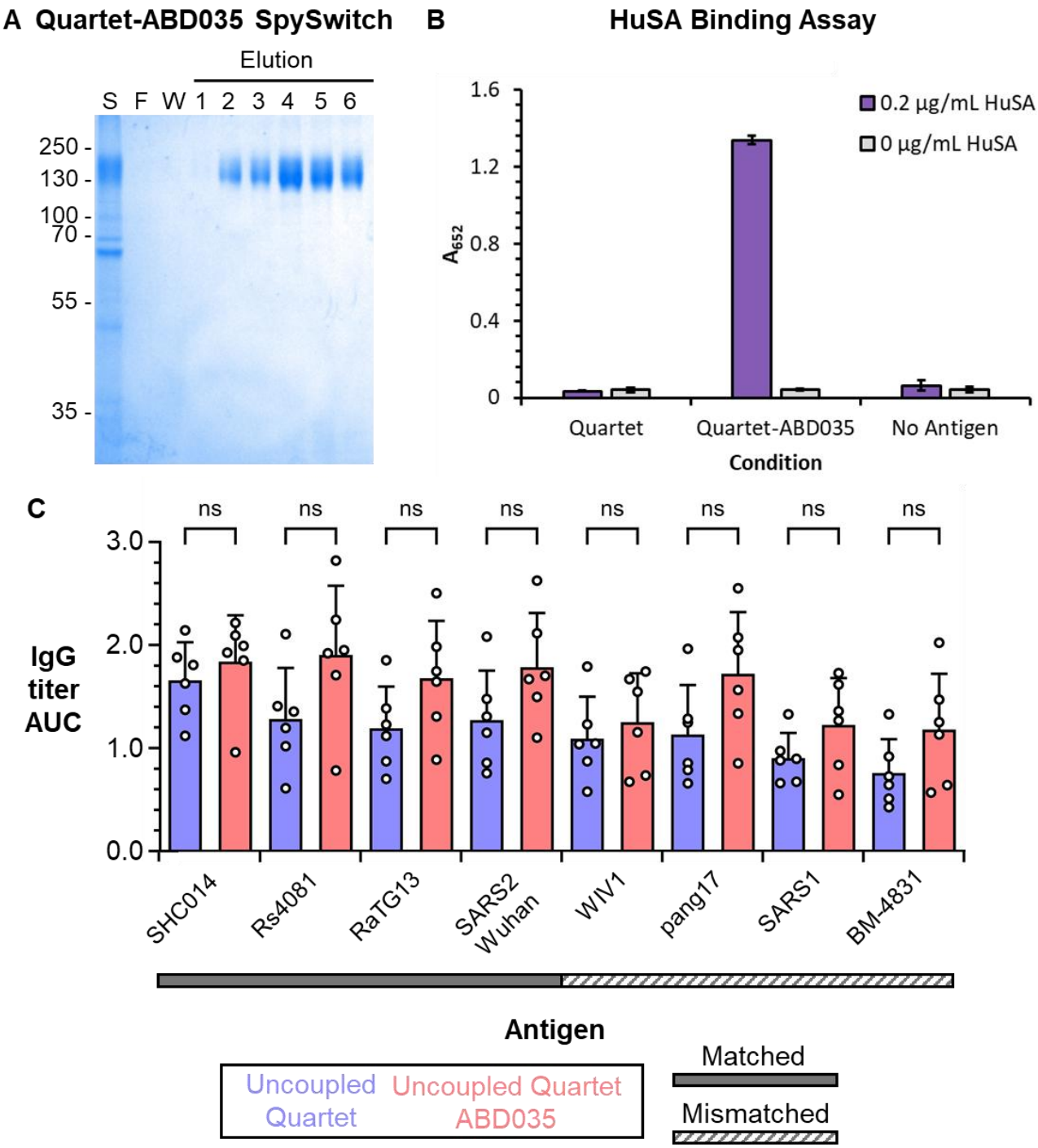

Figure 5.1: Quartet with ABD035 Purification and Immunization. (A) Coomassie/SDS-PAGE analysing the SpySwitch purification of Quartet-ABD035. The lanes include the mammalian supernatant (S), flowthrough (F), wash (W), and elution fractions (E_1 – E_6). **(B)** Results of an albumin binding ELISA. The specified antigen is immobilized to the plate using SpyCatcher2-MBP and is assessed for binding to biotinylated HuSA. Bars represent the mean A_{652} measurement 5 minutes after the addition of TMB (n=3) while the error bars are ±1 standard deviation. **(C)** The area under the curve (AUC) for post-boost antisera elicited by administration of Uncoupled Quartet (blue) and Uncoupled Quartet-ABD035 (red). Binding is assessed for the specified sarbecovirus RBD. Bars represent mean AUC (n=6) with error bars being ±1 standard deviation. Individual points represent the AUC for a single mouse. Significance was calculated with a one-way ANOVA with Bonferroni's multiple comparisons test for the response raised to each immunogen. *P < 0.05, **P < 0.01, ***P < 0.001; ns non-significant.

I performed mouse antisera ELISAs on the post-boost samples. For all tested sarbecovirus RBDs, Quartet-ABD035 raised a greater mean IgG binding response than Quartet. However, none of the differences between Quartet and Quartet-ABD035 response reached statistical significance, when tested using a one-way ANOVA with Bonferroni's multiple comparisons test (Figure 5.1C). The inclusion of ABD035 on the Quartet construct may have had a moderately positive impact on antibody titres but the benefit is not nearly as apparent as it was for the fusion of ABD035 to SARS2 RBD. The inclusion of ABD035 on a Quartet is not comparable to the impact of displaying a Quartet on a nanoparticle.

5.2 Examination of higher dose immunization of Quartet immunogens

Previous Quartet immunizations had achieved neutralization of SARS1 pseudovirus (Figure 4.17C) but the neutralization ID50 was lower than previously reported (A. Cohen et al., 2021; A. A. Cohen et al., 2022). This result was anticipated as our immunizations used 10-fold lower antigen dose than these previous reports. We sought additional insight by performing immunizations in BALB/c mice with10-fold higher antigen dose, and the squalene-based adjuvant AddaVax. All three changes were made to more closely align with these previous immunizations (A. Cohen et al., 2021; A. A. Cohen et al., 2022). I endotoxin-depleted all samples, performed a LA assay to ensure they were at acceptable endotoxin-levels (Brito & Singh, 2011) and aliquoted samples with molar antigenic normalization. Immunizations were performed by Jack Tan (University of Oxford) according to the timeline outlined in Figure 5.2A. This immunization was termed ‘High Dose’ and previous immunization conditions ‘Low Dose’.

I performed mouse antisera ELISAs on post-boost samples. Under the new conditions, Mosaic-8, Quartet Nanocage, and Dual Quartet Nanocage immunogens still raised an enhanced antibody binding response to SARS1 and BtKY72 RBD relative to Homotypic Nanocage.

However, unlike the previous lower dose immunizations, there was no significant difference between the responses raised to any of the tested RBDs by Mosaic-8 and either Quartet immunogen (Figure 5.2).

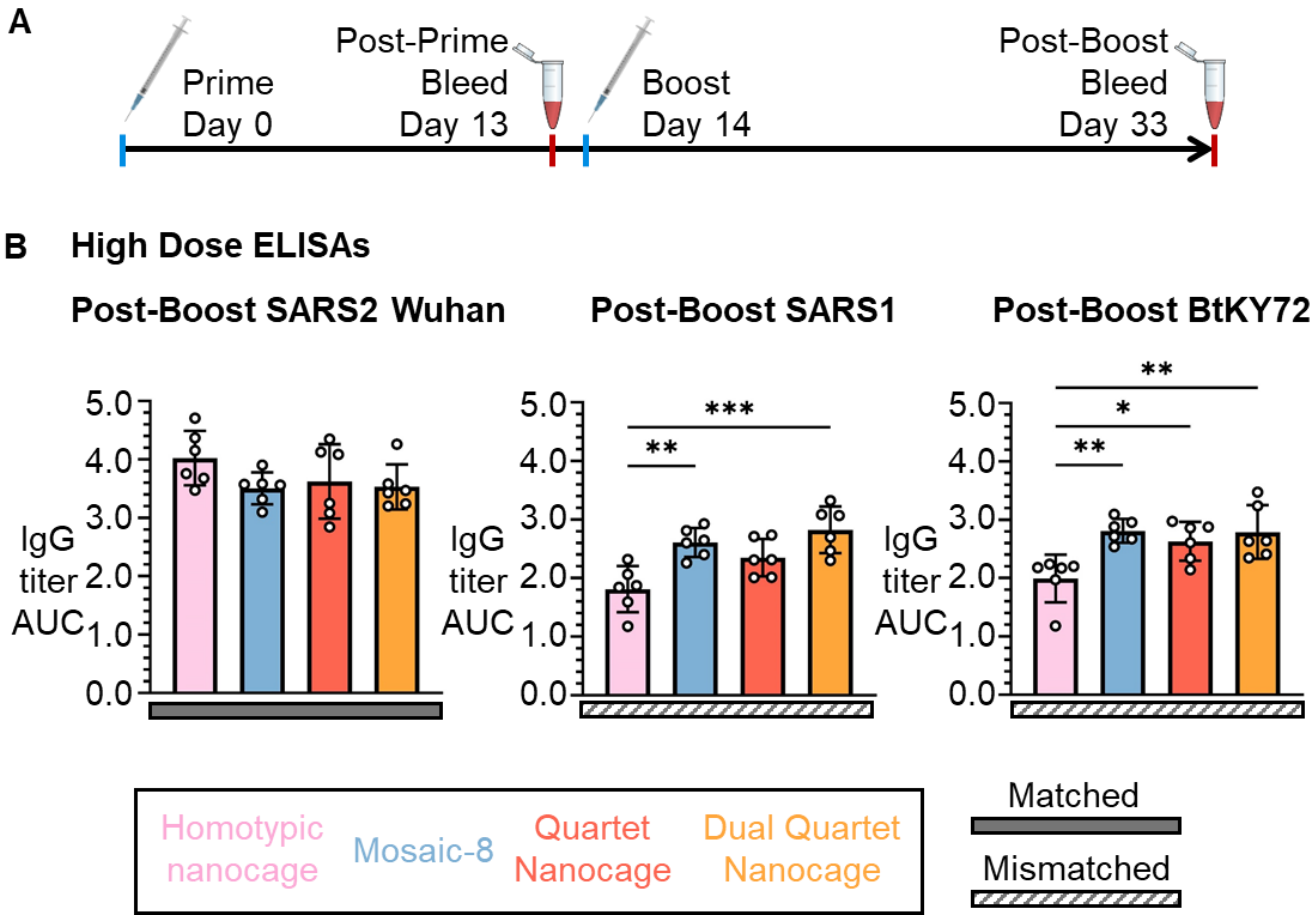

Figure 5.2: High Dose Quartet Immunization ELISAs. (A) Dose administration and sampling timeline for female BALB/c mice immunization. Immunizations were performed at High Dose 0.2 nmol antigen, a 10-fold increase relative to prior immunizations. **(B)** ELISA for post-boost sera assessing IgG binding to SARS2 Wuhan, SARS1 and BtKY72 RBD is shown as the area under the curve (AUC) of a serial dilution. Solid gray rectangles under samples indicate the ELISA is against a component of that vaccine (matched). Striped rectangles indicate the ELISA is against an antigen absent in that vaccine (mismatched). Each dot represents serum from one animal. The mean (n=6) AUC is denoted by a bar, with error bars ± 1 standard deviation. Significance was calculated with an ANOVA test, followed by Tukey's multiple comparison post hoc test. * $p < 0.05$, ** $p < 0.01$, *** $p < 0.001$; other comparisons were non-significant.

Pseudovirus neutralization assays were performed on these High Dose antisera to test the breadth of neutralization across sarbecoviruses. These neutralization assays were performed by Jennifer R. Keeffe, Kaya N. Storm, and Priyanthi N. P. Gnanapragasam (California Institute of Technology). Mosaic-8, Quartet Nanocage, and Dual Quartet Nanocage antisera all induced neutralization of WIV1, SARS1, SHC014, and BtKY72 pseudoviruses at levels greater than the sera elicited from Homotypic Nanocage immunization. Under these immunization conditions, the Dual Quartet Nanocage and Mosaic-8 induced similar neutralization for all tested zoonotic pseudoviruses. Quartet Nanocage performed moderately worse than Mosaic-8 and Dual Quartet Nanocage, at inducing neutralization of BtKY72 and WIV1, but these differences did not reach statistical significance. Neither Homotypic Nanocage, Mosaic-8, Quartet Nanocage, or Dual Quartet Nanocage elicited substantial neutralization of SARS2 Omicron XBB.1 pseudovirus (Figure 5.3).

The High Dose antisera underwent further analysis by yeast-display deep mutational scanning for epitope mapping (Greaney et al., 2021, 2022). These Deep Mutational Scanning assays were performed by Alexander Cohen, Annie Rorick, and Anthony West, Jr. with supervision provided by Pamela Bjorkman (California Institute of Technology).

This assay relies on a SARS2 RBD yeast-display library, that samples all possible single amino acid mutations to RBD. The mutations in this library have been previously characterized for their impact on RBD expression and human ACE2 binding (Starr et al., 2020).

The polyclonal mouse antisera elicited from the High Dose immunization was first used to treat yeast that displayed unmutated RBD. The yeast cells were sorted based on RBD expression and antibody binding. This result provides baseline antisera binding and allows for deviations in antibody binding to be detected.

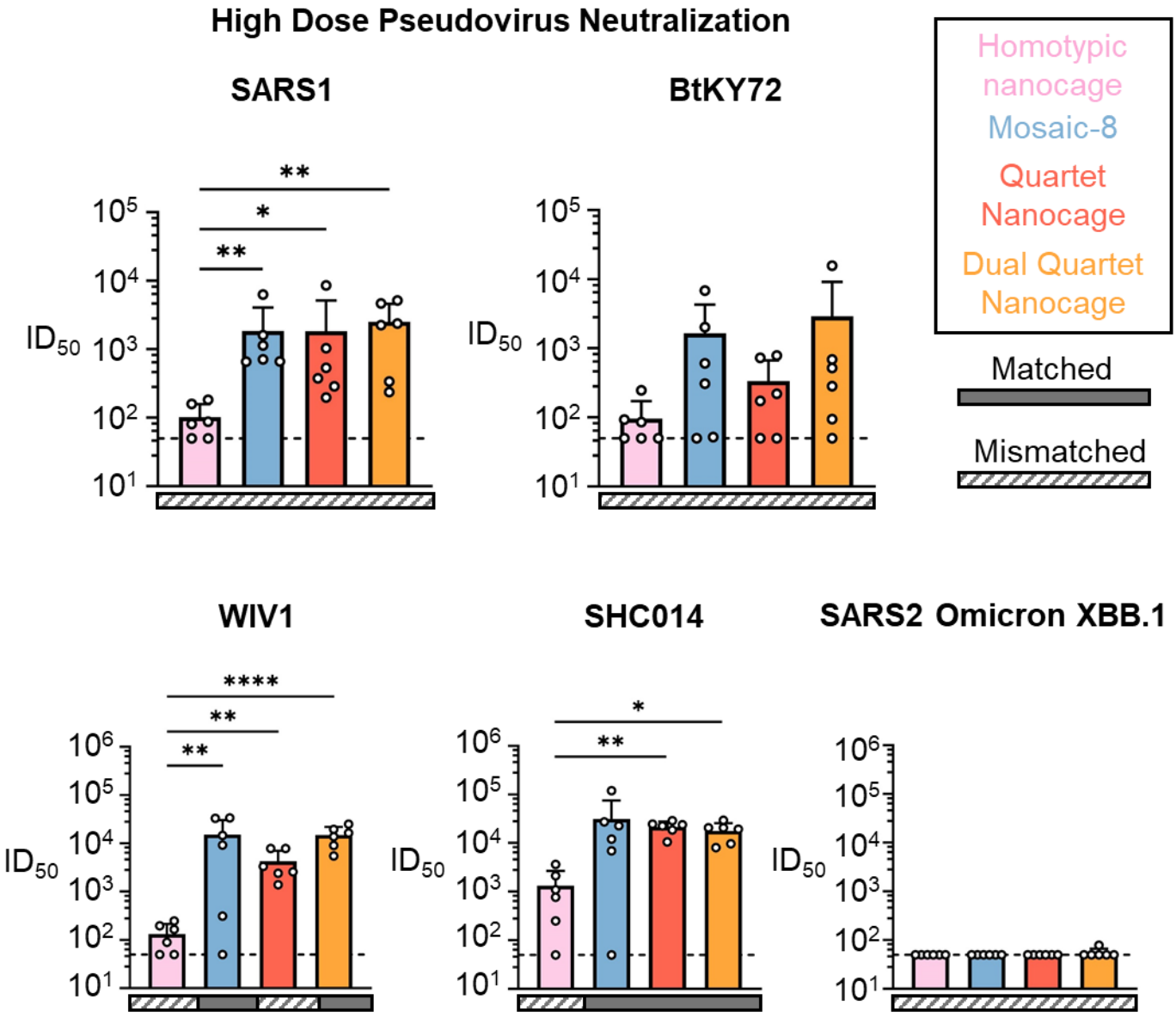

Figure 5.3: Pseudovirus Neutralization by High Dose Quartet Immunization. These figures assess antisera raised by immunizations with 0.2 nmol antigen, a 10-fold increase relative to prior immunizations. Sera is assessed for neutralization of SARS1, BtKY72, WIV1, SHC014, and SARS2 Omicron XBB.1 pseudovirus. Matched RBDs are indicated by solid gray rectangles under the sample, while mismatched RBDs are indicated by striped gray rectangles under the sample. The limit of detection is represented by a dashed horizontal line. Each dot represents the response for one animal. Mean ID50 (n=6) is denoted by a bar, with error bars + 1 standard deviation. Significance was calculated with an ANOVA test, followed by Tukey's multiple comparison post hoc test of ID50 values converted to log10 scale. * $p < 0.05$, ** $p < 0.01$, *** $p < 0.001$; other comparisons were non-significant. These experiments were performed by Jennifer R. Keeffe, Kaya N. Storm, and Priyanthi N. P. Gnanapragasam with supervision by Pamela Bjorkman (California Institute of Technology).

Before treatment, the mutant RBD yeast display library underwent deep sequencing to understand the baseline prevalence of different mutations. The mutant RBD display library was then treated with polyclonal mouse antisera and yeast were sorted by RBD expression and antibody binding. The yeast with RBDs that had reduced antibody binding relative to the unmutated RBD baseline were defined as antibody-escape cells. These antibody-escape cells underwent deep sequencing. Mutations that were overrepresented in the antibody-escape cells relative to the pre-treatment samples are determined to reduce sera binding. The location of mutations that reduce antibody binding can give insight into the profile of the elicited antibodies (A. A. Cohen et al., 2022; Greaney et al., 2021, 2022).

When deep mutational scanning was performed on the High Dose sera, Homotypic Nanocage immunization elicited an antibody profile dominated by Class 1 and Class 2 antibodies (Barnes et al., 2020). These antibodies bind RBD regions that are poorly conserved across sarbecoviruses. The Quartet Nanocage showed variance in the immune response it raised. One mouse showed a Class 1 dominated response and the other two mice showed a Class 3 and Class 4 dominated response. Both the Dual Quartet Nanocage and the Mosaic-8 induced an antibody response dominated by Class 3 and Class 4 antibodies, which are well conserved across sarbecovirus RBDs (Figure 5.4). Deep mutational scanning demonstrates that immunization with Quartet immunogens is capable of altering the binding pattern of individual antibodies and not just the activity of the polyclonal sera.

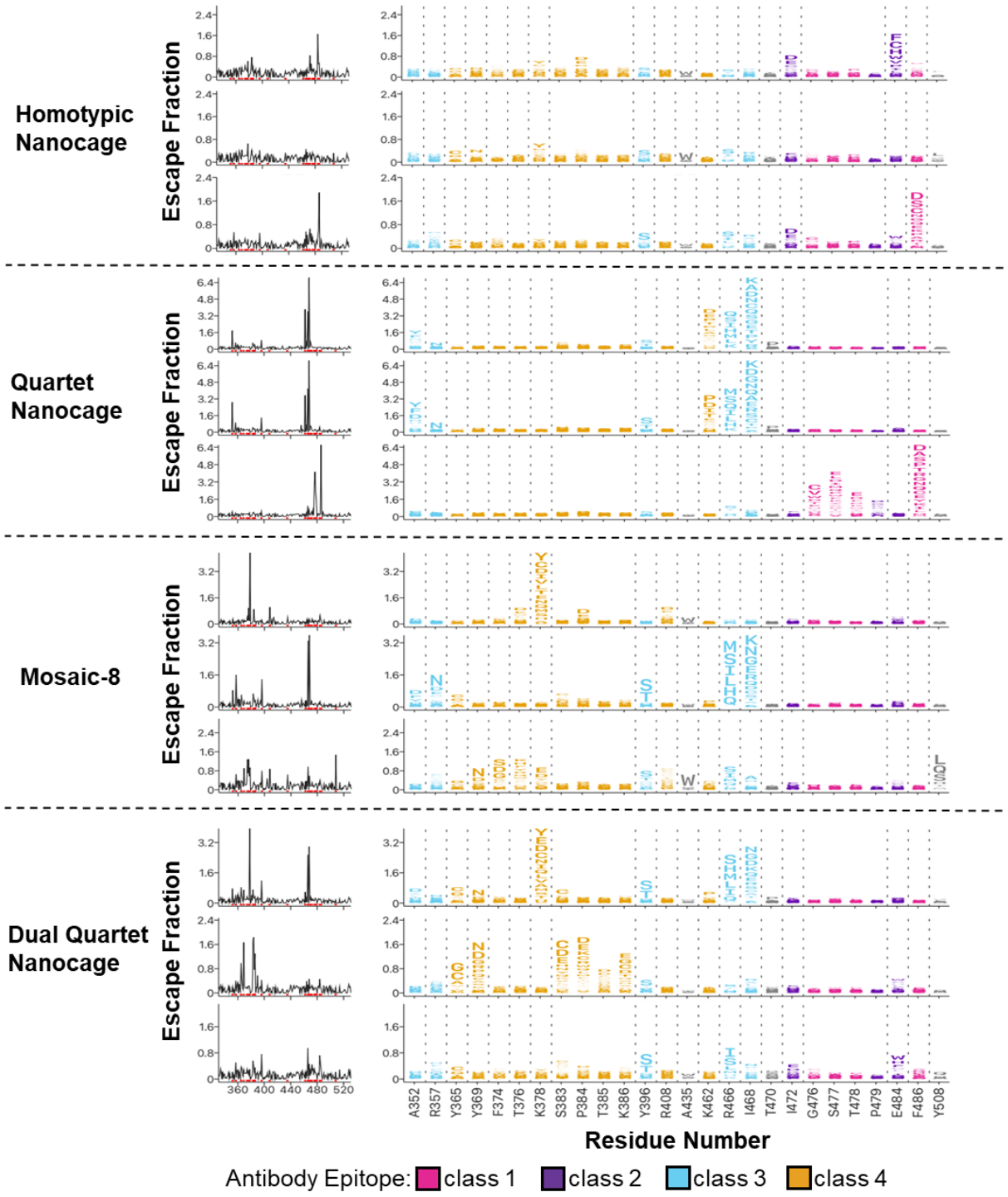

Figure 5.4: Antibody-escape maps for sera from immunization with Quartet and Mosaic antigens. Deep mutational scanning analysis for mice sera (n=3) primed and boosted with 0.2 nmol of each vaccine candidate. The line plots on the left visualize the sum of effects of all mutations at each RBD site on antibody binding; larger values indicate greater escape from antibody binding. Logo plots on the right show mutations that disrupt antibody binding for specific epitopes of interest. Sites are colored by antibody epitope and sites where mutations can introduce a potential N-linked glycosylation site sequon (NxS/T) are gray. The height of each letter represents that mutation's escape fraction. The y-axis is scaled independently for each serum sample. These experiments were performed by Alexander Cohen, Annie Rorick, and Anthony West, Jr. with supervision provided by Pamela Bjorkman (California Institute of Technology).

5.3 Kraken Quartets

While the primary focus of the Quartet Nanocage approach is to provide protection against future zoonotic pathogens, our ideal vaccine candidate would additionally provide protection against circulating SARS2 variants. The Quartet Nanocage elicited a strongly neutralizing response against SARS2 Wuhan and Delta (Figure 4.17). However, the protective neutralization began to wane against SARS2 Omicron BA.1 (Hills et al., 2024) and had been completely ablated by the SARS2 XBB.1 variant (Figure 5.3).

I wanted to demonstrate that Quartet Nanocage vaccines could be updated to protect against circulating SARS2. We chose the variant SARS2 Omicron XBB.1.5 which was prevalent when this work was completed in Spring 2023 (Hadfield et al., 2018).

I cloned a version SpyTag-Quartet which replaced SARS2 Wuhan with SARS2 Omicron XBB.1.5 (Figure 5.5A). The SARS2 Omicron XBB.1.5 variant had received the nickname ‘Kraken’ (Geddes, 2023), leading us to name this updated construct the Kraken Quartet. I expressed Kraken Quartet in Expi293F cells and purified it by SpySwitch. I ran the pooled elution fractions on a reducing SDS-PAGE gel, producing a single band at the expected molecular weight (Figure 5.5B). I ran the Kraken Quartet over an S200 column in PBS pH 7.4 and showed a single dominant peak that corresponded well to previous Quartet elutions (Figure 5.5C).

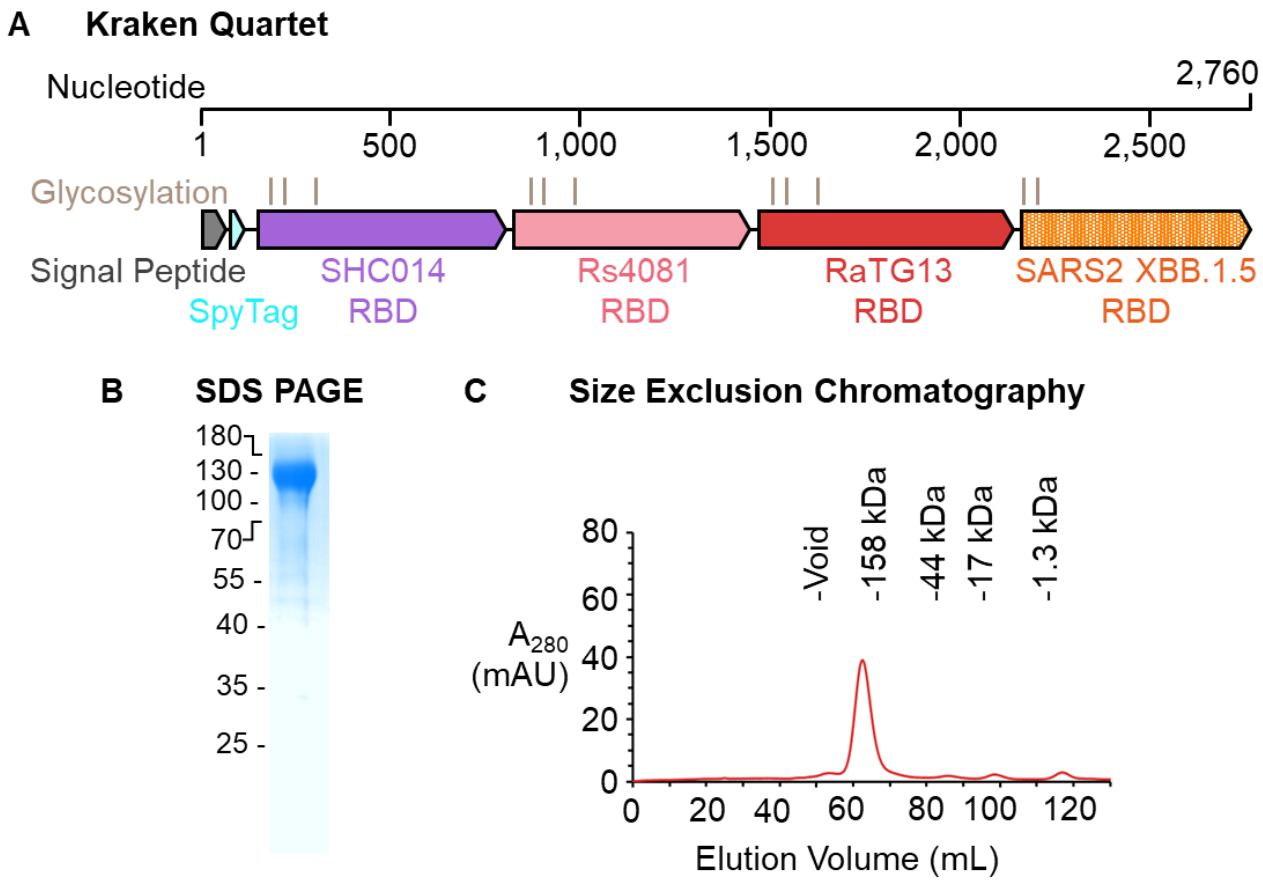

Figure 5.5: Purification of Kraken Quartet. (A) Schematic showing the genetic organization of the Kraken Quartet construct, which has SARS2 XBB.1.5 in place of SARS2 Wuhan. **(B)** Purified Kraken Quartet resolved by reducing SDS-PAGE. **(C)** Kraken Quartet were run over an S200 column in PBS pH 7.4. Bio-Rad gel filtration standards were run over the same column under the same conditions and the elution volume based on these standards are presented.

In addition to a conventional Dual Quartet Nanocage vaccine, I prepared versions of the Homotypic Nanocage, Mosaic-8, and Quartet Nanocage with either Wuhan or XBB.1.5 in the SARS2 position. I endotoxin-depleted the samples, determined they had acceptable endotoxin levels by LAL assay (Brito & Singh, 2011) and aliquoted them normalizing by molar antigen quantity. Immunizations were performed using the 'High Dose' protocol by Jack Tan (University of Oxford).

Given the interest in the response raised to SARS2 variants, I cloned, expressed, and purified new SpyTag-RBD constructs for SARS2 Delta, BQ.1.1, and XBB.1.5. I performed antisera ELSAs on the post-boost samples. All of the Mosaic and Quartet immunogens (both Wuhan

and XBB.1.5) outperformed both Homotypic Nanocages at raising responses to the tested non-SARS2 coronaviruses (WIV1, SCH014, SARS1, and BM48-31). There were no apparent differences in the strength of response raised to the non-SARS2 viruses by any of the Quartet or Mosaic antigens (Figure 5.6). This result is consistent with the previous 'High Dose' immunization.

The Wuhan Homotypic Nanocage raised a greater response to Wuhan and Delta RBD than the XBB.1.5 Homotypic. Conversely, the XBB.1.5 Homotypic Nanocage raised a greater response to BQ.1.1 and XBB.1.5 than the Wuhan Homotypic. Comparing the XBB.1.5 and Wuhan counterparts of Quartet Nanocage and Mosaic-8, the differences were less apparent. For example, looking at the antisera binding to XBB.1.5 RBD, the strongest response was raised by Homotypic XBB.1.5 and the weakest response by Homotypic Wuhan. The Quartet and Mosaic antigens containing XBB.1.5 induced marginally higher binding than their counterparts containing Wuhan, but these differences did not reach statistical significance (Figure 5.6).

Pseudovirus neutralization assays were performed on these antisera by Jennifer R. Keeffe, Kaya N. Storm, and Priyanthi N. P. Gnanapragasam (California Institute of Technology). In these assays there was a clear difference in neutralization based the SARS2 variant present in the immunogen. Immunogens that contained Wuhan were effective at neutralizing Wuhan but not XBB.1.5. Likewise, immunogens containing XBB.1.5 were effective at neutralizing XBB.1.5 but not Wuhan. The Mosaic and Quartet induction of binding to different SARS2 variants did not correlate with neutralization to these different variants. All of the Mosaic and Quartet immunogens (Wuhan and XBB.1.5) were capable of neutralizing the mismatched SARS1 sarbecovirus significantly better than their homotypic counterparts (Figure 5.7). These results show that Quartet Nanocage can be updated to incorporate a circulating variant, while retaining neutralizing breadth against sarbecoviruses.

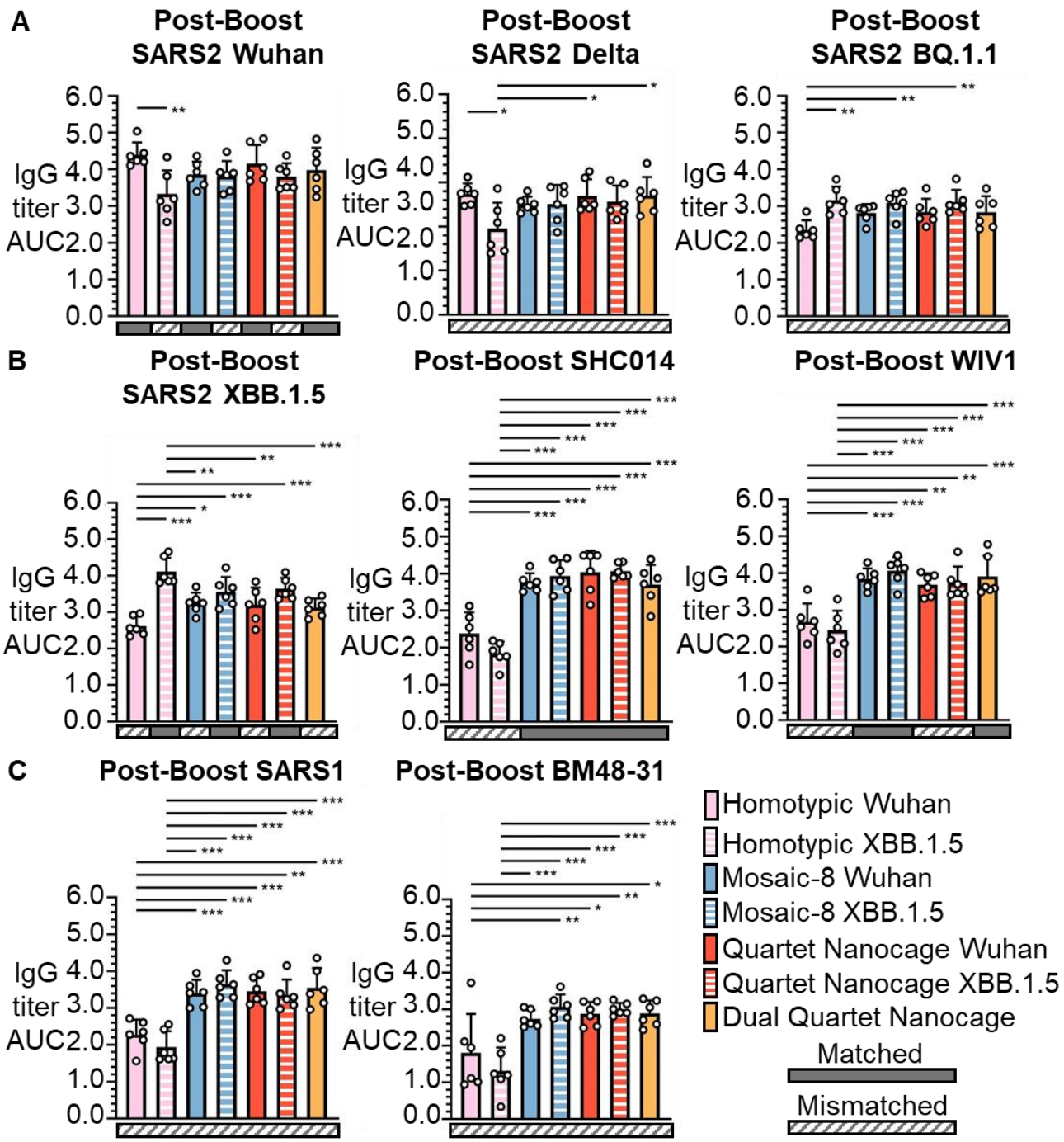

Figure 5.6: ELISA binding for immunogens with Wuhan or Kraken RBD. Post-boost serum IgG ELISAs for mice immunized with the indicated immunogen with 0.2 nmol antigen per dose. The mean AUC (n=6) is denoted by a bar. Immunogens that include a Wuhan RBD have a solid bar, while immunogens that include XBB.1.5 (Kraken) are striped bars. Error bars are ±1 standard deviation. Each dot represents serum from one animal. Solid gray rectangles under samples indicate the ELISA is against a component of that vaccine (matched), while diagonally striped rectangles indicate the ELISA is against an antigen absent in that vaccine (mismatched). Significance was calculated with an ANOVA test using Tukey's post hoc test. * $p < 0.05$, ** $p < 0.01$, *** $p < 0.001$; other comparisons were non-significant.

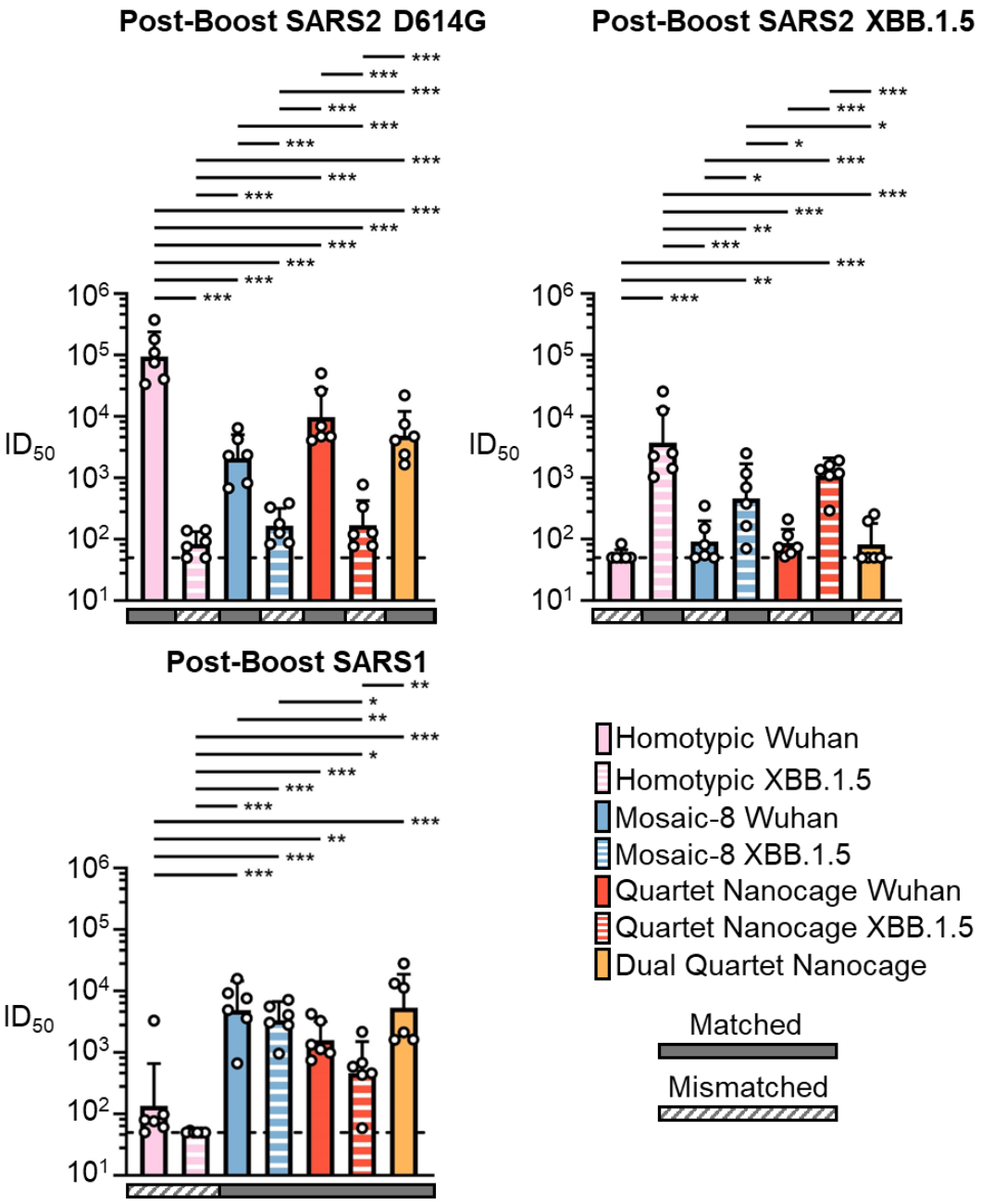

Figure 5.7: Pseudovirus neutralization for Quartet and Mosaic immunogens updated with Kraken RBD. Serum IgG from mice immunized with the indicated immunogen with 0.2 nmol antigen per dose were assessed for pseudovirus neutralization of SARS2 D614G (SARS2 Wuhan with a single point mutation), SARS2 XBB.1.5, and SARS1. Each dot represents serum response from one animal. Solid gray rectangles under samples indicate the ELISA are for matched viruses and diagonally striped rectangles are for mismatched viruses. The mean (n=6) is denoted by a bar, with error bars + 1 standard deviation. Significance was calculated with an ANOVA test, followed by Tukey's multiple comparison post hoc test of ID_{50} values converted to $\log_{10}$ scale. * $p < 0.05$, ** $p < 0.01$, *** $p < 0.001$; other comparisons were non-significant. Bars for immunogens that contain SARS Wuhan are solid. Bars for immunogens that contain SARS Omicron XBB.1.5 (Kraken) are striped. Dashed horizontal lines represent the limit of detection. These experiments were performed by Jennifer R. Keeffe, Kaya N. Storm, and Priyanthi N. P. Gnanapragasam with supervision by Pamela Bjorkman (California Institute of Technology).

5.4 Considering the impact of Quartet flexibility

It is apparent based on monoclonal antibody ELISAs that there is a variance in accessibility to different RBDs when a Quartet is displayed on SpyCatcher003-mi3 (Figure 4.16). Despite this difference, there was consistently no relationship established between the chain location and antibody response elicited. My current hypothesis is that the flexibility between RBDs creates a dynamic nanoparticle surface with multiple different RBDs available.

To investigate this hypothesis, I produced a Quartet where the flexible Glycine-Serine linkers separating the different RBDs was removed (Figure 5.8A). I expressed this No Linker Quartet in Expi293F cells and purified by SpySwitch (Figure 5.8B). Interestingly, No Linker Quartet was purified at comparable levels to previously expressed Quartet constructs. I ran the No Linker Quartet over an S200 column in PBS pH 7.4, demonstrating a single major peak at a similar elution volume as the original Quartet construct (Figure 4.8C).

I coupled the Quartet and No Linker Quartet immunogens to SpyCatcher003-mi3. I performed endotoxin depletion and quantification on the vaccine components ensuring that all immunogens had appropriate endotoxin levels (Brito & Singh, 2011). I aliquoted immunization samples with molar normalization of antigens using a ‘Low Dose’ regimen. Immunizations were performed by Jack Tan (University of Oxford) using VAC 20 adjuvant (Figure 5.9A).

I performed mouse antisera ELISAs on post-boost samples with assistance from Gabrielle Admans (University of Cambridge). There was no significant difference in the immune responses raised to any of the tested RBDs by the No Linker Quartet Nanocage and the conventional Quartet Nanocage. There remained no apparent relationship between an RBDs location on the Quartet chain and the antibody response raised to it for the No Linker Quartet Nanocage (Figure 5.9B). There is a flexible region at both the N and C termini of the sarbecovirus RBDs that constitute the chain. It remains possible that these regions provide

sufficient flexibility to support a dynamic surface arrangement. The success of the No Linker Quartet Nanocage makes the importance of flexible linkers between antigens an open question for the design of future Quartet constructs.

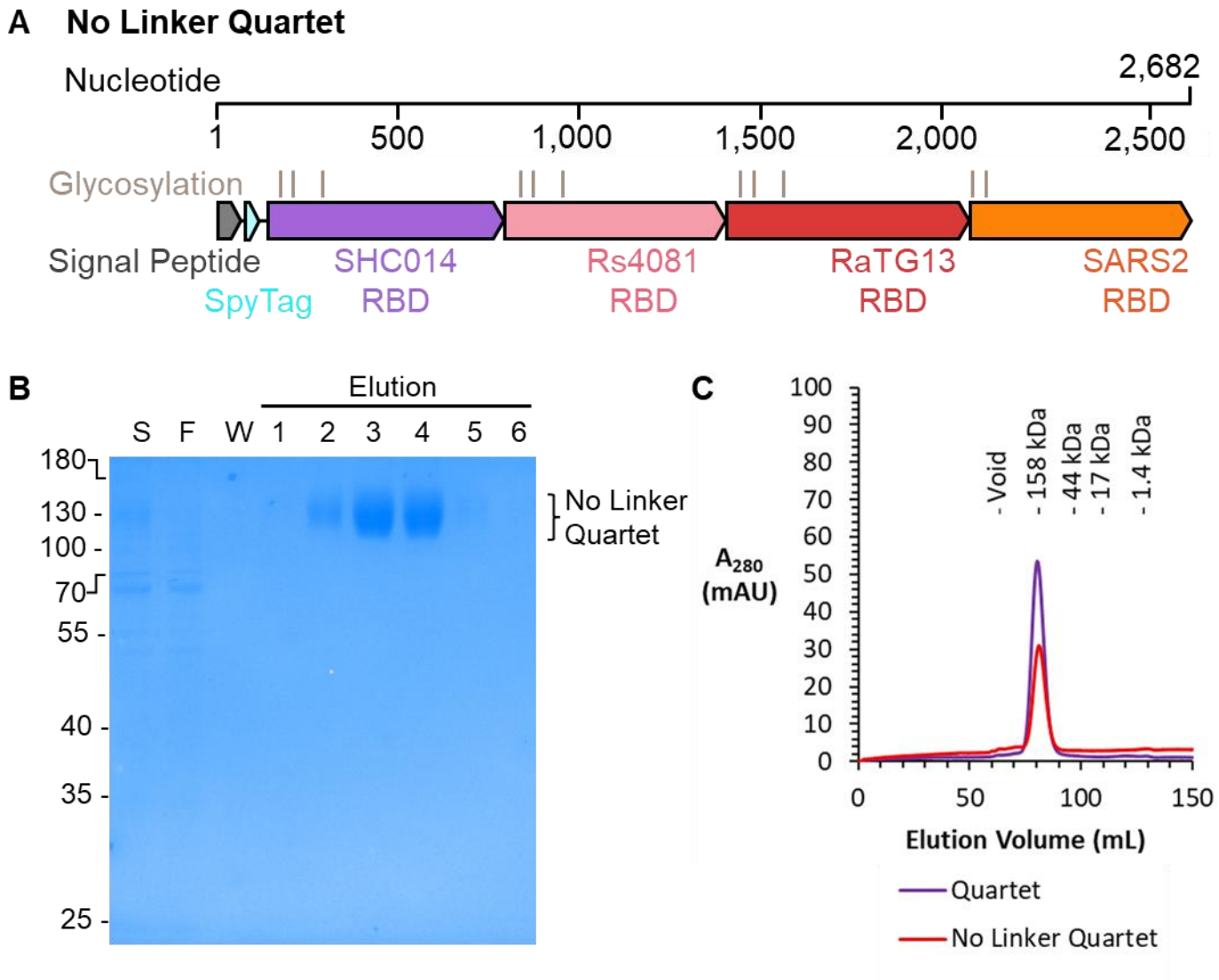

Figure 5.8: Purification of No Linker Quartet. (A) Schematic showing the genetic organization of the No Linker Quartet construct, where Glycine-Serine linkers have been removed between RBDs. **(B)** SpySwitch purification of No Linker Quartet, analysed by Coomassie/SDS-PAGE. The lanes include the supernatant (S), flowthrough (F), wash (W), and elution fractions (1-6). **(C)** No Linker Quartet was run over an S200 column in PBS pH 7.4 (red). Bio-Rad gel filtration standards were run over the same column under the same conditions and the elution volume based on these standards are presented. A previous Quartet SEC trace is included for reference (purple).

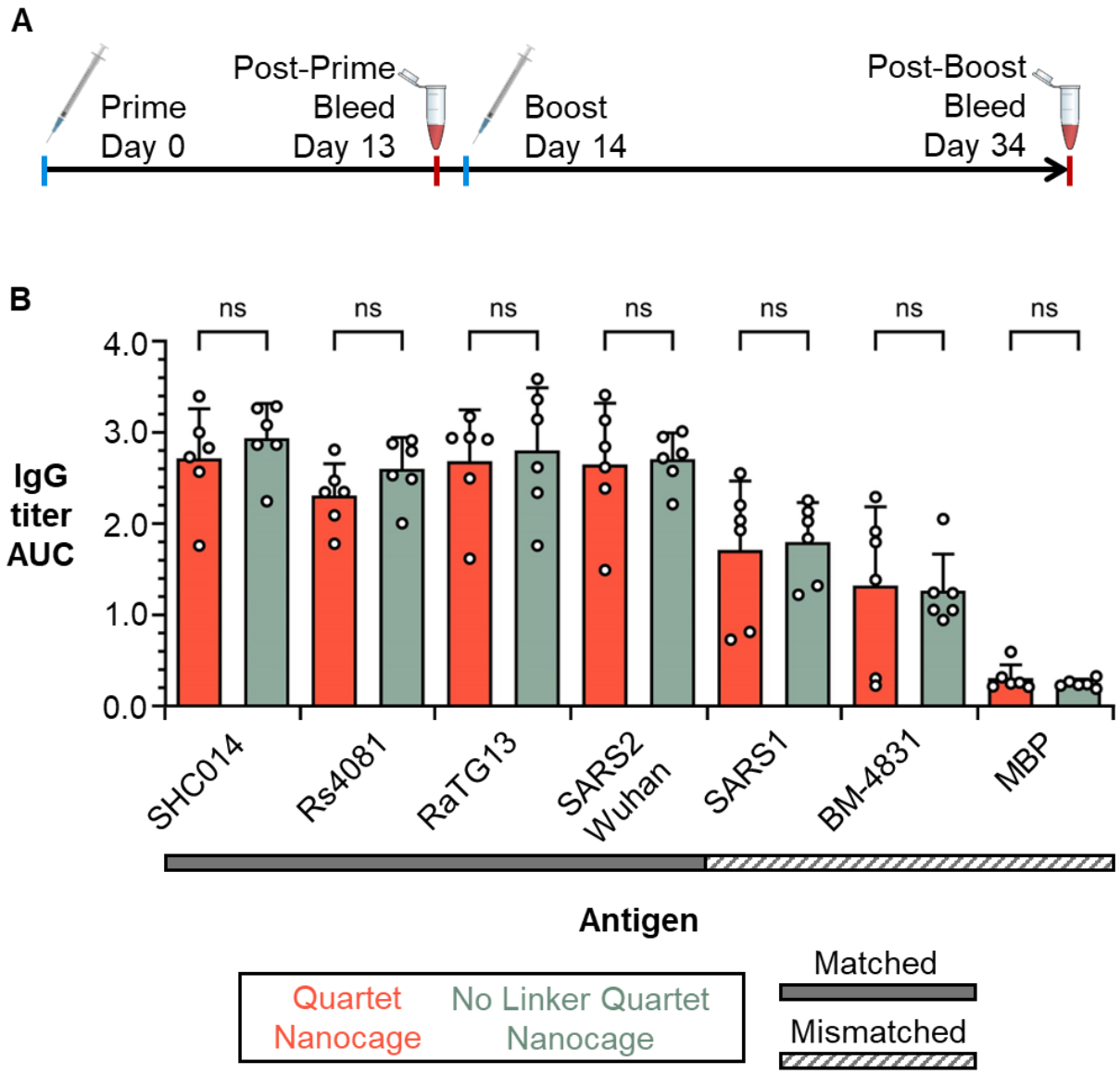

Figure 5.9: Immunogenicity for Quartets with or without linkers. Immunizations were performed with 0.02 nmol Quartet Nanocages with conventional Quartets and No Linker Quartets **(A)** Timeline for immunization doses and sampling. **(B)** ELISA for serum IgG antibodies, presented as area under the curve of a serial dilution of sera. Sera samples are from mice immunized using a conventional Quartet Nanocage (red) or a No Linker Quartet Nanocage (gray). Each dot represents serum from one animal. The mean is denoted by a bar, with error bars + 1 standard deviation, n = 6. ns means non-significant. Solid gray rectangles under samples indicate the ELISAs are against a matched antigen, while diagonally striped rectangles indicate the ELISA is against a mismatched antigen. Statistical comparisons were only made between responses to each antigen with or without linkers. Significance was calculated with a one-way ANOVA with Bonferroni's multiple comparisons test for the response raised to each immunogen. *P < 0.05, **P < 0.01, ***P < 0.001; ns non-significant. Gabrielle Admans (University of Cambridge) contributed to performing these ELISAs.

5.5 The 2017 Quartet

The primary goal of the Quartet Nanocage strategy is to facilitate proactive vaccinology. Under this paradigm vaccines are produced for a zoonotic pathogen before a spillover event has occurred. I have provided robust evidence for the efficacy of Quartet Nanocages against mismatched zoonotic sarbecoviruses which the vaccine was not intentionally designed to protect against. The ultimate test of the Quartet Nanocage would be to see if the vaccine protects against a future sarbecovirus that gains the ability to infect humans.

Given that it is not practical or desirable to wait for such an event to occur, I instead tested whether the Quartet Nanocage strategy could have provided an early response to the COVID-19 pandemic. To this end, I constructed a Quartet using RBDs solely from viruses that had their genomes sequenced and published in 2017 or earlier. I consequently named this construct the 2017 Quartet. I focused on viruses that had been identified as similar to SARS1 and would have been reasonable targets for a hypothetical researcher to include, if they were building a broad vaccine against SARS1 and its relatives.

Under these criteria I included RBDs from Clade 1a SHC014 (Ge et al., 2013b), Clade 2 Rs4081 (Hu et al., 2017b), Clade 1a SARS1 (Bi et al., 2003), and Clade 3 BM48-31 (Drexler et al., 2010). Two of these RBDs, SHC014 and Rs4081, were already present in the original Quartet. RaTG13 and SARS2 were replaced with SARS1 and BM48-31 (Figure 5.10A).

I chose to remove the RaTG13 RBD present in the original Quartet. Although its identity had been published in 2016 (then called RaBtCoV/4991)(Ge et al., 2016), the full genome was not sequenced until 2018 (P. Zhou et al., 2020). There is also a high percentage of RBD sequence similarity between SARS2 and RaTG13 (90%). Homotypic SARS2 Nanocages raise a cross-reactive anti-RaTG13, suggesting RaTG13 may raise a cross-reactive response against SARS2.

I therefore viewed the inclusion of RaTG13 as setting too easy a challenge for the 2017 Quartet and too lucky a break for the hypothetical pre-COVID-19 researcher.

I cloned the 2017 Quartet, expressed the construct in Expi293F cells, and purified via SpySwitch (Figure 5.10B). I ran the 2017 Quartet over an S200 column in PBS pH 7.4 and demonstrated a single dominant peak that eluted at the same approximate volume as the original Quartet (Figure 5.10C). I coupled the 2017 Quartet to SpyCatcher003-mi3, endotoxin-depleted all components, and determined acceptable endotoxin levels by LAL assay (Brito & Singh, 2011). I aliquoted Quartet Nanocage and 2017 Quartet Nanocage samples, normalizing them by molar antigen concentration. Immunizations were performed by Jack Tan (University of Oxford) at 'Low Dose' with VAC 20 adjuvant (Figure 5.11A).

I performed mouse antisera ELISAs on post-boost samples with assistance from Gabrielle Admans (University of Cambridge). The 2017 Quartet Nanocage elicited responses to all of the tested sarbecoviruses that was significantly above the baseline defined by the response to MBP. The 2017 Quartet Nanocage and Quartet Nanocage raised similar responses to the two RBDs that they shared (SHC014 and Rs4081). Predictably, both the Quartet Nanocage and the 2017 Quartet Nanocage raised stronger responses to matched RBDs than mismatched RBDs (Figure 5.11B).

There is a substantial response raised against SARS2 by the 2017 Quartet Nanocage, however, this response was significantly lower than the response raised by the Quartet Nanocage (Figure 5.11B). A key question, therefore, is how effective this may have been at protecting against SARS2. It is not appropriate to make any definitive claims based on comparison between different sets of immunizations. However, given that the immunizations were performed with an identical dose, timeline, mouse strain, and adjuvant, one can make broad comparisons to inform future experiments by comparing the 2017 Quartet Nanocage immunizations with

previous immunizations (Figure 4.11-4.15). The mean anti-SARS2 AUC raised by the 2017 Quartet Nanocage was 1.35 while the mean anti-SARS2 AUC raised by a Homotypic SARS2 Nanocage in a previous experiment was 1.25. This result indicates that the 2017 Quartet Nanocage can raise a similar anti-SARS2 IgG response as a vaccine designed specifically for COVID-19. The Homotypic Nanocage has been shown to elicit potently neutralizing antibodies (T. K. Tan et al., 2021). Further experiments will be required to directly validate this comparison and investigate the neutralization of sera elicited by the 2017 Quartet but initial underline the potential for Quartet Nanocages as a tool for proactive vaccinology.

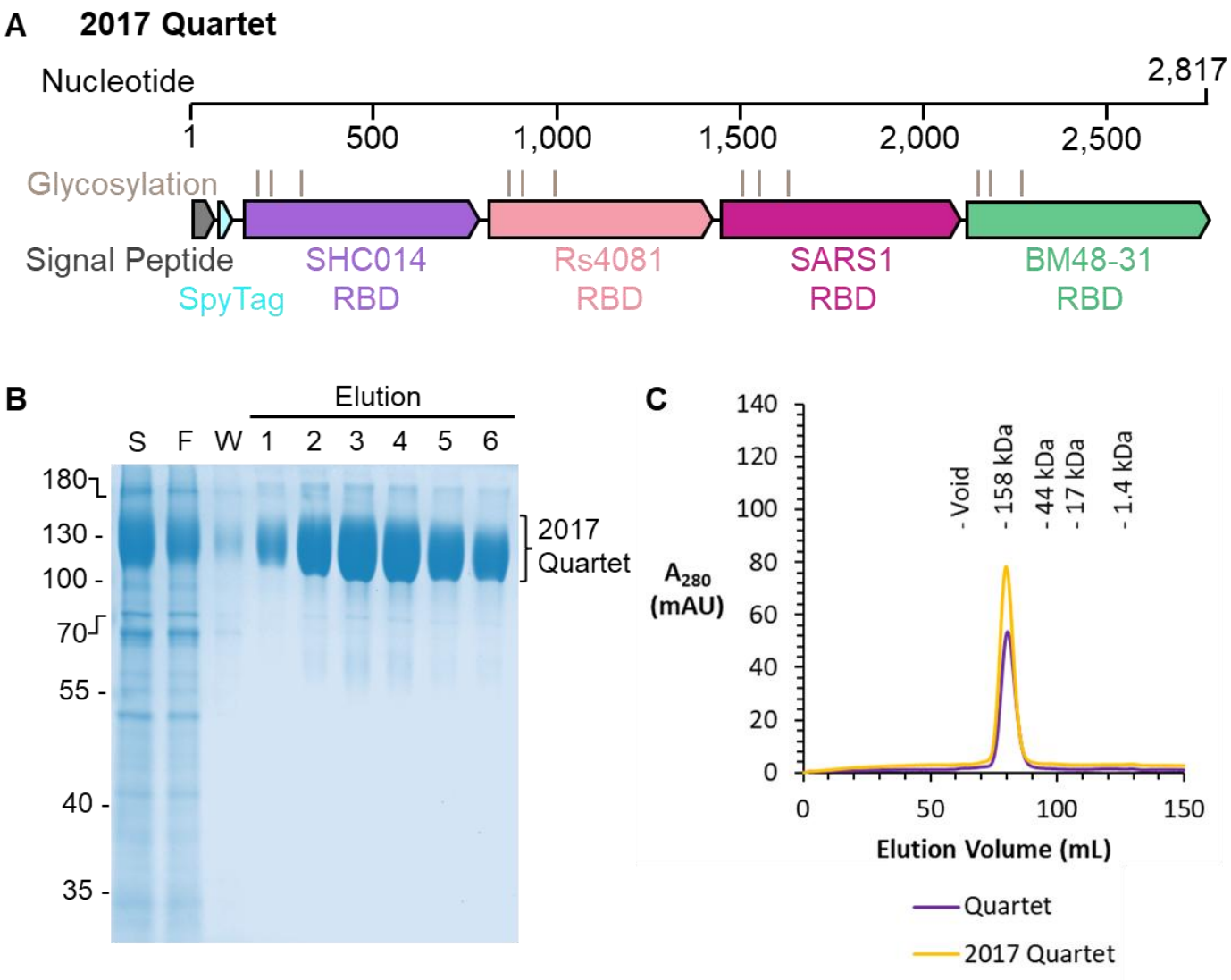

Figure 5.10: Purification of the 2017 Quartet. (A) Schematic showing the genetic organization of the 2017 Quartet. **(B)** SpySwitch purification of 2017 Quartet, analysed by SDS-PAGE with Coomassie staining. The lanes include the supernatant (S), flowthrough (F), wash (W), and elution fractions (1-6). **(C)** SEC for the 2017 Quartet (yellow) in PBS pH 7.4 using an S200 column. A SEC trace for SpyTag-Quartet is included for reference (purple). The elution volume for Bio-Rad gel filtration standards is also presented.

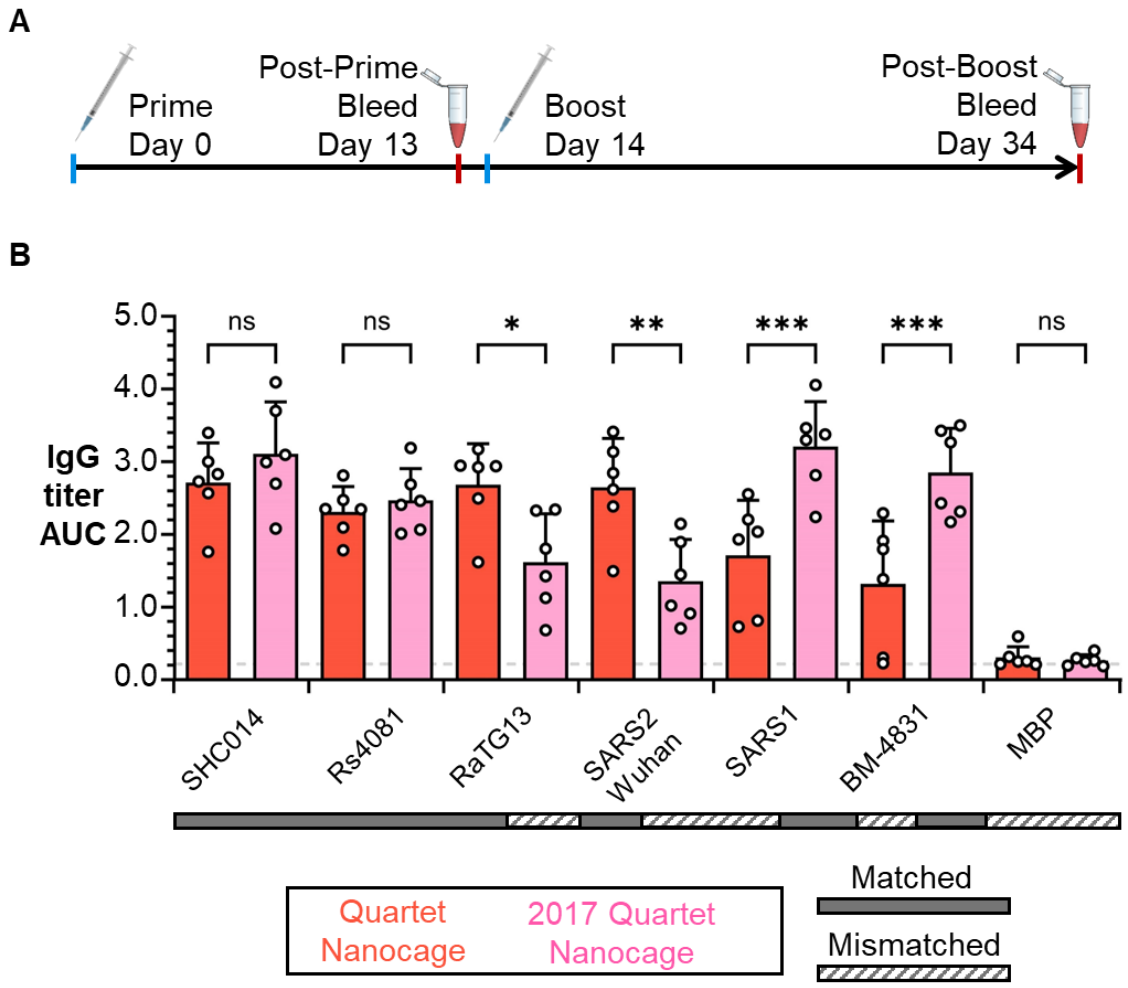

Figure 5.11: Immunogenicity of 2017 Quartet determined by ELISA. Immunizations were performed with 0.02 nmol Quartet Nanocages with conventional Quartets and 2017 Quartets (A) Timeline for immunization doses and sampling. (B) ELISA for post-boost serum IgG antibodies presented as area under the curve of a serial dilution of sera. Sera samples are from mice immunized using a conventional Quartet Nanocage (red) or a 2017 Quartet Nanocage (pink). A dashed horizontal line is used to define a null response based on Quartet Nanocage response raised to MBP. Each dot represents serum from one animal. The mean is denoted by a bar, with error bars + 1 standard deviation, n = 6. ns means non-significant. Solid gray rectangles under samples indicate the ELISAs against a matched antigen, while diagonally striped rectangles indicate the ELISA is against a mismatched antigen. Statistical comparisons were only made between responses to each antigen with or without linkers. Significance was calculated with a one-way ANOVA with Bonferroni's multiple comparisons test for the response raised to each immunogen. *P < 0.05, **P < 0.01, ***P < 0.001; ns non-significant. Gabrielle Admans (University of Cambridge) contributed to performing these ELISAs.

5.6 Applying the Quartet strategy beyond sarbecoviruses

The success of Quartet Nanocages at raising neutralizing antibodies across a range of sarbecoviruses, raises the possibility that the strategy can be applied to other pathogen threats. A logical next target is merbecoviruses. This group of betacoronaviruses is related to Sarbecoviruses and enters host cells using an RBD that binds through ACE2 or DPP4 (Figure 5.12B) (Zumla et al., 2024). The threat looms that the continued evolution of MERS generates improved human-to-human transmission or that a zoonotic merbecovirus evolves to infect humans (Zumla et al., 2024).

To initiate the development of a broad merbecovirus vaccine, I identified a panel of ten merbecoviruses (Figure 5.12A, Table 5.1). I obtained the DNA for RBD for eight of the ten merbecoviruses in this panel. Regulation regarding the export of specific viral DNA delayed obtaining BtVs (Yang et al., 2014 and Neo-CoV (Ithete et al., 2013; Xiong et al., 2022) RBD DNA. Based on RBD sequence conservation, I grouped this panel into six MERS-like RBDs and four Neo-CoV-like members (Figure 5.12A).

For the sarbecoviruses panel used during the generation of the Quartet Nanocage, the RBD amino acid percent identity typically ranged from 70-90%. For the newly constructed panel of merbecoviruses, the percent identity typically ranged from 40-75%. Narrowing on the 'MERS-like' group of merbecoviruses, the percent identity is in the 55-75% range. The conserved residues among 'MERS-like; merbecoviruses tend to be grouped away from the DPP4 binding site (Figure 5.12B, C), similarly to sarbecoviruses Figure 1.5.

I cloned these 8 RBDs in a SpyTag-RBD format. I expressed all eight in Expi293F cells and purified by SpySwitch. A representative gel is presented for the purification of HKU5. Seven of the eight RBDs expressed with yields that ranged from 80-125 mg/L, with HKU25 RBD failing to express.

I designed two merbecovirus Quartets. One was the Broad Merbecovirus Quartet (Figure 5.13A). This Quartet included two MERS-like RBDs (MERS and ITA1/2) and two Neo-CoV-like RBDs (PDF-2180 and Eri-CoV). There is substantially more sequence diversity in this Broad Merbecovirus Quartet than any of the tested sarbecovirus Quartets (36-54% identity) making this Quartet and effective assessment of the limits of antibody breadth that a Quartet Nanocage can elicit.

The other merbecovirus Quartet I designed was the Narrow Merbecovirus Quartet (Figure 5.13C). This Quartet contained the MERS-like RBDs from MERS, ITA1/2, HKU4, and HKU5. The percent identity range of these RBDs was 54-66%. While this Quartet contains more sequence distance than any of the tested sarbecovirus Quartets, there are substantial regions of conservation shared across the four merbecovirus RBDs.

I expressed both Merbecovirus Quartets in Expi293F cells and successfully purified both by SpySwitch (Figure 5.13B,D). The yields for these merbecovirus Quartets were lower than for any of the previously expressed sarbecovirus Quartets. Further optimization of signal peptide, linker length, or inclusion of a carrier protein could be explored to improve yields. However, substantially more protein was produced than would be needed for pre-clinical animal immunizations.

The production of Merbecovirus Quartets demonstrates the versatility of the Quartet strategy. The threat of zoonotic crossover by members of the merbecovirus subgenus makes the development of a broad-spectrum merbecovirus vaccine an important goal for proactive vaccinology. Future work will be required to examine the display of the Merbecovirus Quartets on SpyCatchcer003-mi3 and to determine both the potency and the breadth of the immune response raised by a Merbecovirus Quartet Nanocage in mouse immunizations.

Table 5.1. Summary of merbecovirus RBDs included in the panel.

Name	Host	GenBank	Reference
MERS	*Camelus dromedarius* (dromedary camel); *Homo sapiens* (Human)	JX869059	(van Boheemen et al., 2012)
HKU4	*Tylonycteris pachypus* (lesser bamboo bat)	EF065508	(Woo et al., 2006, 2007)
HKU5	*Pipistrellus abramus* (Japanese house bat or Japanese pipistrelle)	AGP04932	(Woo et al., 2006)
HKU25	*Hypsugo pulveratus* (Chinese pipistrelle)	KX442565	(Lau et al., 2018)
BtVs	*Vespertilio superans* (Asian parti-colored bat)	AHY61337	(Yang et al., 2014)
NeoCoV	*Neoromicia zuluensis* (Zulu pipistrelle or aloe bat)	KC869678.4	(Ithete et al., 2013; Xiong et al., 2022)
PDF-2180	*Pipistrellus hesperidus* (Dusky pipistrelle)	ARJ34226	(Anthony et al., 2017)
HKU31	*Erinaceus amurensis* (Amur hedgehog or Manchurian hedgehog)	UMO75628	(Lau et al., 2019)
EriCoV	*Erinaceus europaeus* (European hedgehog)	KC545383	(Corman, Kallies, et al., 2014)
ITA1/2	*Hypsugo savii* (Savi's pipistrelle) [ITA1] *Pipistrellus kuhlii* (Kuhl's pipistrelle) [ITA2]	MG596802 MG596803	(Moreno et al., 2017)

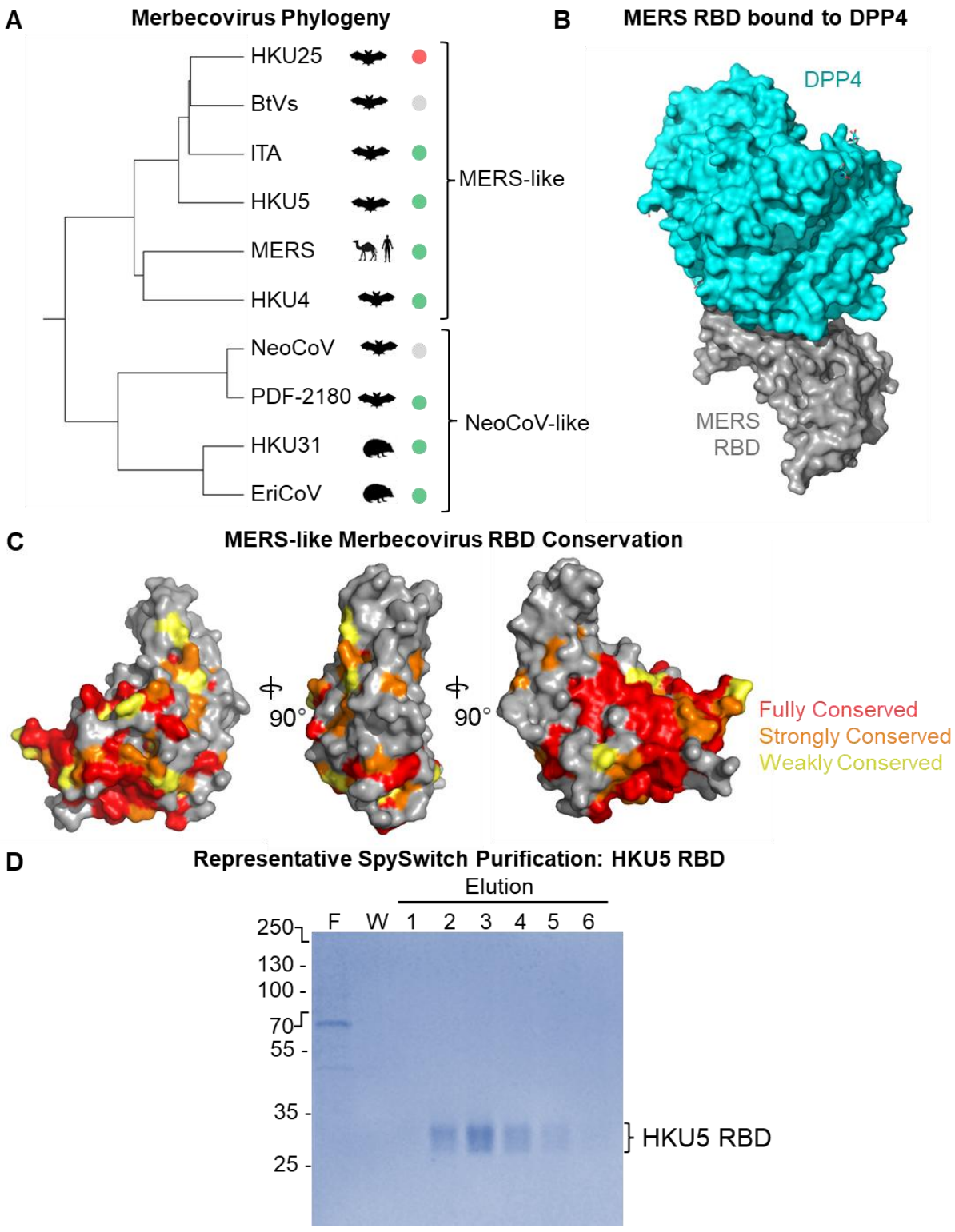

Figure 5.12: Merbecovirus RBD Phylogeny, Structure, and Expression. (A) A phylogenetic tree for the merbecovirus RBDs that were included in this panel. **(B)** MERS RBD (gray) bound to human DPP4 (cyan) (PDB 4L72). **(C)** Conservation of residues between MERS-like merbecoviruses in the study, mapped onto the MERS RBD crystal structure (PDB 4L72). Multiple orientations of the same RBD are shown, represented as the van der Waals surface. **(D)** SDS-PAGE/Coomassie gel for HKU5 SpySwitch purification as a representative for the merbecovirus RBDs. Lanes include flowthrough (F), wash (W), and elution fractions (E1 – E6).

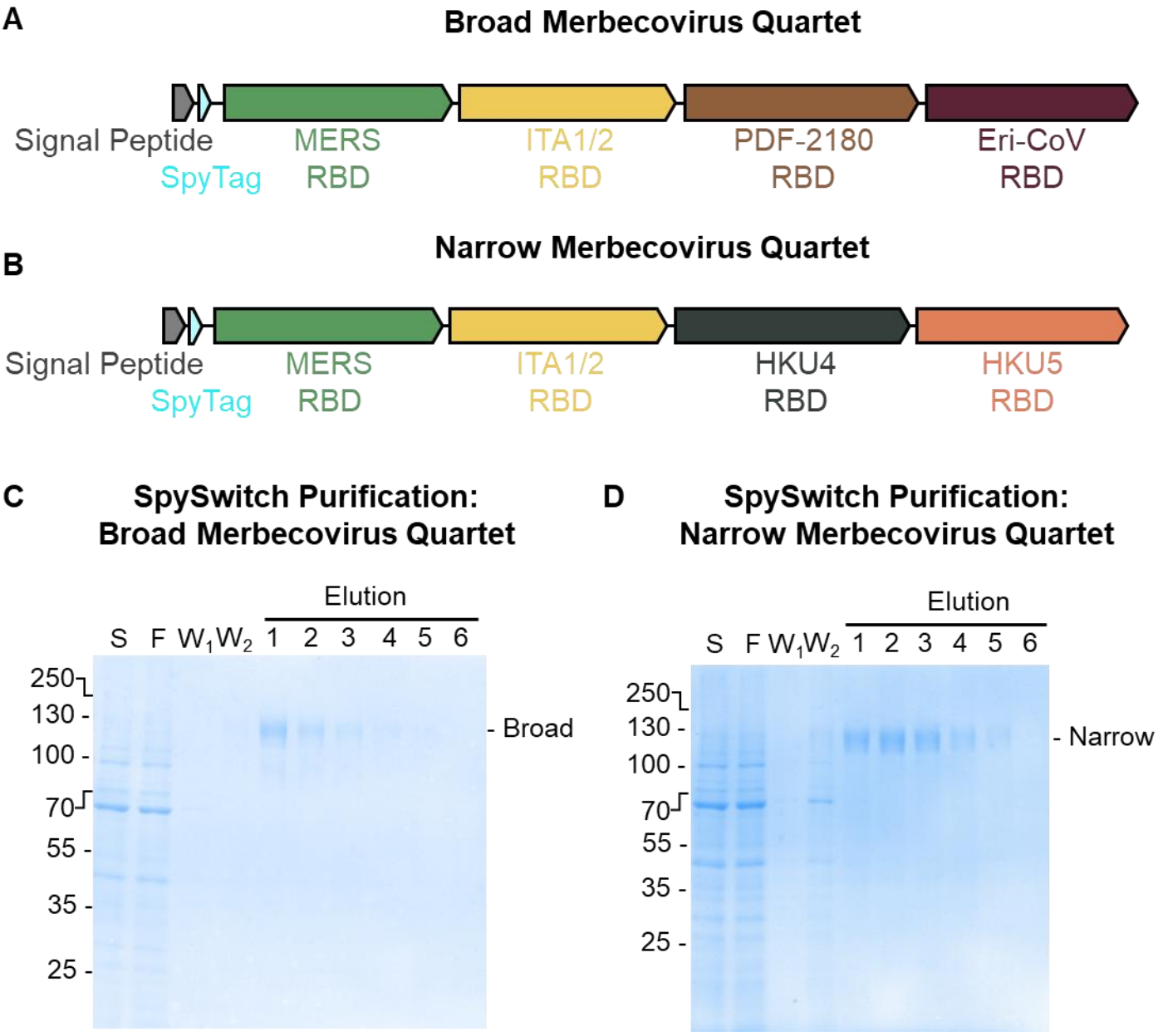

Figure 5.13: Merbecovirus Quartet Expression. Schematic showing the genetic organization of the **(A)** Broad Merbecovirus Quartet and **(B)** Narrow Merbecovirus Quartet. **(C)** SpySwitch Purification of the Broad Merbecovirus Quartet. **(D)** SpySwitch Purification of the Narrow Merbecovirus Quartet. SpySwitch purification is analysed by Coomassie/SDS-PAGE. The lanes include the mammalian supernatant (S), flowthrough (F), wash (W), and elution fractions (1-6).

5.7 Discussion

In this chapter I further examined the Quartet immunization strategy for broadening the induced immune response. This chapter outlines efforts to better understand the underlying mechanism of Quartet Nanocages, to update Quartets to induce neutralizing antibodies against the SARS2 Omicron variants, and to further explore Quartet Nanocages for proactive vaccinology. In the context of proactive vaccinology, I showed that a Quartet Nanocage implemented in 2017 could have provided an effective tool for eliciting SARS2 antibodies before the virus was detected. Additionally, I designed and successfully produced Quartets targeting merbecoviruses which have infected humans or have demonstrated the potential to do so.

Immunization with the single component Uncoupled Quartet has raised a broad immune response that targets both matched and mismatched sarbecoviruses. An effective single-component vaccine could further simplify the vaccine production process and facilitate a more streamlined scale up in production. This effort would remove the need to produce the SpyCatcher003-mi3 Nanocage, to couple the Quartet to the Nanocage, and to have Quality Control (QC) steps to validate successful particle formation and coupling. However, the Uncoupled Quartets have significantly underperformed Quartet Nanocage and Dual Quartet Nanocage immunogens.

In Chapter 3, I outlined the immunogenic benefit of implementing albumin-hitchhiking with soluble SARS2 RBD. I achieved this result by genetically fusing SARS2 RBD to the high-affinity albumin-binding protein domain ABD035. In this chapter, I applied the same strategy with the Quartet and compared the response elicited by Quartet and Quartet-ABD035. The inclusion of a terminal albumin-binding domain increased the mean response against all tested sarbecovirus RBDs but none of these differences reached statistical significance.

While ABD035 fusion may have moderately improved the immune response for a soluble Quartet, it is clear that the fusion did not have the same impact as for the soluble SARS2 RBD. The increase in immune response raised by RBD-ABD035 was largely attributed to albumin-binding increasing the molecular weight of the antigen. This increase made it more likely for the antigen to be trafficked to draining lymph nodes as opposed to undergoing vascular clearance. Above a molecular weight of approximately 45 kDa, proteins tend to be entirely delivered to draining lymph nodes (Miller et al., 2011; Moyer et al., 2016). SARS2 RBD has a molecular weight of 25.4 kDa while SpyTag-Quartet has a molecular weight of 99.6 kDa without including glycosylation. This difference means that, unlike soluble RBD, albumin binding would be unlikely to enhance delivery of the soluble Quartet to draining lymph nodes.

My hypothesis with applying albumin-hitchhiking for the Quartet was that there would still be an improved immune response based on an enhanced immunogen half-life. Albumin has a long serum half-life (19 days) and attachment to albumin is a frequent strategy for improving pharmacokinetics (Tao et al., 2021). If the Quartet-ABD035 improvement in immune response is more than statistical noise, it is possible that an enhanced half-life through albumin-hitchhiking is responsible. Regardless, it is clear that ABD035 fusion is not sufficient to make a soluble Quartet immunogen competitive with a Quartet Nanocage approach. Further work to develop a single-component protein sub-unit vaccine may examine direct fusion to a nanoparticle. This approach has been successfully applied with ferritin and SARS2 spike protein (Powell et al., 2021) and a similar approach could be adopted for Quartets. Direct genetic fusion of ferritin to a Quartet would allow a single protein product to be used for a vaccine. A co-transfection of Quartet-Ferritin and Alternate Quartet-Ferritin could facilitate a Dual Quartet Ferritin Nanocage. This approach would likely require substantial optimization of linkers, sequences, and other factors for efficient expression. It would also remove the plug-and-play modularity of the SpyCatcher003-mi3 system (Rahikainen et al., 2021).

I am currently working with an industrial collaborator to scale-up production of the Quartet Nanocage and Dual Quartet Nanocage vaccine. The relative difficulty or ease of this industrial scale up will influence the emphasis that is placed on further streamlining the soluble Quartet vaccine.

I examined the impact of more closely matching previous immunization experiments (A. A. Cohen et al., 2022) by increasing the dose ten-fold and changing the adjuvant from the alum-based VAC 20 to the squalene-based AddaVax. Under these conditions, Quartet Nanocage and Dual Quartet Nanocage demonstrated potent neutralization against a range of different matched and mismatched sarbecoviruses. However, at this 'High Dose' there was no longer a significant difference in antibody binding or pseudovirus neutralization between the Mosaic-8 and the two Quartet Nanocage immunogens. It is important to note that in mice immunizations, antibody responses can easily be saturated in a way that is difficult to attain in human clinical results (H. L. Davis, 2008; S. P. Graham et al., 2020). It appears that these 'High Dose' immunizations have achieved immune responses that are at the higher end of the dose-response curve and are therefore obscuring critical differences between the vaccine candidates. Comparison of the Mosaic and Quartet strategies at the 'Low Dose' therefore appear to be a more relevant assessment.

Even at this high dose, none of the immunogens raised substantially neutralizing immune response against SARS2 Omicron XBB.1 pseudovirus. This finding is consistent with the level of immune evasion that has been demonstrated by Omicron variants (Uraki et al., 2023). While the overarching goal of our strategy is to protect against future pandemics, the ideal vaccine candidate would be able to protect against circulating variants or, at least, be updatable to match further pathogen evolution.

I assessed the response elicited with Homotypic, Mosaic, and Quartet Nanocage immunogens with either Wuhan or XBB.1.5 in the SARS2 RBD position. Both forms of the Mosaic and Quartet Nanocage immunogens raised antibodies that bound to all tested SARS2 variant RBDs whether matched and mismatched. This result is in contrast to Homotypic Nanocage immunogens, which bound poorly to more distantly related SARS2 variants.

The binding breadth of these immunogens was not reflected with neutralization breadth. Mosaic and Quartet antisera neutralized the mismatched SARS1 and the matched SARS2 variants present in the vaccine. However, all tested vaccines performed poorly at neutralizing the SARS2 variant (XBB.1.5 or Wuhan) pseudovirus that was not represented in the vaccine.

These results demonstrate that the Quartet Nanocage can be effectively updated to incorporate a currently circulating variant. Interestingly, this updated response may come at the cost of ancestral immunity. It would likely be possible to incorporate both XBB.1.5 and Wuhan RBD in the same Quartet (or possibly a Quintet) to achieve a neutralizing response to both. However, this effort may be superfluous, given that the ancestral strain has largely been surpassed by newer variants (Hadfield et al., 2018).

The capacity to update the Quartet with circulating variants is notable. However, it is uncertain how long the efficacy window would be for a variant-chasing vaccine strategy (Uraki et al., 2023). This window may be widened with improvements in predicting viral evolution (Cyrus Maher et al., 2022; W. Han et al., 2023; Taylor & Starr, 2023).

There is evidence that non-neutralizing SARS2 antibodies can still be protective, especially against serious disease and death (Clark et al., 2024; Rahman et al., 2023). These non-neutralizing antibodies are not able to directly prevent viral infection but are capable of recruiting effector cells that contribute to clearance of viruses and infected cells (Clark et al.,

2024; Mader & Dustin, 2024). Given the high binding antibody titres raised against Omicron XBB.1.5 and Omicron BQ.1.1 by the original Quartet Nanocage and Dual Quartet Nanocage, it seems likely that these original vaccines could provide protection for serious disease, but not sterilizing immunity, against these newly evolved SARS2 variants. The results of the upcoming clinical trial for the Mosaic-8b antigen may give further insight into this possibility.

Epitope mapping by DMS for antisera elicited by Quartet and Mosaic immunization was analysed in this chapter. This assay shows that mutations in the evolutionarily conserved Class 3 and Class 4 region reduced binding by antibodies raised with Mosaic-8 and Dual Quartet Nanocage vaccines. The polyclonal antibodies raised by the Homotypic Nanocage showed evidence of binding to the poorly conserved Class 1 and Class 2 region. These results suggest that the antibody profile elicited by Mosaic-8 and Dual Quartet Nanocage has been altered relative to a more conventional Homotypic Nanocage immunization. These results provide strong evidence that the breadth of binding for antibodies raised by the Dual Quartet Nanocage is due to antibodies binding more evolutionarily conserved regions of the antigen.

The DMS results for the Quartet Nanocage was more varied. One of the mice responded with a Class 1/2 dominant response and two of the mice responded with a Class 3/4 dominant response. Along with this result, the Quartet Nanocage generally shows poorer breadth of neutralization than the Dual Quartet Nanocage. This indicates that the Dual Quartet Nanocage is the stronger of the two vaccine candidates based on immunogenic considerations alone. The results of the production scale-up and consultation with regulators regarding nanoparticle homogeneity will provide insight into which candidate is more holistically viable.

As a further test of the Quartet Nanocage mechanism, I produced the No Linker Quartet. Our hypothesis is that the flexibility of the Quartet chain leads to a dynamic nanoparticle surface where all of the RBDs are accessible for BCR interaction. Although there are differences in

RBD accessibility based on monoclonal ELISAs, the working hypothesis is that there is sufficient representation of each RBD at the surface to induce breadth and enhanced RBD-specific responses. Through the production of the No Linker Quartet, I sought to test this hypothesis.

However, immunizations with Quartet or No Linker Quartet displayed on SpyCatcher003-mi3 raise similar immune responses. There was no significant difference in the response raised by the two immunogens to any of the tested RBDs and there were no non-significant patterns evident. Additionally, there was no bias towards different RBDs based on their location on the No Linker Quartet chain. It is possible that the flexible regions at the N- and C-termini of the RBD protein provide a sufficient level of flexibility to maintain this dynamic surface. The presence of these regions maintaining flexibility between the different RBDs may be responsible for the No Linker Quartet retaining high expression levels relative to other Quartets.

A follow-up experiment could build on the production of a Quartet where these flexible regions are removed from the RBDs along with the Glycine-Serine linkers. Unfortunately, I was not able to determine a method to more directly probe the nanoparticle surface. The flexibility between RBDs on the Quartet as well as between the SpyCatcher003 and mi3, mean that cryo-EM and crystallography are not viable (Palamini et al., 2016). In single-particle cryo-EM SpyCatcher003-mi3 displaying SARS2 RBD alone showed minimal electron density for a single RBD, let alone a Quartet (T. K. Tan et al., 2021).

The Quartet Nanocage strategy is designed to provide protection against potential future zoonotic disease outbreaks and Quartet Nanocages elicit broad antibody responses to a variety of mismatched sarbecoviruses. These immune effects include raising responses to Clade 3 sarbecoviruses even though no members of this clade was represented on the vaccine. The

ultimate test of the Quartet Nanocage strategy would be to see whether a zoonotic pathogen capable of infecting humans could be immunized against with a vaccine designed before the cross-over event has occurred.

To gain insight into this possibility, I tested whether a Quartet Nanocage designed with RBDs from viruses discovered by 2017, could raise a response against SARS2. I included RBDs from SHC014 (Ge et al., 2013b), Rs4081 (Hu et al., 2017b), SARS1 (Bi et al., 2003), and BM48-31 (Drexler et al., 2010).

While all of these viruses were sequenced prior to 2017, the SpyCatcher003-mi3 particle was not published until 2021 (Rahikainen et al., 2021). A hypothetical scientist working on this vaccine would have had to use a prior SpyCatcher-based VLP such as SpyCatcher-mi3 (T. U. J. Bruun et al., 2018) or SpyCatcher-AP205 (K. D. Brune et al., 2016), or an alternative self-assembling nanoparticle strategy (Brouwer et al., 2019). However, given the purpose of this exercise is to investigate the proactive nature of the Quartet strategy and any future iterations of Quartet Nanocages would use SpyCatcher003-mi3, I decided not to use an outdated VLP strategy.

Immunizations were performed with Nanocages displaying the original Quartet and the 2017 Quartet. The response raised by the Quartet Nanocage and the 2017 Quartet Nanocage to matched coronavirus RBDs was potent. The response raised by both immunogens to mismatched RBDs was decreased but still strong. Critically, the 2017 Quartet which lacked a SARS2 RBD raised similar antibody titres that were similar to SARS2-specific Homotypic Nanocage. It is important to note that these results were obtained in separate immunizations, although they used the same antigen dose, timeline, adjuvant, and mouse strain. Further analysis of the 2017 Quartet Nanocage would be required to allow direct comparison with the Homotypic Nanocage and to test the elicited antisera for viral neutralization.

The success of the 2017 Quartet at raising an anti-SARS2 response highlights the potential impact of proactive vaccinology. The ability to create vaccines that target large groups of zoonotic viruses means that vaccines can target both known and unknown viruses in that family. This immune breadth allows for vaccines to be validated for safety, efficacy, and production before any members of this group have crossed over into humans. One may consider the impact that the prior development and validation of the 2017 Quartet Nanocage or a similarly broad vaccine could have had on the COVID-19 pandemic. This highlights the potential for proactive vaccinology as a tool for combating future diseases with pandemic potential.

Merbecoviruses have been identified as a possible threat for a future coronavirus pandemic (Gonzalez-Isunza et al., 2023; Tolentino et al., 2024; Zumla et al., 2024). This group includes MERS, which has already demonstrated human-to-human transmission and a high fatality rate in humans (Memish et al., 2020). Continued evolution of MERS could make the disease more easily transmissible between humans (Letko et al., 2018). There are also specific merbecoviruses that have been identified as having the potential to cross over into humans (Gonzalez-Isunza et al., 2023). For example, a relative of HKU4 has been identified circulating in Malayan pangolins that is able to use human DPP4 as a receptor for cell entry as well as host proteases for enhanced cell infection (J. Chen et al., 2023).

There is a larger degree of sequence divergence amongst merbecovirus RBDs when compared with sarbecovirus RBDs. I therefore designed a Broad Merbecovirus Quartet which included members from the entire subgenus as well as a Narrow Merbecovirus Quartet which only included RBDs from MERS-like viruses. Even the average percent identity for the Narrow Merbecovirus Quartet was lower than for any of the tested sarbecovirus Quartets.

Both Merbecovirus Quartets were successfully expressed and purified at a purity and yield appropriate for pre-clinical studies. Further optimization of the constructs signal peptide, linker length, RBD constructs, or the inclusion of a cleavable carrier protein may need to be explored to facilitate large scale production.

Both of the Merbecovirus Quartets are ready for coupling to SpyCatcher003-mi3 and mouse immunization studies. These studies will give important insight into how portable the Quartet Nanocage strategy can be onto other coronaviruses. It will also provide insight into what level of antigen conservation is required for Quartets to induce an antibody response to evolutionarily maintained regions. There remains no approved vaccine against MERS, although there are promising vaccine candidates progressing to clinical trials (Bosaeed & Alharbi, 2023F. An effective Merbecovirus Quartet Nanocage could provide protection against MERS while also targeting potentially dangerous zoonotic merbecoviruses. The synergy of protecting against existing and potential future pathogens could facilitate scaled-up production or uptake of such a vaccine before a future spillover event has occurred.

This chapter has examined methods of improving the efficacy of Quartet vaccines, investigated the underlining mechanism for Quartet-induced breadth of protection, and highlighted the potential for Quartet Nanocages to facilitate proactive vaccinology. The ability to develop a vaccine before a pathogen with pandemic potential emerges is the driving force behind the development of the Quartet vaccine technology.

Chapter 6 – Summary, General Discussion, and Future Outlook

The SpyTag/SpyCatcher system has been used for development of vaccine candidates against a variety of pathogens (A. A. Cohen et al., 2022; Lampinen et al., 2023; S. K. Singh et al., 2017; T. K. Tan et al., 2021; W. Wang et al., 2019). SpyTag/SpyCatcher facilitates production of multicomponent vaccines, where constituent elements can be expressed in different systems, purified under different conditions, and produced at different times and locations (K. D. Brune et al., 2016; T. U. J. Bruun et al., 2018). In this thesis, I explored the use of SpyTag for purification and nanoassembly of proteins for vaccine development. I used SpyDock to purify a COVID-19 immunogen without any additional purification tags and show that fusion with a high affinity albumin binding (Jonsson et al., 2008) significantly increases the elicited immune response. I piloted the newly developed SpySwitch system for affinity purification of a panel of SpyTagged sarbecovirus RBDs and show that each of these RBDs can be coupled to the SpyCatcher003-mi3 nanocage. Using this panel of sarbecovirus RBDs, I probed the breadth of activity for several patient derived monoclonal IgGs and identify two antibodies that bind all tested sarbecoviruses: EY6A and IY2A. Our collaborators demonstrated that IY-2A potently neutralized all tested SARS2 Omicron variants and bound SARS2 RBD using a previously unreported mechanism (K. Y. A. Huang et al., 2023).

I introduced the Quartet strategy where a string of evolutionarily related coronavirus RBDs are genetically fused and expressed as a single polyprotein. When immunized as a soluble protein, I showed that Quartets elicit broad antibody responses against both matched and mismatched coronaviruses. This response was further enhanced when the Quartets were displayed on SpyCatcher003-mi3 to form a Quartet Nanocage. Quartet Nanocages elicited strong and broad immune responses that compared favourably with the Mosaic-8 nanoparticle, a leading anti-sarbecovirus vaccine candidate. Unexpectedly, there was no difference in the immune response to RBDs at different locations on the chain despite monoclonal antibody ELISAs showing

differences in accessibility. When mice were pre-immunized with SARS2 Wuhan Spike, a boost immunization with Mosaic or Quartet Nanocage vaccine candidates was still able to elicit broad immune responses. This is important given that a substantial number of people will have a preexisting immune response to SARS2 through immunization and infection (Mathieu et al., 2021; H. Wang et al., 2022; Watson et al., 2022b; WHO, 2023).

I performed additional experiments to gain insight into the Quartet Nanocage mechanism. I found that Quartet Nanocages without flexible linkers between the RBDs still raised similar responses to each constituent RBD. This suggests that chain flexibility is not responsible the invariant response to different RBDs or that flexible RBD regions provide sufficient chain flexibility without the need for additional linkers. Deep Mutational Scanning was performed by our collaborators to map the epitopes of polyclonal sera elicited by Quartet Nanocages. This assay showed that both Mosaic-8 and Quartet Nanocage vaccines shifted the binding pattern of antibodies to favour the evolutionarily conserved Class 3 and 4 regions of the RBD. Finally, I further explored the application of Quartets for proactive vaccinology. I showed that the 2017 Quartet, composed entirely of sarbecovirus RBDs with sequences published more than a year before the first COVID-19 case was reported, were still able to raise a strong response against SARS2. Additionally, Quartets composed of merbecovirus RBDs were successfully expressed and purified, demonstrating potential future directions for the Quartet immunization strategy.

Merbecoviruses (J. Chen et al., 2023; Gonzalez-Isunza et al., 2023; Tolentino et al., 2024; Zumla et al., 2024) are one of several pathogen groups that have been identified as a threat for future disease outbreaks (Mehand et al., 2018; Morens & Fauci, 2020). Some of these pathogen outbreak threats, like influenza, have already caused pandemic events and future mutations may make the circulating strains more deadly, more transmissible, or more immune evasive (Reperant et al., 2015; Taubenberger & Morens, 2010). Some, such Lassa and Ebola viruses,

have crossed from animal reservoirs into humans, causing deadly outbreaks that could become more dangerous with additional pathogen evolution (Garry, 2023; Mehand et al., 2018; H.-Q. Zhang et al., 2023). Other pathogens lurk undiscovered in animal hosts with the potential to infect humans at every human-animal intersection (Iserson, 2020; Simpson et al., 2020). This risk is especially potent in newly arising interactions that are spurred by habitat decline or climate change (Carlson et al., 2022; Keesing & Ostfeld, 2021; The Lancet, 2023). The unknown nature of this 'Disease X' underlines the importance of developing rapid and flexible health interventions (Iserson, 2020; Simpson et al., 2020).

The remarkable efficacy of SARS2 vaccines at reducing COVID-19 mortality and morbidity (Huespe et al., 2023; Rahmani et al., 2022; Thomas et al., 2021; Voysey et al., 2021) highlights the importance of developing vaccines against these future pandemic threats (Iserson, 2020; Mehand et al., 2018; Simpson et al., 2020). There are extensive efforts at developing vaccines against known human pathogens that have the possibility of causing larger outbreaks (D. Gupta & Mohan, 2023b; Malik et al., 2023; Mane Manohar et al., 2023; Pollard & Bijker, 2021a; Sulis et al., 2023). However, there remains a distinct possibility that evolution of these known pathogens could lead to immune evasion, meaning that a vaccine targeted to conserved regions may be required for robust protection (C. J. Wei et al., 2020; D. Xu et al., 2023).

There remains the open question of how to address currently unknown threats. One answer is the rapid development of targeted vaccines (Saville et al., 2022). A remarkable interdisciplinary effort, a streamlined approval processes, and the application of mRNA and viral vector vaccine technology allowed COVID-19 vaccines to be applied clinically at an unprecedented speed (Daems & Maes, 2022; Excler et al., 2023). It is possible that refinement of these processes could allow for further enhancement of this response against a future outbreak. SpyCatcher functionalized nanoparticles could be a useful tool for this approach with stockpiled

nanoparticles being decorated with newly produced and outbreak-specific SpyTagged antigen (K. D. Brune et al., 2016).

Another answer for addressing unknown threats is to proactively develop vaccines against potential emergent pathogens. With a narrowly focused vaccine it is not possible to proactively develop a vaccine against an unknown threat, but this goal could be made possible by a broadly effective vaccine that protects against a large group of related pathogens (Gouglas et al., 2023). Under this vision, a library of vaccines could be developed with each library member targeting a different group of pathogens that has pandemic potential. These vaccines could be tested robustly to understand the level and breadth of protection afforded. Pilot production runs could be performed and a pipeline could be established for the scale up of library members for when an outbreak is first identified (Saville et al., 2022).

In a particularly ambitious version of this approach, the library members would undergo initial human clinical trials to establish safety. Human sera could be tested for neutralization of known members of the target pathogen family but it would not be possible to establish clinical protection against a potential threat until that pathogen had made the leap into humans. A vaccine stock could be produced and stored for each library member. In the event that a novel outbreak occurred, the appropriate library member or members could begin production scale up and validation against this specific threat. This validation could include using human sera samples stored from the earlier clinical trial. If the vaccine had demonstrated a strong safety profile in previous trials and these initial tests were promising, then emergency use approval could allow rapid implementation of the vaccine at early stage of the outbreak.

There are a variety of approaches to produce the broad vaccines that would be necessary for this proactive vaccine library approach (A. Cohen et al., 2021; Lee et al., 2023; Ng et al., 2022; van Bergen et al., 2023; Walls et al., 2021). The Quartet Nanocages outlined in this thesis are

one such tool. Quartet Nanocages are able to target an immune response towards evolutionarily conserved regions of an antigen which allows for a single vaccine to protect against a variety of related pathogens. A key benefit of the Quartet Nanocage approach is it elicits immune breadth with only one to three components. The exact number of components depends on what version of the Quartet vaccine is finalized. Currently, the greatest level of breadth is achieved with a three-component vaccine (Dual Quartet Nanocage), but it is possible that a two-component vaccine (Quartet Nanocage) may give a better trade-off between simplicity and efficacy. One could envision a vaccine library where each member is a different polyprotein of tandemly linked antigens. SpyTag could be included to facilitate easy multimeric presentation on a SpyCatcher functionalized nanoparticle.

More immediate future work will focus on the further development of Quartet Nanocages as a clinical anti-sarbecovirus vaccine. We are currently working closely with an industrial collaborator to scale up production of Quartets in a Chinese hamster ovary (CHO) cell line. With the demonstration of manufacturing feasibility, our ultimate aim is to gain support to enter Phase 1 clinical trials with a Quartet Nanocage and/or Dual Quartet Nanocage vaccine.

An open question with the clinical application of Quartet Nanocages is the level of protection that would be offered against circulating variants of SARS2. Both Quartet Nanocage and Mosaic vaccines raised antibodies that bound similarly to all tested SARS2 RBDs, namely Wuhan, Delta, XBB.1.5, and BQ.1.1. These results are in contrast to homotypic SARS2 vaccines which elicited more narrow antibody binding responses across the SARS2 variants. However, the antibodies raised by Quartet and Mosaic immunogens that contained Wuhan RBD were poorly neutralizing against XBB.1 pseudovirus. Both Quartet and Mosaic immunogens were successfully updated to replace the SARS2 Wuhan RBD with the then circulating variant XBB.1.5. These updated immunogens elicited a neutralizing response

against XBB.1 pseudovirus and the mismatched SARS1 pseudovirus. However, replacing SARS2 Wuhan with XBB.1.5 lead to a poorly neutralizing response against SARS2 Wuhan pseudovirus. These results highlight the notable immune evasion demonstrated by Omicron variants (Uraki et al., 2023). It seems likely that a neutralizing response could be raised to both Omicron and Wuhan by including both RBDs as part of a single tandemly linked polyprotein. While this may be interesting to examine, it does not appear practically necessary given that the ancestral strain has largely been surpassed by newer variants (Hadfield et al., 2018).

When considering clinical trials, one option would be to update the Quartet to include a circulating variant. However, in the time between Kraken Quartet experiments that I performed and the writing of this thesis, XBB.1.5 has been surpassed by JN.1 and JN.1.1 (Hadfield et al., 2018). In the window of time between a variant being selected for trials and the approval of a vaccine, it is likely that further evolution may have occurred which raises questions about how effective a variant-chasing strategy will be at achieving sterilizing immunity (Uraki et al., 2023).

There is, however, growing evidence that SARS2 antibodies which bind but do not neutralize the virus may still play an important protective role, especially when considering reduction in serious disease and death (Clark et al., 2024; Rahman et al., 2023). These non-neutralizing sera cannot directly prevent viral invasion of cells but remains capable of recruiting effector cells that lead to clearance of viruses and infected cells (Clark et al., 2024; Mader & Dustin, 2024). The high binding titres raised against XBB.1.5 and BQ.1.1 by Wuhan-containing Quartet Nanocages suggest that these vaccines may still provide protection against serious COVID-19 disease, even if they do not provide sterilizing immunity. The results of the upcoming Phase 1 clinical trial for the Mosaic-8b nanoparticle will give important insight into the future of Quartet Nanocage in the context of the circulating SARS2 virus. However, it is important to

remember that the Quartet Nanocage has primarily been introduced as a tool for rapid response to newly infectious diseases, as opposed to a means for boosting against existing circulating human pathogens.

Our clinical development of the Quartet Nanocage strategy has largely focused on a two- or three-component formulation where Quartets are displayed on the SpyCatcher003-mi3 Nanocage. From a manufacturing standpoint, it may be optimal to have the option of an effective one-component vaccine, as long as this option can still provide sufficient protection.

I have shown that an uncoupled soluble Quartet is still capable of raising a robust and mismatched immune response at similar titres to the Mosaic-4 and Mosaic-8 nanoparticles. However, uncoupled Quartet tended to underperform at raising a neutralizing response compared with nanoparticle-based vaccines. It would be desirable to further enhance the immune response raised by a single-component Quartet vaccine. ABD035 was genetically fused to the Quartet in order to facilitate albumin-hitchhiking. This may have provided marginal immune enhancement, but the improvements were not statistically significant and did not approach the level of enhancement that was achieved when a Quartet was displayed on a Nanocage. It may be possible for future research to develop a single-component nanoparticle vaccine by genetically fusing a Quartet to a nanoparticle sub-unit (Powell et al., 2021). However, it is unclear whether this construct could be efficiently expressed, and it is likely that this approach would require optimization (Rahikainen et al., 2021).

Future work on single-component soluble Quartet vaccines should focus on determining whether the immune response raised by an uncoupled Quartet is sufficient to provide protection, how beneficial a single-component vaccine would be from a regulatory and manufacturing standpoint, and what further enhancements can be made to the elicited immune response.

The Quartet immunogen is also well suited for application using vaccine delivery platforms other than protein nanoparticles. As a single polyprotein, Quartet immunogen can be readily administered as an mRNA vaccine (Hoffmann et al., 2023; Z. Zhang, Mateus, et al., 2022). I am currently working with collaborators at the California Institute of Technology and University of California San Francisco to test Quartet immunogens as an mRNA vaccine (Hoffmann et al., 2023). We will compare the responses raised by mRNA encoding a Quartet against a cocktail of mRNA encoding the individual constituent RBDs. Future work may investigate the inclusion of conserved T-cell epitopes to broaden the T-cell mediated immune response along with the humoral immunity (van Bergen et al., 2023).

Quartet immunogens may also be delivered effectively as the antigenic payload of a viral vector platform (Folegatti et al., 2020). This approach could be taken further with a strategy that combines viral vector and protein subunit vaccine delivery. In a recently described approach, an adenoviral capsid was modified to include DogTag (Keeble et al., 2022) in surface-exposed loops (Dicks et al., 2022). DogTag spontaneously forms a covalent bond with DogCatcher in a similar manner to the SpyTag/SpyCatcher system. SARS2 RBD was genetically fused to DogCatcher and was subsequently used to decorate the adenoviral capsid. These decorated adenoviral capsids delivered SARS2 antigen as a protein on its surface and as a genetically encoded payload. This strategy was shown to both enhance the level of anti-SARS2 response and reduce the immune response to the viral vector (Dicks et al., 2022). A similar approach could be applied using DogCatcher-Quartet to decorate the adenoviral surface and delivering a Quartet DNA construct as the payload. Given that the DogCatcher-Quartet protein would be approximately four times the size of a single RBD, it is possible that this strategy would elicit further reduction in anti-vector response.

Another avenue for future Quartet Nanocage research would be expanding the technologies application to other pathogens. The Quartet strategy is best applied to pathogens that have an antigen sufficiently robust to be expressed as a genetic fusion. Otherwise, it may be more appropriate to target the antigen using a mosaic approach. The antigen must also have evolutionarily conserved regions that can elicit protective antibodies. It would be possible to make a Quartet or a Mosaic nanoparticle with antigens that share little to no evolutionary conservation. This approach would be expected to raise responses to the individual antigens present on the particle. However, with no conserved regions to shift an immune response towards, there would be no expectation for a further enhancement of immune breadth.

A potentially impactful next step would be to target other members of the betacoronavirus genus (Llanes et al., 2020). This could include merbecoviruses, nobecoviruses and embecoviruses (which include KHU1 and OC43) (de Klerk et al., 2022; D. X. Liu et al., 2021). Merbecoviruses are an especially intriguing target given that they include a deadly human pathogen (MERS) and several members that have been identified as crossover risks (Gonzalez-Isunza et al., 2023; Tolentino et al., 2024; Zumla et al., 2024). The greater sequence diversity of merbecoviruses also provides an opportunity to test the limitations of the Quartet strategy. When considering the design of a vaccine library, it would be important to understand the level of sequence diversity that can be covered by a single library member.

There is often a balance when seeking breadth of immune response across evolutionarily related pathogens. Broadening the immune response to more evolutionarily diverse pathogens can narrow the regions that are conserved across the group. This immune response can become susceptible to evasion with relatively small mutational drift if the targeted region becomes overly narrow.

Future work could explore a combination of the Quartet and S2 antigen truncation strategy. There is substantial sequence conservation within the S2 region of the spike protein extending beyond sarbecoviruses. Anti-S2 antibodies have shown cross-reactivity but are often poorly neutralizing (Adams et al., 2023; Ng et al., 2022; J. Sun et al., 2020). A vaccine that combined sarbecovirus Quartets and an S2 domain could elicit potently neutralizing antibodies against sarbecoviruses in addition to antisera that binds to a broader range of coronaviruses. Inclusion of a SpyTag on an S2 domain could facilitate multimeric presentation on SpyCatcher functionalized nanoparticle and homotypic S2 nanoparticles could be co-administered with Quartet Nanocage particles. Immunofocusing strategies such as glycosylation to block cryptic epitopes in S2 or the computational construction of a consensus S2 domain could be explored to further enhance the strategy. Through genetic fusion, a polyprotein of S2 and several sarbecovirus RBDs could be attempted in order to produce a single antigen for this strategy.

Future work could also explore a large number of different Quartets with a variety of different betacoronavirus RBDs. Computational approaches have been undertaken to optimize the combination of RBDs present on a mosaic nanoparticle (E. Wang et al., 2024). Similar approaches could be undertaken to develop a panel of optimized Quartets to assess. One option would be to explore this space using high-throughput Eukaryotic cell-free protein synthesis (CFPS) for initial expression screening (Das Gupta et al., 2023). This high-throughput screening would be limited to assessment of expression as a comparably high throughput means of assessing immune response has not been identified. This research could elucidate the boundaries of breadth that can be obtained using the Quartet strategy in addition to validating new vaccine candidates against zoonotic coronaviruses and human pathogens.

The COVID-19 pandemic spurred incredible cross-sector innovation. A culmination of this effort was the implementation of novel, safe, and protective vaccines at unprecedented pace

(Daems & Maes, 2022; Excler et al., 2023). These successes highlight the tremendous impact of a rapid vaccine response to pathogen threats (Mehand et al., 2018; Morens & Fauci, 2020). One method to achieve a fast and efficacious outbreak is to proactively develop vaccines against groups of related pathogens that have pandemic potential. This would allow for an off-the-shelf intervention to be available upon the identification of newly emerged outbreak (Saville et al., 2022). The Quartet Nanocage strategy outlined in this thesis demonstrates that a relatively simple vaccine can elicit broad and potent immune responses and can have the potential to accomplish this vision of proactive vaccinology.

Bibliography

Adams, L. E., Leist, S. R., Dinnon, K. H., West, A., Gully, K. L., Anderson, E. J., Loome, J. F., Madden, E. A., Powers, J. M., Schäfer, A., Sarkar, S., Castillo, I. N., Maron, J. S., McNamara, R. P., Bertera, H. L., Zweigart, M. R., Higgins, J. S., Hampton, B. K., Premkumar, L., … Baric, R. S. (2023). Fc-mediated pan-sarbecovirus protection after alphavirus vector vaccination. *Cell Reports*, *42*(4), 112326. https://doi.org/10.1016/j.celrep.2023.112326

Aida, Y., & Pabst, M. J. (1990). Removal of endotoxin from protein solutions by phase separation using triton X-114. *Journal of Immunological Methods*, *132*(2), 191–195. https://doi.org/10.1016/0022-1759(90)90029-U

Al Kaabi, N., Zhang, Y., Xia, S., Yang, Y., Al Qahtani, M. M., Abdulrazzaq, N., Al Nusair, M., Hassany, M., Jawad, J. S., Abdalla, J., Hussein, S. E., Al Mazrouei, S. K., Al Karam, M., Li, X., Yang, X., Wang, W., Lai, B., Chen, W., Huang, S., … Yang, X. (2021). Effect of 2 Inactivated SARS-CoV-2 Vaccines on Symptomatic COVID-19 Infection in Adults. *JAMA*, *326*(1), 35–45. https://doi.org/10.1001/jama.2021.8565

Alimohamadi, Y., Sepandi, M., Taghdir, M., & Hosamirudsari, H. (2020). Determine the most common clinical symptoms in COVID-19 patients: a systematic review and meta-analysis. *Journal of Preventive Medicine and Hygiene*, *61*(3), E304–E312. https://doi.org/10.15167/2421-4248/jpmh2020.61.3.1530

Alkhovsky, S., Lenshin, S., Romashin, A., Vishnevskaya, T., Vyshemirsky, O., Bulycheva, Y., Lvov, D., & Gitelman, A. (2022). SARS-like Coronaviruses in Horseshoe Bats (Rhinolophus spp.) in Russia, 2020. *Viruses*, *14*(1), 113. https://doi.org/10.3390/v14010113

Almagro Armenteros, J. J., Tsirigos, K. D., Sønderby, C. K., Petersen, T. N., Winther, O., Brunak, S., von Heijne, G., & Nielsen, H. (2019). SignalP 5.0 improves signal peptide predictions using deep neural networks. *Nature Biotechnology*, *37*(4), 420–423. https://doi.org/10.1038/s41587-019-0036-z

Altman, M. O., Angeletti, D., & Yewdell, J. W. (2018). Antibody Immunodominance: The Key to Understanding Influenza Virus Antigenic Drift. *Viral Immunology*, *31*(2), 142–149. https://doi.org/10.1089/vim.2017.0129

Amicone, M., Borges, V., Alves, M. J., Isidro, J., Zé-Zé, L., Duarte, S., Vieira, L., Guiomar, R., Gomes, J. P., & Gordo, I. (2022). Mutation rate of SARS-CoV-2 and emergence of mutators during experimental evolution. *Evolution, Medicine, and Public Health*, *10*(1), 142–155. https://doi.org/10.1093/emph/eoac010

Andrabi, R., Su, C.-Y., Liang, C.-H., Shivatare, S. S., Briney, B., Voss, J. E., Nawazi, S. K., Wu, C.-Y., Wong, C.-H., & Burton, D. R. (2017). Glycans Function as Anchors for Antibodies and Help Drive HIV Broadly Neutralizing Antibody Development. *Immunity*, *47*(3), 524-537.e3. https://doi.org/10.1016/j.immuni.2017.08.006

Anthony, S. J., Gilardi, K., Menachery, V. D., Goldstein, T., Ssebide, B., Mbabazi, R., Navarrete-Macias, I., Liang, E., Wells, H., Hicks, A., Petrosov, A., Byarugaba, D. K., Debbink, K., Dinnon, K. H., Scobey, T., Randell, S. H., Yount, B. L., Cranfield, M., Johnson, C. K., … Mazet, J. A. K. (2017). Further evidence for bats as the evolutionary source of middle east respiratory syndrome coronavirus. *MBio*, *8*(2). https://doi.org/10.1128/mBio.00373-17

Armstrong, J. K. (2009). The occurrence, induction, specificity and potential effect of antibodies against poly(ethylene glycol). In *PEGylated Protein Drugs: Basic Science and Clinical Applications* (pp. 147–168). Birkhäuser Basel. https://doi.org/10.1007/978-3-7643-8679-5_9

Arsiwala, A., Varner, C., McCaffery, J. N., Kell, A., Pendyala, G., Castro, A., Hariharan, V., Moreno, A., & Kane, R. S. (2019). Nanopatterning protein antigens to refocus the immune response. *Nanoscale*, *11*(32), 15307–15311. https://doi.org/10.1039/C9NR05145G

Atyeo, C., Slein, M. D., Fischinger, S., Burke, J., Schäfer, A., Leist, S. R., Kuzmina, N. A., Mire, C., Honko, A., Johnson, R., Storm, N., Bernett, M., Tong, P., Zuo, T., Lin, J., Zuiani, A., Linde, C., Suscovich, T., Wesemann, D. R., … Alter, G. (2021). Dissecting strategies to tune the therapeutic potential of SARS-CoV-2-specific monoclonal antibody CR3022. *JCI Insight*, *6*(1), e143129. https://doi.org/10.1172/jci.insight.143129

Bachmann, M. F., & Jennings, G. T. (2010). Vaccine delivery: a matter of size, geometry, kinetics and molecular patterns. *Nature Reviews Immunology*, *10*(11), 787–796. https://doi.org/10.1038/nri2868

Barnes, C. O., Jette, C. A., Abernathy, M. E., Dam, K. M. A., Esswein, S. R., Gristick, H. B., Malyutin, A. G., Sharaf, N. G., Huey-Tubman, K. E., Lee, Y. E., Robbiani, D. F., Nussenzweig, M. C., West, A. P., & Bjorkman, P. J. (2020). SARS-CoV-2 neutralizing antibody structures inform therapeutic strategies. *Nature*, *588*(7839), 682–687. https://doi.org/10.1038/s41586-020-2852-1

Bar-On, Y., Gruell, H., Schoofs, T., Pai, J. A., Nogueira, L., Butler, A. L., Millard, K., Lehmann, C., Suárez, I., Oliveira, T. Y., Karagounis, T., Cohen, Y. Z., Wyen, C., Scholten, S., Handl, L., Belblidia, S., Dizon, J. P., Vehreschild, J. J., Witmer-Pack, M., … Nussenzweig, M. C. (2018). Safety and antiviral activity of combination HIV-1 broadly neutralizing antibodies in viremic individuals. *Nature Medicine*, *24*(11), 1701–1707. https://doi.org/10.1038/s41591-018-0186-4

Bedi, R., Bayless, N. L., & Glanville, J. (2023). Challenges and Progress in Designing Broad-Spectrum Vaccines Against Rapidly Mutating Viruses. *Annual Review of Biomedical Data Science*, *6*(1), 419–441. https://doi.org/10.1146/annurev-biodatasci-020722-041304

Behrouzi, A., Bouzari, S., Vaziri, F., Fateh, A., Afrough, P., Vijeh Motlagh, A. D., & Siadat, S. D. (2017). Recombinant truncated E protein as a new vaccine candidate against

nontypeable H. influenzae: Its expression and immunogenic evaluation. *Microbial Pathogenesis*, *110*, 431–438. https://doi.org/10.1016/j.micpath.2017.07.025

Berche, P. (2022). Life and death of smallpox. *La Presse Médicale*, *51*(3), 104117. https://doi.org/10.1016/j.lpm.2022.104117

Bhiman, J. N., & Lynch, R. M. (2017). Broadly Neutralizing Antibodies as Treatment: Effects on Virus and Immune System. *Current HIV/AIDS Reports*, *14*(2), 54–62. https://doi.org/10.1007/s11904-017-0352-1

Bi, S., Qin, E., Xu, Z., Li, W., Wang, J., Hu, Y., Liu, Y., Duan, S., Hu, J., Han, Y., Xu, J., Li, Y., Yi, Y., Zhou, Y., Lin, W., Xu, H., Li, R., Zhang, Z., Sun, H., … Yang, H. (2003). Complete genome sequences of the SARS-CoV: the BJ Group (Isolates BJ01-BJ04). *Genomics, Proteomics & Bioinformatics / Beijing Genomics Institute*, *1*(3), 180–192. https://doi.org/10.1016/S1672-0229(03)01023-4

Bianchi, E., Finotto, M., Ingallinella, P., Citron, M., Hrin, R., Lu, M., Geleziunas, R., Miller, M. D., Liang, X., & Pessi, A. (2009). A Strategy for Selectively Shielding Portions of a Peptide/Protein from Immune Response while Maintaining Immunogenicity of Contiguous Epitopes. In *Advances in Experimental Medicine and Biology* (Vol. 611, pp. 359–360). https://doi.org/10.1007/978-0-387-73657-0_158

Bianchi, E., Joyce, J. G., Miller, M. D., Finnefrock, A. C., Liang, X., Finotto, M., Ingallinella, P., McKenna, P., Citron, M., Ottinger, E., Hepler, R. W., Hrin, R., Nahas, D., Wu, C., Montefiori, D., Shiver, J. W., Pessi, A., & Kim, P. S. (2010). Vaccination with peptide mimetics of the gp41 prehairpin fusion intermediate yields neutralizing antisera against HIV-1 isolates. *Proceedings of the National Academy of Sciences*, *107*(23), 10655–10660. https://doi.org/10.1073/pnas.1004261107

Bio-Rad Laboratories. (2023). *Guide to SpyCatcher products supporting TrailBlazer Antibodies*.

Bloom, J. D. (2023). Association between SARS-CoV-2 and metagenomic content of samples from the Huanan Seafood Market. *Virus Evolution*, *9*(2), vead050. https://doi.org/10.1093/ve/vead050

Bloom, J. D., Chan, Y. A., Baric, R. S., Bjorkman, P. J., Cobey, S., Deverman, B. E., Fisman, D. N., Gupta, R., Iwasaki, A., Lipsitch, M., Medzhitov, R., Neher, R. A., Nielsen, R., Patterson, N., Stearns, T., van Nimwegen, E., Worobey, M., & Relman, D. A. (2021). Investigate the origins of COVID-19. *Science*, *372*(6543), 694–694. https://doi.org/10.1126/science.abj0016

Bolze, A., Luo, S., White, S., Cirulli, E. T., Wyman, D., Dei Rossi, A., Machado, H., Cassens, T., Jacobs, S., Schiabor Barrett, K. M., Tanudjaja, F., Tsan, K., Nguyen, J., Ramirez, J. M., Sandoval, E., Wang, X., Wong, D., Becker, D., Laurent, M., … Lee, W. (2022). SARS-CoV-2 variant Delta rapidly displaced variant Alpha in the United States and led to higher viral loads. *Cell Reports Medicine*, *3*(3), 100564. https://doi.org/10.1016/j.xcrm.2022.100564

Boni, M. F. (2008). Vaccination and antigenic drift in influenza. *Vaccine*, *26*, C8–C14. https://doi.org/10.1016/j.vaccine.2008.04.011

Boni, M. F., Lemey, P., Jiang, X., Lam, T. T.-Y., Perry, B. W., Castoe, T. A., Rambaut, A., & Robertson, D. L. (2020). Evolutionary origins of the SARS-CoV-2 sarbecovirus lineage responsible for the COVID-19 pandemic. *Nature Microbiology*, *5*(11), 1408–1417. https://doi.org/10.1038/s41564-020-0771-4

Borgia, A., Kemplen, K. R., Borgia, M. B., Soranno, A., Shammas, S., Wunderlich, B., Nettels, D., Best, R. B., Clarke, J., & Schuler, B. (2015). Transient misfolding dominates multidomain protein folding. *Nature Communications*, *6*, 8861. https://doi.org/10.1038/ncomms9861

Bosaeed, M., & Alharbi, N. K. (2023). Vaccination strategies for mitigation of MERS-CoV outbreaks. *The Lancet Global Health*, *11*(5), e644–e645. https://doi.org/10.1016/S2214-109X(23)00164-X

Bosaeed, M., Balkhy, H. H., Almaziad, S., Aljami, H. A., Alhatmi, H., Alanazi, H., Alahmadi, M., Jawhary, A., Alenazi, M. W., Almasoud, A., Alanazi, R., Bittaye, M., Aboagye, J., Albaalharith, N., Batawi, S., Folegatti, P., Ramos Lopez, F., Ewer, K., Almoaikel, K., … Khalaf Alharbi, N. (2022). Safety and immunogenicity of ChAdOx1 MERS vaccine candidate in healthy Middle Eastern adults (MERS002): an open-label, non-randomised, dose-escalation, phase 1b trial. *The Lancet Microbe*, *3*(1), e11–e20. https://doi.org/10.1016/S2666-5247(21)00193-2

Boyoglu-Barnum, S., Ellis, D., Gillespie, R. A., Hutchinson, G. B., Park, Y.-J., Moin, S. M., Acton, O. J., Ravichandran, R., Murphy, M., Pettie, D., Matheson, N., Carter, L., Creanga, A., Watson, M. J., Kephart, S., Ataca, S., Vaile, J. R., Ueda, G., Crank, M. C., … Kanekiyo, M. (2021). Quadrivalent influenza nanoparticle vaccines induce broad protection. *Nature*, *592*(7855), 623–628. https://doi.org/10.1038/s41586-021-03365-x

Brämswig, K. H., Knittelfelder, R., Gruber, S., Untersmayr, E., Riemer, A. B., Szalai, K., Horvat, R., Kammerer, R., Zimmermann, W., Zielinski, C. C., Scheiner, O., & Jensen-Jarolim, E. (2007). Immunization with Mimotopes Prevents Growth of Carcinoembryonic Antigen–Positive Tumors in BALB/c Mice. *Clinical Cancer Research*, *13*(21), 6501–6508. https://doi.org/10.1158/1078-0432.CCR-07-0692

Brito, L. A., & Singh, M. (2011). Acceptable levels of endotoxin in vaccine formulations during preclinical research. *Journal of Pharmaceutical Sciences*, *100*(1), 34–37. https://doi.org/10.1002/jps.22267

Brouwer, P. J. M., Antanasijevic, A., Berndsen, Z., Yasmeen, A., Fiala, B., Bijl, T. P. L., Bontjer, I., Bale, J. B., Sheffler, W., Allen, J. D., Schorcht, A., Burger, J. A., Camacho, M., Ellis, D., Cottrell, C. A., Behrens, A. J., Catalano, M., del Moral-Sánchez, I., Ketas, T. J., … Sanders, R. W. (2019). Enhancing and shaping the immunogenicity of native-like HIV-1 envelope trimers with a two-component protein nanoparticle. *Nature Communications*, *10*(1). https://doi.org/10.1038/s41467-019-12080-1

Brune, K. (2019). *Extending the scope of covalent peptide-protein conjugation: from purification to expanded nanoassembl*. University of Oxford .

Brune, K. D., & Howarth, M. (2018). New Routes and Opportunities for Modular Construction of Particulate Vaccines: Stick, Click, and Glue. *Frontiers in Immunology*, *9*, 1432. https://doi.org/10.3389/fimmu.2018.01432

Brune, K. D., Leneghan, D. B., Brian, I. J., Ishizuka, A. S., Bachmann, M. F., Draper, S. J., Biswas, S., & Howarth, M. (2016). Plug-and-Display: decoration of Virus-Like Particles via isopeptide bonds for modular immunization. *Scientific Reports*, *6*, 19234. https://doi.org/10.1038/srep19234

Brüssow, H., & Brüssow, L. (2021). Clinical evidence that the pandemic from 1889 to 1891 commonly called the Russian flu might have been an earlier coronavirus pandemic. *Microbial Biotechnology*, *14*(5), 1860–1870. https://doi.org/10.1111/1751-7915.13889

Bruun, T., Do, J., Weidenbacher, P., & Kim, P. (2024). Engineering a SARS-CoV-2 vaccine targeting the RBD cryptic-face via immunofocusing. *BioRxiv*.

Bruun, T. U. J., Andersson, A. M. C., Draper, S. J., & Howarth, M. (2018). Engineering a Rugged Nanoscaffold to Enhance Plug-and-Display Vaccination. *ACS Nano*, *12*(9), 8855–8866. https://doi.org/10.1021/acsnano.8b02805

Buldun, C. M., Jean, J. X., Bedford, M. R., & Howarth, M. (2018). SnoopLigase Catalyzes Peptide-Peptide Locking and Enables Solid-Phase Conjugate Isolation. *Journal of the American Chemical Society*, *140*(8), 3008–3018. https://doi.org/10.1021/JACS.7B13237/SUPPL_FILE/JA7B13237_SI_001.PDF

Burki, T. (2023). First shared SARS-CoV-2 genome: GISAID vs virological.org. *The Lancet Microbe*, *4*(6), e395. https://doi.org/10.1016/S2666-5247(23)00133-7

Caly, L., Druce, J., Roberts, J., Bond, K., Tran, T., Kostecki, R., Yoga, Y., Naughton, W., Taiaroa, G., Seemann, T., Schultz, M. B., Howden, B. P., Korman, T. M., Lewin, S. R., Williamson, D. A., & Catton, M. G. (2020). Isolation and rapid sharing of the 2019 novel coronavirus (SARS-CoV-2) from the first patient diagnosed with COVID-19 in Australia. *Medical Journal of Australia*, *212*(10), 459–462. https://doi.org/10.5694/mja2.50569

Cankat, S., Demael, M. U., & Swadling, L. (2024). In search of a pan-coronavirus vaccine: next-generation vaccine design and immune mechanisms. In *Cellular and Molecular Immunology* (Vol. 21, Issue 2, pp. 103–118). Springer Nature. https://doi.org/10.1038/s41423-023-01116-8

Cao, Y., Yang, R., Lee, I., Zhang, W., Sun, J., Wang, W., & Meng, X. (2021). Characterization of the SARS-CoV-2 E Protein: Sequence, Structure, Viroporin, and Inhibitors. *Protein Science*, *30*(6), 1114–1130. https://doi.org/10.1002/pro.4075

Carlson, C. J., Albery, G. F., Merow, C., Trisos, C. H., Zipfel, C. M., Eskew, E. A., Olival, K. J., Ross, N., & Bansal, S. (2022). Climate change increases cross-species viral

transmission risk. *Nature*, *607*(7919), 555–562. https://doi.org/10.1038/s41586-022-04788-w

Carnell, G. W., Billmeier, M., Vishwanath, S., Suau Sans, M., Wein, H., George, C. L., Neckermann, P., Del Rosario, J. M. M., Sampson, A. T., Einhauser, S., Aguinam, E. T., Ferrari, M., Tonks, P., Nadesalingam, A., Schütz, A., Huang, C. Q., Wells, D. A., Paloniemi, M., Jordan, I., … Heeney, J. L. (2023). Glycan masking of a non-neutralising epitope enhances neutralising antibodies targeting the RBD of SARS-CoV-2 and its variants. *Frontiers in Immunology*, *14*, 1118523. https://doi.org/10.3389/fimmu.2023.1118523

Carrat, F., & Flahault, A. (2007). Influenza vaccine: The challenge of antigenic drift. *Vaccine*, *25*(39–40), 6852–6862. https://doi.org/10.1016/j.vaccine.2007.07.027

Carreño, J. M., Alshammary, H., Tcheou, J., Singh, G., Raskin, A. J., Kawabata, H., Sominsky, L. A., Clark, J. J., Adelsberg, D. C., Bielak, D. A., Gonzalez-Reiche, A. S., Dambrauskas, N., Vigdorovich, V., Alburquerque, B., Amoako, A. A., Banu, R., Beach, K. F., Bermúdez-González, M. C., Cai, G. Y., … Krammer, F. (2022). Activity of convalescent and vaccine serum against SARS-CoV-2 Omicron. *Nature*, *602*(7898), 682–688. https://doi.org/10.1038/s41586-022-04399-5

Cavelti-Weder, C., Timper, K., Seelig, E., Keller, C., Osranek, M., Lässing, U., Spohn, G., Maurer, P., Müller, P., Jennings, G. T., Willers, J., Saudan, P., Donath, M. Y., & Bachmann, M. F. (2016). Development of an Interleukin-1β Vaccine in Patients with Type 2 Diabetes. *Molecular Therapy*, *24*(5), 1003–1012. https://doi.org/10.1038/mt.2015.227

Chargelegue, D., Obeid, O. E., Shaw, D. M., Denbury, A. N., Hobby, P., Hsu, S. C., & Steward, M. W. (1997). Peptide mimics of a conformationally constrained protective epitopes of respiratory syncytial virus fusion protein. *Immunology Letters*, *57*(1–3), 15–17. https://doi.org/10.1016/S0165-2478(97)00045-X

Chaudhary, N., Weissman, D., & Whitehead, K. A. (2021). mRNA vaccines for infectious diseases: principles, delivery and clinical translation. *Nature Reviews Drug Discovery*, *20*(11), 817–838. https://doi.org/10.1038/s41573-021-00283-5

Chen, B. M., Cheng, T. L., & Roffler, S. R. (2021). Polyethylene Glycol Immunogenicity: Theoretical, Clinical, and Practical Aspects of Anti-Polyethylene Glycol Antibodies. *ACS Nano*, *15*(9), 14022–14048. https://doi.org/10.1021/acsnano.1c05922

Chen, B. M., Su, Y. C., Chang, C. J., Burnouf, P. A., Chuang, K. H., Chen, C. H., Cheng, T. L., Chen, Y. T., Wu, J. Y., & Roffler, S. R. (2016). Measurement of Pre-Existing IgG and IgM Antibodies against Polyethylene Glycol in Healthy Individuals. *Analytical Chemistry*, *88*(21), 10661–10666. https://doi.org/10.1021/acs.analchem.6b03109

Chen, J., Yang, X., Si, H., Gong, Q., Que, T., Li, J., Li, Y., Wu, C., Zhang, W., Chen, Y., Luo, Y., Zhu, Y., Li, B., Luo, D., Hu, B., Lin, H., Jiang, R., Jiang, T., Li, Q., … Zhou, P. (2023). A bat MERS-like coronavirus circulates in pangolins and utilizes human DPP4

and host proteases for cell entry. *Cell*, *186*(4), 850-863.e16. https://doi.org/10.1016/j.cell.2023.01.019

Chen, Y., Zhao, X., Zhou, H., Zhu, H., Jiang, S., & Wang, P. (2023). Broadly neutralizing antibodies to SARS-CoV-2 and other human coronaviruses. *Nature Reviews Immunology*, *23*(3), 189–199. https://doi.org/10.1038/s41577-022-00784-3

Chung, Y. H., Volckaert, B. A., & Steinmetz, N. F. (2023). Development of a Modular NTA:His Tag Viral Vaccine for Co-delivery of Antigen and Adjuvant. *Bioconjugate Chemistry*, *34*(1), 269–278. https://doi.org/10.1021/acs.bioconjchem.2c00601

Clark, J., Hoxie, I., Adelsberg, D. C., Sapse, I. A., Andreata-Santos, R., Yong, S., Amanat, F., Tcheou, J., Raskin, A., Singh, G., González-, I., Edgar, J. E., Bournazos, S., Sun, W., Manuel Carreño, J., Ellebedy, A. H., Bajic, G., & Krammer, F. (2024). Protective effect and molecular mechanisms of human non-neutralizing cross-reactive spike antibodies elicited by SARS-CoV-2 mRNA vaccination 2 3. *BioRxiv*. https://doi.org/10.1101/2024.02.28.582613

Cockrell, A. S., Yount, B. L., Scobey, T., Jensen, K., Douglas, M., Beall, A., Tang, X.-C., Marasco, W. A., Heise, M. T., & Baric, R. S. (2016). A mouse model for MERS coronavirus-induced acute respiratory distress syndrome. *Nature Microbiology*, *2*(2), 16226. https://doi.org/10.1038/nmicrobiol.2016.226

Cohen, A. A., Keeffe, J. R., Schiepers, A., Dross, S. E., Greaney, A. J., Rorick, A. V, Gao, H., Gnanapragasam, P. N. P., Fan, C., West, A. P., Ramsingh, A. I., Erasmus, J. H., Pata, J. D., Muramatsu, H., Pardi, N., Lin, P. J. C., Baxter, S., Cruz, R., Quintanar-Audelo, M., … Bjorkman, P. J. (2024). Mosaic sarbecovirus nanoparticles elicit cross-reactive responses in pre-vaccinated animals. *BioRxiv*, 2024.02.08.576722. https://doi.org/10.1101/2024.02.08.576722

Cohen, A. A., van Doremalen, N., Greaney, A. J., Andersen, H., Sharma, A., Starr, T. N., Keeffe, J. R., Fan, C., Schulz, J. E., Gnanapragasam, P. N. P., Kakutani, L. M., West, A. P., Saturday, G., Lee, Y. E., Gao, H., Jette, C. A., Lewis, M. G., Tan, T. K., Townsend, A. R., … Bjorkman, P. J. (2022). Mosaic RBD nanoparticles protect against challenge by diverse sarbecoviruses in animal models. *Science*, *377*(6606), 735–741. https://doi.org/10.1126/science.abf6840

Cohen, A. A., Yang, Z., Gnanapragasam, P. N. P., Ou, S., Dam, K.-M. A., Wang, H., & Bjorkman, P. J. (2021). Construction, characterization, and immunization of nanoparticles that display a diverse array of influenza HA trimers. *PLOS ONE*, *16*(3), e0247963. https://doi.org/10.1371/journal.pone.0247963

Cohen, A., Gnanapragasam, P. N. P., Lee, Y., Hoffman, P., Ou, S., Kakutani, L., Keeffe, J., Wu, H.-J., Howarth, M., West, A., Barnes, C., Nussenzweig, M., & Bjorkman, P. (2021). Mosaic nanoparticles elicit cross-reactive immune responses to zoonotic coronaviruses in mice. *Science*, *371*(6530), 735–741. https://www.science.org

Corman, V. M., Eckerle, I., Memish, Z. A., Liljander, A. M., Dijkman, R., Jonsdottir, H., Juma Ngeiywa, K. J. Z., Kamau, E., Younan, M., Al Masri, M., Assiri, A., Gluecks, I., Musa, B. E., Meyer, B., Müller, M. A., Hilali, M., Bornstein, S., Wernery, U., Thiel, V., … Drosten, C. (2016). Link of a ubiquitous human coronavirus to dromedary camels. *Proceedings of the National Academy of Sciences*, *113*(35), 9864–9869. https://doi.org/10.1073/pnas.1604472113

Corman, V. M., Ithete, N. L., Richards, L. R., Schoeman, M. C., Preiser, W., Drosten, C., & Drexler, J. F. (2014). Rooting the Phylogenetic Tree of Middle East Respiratory Syndrome Coronavirus by Characterization of a Conspecific Virus from an African Bat. *Journal of Virology*, *88*(19), 11297–11303. https://doi.org/10.1128/JVI.01498-14

Corman, V. M., Kallies, R., Philipps, H., Göpner, G., Müller, M. A., Eckerle, I., Brünink, S., Drosten, C., & Drexler, J. F. (2014). Characterization of a Novel Betacoronavirus Related to Middle East Respiratory Syndrome Coronavirus in European Hedgehogs. *Journal of Virology*, *88*(1), 717–724. https://doi.org/10.1128/JVI.01600-13

Correia, B. E., Bates, J. T., Loomis, R. J., Baneyx, G., Carrico, C., Jardine, J. G., Rupert, P., Correnti, C., Kalyuzhniy, O., Vittal, V., Connell, M. J., Stevens, E., Schroeter, A., Chen, M., MacPherson, S., Serra, A. M., Adachi, Y., Holmes, M. A., Li, Y., … Schief, W. R. (2014). Proof of principle for epitope-focused vaccine design. *Nature*, *507*(7491), 201–206. https://doi.org/10.1038/nature12966

Corti, D., Cameroni, E., Guarino, B., Kallewaard, N. L., Zhu, Q., & Lanzavecchia, A. (2017). Tackling influenza with broadly neutralizing antibodies. *Current Opinion in Virology*, *24*, 60–69. https://doi.org/10.1016/j.coviro.2017.03.002

Corti, D., & Lanzavecchia, A. (2013). Broadly Neutralizing Antiviral Antibodies. *Annual Review of Immunology*, *31*(1), 705–742. https://doi.org/10.1146/annurev-immunol-032712-095916

Corti, D., Zhao, J., Pedotti, M., Simonelli, L., Agnihothram, S., Fett, C., Fernandez-Rodriguez, B., Foglierini, M., Agatic, G., Vanzetta, F., Gopal, R., Langrish, C. J., Barrett, N. A., Sallusto, F., Baric, R. S., Varani, L., Zambon, M., Perlman, S., & Lanzavecchia, A. (2015). Prophylactic and postexposure efficacy of a potent human monoclonal antibody against MERS coronavirus. *Proceedings of the National Academy of Sciences of the United States of America*, *112*(33), 10473–10478. https://doi.org/10.1073/pnas.1510199112

Crawford, K. H. D., Eguia, R., Dingens, A. S., Loes, A. N., Malone, K. D., Wolf, C. R., Chu, H. Y., Tortorici, M. A., Veesler, D., Murphy, M., Pettie, D., King, N. P., Balazs, A. B., & Bloom, J. D. (2020). Protocol and Reagents for Pseudotyping Lentiviral Particles with SARS-CoV-2 Spike Protein for Neutralization Assays. *Viruses*, *12*(5), 513. https://doi.org/10.3390/v12050513

Crespo-Bellido, A., & Duffy, S. (2023). The how of counter-defense: viral evolution to combat host immunity. *Current Opinion in Microbiology*, *74*, 102320. https://doi.org/10.1016/j.mib.2023.102320

Cromer, D., Steain, M., Reynaldi, A., Schlub, T. E., Wheatley, A. K., Juno, J. A., Kent, S. J., Triccas, J. A., Khoury, D. S., & Davenport, M. P. (2022). Neutralising antibody titres as predictors of protection against SARS-CoV-2 variants and the impact of boosting: a meta-analysis. *The Lancet Microbe*, *3*(1), e52–e61. https://doi.org/10.1016/S2666-5247(21)00267-6

Cucinotta, D., & Vanelli, M. (2020). WHO Declares COVID-19 a Pandemic. *Acta Bio-Medica : Atenei Parmensis*, *91*(1), 157–160. https://doi.org/10.23750/abm.v91i1.9397

Cuevas-Juárez, E., Liñan-Torres, A., Hernández, C., Kopylov, M., Potter, C. S., Carragher, B., Ramírez, O. T., & Palomares, L. A. (2023). Mimotope discovery as a tool to design a vaccine against Zika and dengue viruses. *Biotechnology and Bioengineering*, *120*(9), 2658–2671. https://doi.org/10.1002/bit.28392

Cyrus Maher, M., Bartha, I., Weaver, S., Di Iulio, J., Ferri, E., Soriaga, L., Lempp, F. A., Hie, B. L., Bryson, B., Berger, B., Robertson, D. L., Snell, G., Corti, D., Virgin, H. W., Kosakovsky Pond, S. L., & Telenti, A. (2022). Predicting the mutational drivers of future SARS-CoV-2 variants of concern. *Sci. Transl. Med*, *14*, 3445. https://www.science.org

Daems, R., & Maes, E. (2022). The Race for COVID-19 Vaccines: Accelerating Innovation, Fair Allocation and Distribution. *Vaccines*, *10*(9), 1450. https://doi.org/10.3390/vaccines10091450

Dai, L., Gao, L., Tao, L., Hadinegoro, S. R., Erkin, M., Ying, Z., He, P., Girsang, R. T., Vergara, H., Akram, J., Satari, H. I., Khaliq, T., Sughra, U., Celi, A. P., Li, F., Li, Y., Jiang, Z., Dalimova, D., Tuychiev, J., … Gao, G. F. (2022). Efficacy and Safety of the RBD-Dimer–Based Covid-19 Vaccine ZF2001 in Adults. *New England Journal of Medicine*, *386*(22), 2097–2111. https://doi.org/10.1056/nejmoa2202261

Davis, H. E., McCorkell, L., Vogel, J. M., & Topol, E. J. (2023). Long COVID: major findings, mechanisms and recommendations. *Nature Reviews Microbiology*, *21*(3), 133–146. https://doi.org/10.1038/s41579-022-00846-2

Davis, H. L. (2008). Novel vaccines and adjuvant systems: The utility of animal models for predicting immunogenicity in humans. *Human Vaccines*, *4*(3), 246–250. https://doi.org/10.4161/hv.4.3.5318

de Klerk, A., Swanepoel, P., Lourens, R., Zondo, M., Abodunran, I., Lytras, S., MacLean, O. A., Robertson, D., Kosakovsky Pond, S. L., Zehr, J. D., Kumar, V., Stanhope, M. J., Harkins, G., Murrell, B., & Martin, D. P. (2022). Conserved recombination patterns across coronavirus subgenera. *Virus Evolution*, *8*(2), veac054. https://doi.org/10.1093/ve/veac054

De Silva, N. S., & Klein, U. (2015). Dynamics of B cells in germinal centres. *Nature Reviews Immunology*, *15*(3), 137–148. https://doi.org/10.1038/nri3804

De Wit, E., Van Doremalen, N., Falzarano, D., & Munster, V. J. (2016). SARS and MERS: Recent insights into emerging coronaviruses. *Nature Reviews Microbiology*, *14*(8), 523–534. https://doi.org/10.1038/nrmicro.2016.81

Deeks, S. G., Overbaugh, J., Phillips, A., & Buchbinder, S. (2015). HIV infection. *Nature Reviews Disease Primers*, *1*(1), 15035. https://doi.org/10.1038/nrdp.2015.35

del Moral-Sánchez, I., & Sliepen, K. (2019). Strategies for inducing effective neutralizing antibody responses against HIV-1. *Expert Review of Vaccines*, *18*(11), 1127–1143. https://doi.org/10.1080/14760584.2019.1690458

Dennis, M. S., Zhang, M., Gloria Meng, Y., Kadkhodayan, M., Kirchhofer, D., Combs, D., & Damico, L. A. (2002). Albumin binding as a general strategy for improving the pharmacokinetics of proteins. *Journal of Biological Chemistry*, *277*(38), 35035–35043. https://doi.org/10.1074/jbc.M205854200

Dhar, M. S., Marwal, R., VS, R., Ponnusamy, K., Jolly, B., Bhoyar, R. C., Sardana, V., Naushin, S., Rophina, M., Mellan, T. A., Mishra, S., Whittaker, C., Fatihi, S., Datta, M., Singh, P., Sharma, U., Ujjainiya, R., Bhatheja, N., Divakar, M. K., … Cherian, S. S. (2021). Genomic characterization and epidemiology of an emerging SARS-CoV-2 variant in Delhi, India. *Science*, *374*(6570), 995–999. https://doi.org/10.1126/science.abj9932

Dhawan, M., Sharma, A., Priyanka, Thakur, N., Rajkhowa, T. K., & Choudhary, O. P. (2022). Delta variant (B.1.617.2) of SARS-CoV-2: Mutations, impact, challenges and possible solutions. *Human Vaccines & Immunotherapeutics*, *18*(5), 2068883. https://doi.org/10.1080/21645515.2022.2068883

Dicks, M. D. J., Rose, L. M., Russell, R. A., Bowman, L. A. H., Graham, C., Jimenez-Guardeño, J. M., Doores, K. J., Malim, M. H., Draper, S. J., Howarth, M., & Biswas, S. (2022). Modular capsid decoration boosts adenovirus vaccine-induced humoral immunity against SARS-CoV-2. *Molecular Therapy*, *30*(12), 3639–3657. https://doi.org/10.1016/j.ymthe.2022.08.002

Ding, P., Zhang, T., Li, Y., Teng, M., Sun, Y., Liu, X., Chai, S., Zhou, E., Jin, Q., & Zhang, G. (2017). Nanoparticle orientationally displayed antigen epitopes improve neutralizing antibody level in a model of porcine circovirus type 2. *International Journal of Nanomedicine*, *Volume 12*, 5239–5254. https://doi.org/10.2147/IJN.S140789

Dixit, A., Bennett, R., Ali, K., Griffin, C., Clifford, R. A., Turner, M., Poston, R., Hautzinger, K., Yeakey, A., Girard, B., Zhou, W., Deng, W., Zhou, H., Schnyder Ghamloush, S., Kuter, B. J., Slobod, K., Miller, J. M., Priddy, F., Das, R., … Warfield, P. (2024). Interim safety and immunogenicity of COVID-19 omicron BA.1 variant-containing vaccine in children in the USA: an open-label non-randomised phase 3 trial. *The Lancet Infectious Diseases*, *24*(7), 687–697. https://doi.org/10.1016/S1473-3099(24)00101-4

Dos Santos, G., Neumeier, E., & Bekkat-Berkani, R. (2016). Influenza: Can we cope better with the unpredictable? *Human Vaccines & Immunotherapeutics*, *12*(3), 699–708. https://doi.org/10.1080/21645515.2015.1086047

Drexler, J. F., Corman, V. M., & Drosten, C. (2014). Ecology, evolution and classification of bat coronaviruses in the aftermath of SARS. *Antiviral Research*, *101*, 45–56. https://doi.org/10.1016/j.antiviral.2013.10.013

Drexler, J. F., Gloza-Rausch, F., Glende, J., Corman, V. M., Muth, D., Goettsche, M., Seebens, A., Niedrig, M., Pfefferle, S., Yordanov, S., Zhelyazkov, L., Hermanns, U., Vallo, P., Lukashev, A., Müller, M. A., Deng, H., Herrler, G., & Drosten, C. (2010). Genomic Characterization of Severe Acute Respiratory Syndrome-Related Coronavirus in European Bats and Classification of Coronaviruses Based on Partial RNA-Dependent RNA Polymerase Gene Sequences. *Journal of Virology*, *84*(21), 11336–11349. https://doi.org/10.1128/jvi.00650-10

Drosten, C., Meyer, B., Müller, M. A., Corman, V. M., Al-Masri, M., Hossain, R., Madani, H., Sieberg, A., Bosch, B. J., Lattwein, E., Alhakeem, R. F., Assiri, A. M., Hajomar, W., Albarrak, A. M., Al-Tawfiq, J. A., Zumla, A. I., & Memish, Z. A. (2014). Transmission of MERS-Coronavirus in Household Contacts. *New England Journal of Medicine*, *371*(9), 828–835. https://doi.org/10.1056/NEJMoa1405858

Du, L., Kou, Z., Ma, C., Tao, X., Wang, L., Zhao, G., Chen, Y., Yu, F., Tseng, C.-T. K., Zhou, Y., & Jiang, S. (2013). A Truncated Receptor-Binding Domain of MERS-CoV Spike Protein Potently Inhibits MERS-CoV Infection and Induces Strong Neutralizing Antibody Responses: Implication for Developing Therapeutics and Vaccines. *PLoS ONE*, *8*(12), e81587. https://doi.org/10.1371/journal.pone.0081587

Du, P., Huang, L., Fang, Y., Zhao, F., Li, Q., Ma, X., Li, R., Chen, Q., Shen, H., Wang, Q., Li, H., & Gao, G. F. (2024). Broad-spectrum Delta-BA.2 tandem-fused heterodimer mRNA vaccine delivered by lipopolyplex. *PLoS Pathogens*, *20*(4), e1012116. https://doi.org/10.1371/journal.ppat.1012116

Du, R., Cui, Q., & Rong, L. (2021). Flu Universal Vaccines: New Tricks on an Old Virus. *Virologica Sinica*, *36*(1), 13–24. https://doi.org/10.1007/s12250-020-00283-6

Dunkelberger, J. R., & Song, W.-C. (2010). Complement and its role in innate and adaptive immune responses. *Cell Research*, *20*(1), 34–50. https://doi.org/10.1038/cr.2009.139

Eccles, R. (2023). Common cold. *Frontiers in Allergy*, *4*, 1224988. https://doi.org/10.3389/falgy.2023.1224988

Egesten, A., Frick, I. M., Mörgelin, M., Olin, A. I., & Björck, L. (2011a). Binding of albumin promotes bacterial survival at the epithelial surface. *Journal of Biological Chemistry*, *286*(4), 2469–2476. https://doi.org/10.1074/jbc.M110.148171

Egesten, A., Frick, I.-M., Mörgelin, M., Olin, A. I., & Björck, L. (2011b). Binding of Albumin Promotes Bacterial Survival at the Epithelial Surface. *Journal of Biological Chemistry*, *286*(4), 2469–2476. https://doi.org/10.1074/jbc.M110.148171

Eggink, D., Goff, P. H., & Palese, P. (2014). Guiding the Immune Response against Influenza Virus Hemagglutinin toward the Conserved Stalk Domain by Hyperglycosylation of the Globular Head Domain. *Journal of Virology*, *88*(1), 699–704. https://doi.org/10.1128/JVI.02608-13

El Sayes, M., Badra, R., Ali, M. A., El-Shesheny, R., & Kayali, G. (2024). Global Distribution and Molecular Evolution of Bat Coronaviruses. *Zoonotic Diseases*, *4*(2), 146–161. https://doi.org/10.3390/zoonoticdis4020014

Ellwanger, J. H., & Chies, J. A. B. (2021). Zoonotic spillover: Understanding basic aspects for better prevention. *Genetics and Molecular Biology*, *44*(1 suppl 1). https://doi.org/10.1590/1678-4685-gmb-2020-0355

Elsner, R. A., & Shlomchik, M. J. (2020). Germinal Center and Extrafollicular B Cell Responses in Vaccination, Immunity, and Autoimmunity. *Immunity*, *53*(6), 1136–1150. https://doi.org/10.1016/j.immuni.2020.11.006

Escolano, A., Gristick, H. B., Abernathy, M. E., Merkenschlager, J., Gautam, R., Oliveira, T. Y., Pai, J., West, A. P., Barnes, C. O., Cohen, A. A., Wang, H., Golijanin, J., Yost, D., Keeffe, J. R., Wang, Z., Zhao, P., Yao, K.-H., Bauer, J., Nogueira, L., … Nussenzweig, M. C. (2019). Immunization expands B cells specific to HIV-1 V3 glycan in mice and macaques. *Nature*, *570*(7762), 468–473. https://doi.org/10.1038/s41586-019-1250-z

Escolano, A., Gristick, H. B., Gautam, R., DeLaitsch, A. T., Abernathy, M. E., Yang, Z., Wang, H., Hoffmann, M. A. G., Nishimura, Y., Wang, Z., Koranda, N., Kakutani, L. M., Gao, H., Gnanapragasam, P. N. P., Raina, H., Gazumyan, A., Cipolla, M., Oliveira, T. Y., Ramos, V., … Bjorkman, P. J. (2021). Sequential immunization of macaques elicits heterologous neutralizing antibodies targeting the V3-glycan patch of HIV-1 Env. *Science Translational Medicine*, *13*(621), eabk1533. https://doi.org/10.1126/scitranslmed.abk1533

Escolano, A., Steichen, J. M., Dosenovic, P., Kulp, D. W., Golijanin, J., Sok, D., Freund, N. T., Gitlin, A. D., Oliveira, T., Araki, T., Lowe, S., Chen, S. T., Heinemann, J., Yao, K.-H., Georgeson, E., Saye-Francisco, K. L., Gazumyan, A., Adachi, Y., Kubitz, M., … Nussenzweig, M. C. (2016). Sequential Immunization Elicits Broadly Neutralizing Anti-HIV-1 Antibodies in Ig Knockin Mice. *Cell*, *166*(6), 1445-1458.e12. https://doi.org/10.1016/j.cell.2016.07.030

Evans, H. M., & Schulemann, W. (1914). The action of vital stains belonging to the benzidine group. *Science*, *39*(1004), 443–454. https://doi.org/10.1126/science.39.1004.443/asset/979606bb-a373-4696-a754-13e7f4ac563b/assets/science.39.1004.443.fp.png

Evans, T. S., Tan, C. W., Aung, O., Phyu, S., Lin, H., Coffey, L. L., Toe, A. T., Aung, P., Aung, T. H., Aung, N. T., Weiss, C. M., Thant, K. Z., Htun, Z. T., Murray, S., Wang, L., Johnson, C. K., & Thu, H. M. (2023). Exposure to diverse sarbecoviruses indicates frequent zoonotic spillover in human communities interacting with wildlife. *International Journal of Infectious Diseases : IJID : Official Publication of the International Society for Infectious Diseases*, *131*, 57–64. https://doi.org/10.1016/J.IJID.2023.02.015

Ewer, K., Sebastian, S., Spencer, A. J., Gilbert, S., Hill, A. V. S., & Lambe, T. (2017). Chimpanzee adenoviral vectors as vaccines for outbreak pathogens. *Human Vaccines & Immunotherapeutics*, *13*(12), 3020–3032. https://doi.org/10.1080/21645515.2017.1383575

Excler, J. L., Saville, M., Privor-Dumm, L., Gilbert, S., Hotez, P. J., Thompson, D., Abdool-Karim, S., & Kim, J. H. (2023). Factors, enablers and challenges for COVID-19 vaccine development. *BMJ Global Health*, *8*(6), e011879. https://doi.org/10.1136/bmjgh-2023-011879

Fairhead, M., & Howarth, M. (2015). Site-specific biotinylation of purified proteins using BirA. *Methods in Molecular Biology*, *1266*, 171–184. https://doi.org/10.1007/978-1-4939-2272-7_12

Falsey, A. R., Sobieszczyk, M. E., Hirsch, I., Sproule, S., Robb, M. L., Corey, L., Neuzil, K. M., Hahn, W., Hunt, J., Mulligan, M. J., McEvoy, C., DeJesus, E., Hassman, M., Little, S. J., Pahud, B. A., Durbin, A., Pickrell, P., Daar, E. S., Bush, L., … Gonzalez-Lopez, A. (2021). Phase 3 Safety and Efficacy of AZD1222 (ChAdOx1 nCoV-19) Covid-19 Vaccine. *New England Journal of Medicine*, *385*(25), 2348–2360. https://doi.org/10.1056/NEJMoa2105290

Fan, Y., Zhao, K., Shi, Z.-L., & Zhou, P. (2019). Bat Coronaviruses in China. *Viruses*, *11*(3), 210. https://doi.org/10.3390/v11030210

Fang, P., Fang, L., Zhang, H., Xia, S., & Xiao, S. (2021). Functions of Coronavirus Accessory Proteins: Overview of the State of the Art. *Viruses*, *13*(6), 1139. https://doi.org/10.3390/v13061139

Finkel, Y., Mizrahi, O., Nachshon, A., Weingarten-Gabbay, S., Morgenstern, D., Yahalom-Ronen, Y., Tamir, H., Achdout, H., Stein, D., Israeli, O., Beth-Din, A., Melamed, S., Weiss, S., Israely, T., Paran, N., Schwartz, M., & Stern-Ginossar, N. (2021). The coding capacity of SARS-CoV-2. *Nature*, *589*(7840), 125–130. https://doi.org/10.1038/s41586-020-2739-1

Fiore, A. E., Bridges, C. B., & Cox, N. J. (2009). *Seasonal Influenza Vaccines* (pp. 43–82). https://doi.org/10.1007/978-3-540-92165-3_3

Flach, C.-F., Svensson, N., Blomquist, M., Ekman, A., Raghavan, S., & Holmgren, J. (2011). A truncated form of HpaA is a promising antigen for use in a vaccine against

Helicobacter pylori. *Vaccine*, *29*(6), 1235–1241. https://doi.org/10.1016/j.vaccine.2010.11.088

Folegatti, P. M., Ewer, K. J., Aley, P. K., Angus, B., Becker, S., Belij-Rammerstorfer, S., Bellamy, D., Bibi, S., Bittaye, M., Clutterbuck, E. A., Dold, C., Faust, S. N., Finn, A., Flaxman, A. L., Hallis, B., Heath, P., Jenkin, D., Lazarus, R., Makinson, R., … Yau, Y. (2020). Safety and immunogenicity of the ChAdOx1 nCoV-19 vaccine against SARS-CoV-2: a preliminary report of a phase 1/2, single-blind, randomised controlled trial. *The Lancet*, *396*(10249), 467–478. https://doi.org/10.1016/S0140-6736(20)31604-4

Frey, S. J., Varner, C., Arsiwala, A., Currier, M. G., Moore, M. L., & Kane, R. S. (2021). The Design of Vaccines Based on the Shielding of Antigenic Site Ø of a Respiratory Syncytial Virus Fusion Protein Immunogen. *Advanced Healthcare Materials*, *10*, 2000714. https://doi.org/10.1002/adhm.202000714

Gao, Q., Bao, L., Mao, H., Wang, L., Xu, K., Yang, M., Li, Y., Zhu, L., Wang, N., Lv, Z., Gao, H., Ge, X., Kan, B., Hu, Y., Liu, J., Cai, F., Jiang, D., Yin, Y., Qin, C., … Qin, C. (2020). Development of an inactivated vaccine candidate for SARS-CoV-2. *Science*, *369*(6499), 77–81. https://doi.org/10.1126/science.abc1932

Gao, Z., Xu, Y., Sun, C., Wang, X., Guo, Y., Qiu, S., & Ma, K. (2021). A systematic review of asymptomatic infections with COVID-19. *Journal of Microbiology, Immunology and Infection*, *54*(1), 12–16. https://doi.org/10.1016/j.jmii.2020.05.001

Garay, R. P., El-Gewely, R., Armstrong, J. K., Garratty, G., & Richette, P. (2012). Antibodies against polyethylene glycol in healthy subjects and in patients treated with PEG-conjugated agents. *Expert Opinion on Drug Delivery*, *9*(11), 1319–1323. https://doi.org/10.1517/17425247.2012.720969

Garry, R. F. (2023). Lassa fever — the road ahead. *Nature Reviews Microbiology*, *21*(2), 87–96. https://doi.org/10.1038/s41579-022-00789-8

Gasteiger, E., Hoogland, C., Gattiker, A., Duvaud, S., Wilkins, M. R., Appel, R. D., & Bairoch, A. (2005). Protein Identification and Analysis Tools on the ExPASy Server. In *The Proteomics Protocols Handbook* (pp. 571–607). Humana Press. https://doi.org/10.1385/1-59259-890-0:571

Ge, X. Y., Li, J. L., Yang, X. Lou, Chmura, A. A., Zhu, G., Epstein, J. H., Mazet, J. K., Hu, B., Zhang, W., Peng, C., Zhang, Y. J., Luo, C. M., Tan, B., Wang, N., Zhu, Y., Crameri, G., Zhang, S. Y., Wang, L. F., Daszak, P., & Shi, Z. L. (2013a). Isolation and characterization of a bat SARS-like coronavirus that uses the ACE2 receptor. *Nature*, *503*(7477), 535–538. https://doi.org/10.1038/nature12711

Ge, X. Y., Li, J. L., Yang, X. Lou, Chmura, A. A., Zhu, G., Epstein, J. H., Mazet, J. K., Hu, B., Zhang, W., Peng, C., Zhang, Y. J., Luo, C. M., Tan, B., Wang, N., Zhu, Y., Crameri, G., Zhang, S. Y., Wang, L. F., Daszak, P., & Shi, Z. L. (2013b). Isolation and characterization of a bat SARS-like coronavirus that uses the ACE2 receptor. *Nature*, *503*(7477), 535–538. https://doi.org/10.1038/nature12711

Ge, X. Y., Wang, N., Zhang, W., Hu, B., Li, B., Zhang, Y. Z., Zhou, J. H., Luo, C. M., Yang, X. Lou, Wu, L. J., Wang, B., Zhang, Y., Li, Z. X., & Shi, Z. L. (2016). Coexistence of multiple coronaviruses in several bat colonies in an abandoned mineshaft. *Virologica Sinica*, *31*(1), 31–40. https://doi.org/10.1007/s12250-016-3713-9

Geddes, L. (2023, October 9). *From Kraken to Pirola: who comes up with the nicknames for COVID-19 variants?* Gavi The Vaccine Alliance. https://www.gavi.org/vaccineswork/kraken-pirola-who-comes-nicknames-covid-19-variants

Geysen, H. M., Rodda, S. J., & Mason, T. J. (1986). A priori delineation of a peptide which mimics a discontinuous antigenic determinant. *Molecular Immunology*, *23*(7), 709–715. https://doi.org/10.1016/0161-5890(86)90081-7

Ghai, R. R., Carpenter, A., Liew, A. Y., Martin, K. B., Herring, M. K., Gerber, S. I., Hall, A. J., Sleeman, J. M., VonDobschuetz, S., & Behravesh, C. B. (2021). Animal Reservoirs and Hosts for Emerging Alphacoronaviruses and Betacoronaviruses. *Emerging Infectious Diseases*, *27*(4), 1015–1022. https://doi.org/10.3201/eid2704.203945

Gibson, D. G., Young, L., Chuang, R.-Y., Venter, J. C., Hutchison, C. A., & Smith, H. O. (2009). Enzymatic assembly of DNA molecules up to several hundred kilobases. *Nature Methods*, *6*(5), 343–345. https://doi.org/10.1038/nmeth.1318

Gilbert, P. B., Donis, R. O., Koup, R. A., Fong, Y., Plotkin, S. A., & Follmann, D. (2022). A Covid-19 Milestone Attained — A Correlate of Protection for Vaccines. *New England Journal of Medicine*, *387*(24), 2203–2206. https://doi.org/10.1056/NEJMp2211314

Gilbert, S. C. (2012). T-cell-inducing vaccines – what's the future. *Immunology*, *135*(1), 19–26. https://doi.org/10.1111/j.1365-2567.2011.03517.x

Goldberg, B. S., & Ackerman, M. E. (2020). Antibody-mediated complement activation in pathology and protection. *Immunology & Cell Biology*, *98*(4), 305–317. https://doi.org/10.1111/imcb.12324

Goldblatt, D., Alter, G., Crotty, S., & Plotkin, S. A. (2022). Correlates of protection against SARS-CoV-2 infection and COVID-19 disease. *Immunological Reviews*, *310*(1), 6–26. https://doi.org/10.1111/imr.13091

Gonzalez-Isunza, G., Jawaid, M. Z., Liu, P., Cox, D. L., Vazquez, M., & Arsuaga, J. (2023). Using machine learning to detect coronaviruses potentially infectious to humans. *Scientific Reports*, *13*(1), 9319. https://doi.org/10.1038/s41598-023-35861-7

Gostin, L. O., & Gronvall, G. K. (2023). The Origins of Covid-19 — Why It Matters (and Why It Doesn't). *New England Journal of Medicine*, *388*(25), 2305–2308. https://doi.org/10.1056/NEJMp2305081

Gouglas, D., Christodoulou, M., & Hatchett, R. (2023). The 100 Days Mission—2022 Global Pandemic Preparedness Summit. *Emerging Infectious Disease*, *29*(3), e221142.

Graham, B. S., Gilman, M. S. A., & McLellan, J. S. (2019). Structure-Based Vaccine Antigen Design. *Annual Review of Medicine*, *70*(1), 91–104. https://doi.org/10.1146/annurev-med-121217-094234

Graham, S. P., McLean, R. K., Spencer, A. J., Belij-Rammerstorfer, S., Wright, D., Ulaszewska, M., Edwards, J. C., Hayes, J. W. P., Martini, V., Thakur, N., Conceicao, C., Dietrich, I., Shelton, H., Waters, R., Ludi, A., Wilsden, G., Browning, C., Bialy, D., Bhat, S., … Lambe, T. (2020). Evaluation of the immunogenicity of prime-boost vaccination with the replication-deficient viral vectored COVID-19 vaccine candidate ChAdOx1 nCoV-19. *Npj Vaccines*, *5*, 69. https://doi.org/10.1038/s41541-020-00221-3

Greaney, A. J., Loes, A. N., Crawford, K. H. D., Starr, T. N., Malone, K. D., Chu, H. Y., & Bloom, J. D. (2021). Comprehensive mapping of mutations in the SARS-CoV-2 receptor-binding domain that affect recognition by polyclonal human plasma antibodies. *Cell Host and Microbe*, *29*(3), 463-476.e6. https://doi.org/10.1016/j.chom.2021.02.003

Greaney, A. J., Starr, T. N., Eguia, R. T., Loes, A. N., Khan, K., Karim, F., Cele, S., Bowen, J. E., Logue, J. K., Corti, D., Veesler, D., Chu, H. Y., Sigal, A., & Bloom, J. D. (2022). A SARS-CoV-2 variant elicits an antibody response with a shifted immunodominance hierarchy. *PLoS Pathogens*, *18*(2), e1010248. https://doi.org/10.1371/journal.ppat.1010248

Greenwood, B. (2014). The contribution of vaccination to global health: past, present and future. *Philosophical Transactions of the Royal Society B: Biological Sciences*, *369*(1645), 20130433. https://doi.org/10.1098/rstb.2013.0433

Gristick, H. B., Hartweger, H., Loewe, M., van Schooten, J., Ramos, V., Oliveira, T. Y., Nishimura, Y., Koranda, N. S., Wall, A., Yao, K. H., Poston, D., Gazumyan, A., Wiatr, M., Horning, M., Keeffe, J. R., Hoffmann, M. A. G., Yang, Z., Abernathy, M. E., Dam, K. M. A., … Bjorkman, P. J. (2023). CD4 binding site immunogens elicit heterologous anti–HIV-1 neutralizing antibodies in transgenic and wild-type animals. *Science Immunology*, *8*(80), eade6364. https://doi.org/10.1126/sciimmunol.ade6364

Guan, Y., Zheng, B. J., He, Y. Q., Liu, X. L., Zhuang, Z. X., Cheung, C. L., Luo, S. W., Li, P. H., Zhang, L. J., Guan, Y. J., Butt, K. M., Wong, K. L., Chan, K. W., Lim, W., Shortridge, K. F., Yuen, K. Y., Peiris, J. S. M., & Poon, L. L. M. (2003). Isolation and Characterization of Viruses Related to the SARS Coronavirus from Animals in Southern China. *Science*, *302*(5643), 276–278. https://doi.org/10.1126/science.1087139

Guerrini, G., Gioria, S., Sauer, A. V., Lucchesi, S., Montagnani, F., Pastore, G., Ciabattini, A., Medaglini, D., & Calzolai, L. (2022). Monitoring Anti-PEG Antibodies Level upon Repeated Lipid Nanoparticle-Based COVID-19 Vaccine Administration. *International Journal of Molecular Sciences*, *23*(16), 8838. https://doi.org/10.3390/IJMS23168838/S1

Gulati, N. M., Stewart, P. L., & Steinmetz, N. F. (2018). Bioinspired Shielding Strategies for Nanoparticle Drug Delivery Applications. *Molecular Pharmaceutics*, *15*(8), 2900–2909. https://doi.org/10.1021/acs.molpharmaceut.8b00292

Guo, Y., He, W., Mou, H., Zhang, L., Chang, J., Peng, S., Ojha, A., Tavora, R., Parcells, M. S., Luo, G., Li, W., Zhong, G., Choe, H., Farzan, M., & Quinlan, B. D. (2021). An Engineered Receptor-Binding Domain Improves the Immunogenicity of Multivalent SARS-CoV-2 Vaccines. *MBio*, *12*(3), e00930-21. https://doi.org/10.1128/mBio.00930-21

Gupta, D., & Mohan, S. (2023a). Influenza vaccine: a review on current scenario and future prospects. *Journal of Genetic Engineering and Biotechnology*, *21*(1), 154. https://doi.org/10.1186/s43141-023-00581-y

Gupta, D., & Mohan, S. (2023b). Influenza vaccine: a review on current scenario and future prospects. *Journal of Genetic Engineering and Biotechnology*, *21*(1), 154. https://doi.org/10.1186/s43141-023-00581-y

Gupta, M. Das, Flaskamp, Y., Roentgen, R., Juergens, H., Armero-Gimenez, J., Albrecht, F., Hemmerich, J., Arfi, Z. A., Neuser, J., Spiegel, H., Schillberg, S., Yeliseev, A., Song, L., Qiu, J., Williams, C., & Finnern, R. (2023). Scaling eukaryotic cell-free protein synthesis achieved with the versatile and high-yielding tobacco BY-2 cell lysate. *Biotechnology and Bioengineering*, *120*(10), 2890–2906. https://doi.org/10.1002/bit.28461

Haagmans, B. L., Al Dhahiry, S. H. S., Reusken, C. B. E. M., Raj, V. S., Galiano, M., Myers, R., Godeke, G.-J., Jonges, M., Farag, E., Diab, A., Ghobashy, H., Alhajri, F., Al-Thani, M., Al-Marri, S. A., Al Romaihi, H. E., Al Khal, A., Bermingham, A., Osterhaus, A. D. M. E., AlHajri, M. M., & Koopmans, M. P. G. (2014). Middle East respiratory syndrome coronavirus in dromedary camels: an outbreak investigation. *The Lancet Infectious Diseases*, *14*(2), 140–145. https://doi.org/10.1016/S1473-3099(13)70690-X

Hadfield, J., Megill, C., Bell, S. M., Huddleston, J., Potter, B., Callender, C., Sagulenko, P., Bedford, T., & Neher, R. A. (2018). NextStrain: Real-time tracking of pathogen evolution. *Bioinformatics*, *34*(23), 4121–4123. https://doi.org/10.1093/bioinformatics/bty407

Haeckel, A., Appler, F., Ariza de Schellenberger, A., & Schellenberger, E. (2016). XTEN as Biological Alternative to PEGylation Allows Complete Expression of a Protease-Activatable Killin-Based Cytostatic. *PLOS ONE*, *11*(6), e0157193. https://doi.org/10.1371/journal.pone.0157193

Hager, K. J., Pérez Marc, G., Gobeil, P., Diaz, R. S., Heizer, G., Llapur, C., Makarkov, A. I., Vasconcellos, E., Pillet, S., Riera, F., Saxena, P., Geller Wolff, P., Bhutada, K., Wallace, G., Aazami, H., Jones, C. E., Polack, F. P., Ferrara, L., Atkins, J., … Ward, B. J. (2022). Efficacy and Safety of a Recombinant Plant-Based Adjuvanted Covid-19 Vaccine. *New England Journal of Medicine*, *386*(22), 2084–2096. https://doi.org/10.1056/NEJMoa2201300

Hallengärd, D., Wahren, B., & Bråve, A. (2013). A Truncated Plasmid-Encoded HIV-1 Reverse Transcriptase Displays Strong Immunogenicity. *Viral Immunology*, *26*(2), 163–166. https://doi.org/10.1089/vim.2012.0083

Halperin, S. A., Ye, L., MacKinnon-Cameron, D., Smith, B., Cahn, P. E., Ruiz-Palacios, G. M., Ikram, A., Lanas, F., Lourdes Guerrero, M., Muñoz Navarro, S. R., Sued, O., Lioznov, D. A., Dzutseva, V., Parveen, G., Zhu, F., Leppan, L., Langley, J. M., Barreto, L., Gou, J., … Zubkova, T. (2022). Final efficacy analysis, interim safety analysis, and immunogenicity of a single dose of recombinant novel coronavirus vaccine (adenovirus type 5 vector) in adults 18 years and older: an international, multicentre, randomised, double-blinded, placebo-controlled phase 3 trial. *The Lancet*, *399*(10321), 237–248. https://doi.org/10.1016/S0140-6736(21)02753-7

Han, J.-F., Qiu, Y., Yu, J.-Y., Wang, H.-J., Deng, Y.-Q., Li, X.-F., Zhao, H., Sun, H.-X., & Qin, C.-F. (2017). Immunization with truncated envelope protein of Zika virus induces protective immune response in mice. *Scientific Reports*, *7*(1), 10047. https://doi.org/10.1038/s41598-017-10595-5

Han, W., Chen, N., Xu, X., Sahil, A., Zhou, J., Li, Z., Zhong, H., Gao, E., Zhang, R., Wang, Y., Sun, S., Cheung, P. P. H., & Gao, X. (2023). Predicting the antigenic evolution of SARS-COV-2 with deep learning. *Nature Communications*, *14*(1), 3478. https://doi.org/10.1038/s41467-023-39199-6

Han, Y., Xu, P., Wang, Y., Zhao, W., Zhang, J., Zhang, S., Wang, J., Jin, Q., & Wu, Z. (2023). Panoramic analysis of coronaviruses carried by representative bat species in Southern China to better understand the coronavirus sphere. *Nature Communications*, *14*(1), 5537. https://doi.org/10.1038/s41467-023-41264-z

Hansen, C. H., Moustsen-Helms, I. R., Rasmussen, M., Søborg, B., Ullum, H., & Valentiner-Branth, P. (2024). Short-term effectiveness of the XBB.1.5 updated COVID-19 vaccine against hospitalisation in Denmark: a national cohort study. *The Lancet Infectious Diseases*, *24*(2), e73–e74. https://doi.org/10.1016/S1473-3099(23)00746-6

Hansson, M., Nygren, P., & Sta˚hl, S. (2000). Design and production of recombinant subunit vaccines. *Biotechnology and Applied Biochemistry*, *32*(2), 95–107. https://doi.org/10.1042/BA20000034

Harding, A., & Heaton, N. (2018). Efforts to Improve the Seasonal Influenza Vaccine. *Vaccines*, *6*(2), 19. https://doi.org/10.3390/vaccines6020019

Hariharan, V., & Kane, R. S. (2020). Glycosylation as a tool for rational vaccine design. *Biotechnology and Bioengineering*, *117*(8), 2556–2570. https://doi.org/10.1002/bit.27361

Harris, C. R., Millman, K. J., van der Walt, S. J., Gommers, R., Virtanen, P., Cournapeau, D., Wieser, E., Taylor, J., Berg, S., Smith, N. J., Kern, R., Picus, M., Hoyer, S., van Kerkwijk, M. H., Brett, M., Haldane, A., del Río, J. F., Wiebe, M., Peterson, P., …

Oliphant, T. E. (2020). Array programming with NumPy. *Nature*, *585*(7825), 357–362. https://doi.org/10.1038/s41586-020-2649-2

Harris, J. M., & Chess, R. B. (2003). Effect of pegylation on pharmaceuticals. *Nature Reviews Drug Discovery*, *2*(3), 214–221. https://doi.org/10.1038/nrd1033

Hartman, H., Wang, Y., Schroeder, H. W., & Cui, X. (2018). Absorbance summation: A novel approach for analyzing high-throughput ELISA data in the absence of a standard. *PLOS ONE*, *13*(6), e0198528. https://doi.org/10.1371/journal.pone.0198528

Hartwell, B. L., Melo, M. B., Xiao, P., Lemnios, A. A., Li, N., Chang, J. Y. H., Yu, J., Gebre, M. S., Chang, A., Maiorino, L., Carter, C., Moyer, T. J., Dalvie, N. C., Rodriguez-Aponte, S. A., Rodrigues, K. A., Silva, M., Suh, H., Adams, J., Fontenot, J., … Irvine, D. J. (2022). Intranasal vaccination with lipid-conjugated immunogens promotes antigen transmucosal uptake to drive mucosal and systemic immunity. *Science Translational Medicine*, *14*(654), eabn1413. https://doi.org/10.1126/scitranslmed.abn1413

Haynes, B. F., Burton, D. R., & Mascola, J. R. (2019). Multiple roles for HIV broadly neutralizing antibodies. *Science Translational Medicine*, *11*(516), eaaz2686. https://doi.org/10.1126/scitranslmed.aaz2686

Haynes, B. F., Wiehe, K., Borrow, P., Saunders, K. O., Korber, B., Wagh, K., McMichael, A. J., Kelsoe, G., Hahn, B. H., Alt, F., & Shaw, G. M. (2023). Strategies for HIV-1 vaccines that induce broadly neutralizing antibodies. *Nature Reviews Immunology*, *23*(3), 142–158. https://doi.org/10.1038/s41577-022-00753-w

He, B., Chai, G., Duan, Y., Yan, Z., Qiu, L., Zhang, H., Liu, Z., He, Q., Han, K., Ru, B., Guo, F.-B., Ding, H., Lin, H., Wang, X., Rao, N., Zhou, P., & Huang, J. (2016). BDB: biopanning data bank. *Nucleic Acids Research*, *44*(D1), D1127–D1132. https://doi.org/10.1093/nar/gkv1100

He, W. ting, Musharrafieh, R., Song, G., Dueker, K., Tse, L. V., Martinez, D. R., Schäfer, A., Callaghan, S., Yong, P., Beutler, N., Torres, J. L., Volk, R. M., Zhou, P., Yuan, M., Liu, H., Anzanello, F., Capozzola, T., Parren, M., Garcia, E., … Andrabi, R. (2022). Targeted isolation of diverse human protective broadly neutralizing antibodies against SARS-like viruses. *Nature Immunology 2022 23:6*, *23*(6), 960–970. https://doi.org/10.1038/s41590-022-01222-1

Heath, P. T., Galiza, E. P., Baxter, D. N., Boffito, M., Browne, D., Burns, F., Chadwick, D. R., Clark, R., Cosgrove, C., Galloway, J., Goodman, A. L., Heer, A., Higham, A., Iyengar, S., Jamal, A., Jeanes, C., Kalra, P. A., Kyriakidou, C., McAuley, D. F., … Toback, S. (2021). Safety and Efficacy of NVX-CoV2373 Covid-19 Vaccine. *New England Journal of Medicine*, *385*(13), 1172–1183. https://doi.org/10.1056/NEJMoa2107659

Heddle, J. G., Chakraborti, S., & Iwasaki, K. (2017). Natural and artificial protein cages: design, structure and therapeutic applications. *Current Opinion in Structural Biology*, *43*, 148–155. https://doi.org/10.1016/j.sbi.2017.03.007

Heikkinen, T., Ikonen, N., & Ziegler, T. (2014). Impact of Influenza B Lineage-Level Mismatch Between Trivalent Seasonal Influenza Vaccines and Circulating Viruses, 1999–2012. *Clinical Infectious Diseases*, *59*(11), 1519–1524. https://doi.org/10.1093/cid/ciu664

Henderson, D. A. (1987). Principles and lessons from the smallpox eradication programme. *Bulletin of the World Health Organization*, *65*(4), 535–546.

Henderson, D. A. (2011). The eradication of smallpox – An overview of the past, present, and future. *Vaccine*, *29*, D7–D9. https://doi.org/10.1016/j.vaccine.2011.06.080

Hernández-Bernal, F., Ricardo-Cobas, M. C., Martín-Bauta, Y., Rodríguez-Martínez, E., Urrutia-Pérez, K., Urrutia-Pérez, K., Quintana-Guerra, J., Navarro-Rodríguez, Z., Piñera-Martínez, M., Rodríguez-Reinoso, J. L., Chávez-Chong, C. O., Baladrón-Castrillo, I., Melo-Suárez, G., Batista-Izquierdo, A., Pupo-Micó, A., Mora-Betancourt, R., Bizet-Almeida, J., Martínez-Rodríguez, M. C., Lobaina-Lambert, L., … Muzio-González, V. L. (2023). A phase 3, randomised, double-blind, placebo-controlled clinical trial evaluation of the efficacy and safety of a SARS-CoV-2 recombinant spike RBD protein vaccine in adults (ABDALA-3 study). *The Lancet Regional Health - Americas*, *21*, 100497. https://doi.org/10.1016/j.lana.2023.100497

Hervé, C., Laupèze, B., Del Giudice, G., Didierlaurent, A. M., & Tavares Da Silva, F. (2019). The how's and what's of vaccine reactogenicity. *Npj Vaccines*, *4*(1), 39. https://doi.org/10.1038/s41541-019-0132-6

Hills, R. A., Tan, T. K., Cohen, A. A., Keeffe, J. R., Keeble, A. H., Gnanapragasam, P. N. P., Storm, K. N., Rorick, A. V., West, A. P., Hill, M. L., Liu, S., Gilbert-Jaramillo, J., Afzal, M., Napier, A., Admans, G., James, W. S., Bjorkman, P. J., Townsend, A. R., & Howarth, M. R. (2024). Proactive vaccination using multiviral Quartet Nanocages to elicit broad anti-coronavirus responses. *Nature Nanotechnology*. https://doi.org/10.1038/s41565-024-01655-9

Hioe, C. E., Visciano, M. L., Kumar, R., Liu, J., Mack, E. A., Simon, R. E., Levy, D. N., & Tuen, M. (2009). The use of immune complex vaccines to enhance antibody responses against neutralizing epitopes on HIV-1 envelope gp120. *Vaccine*, *28*(2), 352–360. https://doi.org/10.1016/j.vaccine.2009.10.040

Hoffmann, M. A. G., Yang, Z., Huey-Tubman, K. E., Cohen, A. A., Gnanapragasam, P. N. P., Nakatomi, L. M., Storm, K. N., Moon, W. J., Lin, P. J. C., West, A. P., & Bjorkman, P. J. (2023). ESCRT recruitment to SARS-CoV-2 spike induces virus-like particles that improve mRNA vaccines. *Cell*, *186*(11), 2380-2391.e9. https://doi.org/10.1016/j.cell.2023.04.024

Holshue, M. L., DeBolt, C., Lindquist, S., Lofy, K. H., Wiesman, J., Bruce, H., Spitters, C., Ericson, K., Wilkerson, S., Tural, A., Diaz, G., Cohn, A., Fox, L., Patel, A., Gerber, S. I., Kim, L., Tong, S., Lu, X., Lindstrom, S., … Pillai, S. K. (2020). First Case of 2019

Novel Coronavirus in the United States. *New England Journal of Medicine*, *382*(10), 929–936. https://doi.org/10.1056/NEJMoa2001191

Hoover, D. M. (2002). DNAWorks: an automated method for designing oligonucleotides for PCR-based gene synthesis. *Nucleic Acids Research*, *30*(10), 43e–443. https://doi.org/10.1093/nar/30.10.e43

Hotez, P. J., & Bottazzi, M. E. (2022). Whole Inactivated Virus and Protein-Based COVID-19 Vaccines. *Annual Review of Medicine*, *73*(1), 55–64. https://doi.org/10.1146/annurev-med-042420-113212

Hsia, Y., Bale, J. B., Gonen, S., Shi, D., Sheffler, W., Fong, K. K., Nattermann, U., Xu, C., Huang, P. S., Ravichandran, R., Yi, S., Davis, T. N., Gonen, T., King, N. P., & Baker, D. (2016). Design of a hyperstable 60-subunit protein icosahedron. *Nature*, *535*(7610), 136–139. https://doi.org/10.1038/nature18010

Hu, B., Zeng, L. P., Yang, X. Lou, Ge, X. Y., Zhang, W., Li, B., Xie, J. Z., Shen, X. R., Zhang, Y. Z., Wang, N., Luo, D. S., Zheng, X. S., Wang, M. N., Daszak, P., Wang, L. F., Cui, J., & Shi, Z. L. (2017a). Discovery of a rich gene pool of bat SARS-related coronaviruses provides new insights into the origin of SARS coronavirus. *PLoS Pathogens*, *13*(11). https://doi.org/10.1371/journal.ppat.1006698

Hu, B., Zeng, L. P., Yang, X. Lou, Ge, X. Y., Zhang, W., Li, B., Xie, J. Z., Shen, X. R., Zhang, Y. Z., Wang, N., Luo, D. S., Zheng, X. S., Wang, M. N., Daszak, P., Wang, L. F., Cui, J., & Shi, Z. L. (2017b). Discovery of a rich gene pool of bat SARS-related coronaviruses provides new insights into the origin of SARS coronavirus. *PLoS Pathogens*, *13*(11), e1006698. https://doi.org/10.1371/journal.ppat.1006698

Huang, C. Q., Vishwanath, S., Carnell, G. W., Chan, A. C. Y., & Heeney, J. L. (2023). Immune imprinting and next-generation coronavirus vaccines. *Nature Microbiology*, *8*(11), 1971–1985. https://doi.org/10.1038/s41564-023-01505-9

Huang, C., Wang, Y., Li, X., Ren, L., Zhao, J., Hu, Y., Zhang, L., Fan, G., Xu, J., Gu, X., Cheng, Z., Yu, T., Xia, J., Wei, Y., Wu, W., Xie, X., Yin, W., Li, H., Liu, M., … Cao, B. (2020). Clinical features of patients infected with 2019 novel coronavirus in Wuhan, China. *The Lancet*, *395*(10223), 497–506. https://doi.org/10.1016/S0140-6736(20)30183-5

Huang, J., Ru, B., Zhu, P., Nie, F., Yang, J., Wang, X., Dai, P., Lin, H., Guo, F.-B., & Rao, N. (2012). MimoDB 2.0: a mimotope database and beyond. *Nucleic Acids Research*, *40*(D1), D271–D277. https://doi.org/10.1093/nar/gkr922

Huang, K. Y. A., Chen, X., Mohapatra, A., Nguyen, H. T. V., Schimanski, L., Tan, T. K., Rijal, P., Vester, S. K., Hills, R. A., Howarth, M., Keeffe, J. R., Cohen, A. A., Kakutani, L. M., Wu, Y. M., Shahed-Al-Mahmud, M., Chou, Y. C., Bjorkman, P. J., Townsend, A. R., & Ma, C. (2023). Structural basis for a conserved neutralization epitope on the receptor-binding domain of SARS-CoV-2. *Nature Communications*, *14*(1), 311. https://doi.org/10.1038/s41467-023-35949-8

Huang, K. Y. A., Zhou, D., Tan, T. K., Chen, C., Duyvesteyn, H. M. E., Zhao, Y., Ginn, H. M., Qin, L., Rijal, P., Schimanski, L., Donat, R., Harding, A., Gilbert-Jaramillo, J., James, W., Tree, J. A., Buttigieg, K., Carroll, M., Charlton, S., Lien, C. E., … Stuart, D. I. (2022). Structures and therapeutic potential of anti-RBD human monoclonal antibodies against SARS-CoV-2. *Theranostics*, *27*(1), 1–17. https://doi.org/10.7150/THNO.65563

Huang, K.-Y. A., Tan, T. K., Chen, T.-H., Huang, C.-G., Harvey, R., Hussain, S., Chen, C.-P., Harding, A., Gilbert-Jaramillo, J., Liu, X., Knight, M., Schimanski, L., Shih, S.-R., Lin, Y.-C., Cheng, C.-Y., Cheng, S.-H., Huang, Y.-C., Lin, T.-Y., Jan, J.-T., … Townsend, A. R. (2021). Breadth and function of antibody response to acute SARS-CoV-2 infection in humans. *PLOS Pathogens*, *17*(2), e1009352. https://doi.org/10.1371/journal.ppat.1009352

Huang, Y., Yang, C., Xu, X., Xu, W., & Liu, S. (2020). Structural and functional properties of SARS-CoV-2 spike protein: potential antivirus drug development for COVID-19. *Acta Pharmacologica Sinica*, *41*(9), 1141–1149. https://doi.org/10.1038/s41401-020-0485-4

Huespe, I. A., Ferraris, A., Lalueza, A., Valdez, P. R., Peroni, M. L., Cayetti, L. A., Mirofsky, M. A., Boietti, B., Gómez-Huelgas, R., Casas-Rojo, J. M., Antón-Santos, J. M., Núñez-Cortés, J. M., Lumbreras, C., Ramos-Rincón, J., Barrio, N. G., Pedrera-Jiménez, M., Martin-Escalante, M. D., Ruiz, F. R., Onieva-García, M. Á., … Gómez-Varela, D. (2023). COVID-19 vaccines reduce mortality in hospitalized patients with oxygen requirements: Differences between vaccine subtypes. A multicontinental cohort study. *Journal of Medical Virology*, *95*(5), e28786. https://doi.org/10.1002/jmv.28786

Humbert, M. V., & Christodoulides, M. (2018). Immunization with recombinant truncated Neisseria meningitidis-Macrophage Infectivity Potentiator (rT-Nm-MIP) protein induces murine antibodies that are cross-reactive and bactericidal for Neisseria gonorrhoeae. *Vaccine*, *36*(27), 3926–3936. https://doi.org/10.1016/j.vaccine.2018.05.069

Hutchinson, G. B., Abiona, O. M., Ziwawo, C. T., Werner, A. P., Ellis, D., Tsybovsky, Y., Leist, S. R., Palandjian, C., West, A., Fritch, E. J., Wang, N., Wrapp, D., Boyoglu-Barnum, S., Ueda, G., Baker, D., Kanekiyo, M., McLellan, J. S., Baric, R. S., King, N. P., … Corbett-Helaire, K. S. (2023). Nanoparticle display of prefusion coronavirus spike elicits S1-focused cross-reactive antibody response against diverse coronavirus subgenera. *Nature Communications*, *14*(1), 6195. https://doi.org/10.1038/s41467-023-41661-4

Imai, N., Gaythorpe, K. A. M., Bhatia, S., Mangal, T. D., Cuomo-Dannenburg, G., Unwin, H. J. T., Jauneikaite, E., & Ferguson, N. M. (2022). COVID-19 in Japan, January–March 2020: insights from the first three months of the epidemic. *BMC Infectious Diseases*, *22*(1), 493. https://doi.org/10.1186/s12879-022-07469-1

Impagliazzo, A., Milder, F., Kuipers, H., Wagner, M. V., Zhu, X., Hoffman, R. M. B., van Meersbergen, R., Huizingh, J., Wanningen, P., Verspuij, J., de Man, M., Ding, Z., Apetri, A., Kükrer, B., Sneekes-Vriese, E., Tomkiewicz, D., Laursen, N. S., Lee, P. S.,

Zakrzewska, A., … Radošević, K. (2015). A stable trimeric influenza hemagglutinin stem as a broadly protective immunogen. *Science*, *349*(6254), 1301–1306. https://doi.org/10.1126/science.aac7263

Isabel, S., Graña-Miraglia, L., Gutierrez, J. M., Bundalovic-Torma, C., Groves, H. E., Isabel, M. R., Eshaghi, A., Patel, S. N., Gubbay, J. B., Poutanen, T., Guttman, D. S., & Poutanen, S. M. (2020). Evolutionary and structural analyses of SARS-CoV-2 D614G spike protein mutation now documented worldwide. *Scientific Reports*, *10*(1), 14031. https://doi.org/10.1038/s41598-020-70827-z

Iserson, K. (2020). The Next Pandemic: Prepare for "Disease X." *Western Journal of Emergency Medicine*, *21*(4), 756–758. https://doi.org/10.5811/westjem.2020.5.48215

Islam, A., Ferdous, J., Islam, S., Sayeed, Md. A., Dutta Choudhury, S., Saha, O., Hassan, M. M., & Shirin, T. (2021). Evolutionary Dynamics and Epidemiology of Endemic and Emerging Coronaviruses in Humans, Domestic Animals, and Wildlife. *Viruses*, *13*(10), 1908. https://doi.org/10.3390/v13101908

Ithete, N. L., Stoffberg, S., Corman, V. M., Cottontail, V. M., Richards, L. R., Schoeman, M. C., Drosten, C., Drexler, J. F., & Preiser, W. (2013). Close Relative of Human Middle East Respiratory Syndrome Coronavirus in Bat, South Africa. *Emerging Infectious Diseases*, *19*(10), 1697–1699. https://doi.org/10.3201/eid1910.130946

Iván, J., Velhner, M., Ursu, K., German, P., Mató, T., Drén, C. N., & Mészáros, J. (2005). Delayed vaccine virus replication in chickens vaccinated subcutaneously with an immune complex infectious bursal disease vaccine: quantification of vaccine virus by real-time polymerase chain reaction. *Canadian Journal of Veterinary Research = Revue Canadienne de Recherche Veterinaire*, *69*(2), 135–142.

Iwasaki, A., & Omer, S. B. (2020). Why and How Vaccines Work. *Cell*, *183*(2), 290–295. https://doi.org/10.1016/j.cell.2020.09.040

Jackson, C. B., Farzan, M., Chen, B., & Choe, H. (2022). Mechanisms of SARS-CoV-2 entry into cells. *Nature Reviews Molecular Cell Biology*, *23*(1), 3–20. https://doi.org/10.1038/s41580-021-00418-x

Jackson, L. A., Anderson, E. J., Rouphael, N. G., Roberts, P. C., Makhene, M., Coler, R. N., McCullough, M. P., Chappell, J. D., Denison, M. R., Stevens, L. J., Pruijssers, A. J., McDermott, A., Flach, B., Doria-Rose, N. A., Corbett, K. S., Morabito, K. M., O'Dell, S., Schmidt, S. D., Swanson, P. A., … Beigel, J. H. (2020). An mRNA Vaccine against SARS-CoV-2 — Preliminary Report. *New England Journal of Medicine*, *383*(20), 1920–1931. https://doi.org/10.1056/NEJMoa2022483

Jahirul Islam, Md., Nawal Islam, N., Siddik Alom, Md., Kabir, M., & Halim, M. A. (2023). A review on structural, non-structural, and accessory proteins of SARS-CoV-2: Highlighting drug target sites. *Immunobiology*, *228*(1), 152302. https://doi.org/10.1016/j.imbio.2022.152302

Jalali, N., Brustad, H. K., Frigessi, A., MacDonald, E. A., Meijerink, H., Feruglio, S. L., Nygård, K. M., Rø, G., Madslien, E. H., & de Blasio, B. F. (2022). Increased household transmission and immune escape of the SARS-CoV-2 Omicron compared to Delta variants. *Nature Communications*, *13*(1), 5706. https://doi.org/10.1038/s41467-022-33233-9

Jeevanandam, J., Barhoum, A., Chan, Y. S., Dufresne, A., & Danquah, M. K. (2018). Review on nanoparticles and nanostructured materials: history, sources, toxicity and regulations. *Beilstein Journal of Nanotechnology*, *9*, 1050–1074. https://doi.org/10.3762/bjnano.9.98

Jette, C. A., Cohen, A. A., Gnanapragasam, P. N. P., Muecksch, F., Lee, Y. E., Huey-Tubman, K. E., Schmidt, F., Hatziioannou, T., Bieniasz, P. D., Nussenzweig, M. C., West, A. P., Keeffe, J. R., Bjorkman, P. J., & Barnes, C. O. (2021). Broad cross-reactivity across sarbecoviruses exhibited by a subset of COVID-19 donor-derived neutralizing antibodies. *Cell Reports*, *36*(13), 109760. https://doi.org/10.1016/j.celrep.2021.109760

Johansson, M. U., Frick, I. M., Nilsson, H., Kraulis, P. J., Hober, S., Jonasson, P., Linhult, M., Nygren, P. Å., Uhlén, M., Björck, L., Drakenberg, T., Forsén, S., & Wikström, M. (2002). Structure, specificity, and mode of interaction for bacterial albumin-binding modules. *Journal of Biological Chemistry*, *277*(10), 8114–8120. https://doi.org/10.1074/jbc.M109943200

Johnston, M. I., & Fauci, A. S. (2008). An HIV Vaccine — Challenges and Prospects. *New England Journal of Medicine*, *359*(9), 888–890. https://doi.org/10.1056/NEJMp0806162

Jonsson, A., Dogan, J., Herne, N., Abrahmsén, L., & Nygren, P. Å. (2008). Engineering of a femtomolar affinity binding protein to human serum albumin. *Protein Engineering, Design and Selection*, *21*(8), 515–527. https://doi.org/10.1093/protein/gzn028

Joyce, M. G., Chen, W.-H., Sankhala, R. S., Hajduczki, A., Thomas, P. V., Choe, M., Martinez, E. J., Chang, W. C., Peterson, C. E., Morrison, E. B., Smith, C., Chen, R. E., Ahmed, A., Wieczorek, L., Anderson, A., Case, J. B., Li, Y., Oertel, T., Rosado, L., … Modjarrad, K. (2021). SARS-CoV-2 ferritin nanoparticle vaccines elicit broad SARS coronavirus immunogenicity. *Cell Reports*, *37*(12), 110143. https://doi.org/10.1016/j.celrep.2021.110143

Ju, Y., Carreño, J. M., Simon, V., Dawson, K., Krammer, F., & Kent, S. J. (2023). Impact of anti-PEG antibodies induced by SARS-CoV-2 mRNA vaccines. *Nature Reviews Immunology*, *23*(3), 135–136. https://doi.org/10.1038/s41577-022-00825-x

Ju, Y., Lee, W. S., Pilkington, E. H., Kelly, H. G., Li, S., Selva, K. J., Wragg, K. M., Subbarao, K., Nguyen, T. H. O., Rowntree, L. C., Allen, L. F., Bond, K., Williamson, D. A., Truong, N. P., Plebanski, M., Kedzierska, K., Mahanty, S., Chung, A. W., Caruso, F., … Kent, S. J. (2022). Anti-PEG Antibodies Boosted in Humans by SARS-CoV-2 Lipid Nanoparticle mRNA Vaccine. *ACS Nano*, *16*(8), 11769–11780. https://doi.org/10.1021/acsnano.2c04543/asset/images/large/nn2c04543_0008.jpeg

Kaku, Y., Okumura, K., Padilla-Blanco, M., Kosugi, Y., Uriu, K., Hinay, A. A., Chen, L., Plianchaisuk, A., Kobiyama, K., Ishii, K. J., Zahradnik, J., Ito, J., & Sato, K. (2024). Virological characteristics of the SARS-CoV-2 JN.1 variant. *The Lancet Infectious Diseases*, *24*(2), e82. https://doi.org/10.1016/S1473-3099(23)00813-7

Kanekiyo, M., Joyce, M. G., Gillespie, R. A., Gallagher, J. R., Andrews, S. F., Yassine, H. M., Wheatley, A. K., Fisher, B. E., Ambrozak, D. R., Creanga, A., Leung, K., Yang, E. S., Boyoglu-Barnum, S., Georgiev, I. S., Tsybovsky, Y., Prabhakaran, M. S., Andersen, H., Kong, W. P., Baxa, U., … Graham, B. S. (2019). Mosaic nanoparticle display of diverse influenza virus hemagglutinins elicits broad B cell responses. *Nature Immunology*, *20*(3), 362–372. https://doi.org/10.1038/s41590-018-0305-x

Kang, Y.-F., Sun, C., Sun, J., Xie, C., Zhuang, Z., Xu, H.-Q., Liu, Z., Liu, Y.-H., Peng, S., Yuan, R.-Y., Zhao, J.-C., & Zeng, M.-S. (2022). Quadrivalent mosaic HexaPro-bearing nanoparticle vaccine protects against infection of SARS-CoV-2 variants. *Nature Communications*, *13*(1), 2674. https://doi.org/10.1038/s41467-022-30222-w

Keeble, A. H., Banerjee, A., Ferla, M. P., Reddington, S. C., Anuar, I. N. A. K., & Howarth, M. (2017). Evolving Accelerated Amidation by SpyTag/SpyCatcher to Analyze Membrane Dynamics. *Angewandte Chemie International Edition*, *56*(52), 16521–16525. https://doi.org/10.1002/anie.201707623

Keeble, A. H., & Howarth, M. (2020). Power to the protein: Enhancing and combining activities using the Spy toolbox. *Chemical Science*, *11*(28), 7281–7291. https://doi.org/10.1039/d0sc01878c

Keeble, A. H., Turkki, P., Stokes, S., Khairil Anuar, I. N. A., Rahikainen, R., Hytönen, V. P., & Howarth, M. (2019). Approaching infinite affinity through engineering of peptide–protein interaction. *Proceedings of the National Academy of Sciences*, *116*(52), 26523–26533. https://doi.org/10.1073/pnas.1909653116

Keeble, A. H., Yadav, V. K., Ferla, M. P., Bauer, C. C., Chuntharpursat-Bon, E., Huang, J., Bon, R. S., & Howarth, M. (2022). DogCatcher allows loop-friendly protein-protein ligation. *Cell Chemical Biology*, *29*(2), 339-350.e10. https://doi.org/10.1016/j.chembiol.2021.07.005

Keesing, F., & Ostfeld, R. S. (2021). Impacts of biodiversity and biodiversity loss on zoonotic diseases. *Proceedings of the National Academy of Sciences*, *118*(17), e2023540118. https://doi.org/10.1073/pnas.2023540118

Kelly, J. A., Woodside, M. T., & Dinman, J. D. (2021). Programmed −1 Ribosomal Frameshifting in coronaviruses: A therapeutic target. *Virology*, *554*, 75–82. https://doi.org/10.1016/j.virol.2020.12.010

Kesheh, M. M., Hosseini, P., Soltani, S., & Zandi, M. (2022). An overview on the seven pathogenic human coronaviruses. *Reviews in Medical Virology*, *32*(2), e2282. https://doi.org/10.1002/rmv.2282

Khailany, R. A., Safdar, M., & Ozaslan, M. (2020). Genomic characterization of a novel SARS-CoV-2. *Gene Reports*, *19*, 100682. https://doi.org/10.1016/j.genrep.2020.100682

Khairil Anuar, I. N. A., Banerjee, A., Keeble, A. H., Carella, A., Nikov, G. I., & Howarth, M. (2019). Spy&Go purification of SpyTag-proteins using pseudo-SpyCatcher to access an oligomerization toolbox. *Nature Communications 2019 10:1*, *10*(1), 1–13. https://doi.org/10.1038/s41467-019-09678-w

Khaledian, E., Ulusan, S., Erickson, J., Fawcett, S., Letko, M. C., & Broschat, S. L. (2022). Sequence determinants of human-cell entry identified in ACE2-independent bat sarbecoviruses: A combined laboratory and computational network science approach. *EBioMedicine*, *79*, 103990. https://doi.org/10.1016/j

Khan, F., Legler, P. M., Mease, R. M., Duncan, E. H., Bergmann-Leitner, E. S., & Angov, E. (2012). Histidine affinity tags affect MSP1 42 structural stability and immunodominance in mice. *Biotechnology Journal*, *7*(1), 133–147. https://doi.org/10.1002/biot.201100331

Khan, I., Saeed, K., & Khan, I. (2019). Nanoparticles: Properties, applications and toxicities. *Arabian Journal of Chemistry*, *12*(7), 908–931. https://doi.org/10.1016/j.arabjc.2017.05.011

Khoury, D. S., Cromer, D., Reynaldi, A., Schlub, T. E., Wheatley, A. K., Juno, J. A., Subbarao, K., Kent, S. J., Triccas, J. A., & Davenport, M. P. (2021). Neutralizing antibody levels are highly predictive of immune protection from symptomatic SARS-CoV-2 infection. *Nature Medicine*, *27*(7), 1205–1211. https://doi.org/10.1038/s41591-021-01377-8

Killerby, M. E., Biggs, H. M., Midgley, C. M., Gerber, S. I., & Watson, J. T. (2020). Middle East Respiratory Syndrome Coronavirus Transmission. *Emerging Infectious Diseases*, *26*(2), 191–198. https://doi.org/10.3201/eid2602.190697

Kim, K., Calabrese, P., Wang, S., Qin, C., Rao, Y., Feng, P., & Chen, X. S. (2022). The roles of APOBEC-mediated RNA editing in SARS-CoV-2 mutations, replication and fitness. *Scientific Reports*, *12*(1), 14972. https://doi.org/10.1038/s41598-022-19067-x

Klasse, P. J. (2014). Neutralization of Virus Infectivity by Antibodies: Old Problems in New Perspectives. *Advances in Biology*, *2014*, 1–24. https://doi.org/10.1155/2014/157895

Knittelfelder, R., Riemer, A. B., & Jensen-Jarolim, E. (2009). Mimotope vaccination – from allergy to cancer. *Expert Opinion on Biological Therapy*, *9*(4), 493–506. https://doi.org/10.1517/14712590902870386

Koch, T., Dahlke, C., Fathi, A., Kupke, A., Krähling, V., Okba, N. M. A., Halwe, S., Rohde, C., Eickmann, M., Volz, A., Hesterkamp, T., Jambrecina, A., Borregaard, S., Ly, M. L., Zinser, M. E., Bartels, E., Poetsch, J. S. H., Neumann, R., Fux, R., … Addo, M. M. (2020). Safety and immunogenicity of a modified vaccinia virus Ankara vector vaccine candidate for Middle East respiratory syndrome: an open-label, phase 1 trial. *The Lancet Infectious Diseases*, *20*(7), 827–838. https://doi.org/10.1016/S1473-3099(20)30248-6

Koho, T., Ihalainen, T. O., Stark, M., Uusi-Kerttula, H., Wieneke, R., Rahikainen, R., Blazevic, V., Marjomäki, V., Tampé, R., Kulomaa, M. S., & Hytönen, V. P. (2015). His-tagged norovirus-like particles: A versatile platform for cellular delivery and surface display. *European Journal of Pharmaceutics and Biopharmaceutics*, *96*, 22–31. https://doi.org/10.1016/j.ejpb.2015.07.002

Korber, B., Fischer, W. M., Gnanakaran, S., Yoon, H., Theiler, J., Abfalterer, W., Hengartner, N., Giorgi, E. E., Bhattacharya, T., Foley, B., Hastie, K. M., Parker, M. D., Partridge, D. G., Evans, C. M., Freeman, T. M., de Silva, T. I., McDanal, C., Perez, L. G., Tang, H., … Wyles, M. D. (2020). Tracking Changes in SARS-CoV-2 Spike: Evidence that D614G Increases Infectivity of the COVID-19 Virus. *Cell*, *182*(4), 812-827.e19. https://doi.org/10.1016/j.cell.2020.06.043

Kozma, G. T., Mészáros, T., Berényi, P., Facskó, R., Patkó, Z., Oláh, C. Z., Nagy, A., Fülöp, T. G., Glatter, K. A., Radovits, T., Merkely, B., & Szebeni, J. (2023). Role of anti-polyethylene glycol (PEG) antibodies in the allergic reactions to PEG-containing Covid-19 vaccines: Evidence for immunogenicity of PEG. *Vaccine*, *41*(31), 4561–4570. https://doi.org/10.1016/J.VACCINE.2023.06.009

Kozma, G. T., Shimizu, T., Ishida, T., & Szebeni, J. (2020). Anti-PEG antibodies: Properties, formation, testing and role in adverse immune reactions to PEGylated nano-biopharmaceuticals. *Advanced Drug Delivery Reviews*, *154*, 163–175. https://doi.org/10.1016/j.addr.2020.07.024

Kraft, J. C., Pham, M. N., Shehata, L., Brinkkemper, M., Boyoglu-Barnum, S., Sprouse, K. R., Walls, A. C., Cheng, S., Murphy, M., Pettie, D., Ahlrichs, M., Sydeman, C., Johnson, M., Blackstone, A., Ellis, D., Ravichandran, R., Fiala, B., Wrenn, S., Miranda, M., … King, N. P. (2022). Antigen- and scaffold-specific antibody responses to protein nanoparticle immunogens. *Cell Reports Medicine*, *3*(10), 100780. https://doi.org/10.1016/j.xcrm.2022.100780

Krammer, F. (2024). The role of vaccines in the COVID-19 pandemic: what have we learned? *Seminars in Immunopathology*, *45*(4–6), 451–468. https://doi.org/10.1007/s00281-023-00996-2

Laidlaw, B. J., & Ellebedy, A. H. (2022). The germinal centre B cell response to SARS-CoV-2. *Nature Reviews Immunology*, *22*(1), 7–18. https://doi.org/10.1038/s41577-021-00657-1

Lamers, M. M., & Haagmans, B. L. (2022). SARS-CoV-2 pathogenesis. *Nature Reviews Microbiology*, *20*(5), 270–284. https://doi.org/10.1038/s41579-022-00713-0

Lampinen, V., Gröhn, S., Soppela, S., Blazevic, V., Hytönen, V. P., & Hankaniemi, M. M. (2023). SpyTag/SpyCatcher display of influenza M2e peptide on norovirus-like particle provides stronger immunization than direct genetic fusion. *Frontiers in Cellular and Infection Microbiology*, *13*, 1216364. https://doi.org/10.3389/fcimb.2023.1216364

Lamson, D. T., Amokrane, F., Mohamed, N., Vu, M., Maurer, D. P., Ronsard, L., Lingwood, D., & Schmidt, A. G. (2023). A modular platform to display multiple hemagglutinin subtypes on a single immunogen. *BioRxiv*. https://doi.org/10.1101/2023.11.09.566478

Landais, E., & Moore, P. L. (2018). Development of broadly neutralizing antibodies in HIV-1 infected elite neutralizers. *Retrovirology*, *15*(1), 61. https://doi.org/10.1186/s12977-018-0443-0

Latzka, J., Gaier, S., Hofstetter, G., Balazs, N., Smole, U., Ferrone, S., Scheiner, O., Breiteneder, H., Pehamberger, H., & Wagner, S. (2011). Specificity of Mimotope-Induced Anti-High Molecular Weight-Melanoma Associated Antigen (HMW-MAA) Antibodies Does Not Ensure Biological Activity. *PLoS ONE*, *6*(5), e19383. https://doi.org/10.1371/journal.pone.0019383

Lau, S. K. P., Luk, H. K. H., Wong, A. C. P., Fan, R. Y. Y., Lam, C. S. F., Li, K. S. M., Ahmed, S. S., Chow, F. W. N., Cai, J.-P., Zhu, X., Chan, J. F. W., Lau, T. C. K., Cao, K., Li, M., Woo, P. C. Y., & Yuen, K.-Y. (2019). Identification of a Novel Betacoronavirus (Merbecovirus) in Amur Hedgehogs from China. *Viruses*, *11*(11), 980. https://doi.org/10.3390/v11110980

Lau, S. K. P., Zhang, L., Luk, H. K. H., Xiong, L., Peng, X., Li, K. S. M., He, X., Zhao, P. S. H., Fan, R. Y. Y., Wong, A. C. P., Ahmed, S. S., Cai, J. P., Chan, J. F. W., Sun, Y., Jin, D., Chen, H., Lau, T. C. K., Kok, R. K. H., Li, W., … Woo, P. C. Y. (2018). Receptor usage of a novel bat lineage C betacoronavirus reveals evolution of middle east respiratory syndrome-related coronavirus spike proteins for human dipeptidyl peptidase 4 binding. *Journal of Infectious Diseases*, *218*(2), 197–207. https://doi.org/10.1093/infdis/jiy018

Lavie, M., Hanoulle, X., & Dubuisson, J. (2018). Glycan Shielding and Modulation of Hepatitis C Virus Neutralizing Antibodies. *Frontiers in Immunology*, *9*, 910. https://doi.org/10.3389/fimmu.2018.00910

Laydon, D. J., Cauchemez, S., Hinsley, W. R., Bhatt, S., & Ferguson, N. M. (2023). Impact of proactive and reactive vaccination strategies for health-care workers against MERS-CoV: a mathematical modelling study. *The Lancet Global Health*, *11*(5), e759–e769. https://doi.org/10.1016/S2214-109X(23)00117-1

Lednicky, J. A., Tagliamonte, M. S., White, S. K., Elbadry, M. A., Alam, M. M., Stephenson, C. J., Bonny, T. S., Loeb, J. C., Telisma, T., Chavannes, S., Ostrov, D. A., Mavian, C., Beau De Rochars, V. M., Salemi, M., & Morris, J. G. (2021). Independent infections of porcine deltacoronavirus among Haitian children. *Nature*, *600*(7887), 133–137. https://doi.org/10.1038/s41586-021-04111-z

Lee, D. B., Kim, H., Jeong, J. H., Jang, U. S., Jang, Y., Roh, S., Jeon, H., Kim, E. J., Han, S. Y., Maeng, J. Y., Magez, S., Radwanska, M., Mun, J. Y., Jun, H. S., Lee, G., Song, M. S., Lee, H. R., Chung, M. S., Baek, Y. H., & Kim, K. H. (2023). Mosaic RBD nanoparticles induce intergenus cross-reactive antibodies and protect against SARS-CoV-2 challenge.

Proceedings of the National Academy of Sciences of the United States of America, *120*(4), e2208425120. https://doi.org/10.1073/pnas.2208425120

Letko, M., Marzi, A., & Munster, V. (2020). Functional assessment of cell entry and receptor usage for SARS-CoV-2 and other lineage B betacoronaviruses. *Nature Microbiology*, *5*(4), 562–569. https://doi.org/10.1038/s41564-020-0688-y

Letko, M., Miazgowicz, K., McMinn, R., Seifert, S. N., Sola, I., Enjuanes, L., Carmody, A., van Doremalen, N., & Munster, V. (2018). Adaptive Evolution of MERS-CoV to Species Variation in DPP4. *Cell Reports*, *24*(7), 1730–1737. https://doi.org/10.1016/j.celrep.2018.07.045

Letko, M., Seifert, S. N., Olival, K. J., Plowright, R. K., & Munster, V. J. (2020). Bat-borne virus diversity, spillover and emergence. *Nature Reviews Microbiology*, *18*(8), 461–471. https://doi.org/10.1038/s41579-020-0394-z

Letvin, N. L. (2005). Progress Toward an HIV Vaccine. *Annual Review of Medicine*, *56*(1), 213–223. https://doi.org/10.1146/annurev.med.54.101601.152349

Leung, N. Y. H., Wai, C. Y. Y., Chu, K. H., & Leung, P. S. C. (2019). Mimotope-based allergen-specific immunotherapy: ready for prime time? *Cellular & Molecular Immunology*, *16*(11), 890–891. https://doi.org/10.1038/s41423-019-0272-7

Levesque, D. L., Boyles, J. G., Downs, C. J., & Breit, A. M. (2021). High Body Temperature is an Unlikely Cause of High Viral Tolerance in Bats. *Journal of Wildlife Diseases*, *57*(1). https://doi.org/10.7589/JWD-D-20-00079

Lewitus, E., Bai, H., & Rolland, M. (2023). Design of a pan-betacoronavirus vaccine candidate through a phylogenetically informed approach. *Science Advances*, *9*(3), eabq4149. https://doi.org/10.1126/sciadv.abq4149

Li, G., Dong, B. X., Liu, Y. H., Li, C. J., & Zhang, L. P. (2013). Gene synthesis method based on overlap extension PCR and DNAWorks program. *Methods in Molecular Biology*, *1073*, 9–17. https://doi.org/10.1007/978-1-62703-625-2_2

Li, W., Shi, Z., Yu, M., Ren, W., Smith, C., Epstein, J. H., Wang, H., Crameri, G., Hu, Z., Zhang, H., Zhang, J., McEachern, J., Field, H., Daszak, P., Eaton, B. T., Zhang, S., & Wang, L.-F. (2005). Bats Are Natural Reservoirs of SARS-Like Coronaviruses. *Science*, *310*(5748), 676–679. https://doi.org/10.1126/science.1118391

Liang, Y., Zhang, J., Yuan, R. Y., Wang, M. Y., He, P., Su, J. G., Han, Z. B., Jin, Y. Q., Hou, J. W., Zhang, H., Zhang, X. F., Shao, S., Hou, Y. N., Liu, Z. M., Du, L. F., Shen, F. J., Zhou, W. M., Xu, K., Gao, R. Q., … Li, Q. M. (2022). Design of a mutation-integrated trimeric RBD with broad protection against SARS-CoV-2. *Cell Discovery*, *8*(1), 17. https://doi.org/10.1038/s41421-022-00383-5

Lin, B., Qing, X., Liao, J., & Zhuo, K. (2020). Role of Protein Glycosylation in Host-Pathogen Interaction. *Cells*, *9*(4), 1022. https://doi.org/10.3390/cells9041022

Lin, S.-C., Liu, W.-C., Jan, J.-T., & Wu, S.-C. (2014). Glycan Masking of Hemagglutinin for Adenovirus Vector and Recombinant Protein Immunizations Elicits Broadly Neutralizing Antibodies against H5N1 Avian Influenza Viruses. *PLoS ONE*, *9*(3), e92822. https://doi.org/10.1371/journal.pone.0092822

Liu, D. X., Liang, J. Q., & Fung, T. S. (2021). Human Coronavirus-229E, -OC43, -NL63, and -HKU1 (Coronaviridae). In *Encyclopedia of Virology* (pp. 428–440). Elsevier. https://doi.org/10.1016/B978-0-12-809633-8.21501-X

Liu, H., Moynihan, K. D., Zheng, Y., Szeto, G. L., Li, A. V., Huang, B., Van Egeren, D. S., Park, C., & Irvine, D. J. (2014). Structure-based programming of lymph-node targeting in molecular vaccines. *Nature*, *507*(7493), 519–522. https://doi.org/10.1038/nature12978

Liu, Y., Cao, W., Sun, M., & Li, T. (2020). Broadly neutralizing antibodies for HIV-1: efficacies, challenges and opportunities. *Emerging Microbes & Infections*, *9*(1), 194–206. https://doi.org/10.1080/22221751.2020.1713707

Llanes, A., Restrepo, C. M., Caballero, Z., Rajeev, S., Kennedy, M. A., & Lleonart, R. (2020). Betacoronavirus Genomes: How Genomic Information has been Used to Deal with Past Outbreaks and the COVID-19 Pandemic. *International Journal of Molecular Sciences*, *21*(12), 4546. https://doi.org/10.3390/ijms21124546

Logunov, D. Y., Dolzhikova, I. V, Shcheblyakov, D. V, Tukhvatulin, A. I., Zubkova, O. V, Dzharullaeva, A. S., Kovyrshina, A. V, Lubenets, N. L., Grousova, D. M., Erokhova, A. S., Botikov, A. G., Izhaeva, F. M., Popova, O., Ozharovskaya, T. A., Esmagambetov, I. B., Favorskaya, I. A., Zrelkin, D. I., Voronina, D. V, Shcherbinin, D. N., … Gintsburg, A. L. (2021). Safety and efficacy of an rAd26 and rAd5 vector-based heterologous prime-boost COVID-19 vaccine: an interim analysis of a randomised controlled phase 3 trial in Russia. *The Lancet*, *397*(10275), 671–681. https://doi.org/10.1016/S0140-6736(21)00234-8

Low, Z. Y., Zabidi, N. Z., Yip, A. J. W., Puniyamurti, A., Chow, V. T. K., & Lal, S. K. (2022). SARS-CoV-2 Non-Structural Proteins and Their Roles in Host Immune Evasion. *Viruses*, *14*(9), 1991. https://doi.org/10.3390/v14091991

Lu, L. L., Suscovich, T. J., Fortune, S. M., & Alter, G. (2018). Beyond binding: antibody effector functions in infectious diseases. *Nature Reviews Immunology*, *18*(1), 46–61. https://doi.org/10.1038/nri.2017.106

Lu, R., Zhao, X., Li, J., Niu, P., Yang, B., Wu, H., Wang, W., Song, H., Huang, B., Zhu, N., Bi, Y., Ma, X., Zhan, F., Wang, L., Hu, T., Zhou, H., Hu, Z., Zhou, W., Zhao, L., … Tan, W. (2020). Genomic characterisation and epidemiology of 2019 novel coronavirus: implications for virus origins and receptor binding. *The Lancet*, *395*(10224), 565–574. https://doi.org/10.1016/S0140-6736(20)30251-8

Luis, A. D., Hayman, D. T. S., O'Shea, T. J., Cryan, P. M., Gilbert, A. T., Pulliam, J. R. C., Mills, J. N., Timonin, M. E., Willis, C. K. R., Cunningham, A. A., Fooks, A. R., Rupprecht, C. E., Wood, J. L. N., & Webb, C. T. (2013). A comparison of bats and

rodents as reservoirs of zoonotic viruses: are bats special? *Proceedings of the Royal Society B: Biological Sciences*, *280*(1756), 20122753. https://doi.org/10.1098/rspb.2012.2753

Lythgoe, K. A., Hall, M., Ferretti, L., de Cesare, M., MacIntyre-Cockett, G., Trebes, A., Andersson, M., Otecko, N., Wise, E. L., Moore, N., Lynch, J., Kidd, S., Cortes, N., Mori, M., Williams, R., Vernet, G., Justice, A., Green, A., Nicholls, S. M., … Golubchik, T. (2021). SARS-CoV-2 within-host diversity and transmission. *Science*, *372*(6539), eabg0821. https://doi.org/10.1126/science.abg0821

Ma, C., Liu, C., Xiong, Q., Gu, M., Shi, L., Wang, C., Si, J., Tong, F., Liu, P., Huang, M., & Yan, H. (2023). Broad host tropism of ACE2-using MERS-related coronaviruses and determinants restricting viral recognition. *Cell Discovery*, *9*(1), 57. https://doi.org/10.1038/s41421-023-00566-8

Ma, Y., Zhao, S., Shen, S., Fang, S., Ye, Z., Shi, Z., & Hong, A. (2015). A novel recombinant slow-release TNF α-derived peptide effectively inhibits tumor growth and angiogensis. *Scientific Reports*, *5*(1), 13595. https://doi.org/10.1038/srep13595

Madeira, F., Park, Y. mi, Lee, J., Buso, N., Gur, T., Madhusoodanan, N., Basutkar, P., Tivey, A. R. N., Potter, S. C., Finn, R. D., & Lopez, R. (2019). The EMBL-EBI search and sequence analysis tools APIs in 2019. *Nucleic Acids Research*, *47*(W1), W636–W641. https://doi.org/10.1093/nar/gkz268

Mader, K., & Dustin, L. B. (2024). Beyond bNAbs: Uses, Risks, and Opportunities for Therapeutic Application of Non-Neutralising Antibodies in Viral Infection. *Antibodies*, *13*(2), 28. https://doi.org/10.3390/antib13020028

Mahomed, S., Garrett, N., Baxter, C., Abdool Karim, Q., & Abdool Karim, S. S. (2021). Clinical Trials of Broadly Neutralizing Monoclonal Antibodies for Human Immunodeficiency Virus Prevention: A Review. *The Journal of Infectious Diseases*, *223*(3), 370–380. https://doi.org/10.1093/infdis/jiaa377

Malik, S., Kishore, S., Nag, S., Dhasmana, A., Preetam, S., Mitra, O., León-Figueroa, D. A., Mohanty, A., Chattu, V. K., Assefi, M., Padhi, B. K., & Sah, R. (2023). Ebola Virus Disease Vaccines: Development, Current Perspectives & Challenges. *Vaccines*, *11*(2), 268. https://doi.org/10.3390/vaccines11020268

Mallajosyula, V. V. A., Citron, M., Ferrara, F., Lu, X., Callahan, C., Heidecker, G. J., Sarma, S. P., Flynn, J. A., Temperton, N. J., Liang, X., & Varadarajan, R. (2014). Influenza hemagglutinin stem-fragment immunogen elicits broadly neutralizing antibodies and confers heterologous protection. *Proceedings of the National Academy of Sciences*, *111*(25), E2514–E2523. https://doi.org/10.1073/pnas.1402766111

Mane Manohar, M. P., Lee, V. J., Chinedum Odunukwe, E. U., Singh, P. K., Mpofu, B. S., & Oxley, M. C. (2023). Advancements in Marburg (MARV) Virus Vaccine Research With Its Recent Reemergence in Equatorial Guinea and Tanzania: A Scoping Review. *Cureus*, *15*(7), e42014. https://doi.org/10.7759/cureus.42014

Marcandalli, J., Fiala, B., Ols, S., Perotti, M., de van der Schueren, W., Snijder, J., Hodge, E., Benhaim, M., Ravichandran, R., Carter, L., Sheffler, W., Brunner, L., Lawrenz, M., Dubois, P., Lanzavecchia, A., Sallusto, F., Lee, K. K., Veesler, D., Correnti, C. E., … King, N. P. (2019). Induction of Potent Neutralizing Antibody Responses by a Designed Protein Nanoparticle Vaccine for Respiratory Syncytial Virus. *Cell*, *176*(6), 1420-1431.e17. https://doi.org/10.1016/j.cell.2019.01.046

Marini, A., Zhou, Y., Li, Y., Taylor, I. J., Leneghan, D. B., Jin, J., Zaric, M., Mekhaiel, D., Long, C. A., Miura, K., & Biswas, S. (2019). A Universal Plug-and-Display Vaccine Carrier Based on HBsAg VLP to Maximize Effective Antibody Response. *Frontiers in Immunology*, *10*, 2931. https://doi.org/10.3389/fimmu.2019.02931

Markov, P. V., Ghafari, M., Beer, M., Lythgoe, K., Simmonds, P., Stilianakis, N. I., & Katzourakis, A. (2023). The evolution of SARS-CoV-2. *Nature Reviews Microbiology*, *21*(6), 361–379. https://doi.org/10.1038/s41579-023-00878-2

Martinez, D. R., Schäfer, A., Leist, S. R., De la Cruz, G., West, A., Atochina-Vasserman, E. N., Lindesmith, L. C., Pardi, N., Parks, R., Barr, M., Li, D., Yount, B., Saunders, K. O., Weissman, D., Haynes, B. F., Montgomery, S. A., & Baric, R. S. (2021). Chimeric spike mRNA vaccines protect against Sarbecovirus challenge in mice. *Science*, *373*(6558), 991–998. https://doi.org/10.1126/science.abi4506

Masters, P. S. (2006). *The Molecular Biology of Coronaviruses* (pp. 193–292). https://doi.org/10.1016/S0065-3527(06)66005-3

Mateu, M. G. (2011). Virus engineering: functionalization and stabilization. *Protein Engineering Design and Selection*, *24*(1–2), 53–63. https://doi.org/10.1093/protein/gzq069

Mathieu, E., Ritchie, H., Ortiz-Ospina, E., Roser, M., Hasell, J., Appel, C., Giattino, C., & Rodés-Guirao, L. (2021). A global database of COVID-19 vaccinations. *Nature Human Behaviour*, *5*(7), 947–953. https://doi.org/10.1038/s41562-021-01122-8

Medeiros-Silva, J., Dregni, A. J., Somberg, N. H., Duan, P., & Hong, M. (2023). Atomic structure of the open SARS-CoV-2 E viroporin. *Science Advances*, *9*(41), eadi9007. https://doi.org/10.1126/sciadv.adi9007

Mehand, M. S., Al-Shorbaji, F., Millett, P., & Murgue, B. (2018). The WHO R&D Blueprint: 2018 review of emerging infectious diseases requiring urgent research and development efforts. *Antiviral Research*, *159*, 63–67. https://doi.org/10.1016/j.antiviral.2018.09.009

Mei, X., Qin, P., Yang, Y., Liao, M., Liang, Q., Zhao, Z., Shi, F., Wang, B., & Huang, Y. (2022). First evidence that an emerging mammalian alphacoronavirus is able to infect an avian species. *Transboundary and Emerging Diseases*, *69*(5), e2006–e2019. https://doi.org/10.1111/tbed.14535

Memish, Z. A., Al-Tawfiq, J. A., Makhdoom, H. Q., Al-Rabeeah, A. A., Assiri, A., Alhakeem, R. F., AlRabiah, F. A., Al Hajjar, S., Albarrak, A., Flemban, H., Balkhy, H., Barry, M.,

Alhassan, S., Alsubaie, S., & Zumla, A. (2014). Screening for Middle East respiratory syndrome coronavirus infection in hospital patients and their healthcare worker and family contacts: a prospective descriptive study. *Clinical Microbiology and Infection*, *20*(5), 469–474. https://doi.org/10.1111/1469-0691.12562

Memish, Z. A., Perlman, S., Van Kerkhove, M. D., & Zumla, A. (2020). Middle East respiratory syndrome. In *The Lancet* (Vol. 395, Issue 10229, pp. 1063–1077). Lancet Publishing Group. https://doi.org/10.1016/S0140-6736(19)33221-0

Menachery, V. D., Graham, R. L., & Baric, R. S. (2017). Jumping species—a mechanism for coronavirus persistence and survival. *Current Opinion in Virology*, *23*, 1–7. https://doi.org/10.1016/j.coviro.2017.01.002

Menachery, V. D., Yount, B. L., Debbink, K., Agnihothram, S., Gralinski, L. E., Plante, J. A., Graham, R. L., Scobey, T., Ge, X. Y., Donaldson, E. F., Randell, S. H., Lanzavecchia, A., Marasco, W. A., Shi, Z. L., & Baric, R. S. (2015). A SARS-like cluster of circulating bat coronaviruses shows potential for human emergence. *Nature Medicine*, *21*(12), 1508–1513. https://doi.org/10.1038/nm.3985

Meng, B., Abdullahi, A., Ferreira, I. A. T. M., Goonawardane, N., Saito, A., Kimura, I., Yamasoba, D., Gerber, P. P., Fatihi, S., Rathore, S., Zepeda, S. K., Papa, G., Kemp, S. A., Ikeda, T., Toyoda, M., Tan, T. S., Kuramochi, J., Mitsunaga, S., Ueno, T., … Gupta, R. K. (2022). Altered TMPRSS2 usage by SARS-CoV-2 Omicron impacts infectivity and fusogenicity. *Nature*, *603*(7902), 706–714. https://doi.org/10.1038/s41586-022-04474-x

Merlot, A. M., Kalinowski, D. S., & Richardson, D. R. (2014). Unraveling the mysteries of serum albumin - more than just a serum protein. *Frontiers in Physiology*, *5*, 299. https://doi.org/10.3389/fphys.2014.00299

Mihindukulasuriya, K. A., Wu, G., St. Leger, J., Nordhausen, R. W., & Wang, D. (2008). Identification of a Novel Coronavirus from a Beluga Whale by Using a Panviral Microarray. *Journal of Virology*, *82*(10), 5084–5088. https://doi.org/10.1128/JVI.02722-07

Miller, N. E., Michel, C. C., Nanjee, M. N., Olszewski, W. L., Miller, I. P., Hazell, M., Olivecrona, G., Sutton, P., Humphreys, S. M., & Frayn, K. N. (2011). Secretion of adipokines by human adipose tissue in vivo: partitioning between capillary and lymphatic transport. *Am J Physiol Endocrinol Metab*, *301*, 659–667. https://doi.org/10.1152/ajpendo.00058.2011.-Peptides

Mitsi, E., Diniz, M. O., Reiné, J., Collins, A. M., Robinson, R. E., Hyder-Wright, A., Farrar, M., Liatsikos, K., Hamilton, J., Onyema, O., Urban, B. C., Solórzano, C., Belij-Rammerstorfer, S., Sheehan, E., Lambe, T., Draper, S. J., Weiskopf, D., Sette, A., Maini, M. K., & Ferreira, D. M. (2023). Respiratory mucosal immune memory to SARS-CoV-2 after infection and vaccination. *Nature Communications*, *14*(1), 6815. https://doi.org/10.1038/s41467-023-42433-w

Modjarrad, K., Roberts, C. C., Mills, K. T., Castellano, A. R., Paolino, K., Muthumani, K., Reuschel, E. L., Robb, M. L., Racine, T., Oh, M., Lamarre, C., Zaidi, F. I., Boyer, J., Kudchodkar, S. B., Jeong, M., Darden, J. M., Park, Y. K., Scott, P. T., Remigio, C., … Maslow, J. N. (2019). Safety and immunogenicity of an anti-Middle East respiratory syndrome coronavirus DNA vaccine: a phase 1, open-label, single-arm, dose-escalation trial. *The Lancet Infectious Diseases*, *19*(9), 1013–1022. https://doi.org/10.1016/S1473-3099(19)30266-X

Mohapatra, R. K., Mishra, S., Rabaan, A. A., Mohanty, A., & Sah, R. (2023a). Human-transmissible sarbecovirus 'Khosta-2' similar to SARS-CoV-2: potential global threat? *Annals of Medicine & Surgery*, *85*(4), 1327–1328. https://doi.org/10.1097/MS9.0000000000000486

Mohapatra, R. K., Mishra, S., Rabaan, A. A., Mohanty, A., & Sah, R. (2023b). Human-transmissible sarbecovirus 'Khosta-2' similar to SARS-CoV-2: potential global threat? *Annals of Medicine & Surgery*, *85*(4), 1327–1328. https://doi.org/10.1097/ms9.0000000000000486

Mohsen, M. O., & Bachmann, M. F. (2022). Virus-like particle vaccinology, from bench to bedside. *Cellular & Molecular Immunology*, *19*(9), 993–1011. https://doi.org/10.1038/s41423-022-00897-8

Moore, Z. S., Seward, J. F., & Lane, J. M. (2006). Smallpox. *The Lancet*, *367*(9508), 425–435. https://doi.org/10.1016/S0140-6736(06)68143-9

Moreno, A., Lelli, D., de Sabato, L., Zaccaria, G., Boni, A., Sozzi, E., Prosperi, A., Lavazza, A., Cella, E., Castrucci, M. R., Ciccozzi, M., & Vaccari, G. (2017). Detection and full genome characterization of two beta CoV viruses related to Middle East respiratory syndrome from bats in Italy. *Virology Journal*, *14*(1), 239. https://doi.org/10.1186/s12985-017-0907-1

Morens, D. M., & Fauci, A. S. (2020). Emerging Pandemic Diseases: How We Got to COVID-19. *Cell*, *182*(5), 1077–1092. https://doi.org/10.1016/j.cell.2020.08.021

Morens, D. M., Holmes, E. C., Davis, A. S., & Taubenberger, J. K. (2011). Global Rinderpest Eradication: Lessons Learned and Why Humans Should Celebrate Too. *The Journal of Infectious Diseases*, *204*(4), 502–505. https://doi.org/10.1093/infdis/jir327

Moseri, A., Sinha, E., Zommer, H., Arshava, B., Naider, F., & Anglister, J. (2017). Immunofocusing using conformationally constrained V3 peptide immunogens improves HIV-1 neutralization. *Vaccine*, *35*(2), 222–230. https://doi.org/10.1016/j.vaccine.2016.11.088

Moss, B., Yu, H., Resch, W., Belghith, A., & Hyatt, R. P. (2023). *WO2024049990 - Nanoparticle-Derived Vaccines Against Poxviruses, And Methods For Making And Using The Same*.

Moss, P. (2022). The T cell immune response against SARS-CoV-2. *Nature Immunology*, *23*(2), 186–193. https://doi.org/10.1038/s41590-021-01122-w

Moyer, T. J., Zmolek, A. C., & Irvine, D. J. (2016). Beyond antigens and adjuvants: Formulating future vaccines. *Journal of Clinical Investigation*, *126*(3), 799–808. https://doi.org/10.1172/JCI81083

Msemburi, W., Karlinsky, A., Knutson, V., Aleshin-Guendel, S., Chatterji, S., & Wakefield, J. (2023). The WHO estimates of excess mortality associated with the COVID-19 pandemic. *Nature*, *613*(7942), 130–137. https://doi.org/10.1038/s41586-022-05522-2

Muik, A., Reul, J., Friedel, T., Muth, A., Hartmann, K. P., Schneider, I. C., Münch, R. C., & Buchholz, C. J. (2017). Covalent coupling of high-affinity ligands to the surface of viral vector particles by protein trans-splicing mediates cell type-specific gene transfer. *Biomaterials*, *144*, 84–94. https://doi.org/10.1016/j.biomaterials.2017.07.032

Muylaert, R. L., Kingston, T., Luo, J., Vancine, M. H., Galli, N., Carlson, C. J., John, R. S., Rulli, M. C., & Hayman, D. T. S. (2022). Present and future distribution of bat hosts of sarbecoviruses: implications for conservation and public health. *Proceedings of the Royal Society B*, *289*, 20220397. https://doi.org/10.1098/RSPB.2022.0397

Nachbagauer, R., Feser, J., Naficy, A., Bernstein, D. I., Guptill, J., Walter, E. B., Berlanda-Scorza, F., Stadlbauer, D., Wilson, P. C., Aydillo, T., Behzadi, M. A., Bhavsar, D., Bliss, C., Capuano, C., Carreño, J. M., Chromikova, V., Claeys, C., Coughlan, L., Freyn, A. W., … Krammer, F. (2021). A chimeric hemagglutinin-based universal influenza virus vaccine approach induces broad and long-lasting immunity in a randomized, placebo-controlled phase I trial. *Nature Medicine*, *27*(1), 106–114. https://doi.org/10.1038/s41591-020-1118-7

Nardy, A. F. F. R., Freire-de-Lima, L., Freire-de-Lima, C. G., & Morrot, A. (2016). The Sweet Side of Immune Evasion: Role of Glycans in the Mechanisms of Cancer Progression. *Frontiers in Oncology*, *6*, 54. https://doi.org/10.3389/fonc.2016.00054

Ng, K. W., Faulkner, N., Finsterbusch, K., Wu, M., Harvey, R., Hussain, S., Greco, M., Liu, Y., Kjaer, S., Swanton, C., Gandhi, S., Beale, R., Gamblin, S. J., Cherepanov, P., McCauley, J., Daniels, R., Howell, M., Arase, H., Wack, A., … Kassiotis, G. (2022). SARS-CoV-2 S2–targeted vaccination elicits broadly neutralizing antibodies. *Science Translational Medicine*, *14*(655), eabn3715. https://doi.org/10.1126/scitranslmed.abn3715

Ober Shepherd, B. L., Scott, P. T., Hutter, J. N., Lee, C., McCauley, M. D., Guzman, I., Bryant, C., McGuire, S., Kennedy, J., Chen, W.-H., Hajduczki, A., Mdluli, T., Valencia-Ruiz, A., Amare, M. F., Matyas, G. R., Rao, M., Rolland, M., Mascola, J. R., De Rosa, S. C., … Gazi, M. (2024). SARS-CoV-2 recombinant spike ferritin nanoparticle vaccine adjuvanted with Army Liposome Formulation containing monophosphoryl lipid A and QS-21: a phase 1, randomised, double-blind, placebo-controlled, first-in-human clinical

trial. *The Lancet Microbe*, *5*(6), e581–e593. https://doi.org/10.1016/S2666-5247(23)00410-X

Olszewska, W., Obeid, O. E., & Steward, M. W. (2000). Protection against Measles Virus-Induced Encephalitis by Anti-mimotope Antibodies: The Role of Antibody Affinity. *Virology*, *272*(1), 98–105. https://doi.org/10.1006/viro.2000.0285

Oordt-Speets, A., Spinardi, J., Mendoza, C., Yang, J., Morales, G., McLaughlin, J. M., & Kyaw, M. H. (2023). Effectiveness of COVID-19 Vaccination on Transmission: A Systematic Review. *COVID*, *3*(10), 1516–1527. https://doi.org/10.3390/covid3100103

O'Rourke, J. P., Daly, S. M., Triplett, K. D., Peabody, D., Chackerian, B., & Hall, P. R. (2014). Development of a Mimotope Vaccine Targeting the Staphylococcus aureus Quorum Sensing Pathway. *PLoS ONE*, *9*(11), e111198. https://doi.org/10.1371/journal.pone.0111198

O'Shea, T. J., Cryan, P. M., Cunningham, A. A., Fooks, A. R., Hayman, D. T. S., Luis, A. D., Peel, A. J., Plowright, R. K., & Wood, J. L. N. (2014). Bat Flight and Zoonotic Viruses. *Emerging Infectious Diseases*, *20*(5), 741–745. https://doi.org/10.3201/eid2005.130539

Palamini, M., Canciani, A., & Forneris, F. (2016). Identifying and visualizing macromolecular flexibility in structural biology. *Frontiers in Molecular Biosciences*, *3*, 47. https://doi.org/10.3389/fmolb.2016.00047

Pallesen, J., Wang, N., Corbett, K. S., Wrapp, D., Kirchdoerfer, R. N., Turner, H. L., Cottrell, C. A., Becker, M. M., Wang, L., Shi, W., Kong, W.-P., Andres, E. L., Kettenbach, A. N., Denison, M. R., Chappell, J. D., Graham, B. S., Ward, A. B., & McLellan, J. S. (2017). Immunogenicity and structures of a rationally designed prefusion MERS-CoV spike antigen. *Proceedings of the National Academy of Sciences*, *114*(35), E7348–E7357. https://doi.org/10.1073/pnas.1707304114

Palm, A.-K. E., & Henry, C. (2019). Remembrance of Things Past: Long-Term B Cell Memory After Infection and Vaccination. *Frontiers in Immunology*, *10*, 1787. https://doi.org/10.3389/fimmu.2019.01787

Palma, M. (2023). Epitopes and Mimotopes Identification Using Phage Display for Vaccine Development against Infectious Pathogens. *Vaccines*, *11*(7), 1176. https://doi.org/10.3390/vaccines11071176

Panagioti, E., Klenerman, P., Lee, L. N., van der Burg, S. H., & Arens, R. (2018). Features of Effective T Cell-Inducing Vaccines against Chronic Viral Infections. *Frontiers in Immunology*, *9*, 276. https://doi.org/10.3389/fimmu.2018.00276

Pang, W., Lu, Y., Zhao, Y.-B., Shen, F., Fan, C.-F., Wang, Q., He, W.-Q., He, X.-Y., Li, Z.-K., Chen, T.-T., Yang, C.-X., Li, Y.-Z., Xiao, S.-X., Zhao, Z.-J., Huang, X.-S., Luo, R.-H., Yang, L.-M., Zhang, M., Dong, X.-Q., … Zheng, Y.-T. (2022). A variant-proof SARS-CoV-2 vaccine targeting HR1 domain in S2 subunit of spike protein. *Cell Research*, *32*(12), 1068–1085. https://doi.org/10.1038/s41422-022-00746-3

Parums, D. V. (2021). Editorial: Revised World Health Organization (WHO) Terminology for Variants of Concern and Variants of Interest of SARS-CoV-2. *Medical Science Monitor*, *27*, e933622. https://doi.org/10.12659/MSM.933622

Patel, K. G., & Swartz, J. R. (2011). Surface Functionalization of Virus-Like Particles by Direct Conjugation Using Azide−Alkyne Click Chemistry. *Bioconjugate Chemistry*, *22*(3), 376–387. https://doi.org/10.1021/bc100367u

Patel, P. N., Dickey, T. H., Hopp, C. S., Diouf, A., Tang, W. K., Long, C. A., Miura, K., Crompton, P. D., & Tolia, N. H. (2022). Neutralizing and interfering human antibodies define the structural and mechanistic basis for antigenic diversion. *Nature Communications*, *13*(1), 5888. https://doi.org/10.1038/s41467-022-33336-3

Peak, I. R., Srikhanta, Y. N., Weynants, V. E., Feron, C., Poolman, J. T., & Jennings, M. P. (2013). Evaluation of Truncated NhhA Protein as a Candidate Meningococcal Vaccine Antigen. *PLoS ONE*, *8*(9), e72003. https://doi.org/10.1371/journal.pone.0072003

Pekar, J. E., Magee, A., Parker, E., Moshiri, N., Izhikevich, K., Havens, J. L., Gangavarapu, K., Malpica Serrano, L. M., Crits-Christoph, A., Matteson, N. L., Zeller, M., Levy, J. I., Wang, J. C., Hughes, S., Lee, J., Park, H., Park, M.-S., Ching Zi Yan, K., Lin, R. T. P., … Wertheim, J. O. (2022). The molecular epidemiology of multiple zoonotic origins of SARS-CoV-2. *Science*, *377*(6609), 960–966. https://doi.org/10.1126/science.abp8337

Peng, L., Fang, Z., Renauer, P. A., McNamara, A., Park, J. J., Lin, Q., Zhou, X., Dong, M. B., Zhu, B., Zhao, H., Wilen, C. B., & Chen, S. (2022). Multiplexed LNP-mRNA vaccination against pathogenic coronavirus species. *Cell Reports*, *40*(5), 111160. https://doi.org/10.1016/j.celrep.2022.111160

Pilapitiya, D., Wheatley, A. K., & Tan, H.-X. (2023). Mucosal vaccines for SARS-CoV-2: triumph of hope over experience. *EBioMedicine*, *92*, 104585. https://doi.org/10.1016/j.ebiom.2023.104585

Pinto, D., Sauer, M. M., Czudnochowski, N., Low, J. S., Tortorici, M. A., Housley, M. P., Noack, J., Walls, A. C., Bowen, J. E., Guarino, B., Rosen, L. E., di Iulio, J., Jerak, J., Kaiser, H., Islam, S., Jaconi, S., Sprugasci, N., Culap, K., Abdelnabi, R., … Veesler, D. (2021). Broad betacoronavirus neutralization by a stem helix–specific human antibody. *Science*, *373*(6559), 1109–1116. https://doi.org/10.1126/science.abj3321

Pipes, L., Wang, H., Huelsenbeck, J. P., & Nielsen, R. (2021). Assessing Uncertainty in the Rooting of the SARS-CoV-2 Phylogeny. *Molecular Biology and Evolution*, *38*(4), 1537–1543. https://doi.org/10.1093/molbev/msaa316

Pitek, A. S., Jameson, S. A., Veliz, F. A., Shukla, S., & Steinmetz, N. F. (2016). Serum albumin ‘camouflage’ of plant virus based nanoparticles prevents their antibody recognition and enhances pharmacokinetics. *Biomaterials*, *89*, 89–97. https://doi.org/10.1016/j.biomaterials.2016.02.032

Pitek, A. S., Jameson, S. A., Veliz, F. A., Shukla, S., & Steinmetz, N. F. (2016). Serum Albumin “Camouflage” of Plant Virus Based Nanoparticles Prevents Their Antibody Recognition and Enhances Pharmacokinetics. *Biomaterials*, *89*, 89–97. https://doi.org/https://doi.org/10.1016/j.biomaterials.2016.02.032

Planas, D., Bruel, T., Staropoli, I., Guivel-Benhassine, F., Porrot, F., Maes, P., Grzelak, L., Prot, M., Mougari, S., Planchais, C., Puech, J., Saliba, M., Sahraoui, R., Fémy, F., Morel, N., Dufloo, J., Sanjuán, R., Mouquet, H., André, E., … Schwartz, O. (2023). Resistance of Omicron subvariants BA.2.75.2, BA.4.6, and BQ.1.1 to neutralizing antibodies. *Nature Communications*, *14*(1), 824. https://doi.org/10.1038/s41467-023-36561-6

Poh, C. M., Carissimo, G., Wang, B., Amrun, S. N., Lee, C. Y.-P., Chee, R. S.-L., Fong, S.-W., Yeo, N. K.-W., Lee, W.-H., Torres-Ruesta, A., Leo, Y.-S., Chen, M. I.-C., Tan, S.-Y., Chai, L. Y. A., Kalimuddin, S., Kheng, S. S. G., Thien, S.-Y., Young, B. E., Lye, D. C., … Ng, L. F. P. (2020). Two linear epitopes on the SARS-CoV-2 spike protein that elicit neutralising antibodies in COVID-19 patients. *Nature Communications*, *11*(1), 2806. https://doi.org/10.1038/s41467-020-16638-2

Polack, F. P., Thomas, S. J., Kitchin, N., Absalon, J., Gurtman, A., Lockhart, S., Perez, J. L., Pérez Marc, G., Moreira, E. D., Zerbini, C., Bailey, R., Swanson, K. A., Roychoudhury, S., Koury, K., Li, P., Kalina, W. V., Cooper, D., Frenck, R. W., Hammitt, L. L., … Gruber, W. C. (2020). Safety and Efficacy of the BNT162b2 mRNA Covid-19 Vaccine. *New England Journal of Medicine*, *383*(27), 2603–2615. https://doi.org/10.1056/NEJMoa2034577

Pollard, A. J., & Bijker, E. M. (2021). A guide to vaccinology: from basic principles to new developments. *Nature Reviews Immunology*, *21*(2), 83–100. https://doi.org/10.1038/s41577-020-00479-7

Powell, A. E., Zhang, K., Sanyal, M., Tang, S., Weidenbacher, P. A., Li, S., Pham, T. D., Pak, J. E., Chiu, W., & Kim, P. S. (2021). A Single Immunization with Spike-Functionalized Ferritin Vaccines Elicits Neutralizing Antibody Responses against SARS-CoV-2 in Mice. *ACS Central Science*, *7*(1), 183–199. https://doi.org/10.1021/acscentsci.0c01405

Puhach, O., Bellon, M., Adea, K., Bekliz, M., Hosszu-Fellous, K., Sattonnet, P., Hulo, N., Kaiser, L., Eckerle, I., & Meyer, B. (2023). SARS-CoV-2 convalescence and hybrid immunity elicits mucosal immune responses. *EBioMedicine*, *98*, 104893. https://doi.org/10.1016/j.ebiom.2023.104893

Qu, P., Faraone, J. N., Evans, J. P., Zheng, Y.-M., Carlin, C., Anghelina, M., Stevens, P., Fernandez, S., Jones, D., Panchal, A. R., Saif, L. J., Oltz, E. M., Zhang, B., Zhou, T., Xu, K., Gumina, R. J., & Liu, S.-L. (2023). Enhanced evasion of neutralizing antibody response by Omicron XBB.1.5, CH.1.1, and CA.3.1 variants. *Cell Reports*, *42*(5), 112443. https://doi.org/10.1016/j.celrep.2023.112443

Qu, P., Xu, K., Faraone, J. N., Goodarzi, N., Zheng, Y.-M., Carlin, C., Bednash, J. S., Horowitz, J. C., Mallampalli, R. K., Saif, L. J., Oltz, E. M., Jones, D., Gumina, R. J., & Liu, S.-L. (2024). Immune evasion, infectivity, and fusogenicity of SARS-CoV-2 BA.2.86 and FLip variants. *Cell*, *187*(3), 585-595.e6. https://doi.org/10.1016/j.cell.2023.12.026

Rabaan, A. A., Alenazy, M. F., Alshehri, A. A., Alshahrani, M. A., Al-Subaie, M. F., Alrasheed, H. A., Al Kaabi, N. A., Thakur, N., Bouafia, N. A., Alissa, M., Alsulaiman, A. M., AlBaadani, A. M., Alhani, H. M., Alhaddad, A. H., Alfouzan, W. A., Ali, B. M. A., Al-Abdulali, K. H., Khamis, F., Bayahya, A., … Dhawan, M. (2023). An updated review on pathogenic coronaviruses (CoVs) amid the emergence of SARS-CoV-2 variants: A look into the repercussions and possible solutions. *Journal of Infection and Public Health*, *16*(11), 1870–1883. https://doi.org/10.1016/j.jiph.2023.09.004

Rahikainen, R., Rijal, P., Tan, T. K., Wu, H. J., Andersson, A. M. C., Barrett, J. R., Bowden, T. A., Draper, S. J., Townsend, A. R., & Howarth, M. (2021). Overcoming Symmetry Mismatch in Vaccine Nanoassembly through Spontaneous Amidation. *Angewandte Chemie - International Edition*, *60*(1), 321–330. https://doi.org/10.1002/anie.202009663

Rahman, Md. O., Kamigaki, T., Thandar, M. M., Haruyama, R., Yan, F., Shibamura-Fujiogi, M., Khin Maung Soe, J., Islam, Md. R., Yoneoka, D., Miyahara, R., Ota, E., & Suzuki, M. (2023). Protection of the third-dose and fourth-dose mRNA vaccines against SARS-CoV-2 Omicron subvariant: a systematic review and meta-analysis. *BMJ Open*, *13*(12), e076892. https://doi.org/10.1136/bmjopen-2023-076892

Rahmani, K., Shavaleh, R., Forouhi, M., Disfani, H. F., Kamandi, M., Oskooi, R. K., Foogerdi, M., Soltani, M., Rahchamani, M., Mohaddespour, M., & Dianatinasab, M. (2022). The effectiveness of COVID-19 vaccines in reducing the incidence, hospitalization, and mortality from COVID-19: A systematic review and meta-analysis. *Frontiers in Public Health*, *10*, 873596. https://doi.org/10.3389/fpubh.2022.873596

Rakhra, K., Abraham, W., Wang, C., Moynihan, K. D., Li, N., Donahue, N., Baldeon, A. D., & Irvine, D. J. (2021). Exploiting albumin as a mucosal vaccine chaperone for robust generation of lung-resident memory T cells. *Science Immunology*, *6*(57), eabd8003. https://doi.org/10.1126/sciimmunol.abd8003

Ramadan, N., & Shaib, H. (2019). Middle East respiratory syndrome coronavirus (MERS-CoV): A review. *Germs*, *9*(1), 35–42. https://doi.org/10.18683/germs.2019.1155

Raran-Kurussi, S., Cherry, S., Zhang, D., & Waugh, D. S. (2017). Removal of affinity tags with TEV protease. In *Methods in Molecular Biology* (Vol. 1586, pp. 221–230). Humana Press Inc. https://doi.org/10.1007/978-1-4939-6887-9_14

Rawool, D. B., Bitsaktsis, C., Li, Y., Gosselin, D. R., Lin, Y., Kurkure, N. V., Metzger, D. W., & Gosselin, E. J. (2008). Utilization of Fc Receptors as a Mucosal Vaccine Strategy against an Intracellular Bacterium, Francisella tularensis. *The Journal of Immunology*, *180*(8), 5548–5557. https://doi.org/10.4049/jimmunol.180.8.5548

Recht, J., Schuenemann, V. J., & Sánchez-Villagra, M. R. (2020). Host Diversity and Origin of Zoonoses: The Ancient and the New. *Animals*, *10*(9), 1672. https://doi.org/10.3390/ani10091672

Redondo, N., Zaldívar-López, S., Garrido, J. J., & Montoya, M. (2021). SARS-CoV-2 Accessory Proteins in Viral Pathogenesis: Knowns and Unknowns. *Frontiers in Immunology*, *12*, 708264. https://doi.org/10.3389/fimmu.2021.708264

Regev-Yochay, G., Lustig, Y., Joseph, G., Gilboa, M., Barda, N., Gens, I., Indenbaum, V., Halpern, O., Katz-Likvornik, S., Levin, T., Kanaaneh, Y., Asraf, K., Amit, S., Rubin, C., Ziv, A., Koren, R., Mandelboim, M., Tokayer, N. H., Meltzer, L., … Kreiss, Y. (2023). Correlates of protection against COVID-19 infection and intensity of symptomatic disease in vaccinated individuals exposed to SARS-CoV-2 in households in Israel (ICoFS): a prospective cohort study. *The Lancet Microbe*, *4*(5), e309–e318. https://doi.org/10.1016/S2666-5247(23)00012-5

Reperant, L. A., Grenfell, B. T., & Osterhaus, A. D. M. E. (2015). Quantifying the risk of pandemic influenza virus evolution by mutation and re-assortment. *Vaccine*, *33*(49), 6955–6966. https://doi.org/10.1016/j.vaccine.2015.10.056

Richter, A. W., & Åkerblom, E. (1984). Polyethylene Glycol Reactive Antibodies in Man: Titer Distribution in Allergic Patients Treated with Monomethoxy Polyethylene Glycol Modified Allergens or Placebo, and in Healthy Blood Donors. *International Archives of Allergy and Immunology*, *74*(1), 36–39. https://doi.org/10.1159/000233512

Riemer, A. B., & Jensen-Jarolim, E. (2007). Mimotope vaccines: Epitope mimics induce anti-cancer antibodies. *Immunology Letters*, *113*(1), 1–5. https://doi.org/10.1016/j.imlet.2007.07.008

Riemer, A. B., Kurz, H., Klinger, M., Scheiner, O., Zielinski, C. C., & Jensen-Jarolim, E. (2005). Vaccination With Cetuximab Mimotopes and Biological Properties of Induced Anti–Epidermal Growth Factor Receptor Antibodies. *JNCI: Journal of the National Cancer Institute*, *97*(22), 1663–1670. https://doi.org/10.1093/jnci/dji373

Robbiani, D. F., Gaebler, C., Muecksch, F., Lorenzi, J. C. C., Wang, Z., Cho, A., Agudelo, M., Barnes, C. O., Gazumyan, A., Finkin, S., Hägglöf, T., Oliveira, T. Y., Viant, C., Hurley, A., Hoffmann, H.-H., Millard, K. G., Kost, R. G., Cipolla, M., Gordon, K., … Nussenzweig, M. C. (2020). Convergent antibody responses to SARS-CoV-2 in convalescent individuals. *Nature*, *584*(7821), 437–442. https://doi.org/10.1038/s41586-020-2456-9

Roberts, D. L., Rossman, J. S., & Jarić, I. (2021). Dating first cases of COVID-19. *PLOS Pathogens*, *17*(6), e1009620. https://doi.org/10.1371/journal.ppat.1009620

Roberts, M. J., Bentley, M. D., & Harris, J. M. (2002). Chemistry for peptide and protein PEGylation. *Advanced Drug Delivery Reviews*, *54*(4), 459–476. https://doi.org/10.1016/S0169-409X(02)00022-4

Rodrigues, C. M. C., & Plotkin, S. A. (2020). Impact of Vaccines; Health, Economic and Social Perspectives. *Frontiers in Microbiology*, *11*, 1526. https://doi.org/10.3389/fmicb.2020.01526

Roemer, C., Sheward, D. J., Hisner, R., Gueli, F., Sakaguchi, H., Frohberg, N., Schoenmakers, J., Sato, K., O'Toole, Á., Rambaut, A., Pybus, O. G., Ruis, C., Murrell, B., & Peacock, T. P. (2023). SARS-CoV-2 evolution in the Omicron era. *Nature Microbiology*, *8*(11), 1952–1959. https://doi.org/10.1038/s41564-023-01504-w

Ruan, L., & Zeng, G. (2008). SARS Epidemic: SARS Outbreaks in Inner-land of China. *Emerging Infections in Asia*, 75–96. https://doi.org/10.1007/978-0-387-75722-3_5

Russell, M. W., & Mestecky, J. (2022). Mucosal immunity: The missing link in comprehending SARS-CoV-2 infection and transmission. *Frontiers in Immunology*, *13*, 957107. https://doi.org/10.3389/fimmu.2022.957107

Sachs, J. D., Karim, S. S. A., Aknin, L., Allen, J., Brosbøl, K., Colombo, F., Barron, G. C., Espinosa, M. F., Gaspar, V., Gaviria, A., Haines, A., Hotez, P. J., Koundouri, P., Bascuñán, F. L., Lee, J. K., Pate, M. A., Ramos, G., Reddy, K. S., Serageldin, I., … Michie, S. (2022). The Lancet Commission on lessons for the future from the COVID-19 pandemic. *The Lancet*, *400*(10359), 1224–1280. https://doi.org/10.1016/S0140-6736(22)01585-9

Sánchez, C. A., Li, H., Phelps, K. L., Zambrana-Torrelio, C., Wang, L.-F., Zhou, P., Shi, Z.-L., Olival, K. J., & Daszak, P. (2022). A strategy to assess spillover risk of bat SARS-related coronaviruses in Southeast Asia. *Nature Communications*, *13*(1), 4380. https://doi.org/10.1038/s41467-022-31860-w

Sandini, S., La Valle, R., Deaglio, S., Malavasi, F., Cassone, A., & De Bernardis, F. (2011). A highly immunogenic recombinant and truncated protein of the secreted aspartic proteases family (rSap2t) of *Candida albicans* as a mucosal anticandidal vaccine. *FEMS Immunology & Medical Microbiology*, *62*(2), 215–224. https://doi.org/10.1111/j.1574-695X.2011.00802.x

Santos, R. A. S., Sampaio, W. O., Alzamora, A. C., Motta-Santos, D., Alenina, N., Bader, M., & Campagnole-Santos, M. J. (2018). The ACE2/Angiotensin-(1–7)/MAS Axis of the Renin-Angiotensin System: Focus on Angiotensin-(1–7). *Physiological Reviews*, *98*(1), 505–553. https://doi.org/10.1152/physrev.00023.2016

Saville, M., Cramer, J. P., Downham, M., Hacker, A., Lurie, N., Van der Veken, L., Whelan, M., & Hatchett, R. (2022). Delivering Pandemic Vaccines in 100 Days — What Will It Take? *New England Journal of Medicine*, *387*(2), e3. https://doi.org/10.1056/nejmp2202669

Schlapschy, M., Binder, U., Borger, C., Theobald, I., Wachinger, K., Kisling, S., Haller, D., & Skerra, A. (2013). PASylation: a biological alternative to PEGylation for extending the plasma half-life of pharmaceutically active proteins. *Protein Engineering Design and Selection*, *26*(8), 489–501. https://doi.org/10.1093/protein/gzt023

Schmidt, F., Weisblum, Y., Muecksch, F., Hoffmann, H.-H., Michailidis, E., Lorenzi, J., Mendoza, P., Rutkowska, M., Bednarski, E., Gaebler, C., Agudelo, M., Cho, A., Wang, Z., Gazumyan, A., Cipolla, M., Caskey, M., Robbiani, D., Nussenzweig, M., Rice, C., … Bieniasz, P. (2020). Measuring SARS-CoV-2 neutralizing antibody activity using pseudotyped and chimeric viruses. *Journal of Experimental Medicine*, *217*(11), e20201181.

Seifert, S. N., Bai, S., Fawcett, S., Norton, E. B., Zwezdaryk, K. J., Robinson, J., Gunn, B., & Letko, M. (2022). An ACE2-dependent Sarbecovirus in Russian bats is resistant to SARS-CoV-2 vaccines. *PLoS Pathogens*, *18*(9), e1010828. https://doi.org/10.1371/journal.ppat.1010828

Sesterhenn, F., Galloux, M., Vollers, S. S., Csepregi, L., Yang, C., Descamps, D., Bonet, J., Friedensohn, S., Gainza, P., Corthésy, P., Chen, M., Rosset, S., Rameix-Welti, M.-A., Éléouët, J.-F., Reddy, S. T., Graham, B. S., Riffault, S., & Correia, B. E. (2019). Boosting subdominant neutralizing antibody responses with a computationally designed epitope-focused immunogen. *PLOS Biology*, *17*(2), e3000164. https://doi.org/10.1371/journal.pbio.3000164

Shafaati, M., Saidijam, M., Soleimani, M., Hazrati, F., Mirzaei, R., Amirheidari, B., Tanzadehpanah, H., Karampoor, S., Kazemi, S., Yavari, B., Mahaki, H., Safaei, M., Rahbarizadeh, F., Samadi, P., & Ahmadyousefi, Y. (2022). A Brief Review on Dna Vaccines in the Era of COVID-19. *Future Virology*, *17*(1), 49–66. https://doi.org/10.2217/fvl-2021-0170

Shah, P., Mistry, J., Reche, P. A., Gatherer, D., & Flower, D. R. (2018). In silico design of Mycobacterium tuberculosis epitope ensemble vaccines. *Molecular Immunology*, *97*, 56–62. https://doi.org/10.1016/j.molimm.2018.03.007

Shapiro, S. Z. (2019). Lessons for general vaccinology research from attempts to develop an HIV vaccine. *Vaccine*, *37*(26), 3400–3408. https://doi.org/10.1016/j.vaccine.2019.04.005

Sharma, J. N., Pattadar, D. K., Mainali, B. P., & Zamborini, F. P. (2018). Size Determination of Metal Nanoparticles Based on Electrochemically Measured Surface-Area-to-Volume Ratios. *Analytical Chemistry*, *90*(15), 9308–9314. https://doi.org/10.1021/acs.analchem.8b01905

Shi, Z., & Hu, Z. (2008). A review of studies on animal reservoirs of the SARS coronavirus. *Virus Research*, *133*(1), 74–87. https://doi.org/10.1016/j.virusres.2007.03.012

Shin, H.-J., Franco, L. H., Nair, V. R., Collins, A. C., & Shiloh, M. U. (2017). A baculovirus-conjugated mimotope vaccine targeting Mycobacterium tuberculosis lipoarabinomannan. *PLOS ONE*, *12*(10), e0185945. https://doi.org/10.1371/journal.pone.0185945

Simpson, S., Kaufmann, M. C., Glozman, V., & Chakrabarti, A. (2020). Disease X: accelerating the development of medical countermeasures for the next pandemic. *The*

Lancet Infectious Diseases, *20*(5), e108–e115. https://doi.org/10.1016/S1473-3099(20)30123-7

Singh, M., Sori, H., Ahuja, R., Meena, J., Sehgal, D., & Panda, A. K. (2020). Effect of N-terminal poly histidine-tag on immunogenicity of Streptococcus pneumoniae surface protein SP0845. *International Journal of Biological Macromolecules*, *163*, 1240–1248. https://doi.org/10.1016/j.ijbiomac.2020.07.056

Singh, P., Anand, A., Rana, S., Kumar, A., Goel, P., Kumar, S., Gouda, K. C., & Singh, H. (2023). Impact of COVID-19 vaccination: a global perspective. *Frontiers in Public Health*, *11*, 1272961. https://doi.org/10.3389/fpubh.2023.1272961

Singh, S. K., Thrane, S., Janitzek, C. M., Nielsen, M. A., Theander, T. G., Theisen, M., Salanti, A., & Sander, A. F. (2017). Improving the malaria transmission-blocking activity of a Plasmodium falciparum 48/45 based vaccine antigen by SpyTag/SpyCatcher mediated virus-like display. *Vaccine*, *35*(30), 3726–3732. https://doi.org/10.1016/j.vaccine.2017.05.054

Skrabalak, S. E., Chen, J., Sun, Y., Lu, X., Au, L., Cobley, C. M., & Xia, Y. (2008). Gold Nanocages: Synthesis, Properties, and Applications. *Accounts of Chemical Research*, *41*(12), 1587–1595. https://doi.org/10.1021/ar800018v

Skwarczynski, M., & Toth, I. (2016). Peptide-based synthetic vaccines. *Chemical Science*, *7*(2), 842–854. https://doi.org/10.1039/c5sc03892h

Sok, D., Moldt, B., & Burton, D. R. (2013). SnapShot: Broadly Neutralizing Antibodies. *Cell*, *155*(3), 728-728.e1. https://doi.org/10.1016/j.cell.2013.10.009

Song, H.-D., Tu, C.-C., Zhang, G.-W., Wang, S.-Y., Zheng, K., Lei, L.-C., Chen, Q.-X., Gao, Y.-W., Zhou, H.-Q., Xiang, H., Zheng, H.-J., Chern, S.-W. W., Cheng, F., Pan, C.-M., Xuan, H., Chen, S.-J., Luo, H.-M., Zhou, D.-H., Liu, Y.-F., … Zhao, G.-P. (2005). Cross-host evolution of severe acute respiratory syndrome coronavirus in palm civet and human. *Proceedings of the National Academy of Sciences*, *102*(7), 2430–2435. https://doi.org/10.1073/pnas.0409608102

Song, J. Y., Choi, W. S., Heo, J. Y., Kim, E. J., Lee, J. S., Jung, D. S., Kim, S.-W., Park, K.-H., Eom, J. S., Jeong, S. J., Lee, J., Kwon, K. T., Choi, H. J., Sohn, J. W., Kim, Y. K., Yoo, B. W., Jang, I.-J., Capeding, M. Z., Roman, F., … Kang, S. G. (2023). Immunogenicity and safety of SARS-CoV-2 recombinant protein nanoparticle vaccine GBP510 adjuvanted with AS03: interim results of a randomised, active-controlled, observer-blinded, phase 3 trial. *EClinicalMedicine*, *64*, 102140. https://doi.org/10.1016/j.eclinm.2023.102140

Sparrow, E., Wood, J. G., Chadwick, C., Newall, A. T., Torvaldsen, S., Moen, A., & Torelli, G. (2021). Global production capacity of seasonal and pandemic influenza vaccines in 2019. *Vaccine*, *39*(3), 512–520. https://doi.org/10.1016/j.vaccine.2020.12.018

Spiteri, G., Fielding, J., Diercke, M., Campese, C., Enouf, V., Gaymard, A., Bella, A., Sognamiglio, P., Sierra Moros, M. J., Riutort, A. N., Demina, Y. V., Mahieu, R., Broas, M., Bengnér, M., Buda, S., Schilling, J., Filleul, L., Lepoutre, A., Saura, C., … Ciancio, B. C. (2020). First cases of coronavirus disease 2019 (COVID-19) in the WHO European Region, 24 January to 21 February 2020. *Eurosurveillance*, *25*(9), 2000178. https://doi.org/10.2807/1560-7917.ES.2020.25.9.2000178

Starr, T. N., Greaney, A. J., Hilton, S. K., Ellis, D., Crawford, K. H. D., Dingens, A. S., Navarro, M. J., Bowen, J. E., Tortorici, M. A., Walls, A. C., King, N. P., Veesler, D., & Bloom, J. D. (2020). Deep Mutational Scanning of SARS-CoV-2 Receptor Binding Domain Reveals Constraints on Folding and ACE2 Binding. *Cell*, *182*(5), 1295-1310.e20. https://doi.org/10.1016/j.cell.2020.08.012

Starr, T. N., Zepeda, S. K., Walls, A. C., Greaney, A. J., Alkhovsky, S., Veesler, D., & Bloom, J. D. (2022). ACE2 binding is an ancestral and evolvable trait of sarbecoviruses. *Nature 2022 603:7903*, *603*(7903), 913–918. https://doi.org/10.1038/s41586-022-04464-z

Sulis, G., Peebles, A., & Basta, N. E. (2023). Lassa fever vaccine candidates: A scoping review of vaccine clinical trials. *Tropical Medicine & International Health*, *28*(6), 420–431. https://doi.org/10.1111/tmi.13876

Sun, J., Zhuang, Z., Zheng, J., Li, K., Wong, R. L.-Y., Liu, D., Huang, J., He, J., Zhu, A., Zhao, J., Li, X., Xi, Y., Chen, R., Alshukairi, A. N., Chen, Z., Zhang, Z., Chen, C., Huang, X., Li, F., … Zhao, J. (2020). Generation of a Broadly Useful Model for COVID-19 Pathogenesis, Vaccination, and Treatment. *Cell*, *182*(3), 734-743.e5. https://doi.org/10.1016/j.cell.2020.06.010

Sun, X., Yi, C., Zhu, Y., Ding, L., Xia, S., Chen, X., Liu, M., Gu, C., Lu, X., Fu, Y., Chen, S., Zhang, T., Zhang, Y., Yang, Z., Ma, L., Gu, W., Hu, G., Du, S., Yan, R., … Sun, B. (2022). Neutralization mechanism of a human antibody with pan-coronavirus reactivity including SARS-CoV-2. *Nature Microbiology*, *7*(7), 1063–1074. https://doi.org/10.1038/s41564-022-01155-3

Tai, W., Chen, J., Zhao, G., Geng, Q., He, L., Chen, Y., Zhou, Y., Li, F., & Du, L. (2019). Rational Design of Zika Virus Subunit Vaccine with Enhanced Efficacy. *Journal of Virology*, *93*(17), e02187-18. https://doi.org/10.1128/JVI.02187-18

Tamura, K., Stecher, G., & Kumar, S. (2021). MEGA11: Molecular Evolutionary Genetics Analysis Version 11. *Molecular Biology and Evolution*, *38*(7), 3022–3027. https://doi.org/10.1093/molbev/msab120

Tamura, T., Ito, J., Uriu, K., Zahradnik, J., Kida, I., Anraku, Y., Nasser, H., Shofa, M., Oda, Y., Lytras, S., Nao, N., Itakura, Y., Deguchi, S., Suzuki, R., Wang, L., Begum, M. M., Kita, S., Yajima, H., Sasaki, J., … Sato, K. (2023). Virological characteristics of the SARS-CoV-2 XBB variant derived from recombination of two Omicron subvariants. *Nature Communications*, *14*(1), 2800. https://doi.org/10.1038/s41467-023-38435-3

Tan, C. C. S., van Dorp, L., & Balloux, F. (2024). The evolutionary drivers and correlates of viral host jumps. *Nature Ecology & Evolution*, *8*(5), 960–971. https://doi.org/10.1038/s41559-024-02353-4

Tan, C.-W., Chia, W.-N., Young, B. E., Zhu, F., Lim, B.-L., Sia, W.-R., Thein, T.-L., Chen, M. I.-C., Leo, Y.-S., Lye, D. C., & Wang, L.-F. (2021). Pan-Sarbecovirus Neutralizing Antibodies in BNT162b2-Immunized SARS-CoV-1 Survivors. *New England Journal of Medicine*, *385*(15), 1401–1406. https://doi.org/10.1056/nejmoa2108453

Tan, S. T., Kwan, A. T., Rodríguez-Barraquer, I., Singer, B. J., Park, H. J., Lewnard, J. A., Sears, D., & Lo, N. C. (2023). Infectiousness of SARS-CoV-2 breakthrough infections and reinfections during the Omicron wave. *Nature Medicine*, *29*(2), 358–365. https://doi.org/10.1038/s41591-022-02138-x

Tan, T. K., Rijal, P., Rahikainen, R., Keeble, A. H., Schimanski, L., Hussain, S., Harvey, R., Hayes, J. W. P., Edwards, J. C., McLean, R. K., Martini, V., Pedrera, M., Thakur, N., Conceicao, C., Dietrich, I., Shelton, H., Ludi, A., Wilsden, G., Browning, C., … Townsend, A. R. (2021). A COVID-19 vaccine candidate using SpyCatcher multimerization of the SARS-CoV-2 spike protein receptor-binding domain induces potent neutralising antibody responses. *Nature Communications*, *12*(1), 542. https://doi.org/10.1038/s41467-020-20654-7

Tang, G., Liu, Z., & Chen, D. (2022). Human coronaviruses: Origin, host and receptor. *Journal of Clinical Virology*, *155*, 105246. https://doi.org/10.1016/j.jcv.2022.105246

Tang, S., Xuan, B., Ye, X., Huang, Z., & Qian, Z. (2016). A Modular Vaccine Development Platform Based on Sortase-Mediated Site-Specific Tagging of Antigens onto Virus-Like Particles. *Scientific Reports*, *6*(1), 25741. https://doi.org/10.1038/srep25741

Tanriover, M. D., Doğanay, H. L., Akova, M., Güner, H. R., Azap, A., Akhan, S., Köse, Ş., Erdinç, F. Ş., Akalın, E. H., Tabak, Ö. F., Pullukçu, H., Batum, Ö., Şimşek Yavuz, S., Turhan, Ö., Yıldırmak, M. T., Köksal, İ., Taşova, Y., Korten, V., Yılmaz, G., … Aksu, K. (2021). Efficacy and safety of an inactivated whole-virion SARS-CoV-2 vaccine (CoronaVac): interim results of a double-blind, randomised, placebo-controlled, phase 3 trial in Turkey. *The Lancet*, *398*(10296), 213–222. https://doi.org/10.1016/S0140-6736(21)01429-X

Tao, H. yu, Wang, R. qi, Sheng, W. jin, & Zhen, Y. su. (2021). The development of human serum albumin-based drugs and relevant fusion proteins for cancer therapy. *International Journal of Biological Macromolecules*, *187*, 24–34. https://doi.org/10.1016/J.IJBIOMAC.2021.07.080

Tariq, H., Batool, S., Asif, S., Ali, M., & Abbasi, B. H. (2022). Virus-Like Particles: Revolutionary Platforms for Developing Vaccines Against Emerging Infectious Diseases. *Frontiers in Microbiology*, *12*, 790121. https://doi.org/10.3389/fmicb.2021.790121

Tarke, A., Zhang, Y., Methot, N., Narowski, T. M., Phillips, E., Mallal, S., Frazier, A., Filaci, G., Weiskopf, D., Dan, J. M., Premkumar, L., Scheuermann, R. H., Sette, A., & Grifoni, A. (2023). Targets and cross-reactivity of human T cell recognition of common cold coronaviruses. *Cell Reports. Medicine*, *4*(6), 101088. https://doi.org/10.1016/j.xcrm.2023.101088

Taubenberger, J. K., & Morens, D. M. (2010). Influenza: the once and future pandemic. *Public Health Reports (Washington, D.C. : 1974)*, *125 Suppl 3*(Suppl 3), 16–26.

Taylor, A. L., & Starr, T. N. (2023). Deep mutational scans of XBB.1.5 and BQ.1.1 reveal ongoing epistatic drift during SARS-CoV-2 evolution. *PLoS Pathogens*, *19*(12), e1011901. https://doi.org/10.1371/journal.ppat.1011901

Tegally, H., Wilkinson, E., Giovanetti, M., Iranzadeh, A., Fonseca, V., Giandhari, J., Doolabh, D., Pillay, S., San, E. J., Msomi, N., Mlisana, K., von Gottberg, A., Walaza, S., Allam, M., Ismail, A., Mohale, T., Glass, A. J., Engelbrecht, S., Van Zyl, G., … de Oliveira, T. (2021). Detection of a SARS-CoV-2 variant of concern in South Africa. *Nature*, *592*(7854), 438–443. https://doi.org/10.1038/s41586-021-03402-9

Temmam, S., Vongphayloth, K., Baquero, E., Munier, S., Bonomi, M., Regnault, B., Douangboubpha, B., Karami, Y., Chrétien, D., Sanamxay, D., Xayaphet, V., Paphaphanh, P., Lacoste, V., Somlor, S., Lakeomany, K., Phommavanh, N., Pérot, P., Dehan, O., Amara, F., … Eloit, M. (2022). Bat coronaviruses related to SARS-CoV-2 and infectious for human cells. *Nature*, *604*(7905), 330–336. https://doi.org/10.1038/s41586-022-04532-4

Ter Meulen, J., Van Den Brink, E. N., Poon, L. L. M., Marissen, W. E., Leung, C. S. W., Cox, F., Cheung, C. Y., Bakker, A. Q., Bogaards, J. A., Van Deventer, E., Preiser, W., Doerr, H. W., Chow, V. T., De Kruif, J., Peiris, J. S. M., & Goudsmit, J. (2006). Human monoclonal antibody combination against SARS coronavirus: Synergy and coverage of escape mutants. *PLoS Medicine*, *3*(7), 1071–1079. https://doi.org/10.1371/journal.pmed.0030237

Teufel, F., Almagro Armenteros, J. J., Johansen, A. R., Gíslason, M. H., Pihl, S. I., Tsirigos, K. D., Winther, O., Brunak, S., von Heijne, G., & Nielsen, H. (2022). SignalP 6.0 predicts all five types of signal peptides using protein language models. *Nature Biotechnology*, *40*(7), 1023–1025. https://doi.org/10.1038/s41587-021-01156-3

The Lancet. (2023). One Health: a call for ecological equity. *The Lancet*, *401*(10372), 169. https://doi.org/10.1016/S0140-6736(23)00090-9

Thomas, S. J., Moreira, E. D., Kitchin, N., Absalon, J., Gurtman, A., Lockhart, S., Perez, J. L., Pérez Marc, G., Polack, F. P., Zerbini, C., Bailey, R., Swanson, K. A., Xu, X., Roychoudhury, S., Koury, K., Bouguermouh, S., Kalina, W. V., Cooper, D., Frenck, R. W., … Jansen, K. U. (2021). Safety and Efficacy of the BNT162b2 mRNA Covid-19 Vaccine through 6 Months. *New England Journal of Medicine*, *385*(19), 1761–1773. https://doi.org/10.1056/NEJMoa2110345

Thrane, S., Janitzek, C. M., Agerbæk, M. Ø., Ditlev, S. B., Resende, M., Nielsen, M. A., Theander, T. G., Salanti, A., & Sander, A. F. (2015). A Novel Virus-Like Particle Based Vaccine Platform Displaying the Placental Malaria Antigen VAR2CSA. *PLOS ONE*, *10*(11), e0143071. https://doi.org/10.1371/journal.pone.0143071

Thrane, S., Janitzek, C. M., Matondo, S., Resende, M., Gustavsson, T., de Jongh, W. A., Clemmensen, S., Roeffen, W., van de Vegte-Bolmer, M., van Gemert, G. J., Sauerwein, R., Schiller, J. T., Nielsen, M. A., Theander, T. G., Salanti, A., & Sander, A. F. (2016). Bacterial superglue enables easy development of efficient virus-like particle based vaccines. *Journal of Nanobiotechnology*, *14*(1), 30. https://doi.org/10.1186/s12951-016-0181-1

Tian, J.-H., Patel, N., Haupt, R., Zhou, H., Weston, S., Hammond, H., Logue, J., Portnoff, A. D., Norton, J., Guebre-Xabier, M., Zhou, B., Jacobson, K., Maciejewski, S., Khatoon, R., Wisniewska, M., Moffitt, W., Kluepfel-Stahl, S., Ekechukwu, B., Papin, J., … Smith, G. (2021). SARS-CoV-2 spike glycoprotein vaccine candidate NVX-CoV2373 immunogenicity in baboons and protection in mice. *Nature Communications*, *12*(1), 372. https://doi.org/10.1038/s41467-020-20653-8

Tiwari, P., Kaila, P., & Guptasarma, P. (2019). Understanding anomalous mobility of proteins on SDS-PAGE with special reference to the highly acidic extracellular domains of human E- and N-cadherins. *Electrophoresis*, *40*(9), 1273–1281. https://doi.org/10.1002/elps.201800219

To, H., Someno, S., Nagai, S., Koyama, T., & Nagano, T. (2010). Immunization with Truncated Recombinant Protein SpaC of Erysipelothrix rhusiopathiae Strain 715 Serovar 18 Confers Protective Immunity against Challenge with Various Serovars. *Clinical and Vaccine Immunology*, *17*(12), 1991–1997. https://doi.org/10.1128/CVI.00213-10

Toledo-Romaní, M. E., García-Carmenate, M., Valenzuela-Silva, C., Baldoquín-Rodríguez, W., Martínez-Pérez, M., Rodríguez-González, M., Paredes-Moreno, B., Mendoza-Hernández, I., González-Mujica Romero, R., Samón-Tabio, O., Velazco-Villares, P., Bacallao-Castillo, J. P., Licea-Martín, E., Rodríguez-Ortega, M., Herrera-Marrero, N., Caballero-González, E., Egües-Torres, L., Duartes-González, R., García-Blanco, S., … Verez-Bencomo, V. (2023). Safety and efficacy of the two doses conjugated protein-based SOBERANA-02 COVID-19 vaccine and of a heterologous three-dose combination with SOBERANA-Plus: a double-blind, randomised, placebo-controlled phase 3 clinical trial. *The Lancet Regional Health - Americas*, *18*, 100423. https://doi.org/10.1016/j.lana.2022.100423

Tolentino, J. E., Lytras, S., Ito, J., & Sato, K. (2024). Recombination analysis on the receptor switching event of MERS-CoV and its close relatives: implications for the emergence of MERS-CoV. *Virology Journal*, *21*(1), 84. https://doi.org/10.1186/s12985-024-02358-2

Tortorici, M. A., Walls, A. C., Joshi, A., Park, Y.-J., Eguia, R. T., Miranda, M. C., Kepl, E., Dosey, A., Stevens-Ayers, T., Boeckh, M. J., Telenti, A., Lanzavecchia, A., King, N. P., Corti, D., Bloom, J. D., & Veesler, D. (2022). Structure, receptor recognition, and

antigenicity of the human coronavirus CCoV-HuPn-2018 spike glycoprotein. *Cell*, *185*(13), 2279-2291.e17. https://doi.org/10.1016/j.cell.2022.05.019

Travieso, T., Li, J., Mahesh, S., Mello, J. D. F. R. E., & Blasi, M. (2022). The use of viral vectors in vaccine development. *Npj Vaccines*, *7*(1), 75. https://doi.org/10.1038/s41541-022-00503-y

Tsouchnikas, G., Zlatkovic, J., Jarmer, J., Strauß, J., Vratskikh, O., Kundi, M., Stiasny, K., & Heinz, F. X. (2015). Immunization with Immune Complexes Modulates the Fine Specificity of Antibody Responses to a Flavivirus Antigen. *Journal of Virology*, *89*(15), 7970–7978. https://doi.org/10.1128/JVI.00938-15

Ueda, G., Antanasijevic, A., Fallas, J. A., Sheffler, W., Copps, J., Ellis, D., Hutchinson, G. B., Moyer, A., Yasmeen, A., Tsybovsky, Y., Park, Y.-J., Bick, M. J., Sankaran, B., Gillespie, R. A., Brouwer, P. J., Zwart, P. H., Veesler, D., Kanekiyo, M., Graham, B. S., … Baker, D. (2020). Tailored design of protein nanoparticle scaffolds for multivalent presentation of viral glycoprotein antigens. *ELife*, *9*, e57659. https://doi.org/10.7554/eLife.57659

Uraki, R., Ito, M., Furusawa, Y., Yamayoshi, S., Iwatsuki-Horimoto, K., Adachi, E., Saito, M., Koga, M., Tsutsumi, T., Yamamoto, S., Otani, A., Kiso, M., Sakai-Tagawa, Y., Ueki, H., Yotsuyanagi, H., Imai, M., & Kawaoka, Y. (2023). Humoral immune evasion of the omicron subvariants BQ.1.1 and XBB. *The Lancet Infectious Diseases*, *23*(1), 30–32. https://doi.org/10.1016/S1473-3099(22)00816-7

Uriu, K., Ito, J., Zahradnik, J., Fujita, S., Kosugi, Y., Schreiber, G., & Sato, K. (2023). Enhanced transmissibility, infectivity, and immune resistance of the SARS-CoV-2 omicron XBB.1.5 variant. *The Lancet Infectious Diseases*, *23*(3), 280–281. https://doi.org/10.1016/S1473-3099(23)00051-8

Valleron, A.-J., Cori, A., Valtat, S., Meurisse, S., Carrat, F., & Boëlle, P.-Y. (2010). Transmissibility and geographic spread of the 1889 influenza pandemic. *Proceedings of the National Academy of Sciences*, *107*(19), 8778–8781. https://doi.org/10.1073/pnas.1000886107

van Bergen, J., Camps, M. G. M., Pardieck, I. N., Veerkamp, D., Leung, W. Y., Leijs, A. A., Myeni, S. K., Kikkert, M., Arens, R., Zondag, G. C., & Ossendorp, F. (2023). Multiantigen pan-sarbecovirus DNA vaccines generate protective T cell immune responses. *JCI Insight*, *8*(21), e172488. https://doi.org/10.1172/jci.insight.172488

van Boheemen, S., de Graaf, M., Lauber, C., Bestebroer, T. M., Raj, V. S., Zaki, A. M., Osterhaus, A. D. M. E., Haagmans, B. L., Gorbalenya, A. E., Snijder, E. J., & Fouchier, R. A. M. (2012). Genomic characterization of a newly discovered coronavirus associated with acute respiratory distress syndrome in humans. *MBio*, *3*(6), e00473-12. https://doi.org/10.1128/mBio.00473-12

van der Lubbe, J. E. M., Verspuij, J. W. A., Huizingh, J., Schmit-Tillemans, S. P. R., Tolboom, J. T. B. M., Dekking, L. E. H. A., Kwaks, T., Brandenburg, B., Meijberg, W., Zahn, R. C., Roozendaal, R., & Kuipers, H. (2018). Mini-HA Is Superior to Full Length

Hemagglutinin Immunization in Inducing Stem-Specific Antibodies and Protection Against Group 1 Influenza Virus Challenges in Mice. *Frontiers in Immunology*, *9*, 2350. https://doi.org/10.3389/fimmu.2018.02350

Vatti, A., Monsalve, D. M., Pacheco, Y., Chang, C., Anaya, J. M., & Gershwin, M. E. (2017). Original antigenic sin: A comprehensive review. *Journal of Autoimmunity*, *83*, 12–21. https://doi.org/10.1016/j.jaut.2017.04.008

Veggiani, G., Nakamura, T., Brenner, M. D., Gayet, R. V., Yan, J., Robinson, C. V., & Howarth, M. (2016). Programmable polyproteams built using twin peptide superglues. *Proceedings of the National Academy of Sciences of the United States of America*, *113*(5), 1202–1207. https://doi.org/10.1073/pnas.1519214113

Vert, M., Doi, Y., Hellwich, K.-H., Hess, M., Hodge, P., Kubisa, P., Rinaudo, M., & Schué, F. (2012). Terminology for biorelated polymers and applications (IUPAC Recommendations 2012). *Pure and Applied Chemistry*, *84*(2), 377–410. https://doi.org/10.1351/PAC-REC-10-12-04

Vester, S. K., Rahikainen, R., Khairil Anuar, I. N. A., Hills, R. A., Tan, T. K., & Howarth, M. (2022). SpySwitch enables pH- or heat-responsive capture and release for plug-and-display nanoassembly. *Nature Communications 2022 13:1*, *13*(1), 1–16. https://doi.org/10.1038/s41467-022-31193-8

Vetter, V., Denizer, G., Friedland, L. R., Krishnan, J., & Shapiro, M. (2018). Understanding modern-day vaccines: what you need to know. *Annals of Medicine*, *50*(2), 110–120. https://doi.org/10.1080/07853890.2017.1407035

Viana, R., Moyo, S., Amoako, D. G., Tegally, H., Scheepers, C., Althaus, C. L., Anyaneji, U. J., Bester, P. A., Boni, M. F., Chand, M., Choga, W. T., Colquhoun, R., Davids, M., Deforche, K., Doolabh, D., du Plessis, L., Engelbrecht, S., Everatt, J., Giandhari, J., … de Oliveira, T. (2022). Rapid epidemic expansion of the SARS-CoV-2 Omicron variant in southern Africa. *Nature*, *603*(7902), 679–686. https://doi.org/10.1038/s41586-022-04411-y

Vigerust, D. J., & Shepherd, V. L. (2007). Virus glycosylation: role in virulence and immune interactions. *Trends in Microbiology*, *15*(5), 211–218. https://doi.org/10.1016/j.tim.2007.03.003

Vijayanand, P., Wilkins, E., & Woodhead, M. (2004). Severe acute respiratory syndrome (SARS): a review. *Clinical Medicine*, *4*(2), 152–160. https://doi.org/10.7861/clinmedicine.4-2-152

Vijgen, L., Keyaerts, E., Moës, E., Thoelen, I., Wollants, E., Lemey, P., Vandamme, A.-M., & Van Ranst, M. (2005). Complete Genomic Sequence of Human Coronavirus OC43: Molecular Clock Analysis Suggests a Relatively Recent Zoonotic Coronavirus Transmission Event. *Journal of Virology*, *79*(3), 1595–1604. https://doi.org/10.1128/JVI.79.3.1595-1604.2005

Virtanen, P., Gommers, R., Oliphant, T. E., Haberland, M., Reddy, T., Cournapeau, D., Burovski, E., Peterson, P., Weckesser, W., Bright, J., van der Walt, S. J., Brett, M., Wilson, J., Millman, K. J., Mayorov, N., Nelson, A. R. J., Jones, E., Kern, R., Larson, E., … Vázquez-Baeza, Y. (2020). SciPy 1.0: fundamental algorithms for scientific computing in Python. *Nature Methods*, *17*(3), 261–272. https://doi.org/10.1038/s41592-019-0686-2

Vishwanath, S., Carnell, G. W., Ferrari, M., Asbach, B., Billmeier, M., George, C., Sans, M. S., Nadesalingam, A., Huang, C. Q., Paloniemi, M., Stewart, H., Chan, A., Wells, D. A., Neckermann, P., Peterhoff, D., Einhauser, S., Cantoni, D., Neto, M. M., Jordan, I., … Heeney, J. L. (2023). A computationally designed antigen eliciting broad humoral responses against SARS-CoV-2 and related sarbecoviruses. *Nature Biomedical Engineering*. https://doi.org/10.1038/s41551-023-01094-2

Vitiello, A., & Ferrara, F. (2021). Brief review of the mRNA vaccines COVID-19. *Inflammopharmacology*, *29*(3), 645–649. https://doi.org/10.1007/s10787-021-00811-0

V'kovski, P., Kratzel, A., Steiner, S., Stalder, H., & Thiel, V. (2021). Coronavirus biology and replication: implications for SARS-CoV-2. *Nature Reviews Microbiology*, *19*(3), 155–170. https://doi.org/10.1038/s41579-020-00468-6

Vlasova, A. N., Diaz, A., Damtie, D., Xiu, L., Toh, T. H., Lee, J. S. Y., Saif, L. J., & Gray, G. C. (2022). Novel Canine Coronavirus Isolated from a Hospitalized Patient With Pneumonia in East Malaysia. *Clinical Infectious Diseases*, *74*(3), 446–454. https://doi.org/10.1093/cid/ciab456

Voysey, M., Clemens, S. A. C., Madhi, S. A., Weckx, L. Y., Folegatti, P. M., Aley, P. K., Angus, B., Baillie, V. L., Barnabas, S. L., Bhorat, Q. E., Bibi, S., Briner, C., Cicconi, P., Collins, A. M., Colin-Jones, R., Cutland, C. L., Darton, T. C., Dheda, K., Duncan, C. J. A., … Zuidewind, P. (2021). Safety and efficacy of the ChAdOx1 nCoV-19 vaccine (AZD1222) against SARS-CoV-2: an interim analysis of four randomised controlled trials in Brazil, South Africa, and the UK. *The Lancet*, *397*(10269), 99–111. https://doi.org/10.1016/S0140-6736(20)32661-1

Walls, A. C., Miranda, M. C., Schäfer, A., Pham, M. N., Greaney, A., Arunachalam, P. S., Navarro, M. J., Tortorici, M. A., Rogers, K., O'Connor, M. A., Shirreff, L., Ferrell, D. E., Bowen, J., Brunette, N., Kepl, E., Zepeda, S. K., Starr, T., Hsieh, C. L., Fiala, B., … Veesler, D. (2021). Elicitation of broadly protective sarbecovirus immunity by receptor-binding domain nanoparticle vaccines. *Cell*, *184*(21), 5432-5447.e16. https://doi.org/10.1016/j.cell.2021.09.015

Wang, E., Cohen, A. A., Caldera, L. F., Keeffe, J. R., Rorick, A. V, Aida, Y. M., Gnanapragasam, P. N. P., Bjorkman, P. J., & Chakraborty, A. K. (2024). Designed mosaic nanoparticles enhance cross-reactive immune responses in mice. *BioRxiv*, 2024.02.28.582544. https://doi.org/10.1101/2024.02.28.582544

Wang, H., Paulson, K. R., Pease, S. A., Watson, S., Comfort, H., Zheng, P., Aravkin, A. Y., Bisignano, C., Barber, R. M., Alam, T., Fuller, J. E., May, E. A., Jones, D. P., Frisch, M. E., Abbafati, C., Adolph, C., Allorant, A., Amlag, J. O., Bang-Jensen, B., … Murray, C. J. L. (2022). Estimating excess mortality due to the COVID-19 pandemic: a systematic analysis of COVID-19-related mortality, 2020–21. *The Lancet*, *399*(10334), 1513–1536. https://doi.org/10.1016/S0140-6736(21)02796-3

Wang, H., Zhang, Y., Huang, B., Deng, W., Quan, Y., Wang, W., Xu, W., Zhao, Y., Li, N., Zhang, J., Liang, H., Bao, L., Xu, Y., Ding, L., Zhou, W., Gao, H., Liu, J., Niu, P., Zhao, L., … Yang, X. (2020). Development of an Inactivated Vaccine Candidate, BBIBP-CorV, with Potent Protection against SARS-CoV-2. *Cell*, *182*(3), 713-721.e9. https://doi.org/10.1016/j.cell.2020.06.008

Wang, L., Maddox, C., Terio, K., Lanka, S., Fredrickson, R., Novick, B., Parry, C., McClain, A., & Ross, K. (2020). Detection and Characterization of New Coronavirus in Bottlenose Dolphin, United States, 2019. *Emerging Infectious Diseases*, *26*(7), 1610–1612. https://doi.org/10.3201/eid2607.200093

Wang, L.-F., Shi, Z., Zhang, S., Field, H., Daszak, P., & Eaton, B. (2006). Review of Bats and SARS. *Emerging Infectious Diseases*, *12*(12), 1834–1840. https://doi.org/10.3201/eid1212.060401

Wang, S. (2017). Optimal Sequential Immunization Can Focus Antibody Responses against Diversity Loss and Distraction. *PLOS Computational Biology*, *13*(1), e1005336. https://doi.org/10.1371/journal.pcbi.1005336

Wang, W., Liu, Z., Zhou, X., Guo, Z., Zhang, J., Zhu, P., Yao, S., & Zhu, M. (2019). Ferritin nanoparticle-based SpyTag/SpyCatcher-enabled click vaccine for tumor immunotherapy. *Nanomedicine: Nanotechnology, Biology and Medicine*, *16*, 69–78. https://doi.org/10.1016/j.nano.2018.11.009

Ward, B. J., Gobeil, P., Séguin, A., Atkins, J., Boulay, I., Charbonneau, P.-Y., Couture, M., D'Aoust, M.-A., Dhaliwall, J., Finkle, C., Hager, K., Mahmood, A., Makarkov, A., Cheng, M. P., Pillet, S., Schimke, P., St-Martin, S., Trépanier, S., & Landry, N. (2021). Phase 1 randomized trial of a plant-derived virus-like particle vaccine for COVID-19. *Nature Medicine*, *27*(6), 1071–1078. https://doi.org/10.1038/s41591-021-01370-1

Watanabe, Y., Allen, J. D., Wrapp, D., McLellan, J. S., & Crispin, M. (2020). Site-specific glycan analysis of the SARS-CoV-2 spike. *Science*, *369*(6501), 330–333. https://doi.org/10.1126/science.abb9983

Watanabe, Y., Mendonça, L., Allen, E. R., Howe, A., Lee, M., Allen, J. D., Chawla, H., Pulido, D., Donnellan, F., Davies, H., Ulaszewska, M., Belij-Rammerstorfer, S., Morris, S., Krebs, A.-S., Dejnirattisai, W., Mongkolsapaya, J., Supasa, P., Screaton, G. R., Green, C. M., … Crispin, M. (2021). Native-like SARS-CoV-2 Spike Glycoprotein Expressed by ChAdOx1 nCoV-19/AZD1222 Vaccine. *ACS Central Science*, *7*(4), 594–602. https://doi.org/10.1021/acscentsci.1c00080

Watson, O. J., Barnsley, G., Toor, J., Hogan, A. B., Winskill, P., & Ghani, A. C. (2022a). Global impact of the first year of COVID-19 vaccination: a mathematical modelling study. *The Lancet Infectious Diseases*, *22*(9), 1293–1302. https://doi.org/10.1016/S1473-3099(22)00320-6

Watson, O. J., Barnsley, G., Toor, J., Hogan, A. B., Winskill, P., & Ghani, A. C. (2022b). Global impact of the first year of COVID-19 vaccination: a mathematical modelling study. *The Lancet Infectious Diseases*, *22*(9), 1293–1302. https://doi.org/10.1016/S1473-3099(22)00320-6

Wei, C. J., Crank, M. C., Shiver, J., Graham, B. S., Mascola, J. R., & Nabel, G. J. (2020). Next-generation influenza vaccines: opportunities and challenges. *Nature Reviews Drug Discovery*, *19*(4), 239–252. https://doi.org/10.1038/s41573-019-0056-x

Wei, C.-J., Crank, M. C., Shiver, J., Graham, B. S., Mascola, J. R., & Nabel, G. J. (2020). Next-generation influenza vaccines: opportunities and challenges. *Nature Reviews Drug Discovery*, *19*(4), 239–252. https://doi.org/10.1038/s41573-019-0056-x

Weidenbacher, P. A., & Kim, P. S. (2019). Protect, modify, deprotect (PMD): A strategy for creating vaccines to elicit antibodies targeting a specific epitope. *Proceedings of the National Academy of Sciences*, *116*(20), 9947–9952. https://doi.org/10.1073/pnas.1822062116

Wen, L., Yang, S., Zhu, P., Yu, Y., Qiu, X., Fu, N., & Liu, Y. (2016). Peptide mimics of a carbohydrate-associated epitope expressed by cancer cells: Identification of vaccine candidates. *Molecular Medicine Reports*, *14*(6), 5237–5244. https://doi.org/10.3892/mmr.2016.5863

West, A. P., Scharf, L., Horwitz, J., Klein, F., Nussenzweig, M. C., & Bjorkman, P. J. (2013). Computational analysis of anti–HIV-1 antibody neutralization panel data to identify potential functional epitope residues. *Proceedings of the National Academy of Sciences*, *110*(26), 10598–10603. https://doi.org/10.1073/pnas.1309215110

WHO. (2023). *WHO COVID-19 dashboard: number of COVID-19 cases reported to WHO*. World Health Organization. https://data.who.int/dashboards/covid19/cases

Widagdo, W., Raj, V. S., Schipper, D., Kolijn, K., van Leenders, G. J. L. H., Bosch, B. J., Bensaid, A., Segalés, J., Baumgärtner, W., Osterhaus, A. D. M. E., Koopmans, M. P., van den Brand, J. M. A., & Haagmans, B. L. (2016). Differential Expression of the Middle East Respiratory Syndrome Coronavirus Receptor in the Upper Respiratory Tracts of Humans and Dromedary Camels. *Journal of Virology*, *90*(9), 4838–4842. https://doi.org/10.1128/JVI.02994-15

Widge, A. T., Hofstetter, A. R., Houser, K. V., Awan, S. F., Chen, G. L., Burgos Florez, M. C., Berkowitz, N. M., Mendoza, F., Hendel, C. S., Holman, L. A., Gordon, I. J., Apte, P., Liang, C. J., Gaudinski, M. R., Coates, E. E., Strom, L., Wycuff, D., Vazquez, S., Stein, J. A., … Zhao, Z. (2023). An influenza hemagglutinin stem nanoparticle vaccine induces

cross-group 1 neutralizing antibodies in healthy adults. *Science Translational Medicine*, *15*(692), eade4790. https://doi.org/10.1126/scitranslmed.ade4790

Wille, M., & Holmes, E. C. (2020). Wild birds as reservoirs for diverse and abundant gamma- and deltacoronaviruses. *FEMS Microbiology Reviews*, *44*(5), 631–644. https://doi.org/10.1093/femsre/fuaa026

Willett, B. J., Grove, J., MacLean, O. A., Wilkie, C., De Lorenzo, G., Furnon, W., Cantoni, D., Scott, S., Logan, N., Ashraf, S., Manali, M., Szemiel, A., Cowton, V., Vink, E., Harvey, W. T., Davis, C., Asamaphan, P., Smollett, K., Tong, L., … Thomson, E. C. (2022). SARS-CoV-2 Omicron is an immune escape variant with an altered cell entry pathway. *Nature Microbiology*, *7*(8), 1161–1179. https://doi.org/10.1038/s41564-022-01143-7

Williams, J. G., Tomer, K. B., Hioe, C. E., Zolla-Pazner, S., & Norris, P. J. (2006). The antigenic determinants on HIV p24 for CD4+ T cell inhibiting antibodies as determined by limited proteolysis, chemical modification, and mass spectrometry. *Journal of the American Society for Mass Spectrometry*, *17*(11), 1560–1569. https://doi.org/10.1016/j.jasms.2006.06.011

Winokur, P., Gayed, J., Fitz-Patrick, D., Thomas, S. J., Diya, O., Lockhart, S., Xu, X., Zhang, Y., Bangad, V., Schwartz, H. I., Denham, D., Cardona, J. F., Usdan, L., Ginis, J., Mensa, F. J., Zou, J., Xie, X., Shi, P.-Y., Lu, C., … Kitchin, N. (2023). Bivalent Omicron BA.1–Adapted BNT162b2 Booster in Adults Older than 55 Years. *New England Journal of Medicine*, *388*(3), 214–227. https://doi.org/10.1056/NEJMoa2213082

Woo, P. C. Y., Huang, Y., Lau, S. K. P., & Yuen, K.-Y. (2010). Coronavirus Genomics and Bioinformatics Analysis. *Viruses*, *2*(8), 1804–1820. https://doi.org/10.3390/v2081803

Woo, P. C. Y., Lau, S. K. P., Lam, C. S. F., Lau, C. C. Y., Tsang, A. K. L., Lau, J. H. N., Bai, R., Teng, J. L. L., Tsang, C. C. C., Wang, M., Zheng, B.-J., Chan, K.-H., & Yuen, K.-Y. (2012). Discovery of Seven Novel Mammalian and Avian Coronaviruses in the Genus Deltacoronavirus Supports Bat Coronaviruses as the Gene Source of Alphacoronavirus and Betacoronavirus and Avian Coronaviruses as the Gene Source of Gammacoronavirus and Deltacoronavirus. *Journal of Virology*, *86*(7), 3995–4008. https://doi.org/10.1128/JVI.06540-11

Woo, P. C. Y., Lau, S. K. P., Li, K. S. M., Poon, R. W. S., Wong, B. H. L., Tsoi, H. wah, Yip, B. C. K., Huang, Y., Chan, K. hung, & Yuen, K. yung. (2006). Molecular diversity of coronaviruses in bats. *Virology*, *351*(1), 180–187. https://doi.org/10.1016/j.virol.2006.02.041

Woo, P. C. Y., Wang, M., Lau, S. K. P., Xu, H., Poon, R. W. S., Guo, R., Wong, B. H. L., Gao, K., Tsoi, H., Huang, Y., Li, K. S. M., Lam, C. S. F., Chan, K., Zheng, B., & Yuen, K. (2007). Comparative Analysis of Twelve Genomes of Three Novel Group 2c and Group 2d Coronaviruses Reveals Unique Group and Subgroup Features. *Journal of Virology*, *81*(4), 1574–1585. https://doi.org/10.1128/jvi.02182-06

Worobey, M., Levy, J. I., Malpica Serrano, L., Crits-Christoph, A., Pekar, J. E., Goldstein, S. A., Rasmussen, A. L., Kraemer, M. U. G., Newman, C., Koopmans, M. P. G., Suchard, M. A., Wertheim, J. O., Lemey, P., Robertson, D. L., Garry, R. F., Holmes, E. C., Rambaut, A., & Andersen, K. G. (2022). The Huanan Seafood Wholesale Market in Wuhan was the early epicenter of the COVID-19 pandemic. *Science*, *377*(6609), 951–959. https://doi.org/10.1126/science.abp8715

Wu, W., Cheng, Y., Zhou, H., Sun, C., & Zhang, S. (2023). The SARS-CoV-2 nucleocapsid protein: its role in the viral life cycle, structure and functions, and use as a potential target in the development of vaccines and diagnostics. *Virology Journal*, *20*(1), 6. https://doi.org/10.1186/s12985-023-01968-6

Xia, S., Zhang, Y., Wang, Y., Wang, H., Yang, Y., Gao, G. F., Tan, W., Wu, G., Xu, M., Lou, Z., Huang, W., Xu, W., Huang, B., Wang, H., Wang, W., Zhang, W., Li, N., Xie, Z., Ding, L., … Yang, X. (2021). Safety and immunogenicity of an inactivated SARS-CoV-2 vaccine, BBIBP-CorV: a randomised, double-blind, placebo-controlled, phase 1/2 trial. *The Lancet Infectious Diseases*, *21*(1), 39–51. https://doi.org/10.1016/S1473-3099(20)30831-8

Xiong, Q., Cao, L., Ma, C., Tortorici, M. A., Liu, C., Si, J., Liu, P., Gu, M., Walls, A. C., Wang, C., Shi, L., Tong, F., Huang, M., Li, J., Zhao, C., Shen, C., Chen, Y., Zhao, H., Lan, K., … Yan, H. (2022). Close relatives of MERS-CoV in bats use ACE2 as their functional receptors. *Nature*, *612*(7941), 748–757. https://doi.org/10.1038/s41586-022-05513-3

Xu, D., Powell, A. E., Utz, A., Sanyal, M., Do, J., Patten, J. J., Moliva, J. I., Sullivan, N. J., Davey, R. A., & Kim, P. S. (2023). Design of universal Ebola virus vaccine candidates via immunofocusing. *BioRxiv*. https://doi.org/10.1101/2023.10.14.562364

Xu, D.-Z., Zhao, K., Guo, L.-M., Chen, X.-Y., Wang, H.-F., Zhang, J.-M., Xie, Q., Ren, H., Wang, W.-X., Li, L.-J., Xu, M., Liu, P., Niu, J.-Q., Bai, X.-F., Shen, X.-L., Yuan, Z.-H., Wang, X.-Y., & Wen, Y.-M. (2008). A Randomized Controlled Phase IIb Trial of Antigen-Antibody Immunogenic Complex Therapeutic Vaccine in Chronic Hepatitis B Patients. *PLoS ONE*, *3*(7), e2565. https://doi.org/10.1371/journal.pone.0002565

Xu, Y., Shi, Y., Zhou, J., Yang, W., Bai, L., Wang, S., Jin, X., Niu, Q., Huang, A., & Wang, D. (2017). Structure-based antigenic epitope and PEGylation improve the efficacy of staphylokinase. *Microbial Cell Factories*, *16*(1), 197. https://doi.org/10.1186/s12934-017-0801-y

Yadav, D., & Dewangan, H. K. (2021). PEGYLATION: an important approach for novel drug delivery system. *Journal of Biomaterials Science, Polymer Edition*, *32*(2), 266–280. https://doi.org/10.1080/09205063.2020.1825304

Yan, L., Zhang, Y., Ge, J., Zheng, L., Gao, Y., Wang, T., Jia, Z., Wang, H., Huang, Y., Li, M., Wang, Q., Rao, Z., & Lou, Z. (2020). Architecture of a SARS-CoV-2 mini replication

and transcription complex. *Nature Communications*, *11*(1), 5874. https://doi.org/10.1038/s41467-020-19770-1

Yang, L., Wu, Z., Ren, X., Yang, F., Zhang, J., He, G., Dong, J., Sun, L., Zhu, Y., Zhang, S., & Jin, Q. (2014). MERS–Related Betacoronavirus in Vespertilio superans Bats, China. *Emerging Infectious Diseases*, *20*(7), 1260–1262. https://doi.org/10.3201/eid2007.140318

Yao, L., Xue, X., Yu, P., Ni, Y., & Chen, F. (2018). Evans Blue Dye: A Revisit of Its Applications in Biomedicine. *Contrast Media and Molecular Imaging*, *2018*, 7628037. https://doi.org/10.1155/2018/7628037

Yassine, H. M., Boyington, J. C., McTamney, P. M., Wei, C.-J., Kanekiyo, M., Kong, W.-P., Gallagher, J. R., Wang, L., Zhang, Y., Joyce, M. G., Lingwood, D., Moin, S. M., Andersen, H., Okuno, Y., Rao, S. S., Harris, A. K., Kwong, P. D., Mascola, J. R., Nabel, G. J., & Graham, B. S. (2015). Hemagglutinin-stem nanoparticles generate heterosubtypic influenza protection. *Nature Medicine*, *21*(9), 1065–1070. https://doi.org/10.1038/nm.3927

Yuan, M., Wu, N. C., Zhu, X., Lee, C.-C. D., So, R. T. Y., Lv, H., Mok, C. K. P., & Wilson, I. A. (2020). A highly conserved cryptic epitope in the receptor binding domains of SARS-CoV-2 and SARS-CoV. *Science*, *368*(6491), 630–633. https://www.science.org

Zakeri, B., Fierer, J. O., Celik, E., Chittock, E. C., Schwarz-Linek, U., Moy, V. T., & Howarth, M. (2012). Peptide tag forming a rapid covalent bond to a protein, through engineering a bacterial adhesin. *Proceedings of the National Academy of Sciences*, *109*(12), E690–E697. https://doi.org/10.1073/pnas.1115485109

Zandi, M., Shafaati, M., Kalantar-Neyestanaki, D., Pourghadamyari, H., Fani, M., Soltani, S., Kaleji, H., & Abbasi, S. (2022). The role of SARS-CoV-2 accessory proteins in immune evasion. *Biomedicine & Pharmacotherapy*, *156*, 113889. https://doi.org/10.1016/j.biopha.2022.113889

Zhang, H.-Q., Zhang, Q.-Y., Yuan, Z.-M., & Zhang, B. (2023). The potential epidemic threat of Ebola virus and the development of a preventive vaccine. *Journal of Biosafety and Biosecurity*, *5*(2), 67–78. https://doi.org/10.1016/j.jobb.2023.05.001

Zhang, J., Dong, X., Liu, G., & Gao, Y. (2022). Risk and Protective Factors for COVID-19 Morbidity, Severity, and Mortality. *Clinical Reviews in Allergy & Immunology*, *64*(1), 90–107. https://doi.org/10.1007/s12016-022-08921-5

Zhang, L., Jackson, C. B., Mou, H., Ojha, A., Peng, H., Quinlan, B. D., Rangarajan, E. S., Pan, A., Vanderheiden, A., Suthar, M. S., Li, W., Izard, T., Rader, C., Farzan, M., & Choe, H. (2020). SARS-CoV-2 spike-protein D614G mutation increases virion spike density and infectivity. *Nature Communications*, *11*(1), 6013. https://doi.org/10.1038/s41467-020-19808-4

Zhang, Z., Mateus, J., Coelho, C. H., Dan, J. M., Moderbacher, C. R., Gálvez, R. I., Cortes, F. H., Grifoni, A., Tarke, A., Chang, J., Escarrega, E. A., Kim, C., Goodwin, B., Bloom, N. I., Frazier, A., Weiskopf, D., Sette, A., & Crotty, S. (2022). Humoral and cellular immune memory to four COVID-19 vaccines. *Cell*, *185*(14), 2434-2451.e17. https://doi.org/10.1016/j.cell.2022.05.022

Zhang, Z., Nomura, N., Muramoto, Y., Ekimoto, T., Uemura, T., Liu, K., Yui, M., Kono, N., Aoki, J., Ikeguchi, M., Noda, T., Iwata, S., Ohto, U., & Shimizu, T. (2022). Structure of SARS-CoV-2 membrane protein essential for virus assembly. *Nature Communications*, *13*(1), 4399. https://doi.org/10.1038/s41467-022-32019-3

Zhou, D., Duyvesteyn, H. M. E., Chen, C. P., Huang, C. G., Chen, T. H., Shih, S. R., Lin, Y. C., Cheng, C. Y., Cheng, S. H., Huang, Y. C., Lin, T. Y., Ma, C., Huo, J., Carrique, L., Malinauskas, T., Ruza, R. R., Shah, P. N. M., Tan, T. K., Rijal, P., … Huang, K. Y. A. (2020). Structural basis for the neutralization of SARS-CoV-2 by an antibody from a convalescent patient. *Nature Structural and Molecular Biology*, *27*(10), 950–958. https://doi.org/10.1038/s41594-020-0480-y

Zhou, P., Yang, X. Lou, Wang, X. G., Hu, B., Zhang, L., Zhang, W., Si, H. R., Zhu, Y., Li, B., Huang, C. L., Chen, H. D., Chen, J., Luo, Y., Guo, H., Jiang, R. Di, Liu, M. Q., Chen, Y., Shen, X. R., Wang, X., … Shi, Z. L. (2020). A pneumonia outbreak associated with a new coronavirus of probable bat origin. *Nature*, *579*(7798), 270–273. https://doi.org/10.1038/s41586-020-2012-7

Zhou, T., Doria-Rose, N. A., Cheng, C., Stewart-Jones, G. B. E., Chuang, G.-Y., Chambers, M., Druz, A., Geng, H., McKee, K., Kwon, Y. Do, O'Dell, S., Sastry, M., Schmidt, S. D., Xu, K., Chen, L., Chen, R. E., Louder, M. K., Pancera, M., Wanninger, T. G., … Kwong, P. D. (2017). Quantification of the Impact of the HIV-1-Glycan Shield on Antibody Elicitation. *Cell Reports*, *19*(4), 719–732. https://doi.org/10.1016/j.celrep.2017.04.013

Zhu, G., Lynn, G. M., Jacobson, O., Chen, K., Liu, Y., Zhang, H., Ma, Y., Zhang, F., Tian, R., Ni, Q., Cheng, S., Wang, Z., Lu, N., Yung, B. C., Wang, Z., Lang, L., Fu, X., Jin, A., Weiss, I. D., … Chen, X. (2017). Albumin/vaccine nanocomplexes that assemble in vivo for combination cancer immunotherapy. *Nature Communications*, *8*(1), 1954. https://doi.org/10.1038/s41467-017-02191-y

Zhu, N., Zhang, D., Wang, W., Li, X., Yang, B., Song, J., Zhao, X., Huang, B., Shi, W., Lu, R., Niu, P., Zhan, F., Ma, X., Wang, D., Xu, W., Wu, G., Gao, G. F., & Tan, W. (2020). A Novel Coronavirus from Patients with Pneumonia in China, 2019. *New England Journal of Medicine*, *382*(8), 727–733. https://doi.org/10.1056/NEJMoa2001017

Zinsli, L. V., Stierlin, N., Loessner, M. J., & Schmelcher, M. (2021). Deimmunization of protein therapeutics – Recent advances in experimental and computational epitope prediction and deletion. *Computational and Structural Biotechnology Journal*, *19*, 315–329. https://doi.org/10.1016/j.csbj.2020.12.024

Zumla, A., Peiris, M., Memish, Z. A., & Perlman, S. (2024). Anticipating a MERS-like coronavirus as a potential pandemic threat. *The Lancet*, *403*(10438), 1729–1731. https://doi.org/10.1016/S0140-6736(24)00641-X

Appendix 1 – Protein Sequences

SpySwitch

MSYYHHHHHHGSGGSGAMVTTLSGLSGEQGPSGDMTTEEDSATHIHFHKHDEDGRE
LAGATMELRDCSGKTISTWITDGHVKDFYLYPGKYTFVATAAPDGHHVATPIEFTINE
DGQVTVDGEATEGDPHTGSSGS

HuSA-AviTag-HisTag

MVWVTFISLLFLFSSAYSRGVFRRDAHKSEVAHRFKDLGEENFKALVLIAFAQYLQQ
CPFEDHVKLVNEVTEFAKTCVADESAENCDKSLHTLFGDKLCTVATLRETYGEMADC
CAKQEPERNECFLQHKDDNPNLPRLVRPEVDVMCTAFHDNEETFLKKYLYEIARRHP
YFYAPELLFFAKRYKAAFTECCQAADKAACLLPKLDELRDEGKASSAKQRLKCASLQ
KFGERAFKAWAVARLSQRFPKAEFAEVSKLVTDLTKVHTECCHGDLLECADDRADLA
KYICENQDSISSKLKECCEKPLLEKSHCIAEVENDEMPADLPSLAADFVESKDVCKNY
AEAKDVFLGMFLYEYARRHPDYSVVLLLRLAKTYETTLEKCCAAADPHECYAKVFD
EFKPLVEEPQNLIKQNCELFEQLGEYKFQNALLVRYTKKVPQVSTPTLVEVSRNLGKV
GSKCCKHPEAKRMPCAEDYLSVVLNQLCVLHEKTPVSDRVTKCCTESLVNRRPCFSA
LEVDETYVPKEFNAETFTFHADICTLSEKERQIKKQTALVELVKHKPKATKEQLKAVM
DDFAAFVEKCCKADDKETCFAEEGKKLVAASQVALGLGLNDIFEAQKIEWHEWNHR
DRNLPPLAPLGPHHHHHH

SpyTag-MBP

MGSSHHHHHHSSGLVPRGSHMGAHIVMVDAYKPTKGSGESGKIEEGKLVIWINGDK
GYNGLAEVGKKFEKDTGIKVTVEHPDKLEEKFPQVAATGDGPDIIFWAHDRFGGYAQ
SGLLAEITPDKAFQDKLYPFTWDAVRYNGKLIAYPIAVEALSLIYNKDLLPNPPKTWEE
IPALDKELKAKGKSALMFNLQEPYFTWPLIAADGGYAFKYENGKYDIKDVGVDNAG
AKAGLTFLVDLIKNKHMNADTDYSIAEAAFNKGETAMTINGPWAWSNIDTSKVNYG
VTVLPTFKGQPSKPFVGVLSAGINAASPNKELAKEFLENYLLTDEGLEAVNKDKPLG
AVALKSYEEELAKDPRIAATMENAQKGEIMPNIPQMSAFWYAVRTAVINAASGRQTV
DEALKDAQTNSSS

SpyCatcher003-mi3 (SC3-mi3)

MGSSVTTLSGLSGEQGPSGDMTTEEDSATHIKFSKRDEDGRELAGATMELRDSSGKTI
STWISDGHVKDFYLYPGKYTFVETAAPDGYEVATPIEFTVNEDGQVTVDGEATEGDA
HTGGSGGSGGSGGSMKMEELFKKHKIVAVLRANSVEEAKKKALAVFLGGVHLIEITF
TVPDADTVIKELSFLKEMGAIIGAGTVTSVEQARKAVESGAEFIVSPHLDEEISQFAKE
KGVFYMPGVMTPTELVKAMKLGHTILKLFPGEVVGPQFVKAMKGPFPNVKFVPTGG
VNLDNVCEWFKAGVLAVGVGSALVKGTPVEVAEKAKAFVEKIRGCTEGSGEPEA

SpyCatcher002-MBP

MGSSHHHHHHDYDIPTTENLYFQGAMVTTLSGLSGEQGPSGDMTTEEDSATHIKFSK
RDEDGRELAGATMELRDSSGKTISTWISDGHVKDFYLYPGKYTFVETAAPDGYEVAT
AITFTVNEQGQVTVNGEATKGDAHTGSSGSGKIEEGKLVIWINGDKGYNGLAEVGK
KFEKDTGIKVTVEHPDKLEEKFPQVAATGDGPDIIFWAHDRFGGYAQSGLLAEITPDK
AFQDKLYPFTWDAVRYNGKLIAYPIAVEALSLIYNKDLLPNPPKTWEEIPALDKELKA
KGKSALMFNLQEPYFTWPLIAADGGYAFKYENGKYDIKDVGVDNAGAKAGLTFLVD
LIKNKHMNADTDYSIAEAAFNKGETAMTINGPWAWSNIDTSKVNYGVTVLPTFKGQ
PSKPFVGVLSAGINAASPNKELAKEFLENYLLTDEGLEAVNKDKPLGAVALKSYEEEL
AKDPRIAATMENAQKGEIMPNIPQMSAFWYAVRTAVINAASGRQTVDEALKDAQTNS
SS

SpyTag-RBD[SARS2 Wuhan]

MNTQILVFALIAIIPTNADKIGSGAHIVMVDAYKPTKGSGGSGGSGTGNITNLCPFGEV
FNATRFASVYAWNRKRISNCVADYSVLYNSASFSTFKCYGVSPTKLNDLCFTNVYADS
FVIRGDEVRQIAPGQTGKIADYNYKLPDDFTGCVIAWNSNNLDSKVGGNYNYLYRLF
RKSNLKPFERDISTEIYQAGSTPCNGVEGFNCYFPLQSYGFQPTNGVGYQPYRVVVLS
FELLHAPATVCGPKK

SpyTag-RBD[SARS2 Wuhan]-ABD035

MNTQILVFALIAIIPTNADKIGSGAHIVMVDAYKPTKGSGGSGGSGTGNITNLCPFGEV
FNATRFASVYAWNRKRISNCVADYSVLYNSASFSTFKCYGVSPTKLNDLCFTNVYADS
FVIRGDEVRQIAPGQTGKIADYNYKLPDDFTGCVIAWNSNNLDSKVGGNYNYLYRLF
RKSNLKPFERDISTEIYQAGSTPCNGVEGFNCYFPLQSYGFQPTNGVGYQPYRVVVLS
FELLHAPATVCGPKKGGSGTGLAEAKVLANRELDKYGVSDFYKRLINKAKTVEGVE
ALKLHILAALP

SpyTag-RBD[SARS2 Wuhan] K378N

MNTQILVFALIAIIPTNADKIGSGAHIVMVDAYKPTKGSGGSGGSGTGNITNLCPFGEV
FNATRFASVYAWNRKRISNCVADYSVLYNSASFSTFNCYGVSPTKLNDLCFTNVYADS
FVIRGDEVRQIAPGQTGKIADYNYKLPDDFTGCVIAWNSNNLDSKVGGNYNYLYRLF
RKSNLKPFERDISTEIYQAGSTPCNGVEGFNCYFPLQSYGFQPTNGVGYQPYRVVVLS
FELLHAPATVCGPKK

SpyTag-RBD[SARS2 Wuhan] K378Q

MNTQILVFALIAIIPTNADKIGSGAHIVMVDAYKPTKGSGGSGGSGTGNITNLCPFGEV
FNATRFASVYAWNRKRISNCVADYSVLYNSASFSTFQCYGVSPTKLNDLCFTNVYADS
FVIRGDEVRQIAPGQTGKIADYNYKLPDDFTGCVIAWNSNNLDSKVGGNYNYLYRLF
RKSNLKPFERDISTEIYQAGSTPCNGVEGFNCYFPLQSYGFQPTNGVGYQPYRVVVLS
FELLHAPATVCGPKK

SpyTag-Quartet

MNTQILVFALIAIIPTNADKIGSGAHIVMVDAYKPTKGSGGSGGSGTGRVAPSKEVVRF
PNITNLCPFGEVFNATTFPSVYAWERKRISNCVADYSVLYNSTSFSTFKCYGVSATKLN
DLCFSNVYADSFVVKGDDVRQIAPGQTGVIADYNYKLPDDFLGCVLAWNTNSKDSS
TSGNYNYLYRWVRRSKLNPYERDLSNDIYSPGGQSCSAVGPNCYNPLRPYGFFTTAG
VGHQPYRVVVLSFELLNAPATVCGPKLSTDLIKNQGSGGSGGSGRVSPTHEVVRFPNI
TNRCPFDKVFNASRFPNVYAWERTKISDCVADYTVLYNSTSFSTFKCYGVSPSKLIDL
CFTSVYADTFLIRSSEVRQVAPGETGVIADYNYKLPDDFTGCVIAWNTAKQDQGQYY
YRSSRKTKLKPFERDLTSDENGVRTLSTYDFYPNVPIEYQATRVVVLSFELLNAPATVC
GPKLSTALVKNQCVNFGSGGTGGSGRVQPTDSIVRFPNITNLCPFGEVFNATTFASVY
AWNRKRISNCVADYSVLYNSTSFSTFKCYGVSPTKLNDLCFTNVYADSFVITGDEVRQ
IAPGQTGKIADYNYKLPDDFTGCVIAWNSKHIDAKEGGNFNYLYRLFRKANLKPFER
DISTEIYQAGSKPCNGQTGLNCYYPLYRYGFYPTDGVGHQPYRVVVLSFELLNAPATV
CGPKKSTNLVKNKCVNFGTGGSGGSGNITNLCPFGEVFNATRFASVYAWNRKRISNC
VADYSVLYNSASFSTFKCYGVSPTKLNDLCFTNVYADSFVIRGDEVRQIAPGQTGKIA
DYNYKLPDDFTGCVIAWNSNNLDSKVGGNYNYLYRLFRKSNLKPFERDISTEIYQAG
STPCNGVEGFNCYFPLQSYGFQPTNGVGYQPYRVVVLSFELLHAPATVCGPKKT

Quartet-SpyTag

MNTQILVFALIAIIPTNADKIGSGKLGYIEFYKVEKGSGESGSGRVAPSKEVVRFPNITN
LCPFGEVFNATTFPSVYAWERKRISNCVADYSVLYNSTSFSTFKCYGVSATKLNDLCFS
NVYADSFVVKGDDVRQIAPGQTGVIADYNYKLPDDFLGCVLAWNTNSKDSSTSGNY
NYLYRWVRRSKLNPYERDLSNDIYSPGGQSCSAVGPNCYNPLRPYGFFTTAGVGHQP
YRVVVLSFELLNAPATVCGPKLSTDLIKNQGSGGSGGSGRVSPTHEVVRFPNITNRCPF
DKVFNASRFPNVYAWERTKISDCVADYTVLYNSTSFSTFKCYGVSPSKLIDLCFTSVY
ADTFLIRSSEVRQVAPGETGVIADYNYKLPDDFTGCVIAWNTAKQDQGQYYYRSSRK
TKLKPFERDLTSDENGVRTLSTYDFYPNVPIEYQATRVVVLSFELLNAPATVCGPKLST
ALVKNQCVNFGSGGTGGSGRVQPTDSIVRFPNITNLCPFGEVFNATTFASVYAWNRKR
ISNCVADYSVLYNSTSFSTFKCYGVSPTKLNDLCFTNVYADSFVITGDEVRQIAPGQT
GKIADYNYKLPDDFTGCVIAWNSKHIDAKEGGNFNYLYRLFRKANLKPFERDISTEIY
QAGSKPCNGQTGLNCYYPLYRYGFYPTDGVGHQPYRVVVLSFELLNAPATVCGPKK
STNLVKNKCVNFGTGGSGGSGNITNLCPFGEVFNATRFASVYAWNRKRISNCVADYS
VLYNSASFSTFKCYGVSPTKLNDLCFTNVYADSFVIRGDEVRQIAPGQTGKIADYNYK
LPDDFTGCVIAWNSNNLDSKVGGNYNYLYRLFRKSNLKPFERDISTEIYQAGSTPCNG
VEGFNCYFPLQSYGFQPTNGVGYQPYRVVVLSFELLHAPATVCGPKKTGGGGGDIPA
TYEFTDGKHYITNEPLPPKGGGGGGAHIVMVDAYKPTK

Alternate Quartet

MNTQILVFALIAIIPTNADKIGSGAHIVMVDAYKPTKGSGGSGGSGTGRVQPTISIVRFP
NITNLCPFGEVFNASKFASVYAWNRKRISNCVADYSVLYNSTSFSTFKCYGVSPTKLN
DLCFTNVYADSFVVKGDEVRQIAPGQTGVIADYNYKLPDDFTGCVIAWNSVKQDAL
TGGNYGYLYRLFRKSKLKPFERDISTEIYQAGSTPCNGQVGLNCYYPLERYGFHPTTG
VNYQPFRVVVLSFELLNGPATVCGPKLSTTLVKDKCVNFGSGGSGGTGRILPSTEVVR
FPNITNFCPFDKVFNATRFPNVYAWQRTKISDCIADYTVLYNSTSFSTFKCYGVSPSKLI
DLCFTSVYADTFLIRFSEVRQIAPGETGVIADYNYKLPDDFTGCVLAWNTAQQDIGSY
FYRSHRAVKLKPFERDLSSDENGVRTLSTYDFNPNVPLDYQATRVVVLSFELLNAPAT
VCGPKLSTQLVKNRCVNFGSGGSGGSGRVSPVTEVVRFPNITNLCPFDKVFNATRFPS
VYAWERTKISDCVADYTVFYNSTSFSTFNCYGVSPSKLIDLCFTSVYADTFLIRFSEVR
QVAPGQTGVIADYNYKLPDDFTGCVIAWNTAKQDVGSYFYRSHRSSKLKPFERDLSS
EENGVRTLSTYDFNQNVPLEYQATRVVVLSFELLNAPATVCGPKLSTSLVKNQCVNF
GSGGSGGTGRVAPSKEVVRFPNITNLCPFGEVFNATTFPSVYAWERKRISNCVADYSV
LYNSTSFSTFKCYGVSATKLNDLCFSNVYADSFVVKGDDVRQIAPGQTGVIADYNYK
LPDDFTGCVLAWNTRNIDATQTGNYNYKYRSLRHGKLRPFERDISNVPFSPDGKPCT
PPAFNCYWPLNDYGFYITNGIGYQPYRVVVLSFELLNAPATVCGPKLSTDLIKNQCVN
F

Quartet[SARS1]

MNTQILVFALIAIIPTNADKIGSGAHIVMVDAYKPTKGSGGSGGSGTGRVAPSKEVVRF
PNITNLCPFGEVFNATTFPSVYAWERKRISNCVADYSVLYNSTSFSTFKCYGVSATKLN
DLCFSNVYADSFVVKGDDVRQIAPGQTGVIADYNYKLPDDFLGCVLAWNTNSKDSS
TSGNYNYLYRWVRRSKLNPYERDLSNDIYSPGGQSCSAVGPNCYNPLRPYGFFTTAG
VGHQPYRVVVLSFELLNAPATVCGPKLSTDLIKNQGSGGSGGSGRVSPTHEVVRFPNI
TNRCPFDKVFNASRFPNVYAWERTKISDCVADYTVLYNSTSFSTFKCYGVSPSKLIDL
CFTSVYADTFLIRSSEVRQVAPGETGVIADYNYKLPDDFTGCVIAWNTAKQDQGQYY
YRSSRKTKLKPFERDLTSDENGVRTLSTYDFYPNVPIEYQATRVVVLSFELLNAPATVC
GPKLSTALVKNQCVNFGSGGTGGSGRVQPTDSIVRFPNITNLCPFGEVFNATTFASVY
AWNRKRISNCVADYSVLYNSTSFSTFKCYGVSPTKLNDLCFTNVYADSFVITGDEVRQ
IAPGQTGKIADYNYKLPDDFTGCVIAWNSKHIDAKEGGNFNYLYRLFRKANLKPFER
DISTEIYQAGSKPCNGQTGLNCYYPLYRYGFYPTDGVGHQPYRVVVLSFELLNAPATV
CGPKKSTNLVKNKCVNFGTGGSGGSGRVVPSGDVVRFPNITNLCPFGEVFNATKFPS
VYAWERKKISNCVADYSVLYNSTFFSTFKCYGVSATKLNDLCFSNVYADSFVVKGDD
VRQIAPGQTGVIADYNYKLPDDFMGCVLAWNTRNIDATSTGNYNYKYRYLRHGKLR
PFERDISNVPFSPDGKPCTPPALNCYWPLNDYGFYTTTGIGYQPYRVVVLSFELLNAP
ATVCGPKLSTDLIKNQCVNF

Kraken Quartet

MNTQILVFALIAIIPTNADKIGSGAHIVMVDAYKPTKGSGGSGGSGTGRVAPSKEVVRF
PNITNLCPFGEVFNATTFPSVYAWERKRISNCVADYSVLYNSTSFSTFKCYGVSATKLN
DLCFSNVYADSFVVKGDDVRQIAPGQTGVIADYNYKLPDDFLGCVLAWNTNSKDSS
TSGNYNYLYRWVRRSKLNPYERDLSNDIYSPGGQSCSAVGPNCYNPLRPYGFFTTAG
VGHQPYRVVVLSFELLNAPATVCGPKLSTDLIKNQGSGGSGGSGRVSPTHEVVRFPNI
TNRCPFDKVFNASRFPNVYAWERTKISDCVADYTVLYNSTSFSTFKCYGVSPSKLIDL
CFTSVYADTFLIRSSEVRQVAPGETGVIADYNYKLPDDFTGCVIAWNTAKQDQGQYY
YRSSRKTKLKPFERDLTSDENGVRTLSTYDFYPNVPIEYQATRVVVLSFELLNAPATVC
GPKLSTALVKNQCVNFGSGGTGGSGRVQPTDSIVRFPNITNLCPFGEVFNATTFASVY
AWNRKRISNCVADYSVLYNSTSFSTFKCYGVSPTKLNDLCFTNVYADSFVITGDEVRQ
IAPGQTGKIADYNYKLPDDFTGCVIAWNSKHIDAKEGGNFNYLYRLFRKANLKPFER
DISTEIYQAGSKPCNGQTGLNCYYPLYRYGFYPTDGVGHQPYRVVVLSFELLNAPATV
CGPKKSTNLVKNKCVNFGTGGSGGSGRVQPTESIVRFPNITNLCPFHEVFNATTFASV
YAWNRKRISNCVADYSVIYNFAPFFAFKCYGVSPTKLNDLCFTNVYADSFVIRGNEVS
QIAPGQTGNIADYNYKLPDDFTGCVIAWNSNKLDSKPSGNYNYLYRLFRKSKLKPFE
RDISTEIYQAGNKPCNGVAGPNCYSPLQSYGFRPTYGVGHQPYRVVVLSFELLHAPAT
VCGPKK

No Linker Quartet

MNTQILVFALIAIIPTNADKIGSGAHIVMVDAYKPTKGSGGSGGSGTGRVAPSKEVVRF
PNITNLCPFGEVFNATTFPSVYAWERKRISNCVADYSVLYNSTSFSTFKCYGVSATKLN
DLCFSNVYADSFVVKGDDVRQIAPGQTGVIADYNYKLPDDFLGCVLAWNTNSKDSS
TSGNYNYLYRWVRRSKLNPYERDLSNDIYSPGGQSCSAVGPNCYNPLRPYGFFTTAG
VGHQPYRVVVLSFELLNAPATVCGPKLSTDLIKNQRVSPTHEVVRFPNITNRCPFDKV
FNASRFPNVYAWERTKISDCVADYTVLYNSTSFSTFKCYGVSPSKLIDLCFTSVYADTF
LIRSSEVRQVAPGETGVIADYNYKLPDDFTGCVIAWNTAKQDQGQYYYRSSRKTKLK
PFERDLTSDENGVRTLSTYDFYPNVPIEYQATRVVVLSFELLNAPATVCGPKLSTALVK
NQCVNFRVQPTDSIVRFPNITNLCPFGEVFNATTFASVYAWNRKRISNCVADYSVLYN
STSFSTFKCYGVSPTKLNDLCFTNVYADSFVITGDEVRQIAPGQTGKIADYNYKLPDD
FTGCVIAWNSKHIDAKEGGNFNYLYRLFRKANLKPFERDISTEIYQAGSKPCNGQTGL
NCYYPLYRYGFYPTDGVGHQPYRVVVLSFELLNAPATVCGPKKSTNLVKNKCVNFNI
TNLCPFGEVFNATRFASVYAWNRKRISNCVADYSVLYNSASFSTFKCYGVSPTKLNDL
CFTNVYADSFVIRGDEVRQIAPGQTGKIADYNYKLPDDFTGCVIAWNSNNLDSKVGG
NYNYLYRLFRKSNLKPFERDISTEIYQAGSTPCNGVEGFNCYFPLQSYGFQPTNGVGY
QPYRVVVLSFELLHAPATVCGPKKT

2017 Quartet

MNTQILVFALIAIIPTNADKIGSGAHIVMVDAYKPTKGSGGSGGSGTGRVAPSKEVVRF
PNITNLCPFGEVFNATTFPSVYAWERKRISNCVADYSVLYNSTSFSTFKCYGVSATKLN
DLCFSNVYADSFVVKGDDVRQIAPGQTGVIADYNYKLPDDFLGCVLAWNTNSKDSS
TSGNYNYLYRWVRRSKLNPYERDLSNDIYSPGGQSCSAVGPNCYNPLRPYGFFTTAG
VGHQPYRVVVLSFELLNAPATVCGPKLSTDLIKNQGSGGSGGSGRVSPTHEVVRFPNI
TNRCPFDKVFNASRFPNVYAWERTKISDCVADYTVLYNSTSFSTFKCYGVSPSKLIDL
CFTSVYADTFLIRSSEVRQVAPGETGVIADYNYKLPDDFTGCVIAWNTAKQDQGQYY
YRSSRKTKLKPFERDLTSDENGVRTLSTYDFYPNVPIEYQATRVVVLSFELLNAPATVC
GPKLSTALVKNQCVNFGSGGTGGSGRVVPSGDVVRFPNITNLCPFGEVFNATKFPSVY
AWERKKISNCVADYSVLYNSTFFSTFKCYGVSATKLNDLCFSNVYADSFVVKGDDVR
QIAPGQTGVIADYNYKLPDDFMGCVLAWNTRNIDATSTGNYNYKYRYLRHGKLRPF
ERDISNVPFSPDGKPCTPPALNCYWPLNDYGFYTTTGIGYQPYRVVVLSFELLNAPAT
VCGPKLSTDLIKNQCVNFGTGGSGGSGRVTPTTEVVRFPNITQLCPFNEVFNITSFPSV
YAWERMRITNCVADYSVLYNSSASFSTFQCYGVSPTKLNDLCFSSVYADYFVVKGDD
VRQIAPAQTGVIADYNYKLPDDFTGCVIAWNTNSLDSSNEFFYRRFRHGKIKPYGRD
LSNVLFNPSGGTCSAEGLNCYKPLASYGFTQSSGIGFQPYRVVVLSFELLNAPATVCG
PKQSTELVKNKCVNF

SpyTag-RBD_Beta

MNTQILVFALIAIIPTNADKIGSGAHIVMVDAYKPTKGSGGSGGSGTGNITNLCPFGEV
FNATRFASVYAWNRKRISNCVADYSVLYNSASFSTFKCYGVSPTKLNDLCFTNVYADS
FVIRGDEVRQIAPGQTGNIADYNYKLPDDFTGCVIAWNSNNLDSKVGGNYNYLYRLF
RKSNLKPFERDISTEIYQAGSTPCNGVKGFNCYFPLQSYGFQPTYGVGYQPYRVVVLS
FELLHAPATVCGPKK

SpyTag-RBD_Delta

MNTQILVFALIAIIPTNADKIGSGAHIVMVDAYKPTKGSGGSGGSGTGNITNLCPFGEV
FNATRFASVYAWNRKRISNCVADYSVLYNSASFSTFKCYGVSPTKLNDLCFTNVYADS
FVIRGDEVRQIAPGQTGKIADYNYKLPDDFTGCVIAWNSNNLDSKVGGNYNYRYRLF
RKSNLKPFERDISTEIYQAGSKPCNGVEGFNCYFPLQSYGFQPTNGVGYQPYRVVVLS
FELLHAPATVCGPKK

SpyTag-RRBD_XBB.1.5

MNTQILVFALIAIIPTNADKIGSGAHIVMVDAYKPTKGSGGSGGSGTGNITNLCPFHEV
FNATTFASVYAWNRKRISNCVADYSVIYNFAPFFAFKCYGVSPTKLNDLCFTNVYADS
FVIRGNEVSQIAPGQTGNIADYNYKLPDDFTGCVIAWNSNKLDSKPSGNYNYLYRLF
RKSKLKPFERDISTEIYQAGNKPCNGVAGPNCYSPLQSYGFRPTYGVGHQPYRVVVL
SFELLHAPATVCGPKK

SpyTag-RBD_BQ.1.1

MNTQILVFALIAIIPTNADKIGSGAHIVMVDAYKPTKGSGGSGGSGTGNITNLCPFDEV
FNATTFASVYAWNRKRISNCVADYSVLYNFAPFFAFKCYGVSPTKLNDLCFTNVYADS
FVIRGNEVSQIAPGQTGNIADYNYKLPDDFTGCVIAWNSNKLDSTVGGNYNYRYRLF
RKSKLKPFERDISTEIYQAGNKPCNGVAGVNCYFPLQSYGFRPTYGVGHQPYRVVVL
SFELLHAPATVCGPKK

SARS2-His8-SpyTag003

MPALLSLVSLLSVLLMGCVAQRVQPTESIVRFPNITNLCPFGEVFNATRFASVYAWNR
KRISNCVADYSVLYNSASFSTFKCYGVSPTKLNDLCFTNVYADSFVIRGDEVRQIAPG
QTGKIADYNYKLPDDFTGCVIAWNSNNLDSKVGGNYNYLYRLFRKSNLKPFERDIST
EIYQAGSTPCNGVEGFNCYFPLQSYGFQPTNGVGYQPYRVVVLSFELLHAPATVCGP
KKSTNLVKNKGGGGSGGGGSHHHHHHHHGGGGSGGGSGGGSGSGRGVPHIVMVD
AYKRYK

SARS1-His8-SpyTag003

MPALLSLVSLLSVLLMGCVARVVPSGDVVRFPNITNLCPFGEVFNATKFPSVYAWERK
KISNCVADYSVLYNSTFFSTFKCYGVSATKLNDLCFSNVYADSFVVKGDDVRQIAPG
QTGVIADYNYKLPDDFMGCVLAWNTRNIDATSTGNYNYKYRYLRHGKLRPFERDIS
NVPFSPDGKPCTPPALNCYWPLNDYGFYTTTGIGYQPYRVVVLSFELLNAPATVCGPK
LSTDLIKNQCVNFGGGGSGGGGSHHHHHHHHGGGGSGGGSGGGSGSGRGVPHIVM
VDAYKRYK

RaTG13-His8-SpyTag003

MPALLSLVSLLSVLLMGCVARVQPTDSIVRFPNITNLCPFGEVFNATTFASVYAWNRK
RISNCVADYSVLYNSTSFSTFKCYGVSPTKLNDLCFTNVYADSFVITGDEVRQIAPGQT
GKIADYNYKLPDDFTGCVIAWNSKHIDAKEGGNFNYLYRLFRKANLKPFERDISTEIY
QAGSKPCNGQTGLNCYYPLYRYGFYPTDGVGHQPYRVVVLSFELLNAPATVCGPKK
STNLVKNKCVNFGGGGSGGGGSHHHHHHHHGGGGSGGGSGGGSGSGRGVPHIVMV
DAYKRYK

SHC014-His8-SpyTag003

MPALLSLVSLLSVLLMGCVARVAPSKEVVRFPNITNLCPFGEVFNATTFPSVYAWERK
RISNCVADYSVLYNSTSFSTFKCYGVSATKLNDLCFSNVYADSFVVKGDDVRQIAPGQ
TGVIADYNYKLPDDFLGCVLAWNTNSKDSSTSGNYNYLYRWVRRSKLNPYERDLSN
DIYSPGGQSCSAVGPNCYNPLRPYGFFTTAGVGHQPYRVVVLSFELLNAPATVCGPKL
STDLIKNQGGGGSGGGGSHHHHHHHHGGGGSGGGSGGGSGSGRGVPHIVMVDAYK
RYK

Rs4081-His8-SpyTag003

MPALLSLVSLLSVLLMGCVARVSPTHEVVRFPNITNRCPFDKVFNASRFPNVYAWERT
KISDCVADYTVLYNSTSFSTFKCYGVSPSKLIDLCFTSVYADTFLIRSSEVRQVAPGETG
VIADYNYKLPDDFTGCVIAWNTAKQDQGQYYYRSSRKTKLKPFERDLTSDENGVRT
LSTYDFYPNVPIEYQATRVVVLSFELLNAPATVCGPKLSTALVKNQCVNFGGGGSGGG
GSHHHHHHHHGGGGSGGGSGGGSGSGRGVPHIVMVDAYKRYK

pang17-His8-SpyTag003

MPALLSLVSLLSVLLMGCVARVQPTISIVRFPNITNLCPFGEVFNASKFASVYAWNRKR
ISNCVADYSVLYNSTSFSTFKCYGVSPTKLNDLCFTNVYADSFVVKGDEVRQIAPGQT
GVIADYNYKLPDDFTGCVIAWNSVKQDALTGGNYGYLYRLFRKSKLKPFERDISTEI
YQAGSTPCNGQVGLNCYYPLERYGFHPTTGVNYQPFRVVVLSFELLNGPATVCGPKL
STTLVKDKCVNFGGGGSGGGGSHHHHHHHHGGGGSGGGSGGGSGSGRGVPHIVMV
DAYKRYK

RmYN02-His8-SpyTag003

MPALLSLVSLLSVLLMGCVARILPSTEVVRFPNITNFCPFDKVFNATRFPNVYAWQRT
KISDCIADYTVLYNSTSFSTFKCYGVSPSKLIDLCFTSVYADTFLIRFSEVRQIAPGETG
VIADYNYKLPDDFTGCVLAWNTAQQDIGSYFYRSHRAVKLKPFERDLSSDENGVRTL
STYDFNPNVPLDYQATRVVVLSFELLNAPATVCGPKLSTQLVKNRCVNFGGGGSGGG
GSHHHHHHHHGGGGSGGGSGGGSGSGRGVPHIVMVDAYKRYK

Rf1-His8-SpyTag003

MPALLSLVSLLSVLLMGCVARVSPVTEVVRFPNITNLCPFDKVFNATRFPSVYAWERT
KISDCVADYTVFYNSTSFSTFNCYGVSPSKLIDLCFTSVYADTFLIRFSEVRQVAPGQT
GVIADYNYKLPDDFTGCVIAWNTAKQDVGSYFYRSHRSSKLKPFERDLSSEENGVRT
LSTYDFNQNVPLEYQATRVVVLSFELLNAPATVCGPKLSTSLVKNQCVNFGGGGSGG
GGSHHHHHHHHGGGGSGGGSGGGSGSGRGVPHIVMVDAYKRYK

WIV1-His8-SpyTag003

MPALLSLVSLLSVLLMGCVARVAPSKEVVRFPNITNLCPFGEVFNATTFPSVYAWERK
RISNCVADYSVLYNSTSFSTFKCYGVSATKLNDLCFSNVYADSFVVKGDDVRQIAPGQ
TGVIADYNYKLPDDFTGCVLAWNTRNIDATQTGNYNYKYRSLRHGKLRPFERDISNV
PFSPDGKPCTPPAFNCYWPLNDYGFYITNGIGYQPYRVVVLSFELLNAPATVCGPKLS
TDLIKNQCVNFGGGGSGGGGSHHHHHHHHGGGGSGGGSGGGSGSGRGVPHIVMVD
AYKRYK

Yun11-His8-SpyTag003

MPALLSLVSLLSVLLMGCVARVSPSTEVIRFPNITNRCPFDRVFNASRFPSVYAWERTKI
SDCVADYTVLYNSTSFSTFKCYGVSPSKLIDLCFTSVYADTFLIRFSEVRQIAPGETGVI
ADYNYKLPDEFTGCVIAWNTANQDRGQYYYRSSRKTKLKPFERDLSSDENGVRTLS
TYDFYPSVPLEYQATRVVVLSFELLNAPATVCGPKLSTSLIKNQCVNFGGGGSGGGGS
HHHHHHHHGGGGSGGGSGGGSGSGRGVPHIVMVDAYKRYK

BM4831-His8-SpyTag003

MPALLSLVSLLSVLLMGCVARVTPTTEVVRFPNITQLCPFNEVFNITSFPSVYAWERMR
ITNCVADYSVLYNSSASFSTFQCYGVSPTKLNDLCFSSVYADYFVVKGDDVRQIAPAQ
TGVIADYNYKLPDDFTGCVIAWNTNSLDSSNEFFYRRFRHGKIKPYGRDLSNVLFNPS
GGTCSAEGLNCYKPLASYGFTQSSGIGFQPYRVVVLSFELLNAPATVCGPKQSTELVK
NKCVNFGGGGSGGGGSHHHHHHHHGGGGSGGGSGGGSGSGRGVPHIVMVDAYKR
YK

BtKY72-His8-SpyTag003

MPALLSLVSLLSVLLMGCVARVSPSTEVVRFPNITNLCPFGQVFNASNFPSVYAWERL
RISDCVADYAVLYNSSSSFSTFKCYGVSPTKLNDLCFSSVYADYFVVKGDDVRQIAPA
QTGVIADYNYKLPDDFTGCVLAWNTNSVDSKSGNNFYYRLFRHGKIKPYERDISNVL
YNSAGGTCSSISQLGCYEPLKSYGFTPTVGVGYQPYRVVVLSFELLNAPATVCGPKKS
TELVKNKCVNFGGGGSGGGGSHHHHHHHHGGGGSGGGSGGGSGSGRGVPHIVMV
DAYKRYK

SpyTag-RBD_HKU25

MNTQILVFALIAIIPTNADKIGSGAHIVMVDAYKPTKGSGGSGGSGTGSGKECDFSPM
LTGTPPQVYNFRRLVFTDCNYNLTKLLSLFQVSEFSCHQVSPDALASGCYSSLTVDYF
AYPTSLASYLQQGSTGEITQYNYKQDFSNPTCRILATAPANITLTKPSNYNWLTQCYK
GSAFGNQPHYVQTGQYTPCLGLAVQGFSAAYQSHRDPITKLVATGNIAAMTDNLQM
AFIISVQYGTDTNSVCPMQ

SpyTag-RBD_ITA1/2

MNTQILVFALIAIIPTNADKIGSGAHIVMVDAYKPTKGSGGSGGSGTGQGVECDFSKL
FKAAPPQIYNFSRLVFTNCNYNLTKLLSLFHVSEFSCHQVSPSALASGCYSSLTVDYFA
YPLYLASYLQQGSTGEIAQYNYKQDFSNPTCRILASVPANVSIPKPDKYIWLSQCYSFS
AYSGDVPHYVLPGQYTPCLYLTSSGFDNSYQTNRDFQNKMAATGVISSMTDNLQMA
FVISVQYGTDTNSVCPMQ

SpyTag-RBD_HKU5

MNTQILVFALIAIIPTNADKIGSGAHIVMVDAYKPTKGSGGSGGSGTGTTQECDFTPM
LTGTPPPIYNFKRLVFTNCNYNLTKLLSLFQVSEFSCHQVSPSSLATGCYSSLTVDYFAY
STDMSSYLQPGSAGEIVQFNYKQDFSNPTCRVLATVPQNLTTITKPSNYAYLTECYKTS
AYGKNYLYNAPGGYTPCLSLASRGFSTKYQSHSDGELTTTGYIYPVTGNLQMAFIISV
QYGTDTNSVCPMQ

SpyTag-RBD_MERS

MNTQILVFALIAIIPTNADKIGSGAHIVMVDAYKPTKGSGGSGGSGTGEGVECDFSPLL
SGTPPQVYNFKRLVFTNCNYNLTKLLSLFSVNDFTCSQISPAAIASNCYSSLILDYFSYP
LSMKSDLSVSSAGPISQFNYKQSFSNPTCLILATVPHNLTTITKPLKYSYINKCSRLLSD
DRTEVPQLVNANQYSPCVSIVPSTVWEDGDYYRKQLSPLEGGGWLVASGSTVAMTE
QLQMGFGITVQYGTDTNSVCPKL

SpyTag-RBD_HKU4

MNTQILVFALIAIIPTNADKIGSGAHIVMVDAYKPTKGSGGSGGSGTGNATECDFSPM
LTGVAPQVYNFKRLVFSNCNYNLTKLLSLFAVDEFSCNGISPDAIARGCYSTLTVDYFA
YPLSMKSYIRPGSAGNIPLYNYKQSFANPTCRVMASVPANVTITKPQAYGYISKCSRLT
GANQDVETPLYINPGEYSICRDFSPGGFSEDGQVFKRTLTQFEGGGLLIGVGTKVPMT
DNLQMSFIISVQYGTGTDSVCPML

SpyTag-RBD_PDF-2180

MNTQILVFALIAIIPTNADKIGSGAHIVMVDAYKPTKGSGGSGGSGTGVYPDCNFTDL
FRENAPTIMQYKRQVFTRCNYNLTLLLSLVQVDEFVCDKITPEALATGCYSSLTVDWF
AFPYAWKSYLAIGSADRIVRFNYNQDYSNPSCRIHSKVNSSVGISYSGLYSYITNCNY
GGFNKDDVVKPGGRASQPCVTGALNSPTNGQVWSFNFGGVPYRTSRLTYTDHLKNP
LDMVYVITVKYEPGAETVCPKQ

SpyTag-RBD_HKU31

MNTQILVFALIAIIPTNADKIGSGAHIVMVDAYKPTKGSGGSGGSGTGDLEECALDVL
FKNNAPPIANYSRRVFTNCNYNLTKLLSLVEVDEFVCDKTTPESLATGCYSSLVVDWF
ALPLSMKSTLAIGSAEAISMFNYNQDYSNPTCRIHATINSNVSSSLNFTATGNYAYISRC
QGTDGKPILLQKGQLPNIACRSGVLGLPNDVDYFGYSFNGHIFYIGRKSYTPKTSEGN
IQMVYVITANYAEGPNNVCPLK

SpyTag-RBD_EriCoV

MNTQILVFALIAIIPTNADKIGSGAHIVMVDAYKPTKGSGGSGGSGTGELTECDLDVLF
KNDAPIIANYSRRVFTNCNYNLTKLLSLVQVDEFVCHKTTPEALATGCYSSLTVDWFA
LPFSMKSTLAIGSAEAISMFNYNQDYSNPTCRIHAAVTANVSTALNFTANANYAYISRC
QGVDGKPILLQPGQMTNIACRSGVLARPSDADYFGYSFQGRNYYLGRKSYKPKTDE
GDVQMVYVITPKYDKGPDTVCPLK

Br1 Quartet

MNTQILVFALIAIIPTNADKIGSGAHIVMVDAYKPTKGSGGSGGSGTGEGVECDFSPLL
SGTPPQVYNFKRLVFTNCNYNLTKLLSLFSVNDFTCSQISPAAIASNCYSSLILDYFSYP
LSMKSDLSVSSAGPISQFNYKQSFSNPTCLILATVPHNLTTITKPLKYSYINKCSRLLSD
DRTEVPQLVNANQYSPCVSIVPSTVWEDGDYYRKQLSPLEGGGWLVASGSTVAMTE
QLQMGFGITVQYGTDTNSVCPKLGSGGSGGSGQGVECDFSKLFKAAPPQIYNFSRLV
FTNCNYNLTKLLSLFHVSEFSCHQVSPSALASGCYSSLTVDYFAYPLYLASYLQQGST
GEIAQYNYKQDFSNPTCRILASVPANVSIPKPDKYIWLSQCYSFSAYSGDVPHYVLPG
QYTPCLYLTSSGFDNSYQTNRDFQNKMAATGVISSMTDNLQMAFVISVQYGTDTNSV
CPMQGSGGTGGSGVYPDCNFTDLFRENAPTIMQYKRQVFTRCNYNLTLLLSLVQVD
EFVCDKITPEALATGCYSSLTVDWFAFPYAWKSYLAIGSADRIVRFNYNQDYSNPSCR
IHSKVNSSVGISYSGLYSYITNCNYGGFNKDDVVKPGGRASQPCVTGALNSPTNGQV
WSFNFGGVPYRTSRLTYTDHLKNPLDMVYVITVKYEPGAETVCPKQGTGGSGGSGE
LTECDLDVLFKNDAPIIANYSRRVFTNCNYNLTKLLSLVQVDEFVCHKTTPEALATGC
YSSLTVDWFALPFSMKSTLAIGSAEAISMFNYNQDYSNPTCRIHAAVTANVSTALNFT
ANANYAYISRCQGVDGKPILLQPGQMTNIACRSGVLARPSDADYFGYSFQGRNYYLG
RKSYKPKTDEGDVQMVYVITPKYDKGPDTVCPLK

Nr1 Quartet

MNTQILVFALIAIIPTNADKIGSGAHIVMVDAYKPTKGSGGSGGSGTGEGVECDFSPLL
SGTPPQVYNFKRLVFTNCNYNLTKLLSLFSVNDFTCSQISPAAIASNCYSSLILDYFSYP
LSMKSDLSVSSAGPISQFNYKQSFSNPTCLILATVPHNLTTITKPLKYSYINKCSRLLSD
DRTEVPQLVNANQYSPCVSIVPSTVWEDGDYYRKQLSPLEGGGWLVASGSTVAMTE
QLQMGFGITVQYGTDTNSVCPKLGSGGSGGSGQGVECDFSKLFKAAPPQIYNFSRLV
FTNCNYNLTKLLSLFHVSEFSCHQVSPSALASGCYSSLTVDYFAYPLYLASYLQQGST
GEIAQYNYKQDFSNPTCRILASVPANVSIPKPDKYIWLSQCYSFSAYSGDVPHYVLPG
QYTPCLYLTSSGFDNSYQTNRDFQNKMAATGVISSMTDNLQMAFVISVQYGTDTNSV
CPMQGSGGTGGSGNATECDFSPMLTGVAPQVYNFKRLVFSNCNYNLTKLLSLFAVDE
FSCNGISPDAIARGCYSTLTVDYFAYPLSMKSYIRPGSAGNIPLYNYKQSFANPTCRVM
ASVPANVTITKPQAYGYISKCSRLTGANQDVETPLYINPGEYSICRDFSPGGFSEDGQV
FKRTLTQFEGGGLLIGVGTKVPMTDNLQMSFIISVQYGTGTDSVCPMLGTGGSGGSG
TTQECDFTPMLTGTPPPIYNFKRLVFTNCNYNLTKLLSLFQVSEFSCHQVSPSSLATGC
YSSLTVDYFAYSTDMSSYLQPGSAGEIVQFNYKQDFSNPTCRVLATVPQNLTTITKPSN
YAYLTECYKTSAYGKNYLYNAPGGYTPCLSLASRGFSTKYQSHSDGELTTTGYIYPVT
GNLQMAFIISVQYGTDTNSVCPMQ

SARS2 Wuhan HexaPro Spike

MFVFLVLLPLVSSQCVNLTTRTQLPPAYTNSFTRGVYYPDKVFRSSVLHSTQDLFLPFF
SNVTWFHAIHVSGTNGTKRFDNPVLPFNDGVYFASTEKSNIIRGWIFGTTLDSKTQSL
LIVNNATNVVIKVCEFQFCNDPFLGVYYHKNNKSWMESEFRVYSSANNCTFEYVSQP
FLMDLEGKQGNFKNLREFVFKNIDGYFKIYSKHTPINLVRDLPQGFSALEPLVDLPIGI
NITRFQTLLALHRSYLTPGDSSSGWTAGAAAYYVGYLQPRTFLLKYNENGTITDAVD
CALDPLSETKCTLKSFTVEKGIYQTSNFRVQPTESIVRFPNITNLCPFGEVFNATRFASV
YAWNRKRISNCVADYSVLYNSASFSTFKCYGVSPTKLNDLCFTNVYADSFVIRGDEV
RQIAPGQTGKIADYNYKLPDDFTGCVIAWNSNNLDSKVGGNYNYLYRLFRKSNLKPF
ERDISTEIYQAGSTPCNGVEGFNCYFPLQSYGFQPTNGVGYQPYRVVVLSFELLHAPA
TVCGPKKSTNLVKNKCVNFNFNGLTGTGVLTESNKKFLPFQQFGRDIADTTDAVRDP
QTLEILDITPCSFGGVSVITPGTNTSNQVAVLYQDVNCTEVPVAIHADQLTPTWRVYST
GSNVFQTRAGCLIGAEHVNNSYECDIPIGAGICASYQTQTNSPGSASSVASQSIIAYTM
SLGAENSVAYSNNSIAIPTNFTISVTTEILPVSMTKTSVDCTMYICGDSTECSNLLLQYG
SFCTQLNRALTGIAVEQDKNTQEVFAQVKQIYKTPPIKDFGGFNFSQILPDPSKPSKRS
PIEDLLFNKVTLADAGFIKQYGDCLGDIAARDLICAQKFNGLTVLPPLLTDEMIAQYT
SALLAGTITSGWTFGAGPALQIPFPMQMAYRFNGIGVTQNVLYENQKLIANQFNSAIG
KIQDSLSSTPSALGKLQDVVNQNAQALNTLVKQLSSNFGAISSVLNDILSRLDPPEAE
VQIDRLITGRLQSLQTYVTQQLIRAAEIRASANLAATKMSECVLGQSKRVDFCGKGY
HLMSFPQSAPHGVVFLHVTYVPAQEKNFTTAPAICHDGKAHFPREGVFVSNGTHWFV
TQRNFYEPQIITTDNTFVSGNCDVVIGIVNNTVYDPLQPELDSFKEELDKYFKNHTSP
DVDLGDISGINASVVNIQKEIDRLNEVAKNLNESLIDLQELGKYEQGSGYIPEAPRDG
QAYVRKDGEWVLLSTFLGRSLEVLFQGPGHHHHHHHHSAWSHPQFEKGGGSGGGG
SGGSAWSHPQFEK

Appendix 2 – Sequence alignment of Sarbecovirus RBDs